

CHARACTERIZING THE PROGRESSION OF DISEASE  
ASSOCIATED WITH HUMAN MENISCAL PATHOLOGY

---

A Dissertation presented to  
the Faculty of the Graduate School  
at the University of Missouri-Columbia

---

In Partial Fulfillment  
of the Requirements for the Degree  
Doctor of Philosophy

---

by  
BRANDON L. ROLLER, M.D.  
Dr. James L. Cook, Dissertation Supervisor

JULY 2013

© Copyright by Dr. Brandon Roller 2013

All Rights Reserved

The undersigned, appointed by the dean of the Graduate School, have examined the dissertation entitled

**CHARACTERIZING THE PROGRESSION OF DISEASE  
ASSOCIATED WITH HUMAN MENISCAL PATHOLOGY**

presented by Dr. Brandon L. Roller,

a candidate for the degree of doctor of philosophy, and hereby certify that, in their opinion, it is worthy of acceptance.

---

Professor James L. Cook

---

Professor Derek B. Fox

---

Professor Aaron M. Stoker

---

Professor Keiichi Kuroki

## ACKNOWLEDGEMENTS

Sincere appreciation is dedicated to each of the committee members for their consistent words of encouragement and their helpful guidance that led to the completion of this degree. Without their leadership, I would not have developed the skillset of a research scientist which provides a continual foundation for the career field I find myself within today. Dr. Aaron Stoker spent countless hours working with me in the laboratory to perfect my techniques and teach me how to critically design research protocols. Drs. Derek Fox and Keiichi Kuroki continually offered their time and direction through the resolution of critical questions that spawned from each research project that I pursued. I would like to especially thank Dr. James Cook. Not only was he instrumental in my growth within the fields of pathobiology and orthopaedics; but he has been vitally influential in a more personal way as well. He has taught me to be a respectful and generous person by showing extraordinary humility and a willingness to serve others. Dr. Cook will continue to be my advisor and mentor far after the completion of this degree. I would also like to expressly thank my beautiful wife, Amy. Her endless love, tremendous patience, and inspiring support have helped me to persevere through the process of completing this degree while pursuing a new career path. God has truly blessed me with the people he has placed in my life and the path through which he continually guides me ... Thank You!

## TABLE OF CONTENTS

ACKNOWLEDGEMENTS .....	ii
LIST OF FIGURES .....	vii
LIST OF TABLES .....	ix
ACADEMIC ABSTRACT .....	xi
CHAPTER	
1. Introduction .....	1
References .....	3
2. Literature Review .....	4
Macroscopic meniscal changes .....	4
Biomechanical meniscal changes .....	6
Microscopic meniscal changes .....	8
Biochemical meniscal changes .....	12
Molecular meniscal changes .....	17
Conclusion .....	21
References .....	23
3. Characterization of knee meniscal pathology: correlation of gross, histologic, biochemical, molecular, and radiographic measures of disease .....	29
Experimental purpose and hypothesis .....	29
Materials and methods .....	30
Tissue collection, gross evaluation, and tissue storage .....	30
Histologic evaluation .....	31
Biochemical evaluation .....	31
Molecular evaluation .....	33

Radiographic evaluation .....	36
Statistical evaluation .....	38
Results .....	38
Gross evaluation .....	39
Histologic evaluation .....	39
Biochemical evaluation .....	40
Molecular evaluation .....	41
Radiographic evaluation .....	42
Correlations .....	43
Discussion .....	43
Gross evaluation .....	43
Histologic evaluation.....	45
Biochemical evaluation.....	47
Molecular evaluation.....	51
Radiographic evaluation.....	60
Conclusions .....	62
References .....	74
<b>4. Characterization of meniscal pathology with molecular and proteomic analyses.....</b>	<b>81</b>
Experimental purpose and hypothesis .....	81
Materials and methods .....	82
Tissue collection and tissue storage .....	82
Microarray analysis .....	85
Proteomics analysis .....	87
Results .....	91

Microarray analysis .....	91
Proteomics analysis .....	91
Discussion .....	92
Genes and proteins associated with ECM production .....	92
Genes and proteins associated with vascularity .....	98
Genes and proteins associated with anti-degradation and degradation ....	102
Genes and proteins associated with the cytoskeleton .....	106
Genes and proteins associated with signaling and energy pathways .....	108
Limitations .....	110
Conclusions .....	111
References .....	136
 5. Identification of novel synovial fluid biomarkers that correlate with meniscal pathology .....	144
Experimental purpose and hypothesis .....	144
Materials and methods .....	145
Synovial fluid collection and storage .....	145
Proteomics analysis .....	146
Results .....	148
Discussion .....	149
Extracellular Superoxide Dismutase [Cu-Zn] (SOD3) .....	149
Isoform A and C of Proteoglycan 4 (PRG4) .....	152
Apolipoprotein B-100 (APOB) .....	153
C4b Binding Protein Alpha Chain (C4BPA) .....	156
Low-density Lipoprotein Receptor Related Protein 1 (LRP1) .....	157
Aggrecan (ACAN) .....	158

Isoform V0 of Versican Core Protein (VCAN) .....	160
Hyaluronan and Proteoglycan Link Protein 1 (HAPLN1) .....	161
Lymphatic Vessel Endothelial Hyaluronic Acid Receptor 1 (LYVE1) .....	162
Cartilage Intermediate Layer Protein 1 (CILP) .....	163
Isoform 1 of Collagen Alpha-3 (VI) Chain (COL6A3) .....	164
Haptoglobin (HP) and Isoform 1 of Haptoglobin Related Protein (HRP) .....	165
Ceruloplasmin (CP) .....	166
Beta-2-Microglobulin (B2M) .....	168
Fibroblast Growth Factor Binding Protein 2 (FGFBP2) .....	169
Insulin Like Growth Factor Binding Protein 6 (IGFBP6) .....	170
Isoform 1 of Target of Nesh-SH3 Binding Protein (ABI3BP) .....	171
Conclusions .....	171
References .....	197
VITA .....	206

## LIST OF FIGURES

Figure	Page
2-1 Axial view of medial and lateral meniscus.....	22
2-2 Coronal section of the knee depicting vascular branches into the peripheral border of the medial meniscus.....	22
2-3 Meniscal collagen ultrastructure.....	22
3-1 Meniscal tissue histologic scoring system.....	64
4-1 Expression levels of genes associated with synthesis .....	120
4-2 Expression levels of genes associated with vascularity.....	121
4-3 Expression levels of genes associated with anti-degradation and degradation.....	122
4-4 Expression levels of genes associated with signaling pathways .....	123
4-5 Proteomics gel .....	124
4-6 ECM proteins.....	131
4-7 Proteins associated with vascularity .....	132
4-8 Degredative and potentially anti-degradative proteins .....	133
4-9 Cytoskeleton proteins and proteins involved in glycolysis pathway.....	134
4-10 Proteins associated with signaling .....	135
5-1 Extracellular Superoxide Dismutase [Cu-Zn] .....	190
5-2 Isoform A of Proteoglycan 4 .....	190
5-3 Isoform C of Proteoglycan 4 .....	190
5-4 Apolipoprotein B-100.....	191

5-5	C4b Binding Protein Alpha Chain.....	191
5-6	Low-density Lipoprotein Receptor Related Protein 1 .....	191
5-7	Aggrecan.....	192
5-8	Isoform V0 of Versican Core Protein.....	192
5-9	Hyaluronan and Proteoglycan Link Protein 1 .....	192
5-10	Lymphatic Vessel Endothelial Hyaluronic Acid Receptor 1.....	193
5-11	Cartilage Intermediate Layer Protein 1 .....	193
5-12	Isoform 1 of Collagen Alpha-3 (VI) Chain .....	193
5-13	Haptoglobin .....	194
5-14	Isoform 1 of Haptoglobin Related Protein .....	194
5-15	Ceruloplasmin.....	194
5-16	Beta-2 Microglobulin .....	195
5-17	Fibroblast Growth Factor Binding Protein 2 .....	195
5-18	Insulin Like Growth Factor Binding Protein 6.....	195
5-19	Isoform 1 of Target of Nesh-SH3 Binding Protein .....	196

## LIST OF TABLES

Table		Page
3-1	Gross score .....	65
3-2	Histologic total score.....	65
3-2a	Histologic architecture score.....	65
3-2b	Histologic matrix score .....	66
3-2c	Histologic proliferative score.....	66
3-3	Water content % .....	66
3-4	Proteoglycan content.....	67
3-5	Collagen content.....	67
3-6	Collagen I expression.....	67
3-7	Collagen II expression.....	68
3-8	Collagen III expression .....	68
3-9	Collagen VI expression.....	68
3-10	MMP-1 expression.....	69
3-11	MMP-2 expression.....	69
3-12	MMP-3 expression.....	69
3-13	MMP-13 expression.....	70
3-14	VEGF expression .....	70
3-15	Radiographic measurement.....	71
3-16	Radiographic total score.....	71

3-16a	Radiographic osteophyte score .....	71
3-16b	Radiographic narrowing score .....	71
3-17	Correlations .....	72
4-1	Patient information.....	113
4-2	Microarray analysis.....	114
4-3	Proteomics analysis.....	125
5-1	Patient demographics .....	175
5-2	Proteomics analysis .....	176
5-3	Proteins of interest.....	189

CHARACTERIZING THE PROGRESSION OF DISEASE  
ASSOCIATED WITH HUMAN MENISCAL PATHOLOGY

Brandon L. Roller, M.D.

Dr. James L. Cook, Dissertation Supervisor

ABSTRACT

Meniscal fibrocartilaginous structures are subject to numerous stresses when performing its necessary functions to maintain intra-articular homeostasis. Pathological events causing a loss of tissue integrity will result in meniscal dysfunction, which will inevitably lead to the debilitating disease of osteoarthritis. When working to characterize osteoarthritic meniscal pathology, it was evident that the clinical assessment of radiography will correlate with gross and histologic measures of disease. These three scoring methods correlated well with the biochemical and molecular changes that occur when comparing normal to osteoarthritic menisci and medial to lateral osteoarthritic menisci. In order to more fully differentiate the abundant transformations that occur between aged-normal, meniscectomy, and osteoarthritic menisci, microarray and mass spectrometry analyses were utilized. Pathologic menisci appeared to haphazardly attempt an increase of its extracellular matrix components, some captivating markers of vascularity were increased, and a protein of potential therapeutic value was identified. Proteomic analysis was further utilized to study synovial fluid markers associated with meniscal disease and was able to identify a number of proteins with biomarker potential and a few additional proteins of therapeutic significance. These studies identified novel data that help to define the pathological changes a meniscus undergoes upon degradation.

## CHAPTER 1:

### INTRODUCTION

Joint problems are the foremost disability in the United States, resulting in associated costs of over \$90 billion annually. Osteoarthritis (OA), the most common type of degenerative joint disease in the knee, is often related to meniscal pathology. The medial and lateral menisci are fibrocartilaginous structures positioned between the femoral condyles and tibial plateau. Overall, approximately one million operative procedures are performed each year in the United States to address problems related to knee menisci.<sup>1</sup> The majority of these surgeries require resection of a portion of the meniscus resulting in deficient meniscal function within the knee joint. Knee menisci are exposed to tensile, shear, and compressive stresses during activities of daily living.<sup>2</sup> Menisci must be maintained in their normal size, shape, and composition in order to perform their necessary functions in the knee including stability, congruity, load distribution, shock absorption, lubrication, and joint nutrition. Loss of meniscal integrity causes a lack of protection of articular cartilage, which inevitably will lead to osteoarthritis, pain, and disability in affected individuals.<sup>3-9</sup> Since meniscal morphology plays a vital role in maintaining normal knee function, the amount of resected meniscal tissue directly correlates with the rate and severity of progression of OA and the degree of joint dysfunction.<sup>2,10,11</sup> Multiple reports document that substantial articular cartilage and bone changes will occur from even partial meniscectomies within 5 to 15 years, and that the pathologic changes correlate directly with the amount of meniscus resected at surgery.<sup>3-9</sup> Treatment of meniscal pathology is very limited with respect to successful preservation of functional meniscal tissue. When a meniscal repair procedure is not

feasible, specifically when avascular tears are present, a partial meniscectomy is performed in the majority of patients, potentially dooming the knee to progressive deterioration.<sup>12</sup>

A great deal of progress is required before the common problem of the meniscal deficient knee can be comprehensively managed. The major impediment to addressing this problem is the lack of critical data. Although the meniscus has been studied for years, relatively limited data are available regarding comprehensive characterization of meniscal pathology with respect to the molecular, biochemical, and histologic aspects of disease. It is important to determine the changes that occur from a normal meniscus, to a meniscus that has an avascular lesion or vascular lesion, to a meniscus associated with degenerative joint disease and OA. Understanding these basic science components of meniscal disorders should provide an avenue for determining etiopathogenesis, optimizing diagnostic strategies, evaluating possible treatment options, and determining prognosis for patients. In order to address this goal, our strategy is to comprehensively assess meniscal pathology and correlate clinical and basic science data in pursuit of finding clinically relevant answers for this common problem in people.

## References

1. *Medical Data International, Newport Beach, CA, USA.* September 2003.
2. Fithian DC, Kelly MA, Mow VC. Material properties and structure-function relationships in the menisci. *Clinical Orthopaedics and Related Research.* 1990(252):19-31.
3. Andersson-Molina H, Karlsson H, Rockborn P. Arthroscopic partial and total meniscectomy: A long-term follow-up study with matched controls. *Arthroscopy.* 2002;18(2):183-189.
4. Bonneux I, Vandekerckhove B. Arthroscopic partial lateral meniscectomy long-term results in athletes. *Acta Orthopaedica Belgica.* 2002;68(4):356-361.
5. Chatain F, Robinson AHN, Adeleine P, Chambat P, Neyret P. The natural history of the knee following arthroscopic medial meniscectomy. *Knee Surgery, Sports Traumatology, Arthroscopy.* 2001;9(1):15-18.
6. Ciccuttini FM, Forbes A, Yuanyuan W, Rush G, Stuckey SL. Rate of knee cartilage loss after partial meniscectomy. *Journal of Rheumatology.* 2002;29(9):1954-1956.
7. McKinley TO, English DK, Bay BK. Trabecular bone strain changes resulting from partial and complete meniscectomy. *Clinical Orthopaedics and Related Research.* 2003(407):259-267.
8. van Tienen TG, Heijkants RG, de Groot JH, et al. Presence and mechanism of knee articular cartilage degeneration after meniscal reconstruction in dogs. *Osteoarthritis and Cartilage.* 2003;11(1):78-84.
9. Wyland DJ, Guilak F, Elliott DM, Setton LA, Vail TP. Chondropathy after meniscal tear or partial meniscectomy in a canine model. *Journal of Orthopaedic Research.* 2002;20(5):996-1002.
10. Cook JL, Fox DB, Malaviya P, et al. Evaluation of small intestinal submucosa grafts for meniscal regeneration in a clinically relevant posterior meniscectomy model in dogs. *The journal of knee surgery.* 2006;19(3):159-167.
11. Cook JL, Fox DB, Malaviya P, et al. Long-term outcome for large meniscal defects treated with small intestinal submucosa in a dog model. *American Journal of Sports Medicine.* 2006;34(1):32-42.
12. Cook JL. The current status of treatment for large meniscal defects. *Clinical Orthopaedics and Related Research.* 2005(435):88-95.

## CHAPTER 2:

### LITERATURE REVIEW

Medial and lateral menisci are integral components within the knee joint ensuring normal articular homeostasis. When either meniscus undergoes a pathologic event such as an acute tear or chronic degeneration, a cascade of changes will occur on a macroscopic, biomechanical, microscopic, biochemical, and molecular level. Understanding these events becomes imperative when attempting to characterize how meniscal disease progresses and eventually leads to osteoarthritis.

#### **Macroscopic meniscal changes**

Medial and lateral menisci have a C-shaped appearance when viewed in an axial plane and a wedged appearance when viewed in a coronal plane (Figure 1 and 2). The medial meniscus has firm anterior and posterior attachment sites to the tibial plateau and is supported at its midpoint by the deep medial ligament. The lateral meniscus also has anterior and posterior horn attachment sites to the tibial plateau but it is more mobile than the medial because the horns have a closer proximity to each other, and because there is an area of detachment from the capsule posterolaterally.<sup>1</sup> The medial meniscus covers and protects less of the tibial plateau than the lateral with meniscus-to-plateau ratios of 0.64 and 0.84, respectively.<sup>2</sup> When a tear occurs and a partial meniscectomy is performed, the meniscus-to-plateau ratio will decrease and the contact surface area between the femoral condyle and plateau will increase; this in turn leads to some very distinct characteristic changes within the joint over time.

Some long term data has shown that radiographic changes will depend on the amount of meniscus removed. With increasing amount of tissue removed, there was a correlation with joint space narrowing.<sup>3,4</sup> For lateral menisci more specifically, Fairbank changes were noted on radiography within 8 years for 93% of the patients.<sup>5</sup> Increasing the amount of meniscus removed correlates with more intense cartilage lesions. A canine study compared intact menisci with incomplete partial meniscectomy, partial meniscectomy, subtotal meniscectomy, and total meniscectomy. The degenerative lesions found on the tibial plateau and femoral condyle was proportional to the amount of meniscal tissue removed.<sup>6</sup> A separate canine study looked to compare a meniscal tear to partial meniscectomy of the posterior medial meniscus. Both lesions lead to significantly greater gross chondropathy compared to the unoperated contralateral control. They also noted a decrease in cartilage tensile stiffness, which significantly correlated with the increase in gross chondropathy. Interestingly, there was not a difference between the meniscal tear group or meniscectomy group.<sup>7</sup> Articular cartilage volume loss will also occur due to partial meniscectomies. Magnetic resonance imaging (MRI) was used to measure the cartilage loss within patients and found that a 6.9% per year loss of volume was noted when compared to controls after adjustment for age, body max index (BMI), and sex. This study demonstrates that the articular cartilage can be affected within as little as 3 years after a partial meniscectomy.<sup>8</sup> The amount of initial articular cartilage damage noticed during surgical intervention has also been shown to correlate with the type of avascular tear that occurs. Radial and degenerative tear types were associated with increased cartilage damage when compared to flap and longitudinal tears (cartilage damage rates of 65% and 85% vs. 12% and 0%, respectively). An increase in duration

between injury and surgical intervention also correlated with increased prevalence of cartilage degradation within the adjacent tissue.<sup>9</sup> An in vivo study looked at longitudinal, avascular lesions more specifically. These lesions were created in rabbit medial menisci and after 3 months, one group was repaired, a second was left untreated, and a third underwent meniscectomy. Cartilage changes were more pronounced in the meniscectomy group when compared to the repair and untreated groups. However, cartilage damage was noticed within all pathologic groups which would indicate that even a longitudinal lesion will cause cartilage damage over time.<sup>10</sup> The longitudinal lesion may protect the articular cartilage initially, but unless it is repaired in a timely fashion, the progression of the tear and progression of articular damage will continue.

### **Biomechanical meniscal changes**

Intact menisci are able to distribute the contact pressure within a joint by maximizing the contact area and distribution of forces. Fifty percent of the joint load for the medial compartment is transmitted through the medial meniscus, and seventy percent of the joint load in the lateral compartment is transmitted through the lateral meniscus.<sup>11</sup> For an intact medial meniscus, the contact pressure is less in the anterior and central regions and greater within the posterior region. However, the lateral meniscus appears to have a more uniform amount of pressure present throughout the three regions.<sup>12</sup> After a meniscal tear occurs, the structure and integrity of the meniscal tissue will be altered. For example, vertical radial tears and complex degenerative tears will disrupt the circumferential fibers demonstrated in Figure 3. These fibers normally are able to distribute an axial load circumferentially via hoop stresses.<sup>13</sup> The more circumferential

fibers that are disrupted, the less axial load the meniscus can accommodate for. Another type of tear where the mechanics of the meniscus are altered is the common bucket handle tear. A recent study was able to demonstrate the differences between an intact meniscus, bucket handle tear, partial meniscectomy, and meniscal repair. The stifles that had a partial meniscectomy had significantly lower contact areas, along with higher mean and peak contact pressures when compared to controls. There was no statistical difference when comparing the bucket handle tear to the partial meniscectomy group. However, the meniscal repair groups were able to restore contact mechanics within the stifle.<sup>14</sup> Bucket handle tears disrupt the radial fibers shown in Figure 3 that run perpendicular to the circumferential collagen fibers. These types of tears may originate from a non-displaced vertical longitudinal tear that progresses into a displaced bucket handle tear. This study was able to show how joint mechanics are altered when a tear is not repaired and progresses to a displaced bucket handle.

When a partial meniscectomy is performed to treat these types of tears, a cascade of destruction will occur. As part of the meniscus is removed, the contact area between the meniscus and articular surfaces will decrease. With this change comes an increase in contact pressures. Contact forces have been reported as increasing 350% when less than one-third of the meniscus has been resected.<sup>11</sup> Peak contact pressures have been shown to increase by 65% after partial meniscectomy within a human cadaveric study.<sup>15</sup> Thieman et al used a canine partial meniscectomy model to show a 35% decrease in contact area, 57% increase in mean contact pressure, and 55% increase in peak contact pressure.<sup>14</sup> Zielinska was able to demonstrate a direct relationship with respect to the amount of meniscus removed and the maximum and mean contact pressures that result.

When removing the avascular portion of the medial meniscus (60%) he found that the contact pressure within the remaining medial meniscus increased 65%, and increased 55% for the medial tibial plateau.<sup>12</sup> Shear stresses will also increase with the removal of meniscal tissue. Complete meniscectomy results in a 150% increase in maximum shear stress at the bone-cartilage interface and a 460% increase at the cartilage interfaces.<sup>16</sup> These studies represent the importance of the entire meniscus being present within the joint in order to maintain normal contact forces and pressures. When an avascular tear occurs and is treated with a partial meniscectomy, it is very clear that the joint will never function under its normal parameters again.

### **Microscopic meniscal changes**

With extra-articular tendon and ligament tissue repair, a fibrin clot initially forms at the site of injury and is then invaded by fibroblasts which lay down collagen fibers. A similar fibrin clot can also occur within the vascular zone of the meniscus if a tear occurs. Vessels proliferate through this fibrin scaffold along with undifferentiated cells in order to create fibrovascular scar tissue.<sup>17</sup> However, the percentage of each meniscus that contains vascularity is limited (Figure 2). Fetal menisci have vascular channels throughout the entire meniscus; after birth the vascularity of the central portion begins to decrease. By the time an individual is 10 years old, meniscal blood vessels will mainly be located within the peripheral one-third of the meniscus.<sup>2</sup> Vascular penetration for adult menisci ranges between 10-30%.<sup>1</sup> Because of the lack of vascularity, a fibrin clot will not form within a tear that involves the central avascular portion. Vascular channels provide the fibrinogen required to initiate and maintain a clot. Without the formation of

fibrin, bridging scaffolds across avascular meniscal tears will not occur post injury. This lack of a fibrovascular scar being formed at the tear site is part of the reason why avascular meniscal tears do not heal effectively.<sup>9</sup> In addition to lacking the ability to form a fibrovascular scar, the avascular inner meniscal tissue has been shown to demonstrate a lower intrinsic healing ability when compared to peripheral meniscal tissue. In an in vitro study, a 1.5 mm-diameter plug was removed from the inner avascular meniscal zone; the defect was then replaced with a similar sized plug from the peripheral meniscal zone, or the original avascular plug was implanted back into the defect. After culturing for six weeks, the group that received a meniscal plug from the peripheral zone had significantly better gross and histologic examination scores. It was described that a healing response within meniscal tissue is likely not solely dependent on the vascularity of the tissue. A regional, cellular difference within the meniscus tissue appears to contribute to peripheral meniscal tears eliciting a healing response while central meniscal tears are unable to stimulate a similar response.<sup>18</sup>

Avascular tears of the meniscus have been described as going through three phases after the initial injury occurs according to histologic evaluation. After the initial injury, the tear characteristics are smooth with minimal fraying along the tissue edge. A large influx of neutrophils or lymphocytes does not appear within the torn region; cells found within the torn region of the meniscus appear to have a more chondrocytic phenotype with a round appearance. The second distinctive phase has been described to occur between 3-9 months, and is labeled as the perimeniscal proliferation phase. For longitudinal and flap tears, synovial cells appear to encapsulate the torn part of the meniscus and make up the superficial layer. Within this layer, cells are positive for the

CD68 marker, representing an influx of monocytes/macrophages. Underneath this layer, there exists a thicker layer of cells with a fibroblastic appearance. Neovascularization is not present within the tissue. For radial tears, the tissue is much more macerated and has a frond-like appearance. The third phase consists of a remodeling phase which has been identified as taking place at a time period greater than 9 months post injury. The tissue becomes much denser with very little fatty synovial tissue overlying the torn menisci. CD68 positive cells are now found within the superficial layer as well as the underlying perimeniscal layer. These specimens also appear to contain a greater degree of TUNEL+ cells indicating increased DNA fragmentation from apoptotic signaling cascades. Specimens that are at least 9 months post injury have a higher DNA fragmentation rate when compared to specimens isolated between 1 and 12 weeks (20% vs. 1%, respectively). In addition, it has been noted that radial and degenerative tears will receive the worst histologic scores through these three phases post injury when compared to other tear types. As one would expect, a correlation exists between worsening histologic scores and duration after initial injury.<sup>9</sup>

As indicated through the previous study, apoptosis appears to play a role within avascular meniscal tears. A separate study looked at meniscal tissue collected during surgical intervention and was divided into two groups: degenerative or traumatic. These tissue samples were compared to normal meniscal tissues collected from cadavers. The study found that the mean indexes of apoptosis was significantly increased for the pathologic groups when compared to the normal group (normal = 0.237, traumatic = 0.725, degenerative = 0.497). The apoptotic cells were found within the superficial and middle zones and were distributed throughout the torn edges as well.

Minimal apoptotic cells were found within the normal group and were only found along the surface.<sup>19</sup> This finding was also present within a rabbit anterior cruciate ligament (ACL) transection model, which found increased apoptotic cells within medial menisci with bucket handle tears.<sup>20</sup> A separate rabbit study performed ACL transections and isolated menisci after 9 weeks. All menisci demonstrated degenerative changes and an increased amount of apoptotic cells within the central portion where the chondrocytic type of cells were present.<sup>21</sup> A third ACL transection study demonstrated an increase in DNA fragmentation associated with an increased number of apoptotic cells in the medial meniscus.<sup>22</sup> One hypothesis on why there is an increased amount of apoptotic cells found within injured tissue is because of the acute/chronic mechanical stresses that cause the disruption of the tissue.<sup>19</sup> This type of mechanical overloading leading to apoptosis, matrix degradation, and the release of pro-inflammatory mediators has been described to occur within cartilage and menisci.<sup>23,24</sup> The role of apoptosis is to remove the damaged cells before the cell contents are released leading to the progression of inflammatory cascades.

In addition to an increased amount of cells undergoing programmed cell death, it has been described that meniscal pathology leads to an increased amount of cellularity. Within pathologic menisci there is a disruption of normal cellular networks which may lead to increased cellularity.<sup>25</sup> A separate study found that an increase in cellularity was more prevalent within younger, non-osteoarthritic, patients that sustained a tear of the meniscus when compared to older patients (>40 years), whom had tears that were degenerative in nature. Interestingly, this study also found an increased amount of DNA fragmentation within tears that had a lower cell density and within tears that had not been

treated for longer periods of time.<sup>9</sup> A separate study contradicts some of these findings by describing a reduction of tissue cellularity within menisci after ACL transection in rabbits. However, it goes on to describe that apoptotic cells were prominent in the degenerated areas of the meniscus along with clusters of chondrocytes, many of which were apoptotic.<sup>21</sup> Needless to say, on a microscopic level it is apparent that apoptosis is a natural progression within meniscal tissue following injury. An increased amount of cellularity may or may not be present, but within these groups of cells, programmed cell death is occurring.

### **Biochemical meniscal changes**

Collagen fibers arranged mainly in a circumferential pattern along with perpendicular radial fibers along the superficial and deep layers are what provide the main biomechanical integrity of the meniscus. Degenerative menisci undergo a change in this pattern leaving the menisci less functional. Osteoarthritic menisci have been shown to have coarser collagen fibers in a less organized fashion. The amount of distinct circumferential and radial fibers appears to be reduced.<sup>25</sup> For degenerative menisci post ACL transection, there has been an association of increased collagen types I, II, and III. All three were found in the peripheral region and associated with increased proteoglycan staining. For the inner avascular portion of the medial meniscus, there was an increased staining for type II collagen.<sup>20</sup> This increase in collagen deposition is associated with a disorganization of fiber orientation that results due to degeneration.

When the meniscus undergoes degeneration, fragmentation of the normal extracellular matrix occurs. Aggrecan is a large proteoglycan that can be isolated as one

of the main proteoglycans within meniscal tissue. When analyzing the ovine menisci, it was identified that the aggrecan concentration was highest in the inner tip at birth and then aggrecan presence increased throughout the rest of the meniscus after 19 months and 10 years of life.<sup>26</sup> Aggrecan concentration within canine meniscal tissue follows the following pattern: medial greater than lateral, inner portions greater than peripheral portions. Aggrecan fragments have been isolated within synovial fluid of osteoarthritic patients, and it has been concluded that since the menisci make up a significant portion of the tissue within the knee, aggrecan presence within synovial fluid could be due to meniscus injury.<sup>27</sup> One study analyzed the G1 fragment of aggrecan utilizing immunohistochemistry (IHC) and correlated the presence of these fragments with grades of meniscal degeneration. For higher grades of degeneration, 48% of the patients were found to have extracellular deposits of this aggrecan fragment. With a lower grade of degradation, no deposits of this fragment were found.<sup>28</sup> One of the small leucine-rich proteoglycans, decorin, was found to be consistently fragmented within osteoarthritic degenerative menisci as well.<sup>29</sup> Interestingly, the gene expression for this proteoglycan within medial and lateral menisci were found to be at significantly lower levels within post ACL transected rabbits when compared to normal.<sup>20</sup> Decorin is the dominant, non-aggregating proteoglycan within menisci and helps to maintain the tissue integrity and strength of the menisci through binding interactions with type I collagen fibrils.<sup>30</sup> The initial “repair” process that the meniscal tissue undergoes post-injury does not appear to involve an increase within decorin production. Instead it is found mainly as breakdown products. In a separate study it was found that glycosaminoglycan (GAG) content will decrease initially following ACL transection but will increase substantially with chronic

ACL insufficiency.<sup>31</sup> The question becomes what specific proteoglycans lead to the increase in GAG content. Along with GAG changes and a looser fibrillar meshwork within menisci, the water content will also change. For degenerative menisci, the water content becomes significantly elevated within the meniscus.<sup>32</sup>

Other proteins that have been associated with degenerative menisci are osteopontin, osteonectin, and alkaline phosphatase. Increased IHC staining for these three proteins has been identified within osteoarthritic menisci when compared to control menisci.<sup>25</sup> These proteins are associated with bone-forming chondrocytes, hypertrophic chondrocytes, and mineralization of the extracellular matrix.<sup>33</sup> The presence of these three components suggests that the meniscal chondrocytic type cells have differentiated into a hypertrophic phenotype.<sup>25</sup> Alkaline phosphatase can result in precipitation of calcium, which has been isolated in areas of increased meniscal degeneration, around hypertrophic chondrocytes, and around apoptotic bodies. Increased levels of alkaline phosphatase activity has also been localized within end stage osteoarthritic cartilage.<sup>34</sup> The presence of these calcium deposits and associated proteins may be a marker of increased meniscal degeneration.

Proteoglycan 4 (lubricin) is found within synovial fluid but is also found along the articular surface within the superficial zone of cartilage and along the femoral and tibial surface of the meniscus along the radial and circumferential fibers. This molecule is associated with lubrication of the joint and has a protective feature due to the fact that it can dissipate strain energy.<sup>35</sup> Lubricin is produced by chondrocytes, synovial cells, and meniscal cells.<sup>36</sup> The progression of osteoarthritis leads to reduced levels of this lubricating glycoprotein. Lubricin was statistically reduced during the early stages of the

osteoarthritic pathway following ACL injury when compared to the contralateral uninjured knee.<sup>37</sup> Another study used an ovine meniscectomy model to induce degenerative changes within the joint. Immunostaining of lubricin within the articular cartilage had dissipated by the three month time point. There was also a significant decrease within the mRNA levels measured.<sup>38</sup> The presence or absence of lubricin within the meniscus was not evaluated in this study since it was a meniscectomy model. However, it can be hypothesized that the levels of lubricin along the meniscal surface will also be reduced when meniscal degeneration occurs.

Physiologically, there is a balance between the production of reactive oxygen species (ROS) through cellular metabolism and the level of endogenous antioxidants needed to protect tissues from oxidative damage. When the production of ROS increases or the level of antioxidants decreases, oxidative stress occurs. The process of forming ROS begins with a one-electron reduction of oxygen to form the superoxide ( $O_2^-$ ), which can go through dismutation to hydrogen peroxide ( $H_2O_2$ ) or react with nitric oxide (NO) producing a toxic product called peroxynitrite ( $ONOO^-$ ). The breakdown product of peroxynitrite can create a highly toxic hydroxyl radical ( $\cdot OH$ ). Excess presence of these ROS will lead to pathophysiologic catastrophes. Superoxide dismutases (SOD) are antioxidants that catalyze the dismutation of two superoxide radicals into oxygen and hydrogen peroxide, hydrogen peroxide can then be removed by glutathione peroxidase or catalase.<sup>39,40</sup> The third SOD isozyme is termed extracellular superoxide dismutase (SOD3), and is the predominant SOD in plasma, synovial fluid, and other extracellular fluids.<sup>41-43</sup> Collagens are targets for oxygen free radicals; hydroxyl radicals can cleave collagen into small peptides.<sup>44</sup> SOD3 binds specifically to type I collagen through the

heparin-binding region and protects it from oxidative fragmentation.<sup>45</sup> Regan et al. obtained human cartilage from cadaver donors younger than 40 (no history of arthritis, no articular cartilage defects), from patients undergoing bipolar joint replacement due to a displaced fracture of the femoral neck (no radiographic signs of arthritis or articular cartilage defects), and from patients undergoing total joint replacement due to osteoarthritis. The OA patients had significantly decreased SOD3 protein levels when compared to the younger and older controls, determined by enzyme-linked immunosorbent assay (ELISA) (four fold lower levels than cartilage from patients with a hip fracture). SOD3 immunolocalization within OA specimens showed a pattern of decreased SOD3 protein in the matrix but increased intracellular staining. OA patients also had increased levels of SOD3 mRNA. Controls had a smooth distribution of staining in the ECM with variable intracellular staining. They postulated that a period of compensation may be present when increased oxidative stress occurs but over time an inadequate production of SOD3 and loss of binding sites for SOD3 prevents this protein from being able to adequately counteract the increase in reactive oxygen species associated with OA. They concluded that an “inadequate control of reactive oxygen species plays a role in the pathophysiology of OA.”<sup>46</sup> The same can be hypothesized for meniscal degeneration and meniscal pathology.

The complement system also plays a role within meniscal degeneration. When analyzing tissue from partial meniscectomies, diffuse C4d deposits can be found in the extracellular matrix in areas where mucoid degeneration or fibrillation is most prevalent. C4d deposits were not found within the avascular extracellular matrix (ECM) for the control group. C4d is the final degradation product after cleavage of the C4 component.

C4d in turn is fairly stable and will bind to the closest protein. The role C4d plays within meniscal degradation is not fully understood but it leads one to believe that the complement cascade may be involved in the process of meniscal pathology.<sup>47</sup>

Many signals and pathways exist and become activated when the body is reacting toward pathologic triggers from a traumatic event, degeneration, inflammation, etc. One pathway that has been identified with the progression of meniscal degeneration is the p38 mitogen-activated protein kinase (MAPK) signal transduction pathway. Meniscal cell receptors may respond to outside inflammatory mediators by triggering the p38 cascade: phosphorylation of p38 leads to phosphorylation of the inhibitor of nuclear factor of kappa light polypeptide gene enhancer in B cells (NF-κB) → the inhibitor will undergo poly-ubiquitination and degradation → this releases NF-κB and allows it to enter the nucleus → promotes the transcription of inflammatory genes such as tumor necrosis factor alpha (TNF-α), interleukin 1 beta (IL-1β), IL-6, IL-8, and cyclooxygenase (COX). IHC has been utilized to identify the presence of p38 within the cytoplasm and nucleus of meniscal cells after they had been torn; the level was significantly higher in degenerated menisci when compared to non-degenerated. This increased amount of p38 in degenerative menisci also correlated with the increase of NF-κB.<sup>48</sup> This pathway may play a significant role in the degenerative process of a meniscus after it sustains a tear.

### **Molecular meniscal changes**

The central and peripheral regions of the meniscus differ with respect to vascularity and they differ with respect to ECM production. The peripheral region is vascular and has a more fibroblastic phenotype when compared to the avascular, more

chondrocytic phenotype of the central meniscus. Because of the difference in “phenotype” one would also expect a difference in gene expression when tissue is injured. For the unaltered state, the central region has a higher gene expression for collagen II and aggrecan; but, it has a lower expression for collagen I when compared to the outer region.<sup>49,50</sup> When an injury to the avascular zone of the meniscus occurs, it can be hypothesized that an increase in these genes will be present with the premise of trying to repair the injured tissue. This was represented when an ACL transected rabbit study was able to show an increase in type II collagen and aggrecan gene expression within the inner portion of the meniscus after sustaining bucket handle tears.<sup>20</sup> A different study looked at collagen I and VI gene expression for the entire meniscus post ACL transection. Both were shown to be at significantly increased levels when compared to the control. Collagen VI has been associated with remodeling and may help with meniscal cell movement and anchorage along with helping to organize the newly formed ECM.<sup>51</sup> Hellio Le Graverand conducted gene expression analyses for a number of mRNAs in order to identify differences in the meniscus post ACL transection. This study looked at the expression levels for the meniscus as a whole instead of separating out the central and peripheral regions. In both menisci at 3 and 8 weeks, the following mRNA levels were significantly increased compared to the control group: collagen I and tissue inhibitor of metalloproteinase 1 (TIMP-1). The following were decreased at 3 and 8 weeks: decorin, TNF- $\alpha$ , insulin-like growth factor 2 (IGF-2). For the medial meniscus alone, type II collagen, biglycan, inducible nitric oxide synthase (iNOS), and plasminogen activator inhibitor type 1 (PAI-1) were increased at both time points; type III collagen, aggrecan, and COX-2 were increased at 3 weeks; matrix

metalloproteinase 1 (MMP-1) was increased at 8 weeks. For the lateral meniscus alone, type III collagen was increased at 3 weeks, fibromodulin was decreased at 3 weeks, and biglycan was increased at 8 weeks.<sup>22</sup> This study was able to demonstrate that a complex array of molecular alterations will occur after the transection of an ACL as the meniscus is trying to cope with the deteriorating inflammatory and mechanical environment.

In addition to the extracellular matrix being altered during meniscal pathological changes, the degree of catabolic activity will also be affected. When meniscal explants were stressed with a 20% dynamic compressive strain there was an increased release of GAG content and nitric oxide (NO) into culture media along with an up regulation of IL-1.<sup>52,53</sup> Zielinska et al wanted to evaluate two different strain patterns to see what the difference would be with respect to catabolic gene expression. A lower 10% dynamic compressive strain revealed significant increases in aggrecan, COX-2, and a disintegrin and metalloproteinase with thrombospondin motifs 5 (ADAMTS-5) gene expression. When increasing this dynamic strain to 20%, additional catabolic genes were expressed at increased levels when compared to no dynamic loading: MMP-1, MMP-3, MMP-13, and ADAMTS-4.<sup>24</sup> The level of 20% axial strains correlates with the strain levels that occur after 30% of the meniscus is removed.<sup>12</sup> When a partial meniscectomy occurs, increased stresses will occur causing the production of catabolic enzymes. These enzymes in turn cause matrix degradation and fragmentation.<sup>24</sup> This finding correlates with the increased amount of aggrecan and decorin fragments that occur during meniscal pathology as described in previous reports. A separate study analyzed the production of catabolic enzymes by meniscal explants following TNF- $\alpha$  induction. There was increased production of MMP-3 and ADAMTS-4; decreased production of type I collagen,

aggrecan, and type II collagen; and variable expression of MMP-1, MMP-2, MMP-13, and ADAMTS-5. An increase in GAG release, aggrecan neoepitope NITEGE, and NO production also occurred. Interestingly, when TIMP-3 was added, this decreased the GAG release and NITEGE production.<sup>54</sup> An in vivo rat ACL rupture model also revealed an increase in catabolic gene expression within intra-articular joint tissues. MMP-2, MMP-13, CD147 (extracellular matrix metalloproteinase inducer), along with TIMP-1 were elevated within the meniscus, cartilage, ACL, posterior cruciate ligament (PCL), and synovium.<sup>55</sup> The increased presence of catabolic proteins due to abnormal joint stresses, amplified inflammatory markers, and mechanical injury will cause a cascade of degradation for all tissues within the joint.

For normal menisci, inducible nitric oxide synthase has been shown to be expressed at higher levels within the central region when compared to the peripheral region.<sup>49,50</sup> When pathological events invoke changes to the central avascular meniscus, an increased level of inducible nitric oxide synthase will likely be present and contribute to the cascade of destructive events. A study by Kobayashi et al was able to confirm this hypothesis. They performed partial medial meniscectomies within rabbits and then measured NO production, gene expression of iNOS, IHC staining for nitrotyrosine (marker for peroxynitrite-mediated NO action in vivo), and the presence of apoptotic cells within the peripheral and central zones of the meniscus and articular cartilage. It was determined that all four were at higher levels within the central region of the medial meniscus, and within articular cartilage.<sup>56</sup> Hashimoto et al performed a similar study except they analyzed degenerative menisci post ACL transection. The media from meniscal cultures had elevated nitrite levels, nitrotyrosine was prominent within the

meniscal tissue, and a high number of apoptotic cells were present in the medial portion of the meniscus.<sup>21</sup> These studies help to confirm the production of nitric oxide by inducible nitric oxide synthase within the central region of the meniscus after injury. It also shows that NO will have a negative effect on tissue by reacting with superoxides to form peroxynitrite which causes the formation of nitrotyrosines (product of tyrosine nitration). Lastly, it demonstrated the role it plays with induction of apoptosis at the injury site.

## **Conclusion**

The meniscus is a complex structure containing regional variances with respect to cellular morphology and function along with extracellular composition and structure. Even though a great deal of work has been conducted attempting to characterize the meniscus, there remains many unanswered questions. This is especially evident when analyzing meniscal treatment options which are fairly rudimentary when compared to other pathologies treated within the body. When menisci are torn and undergo degeneration, the majority of cases undergo limited resection, small percentages are repaired, and even smaller percentages are replaced. In order to build upon the treatment algorithm of meniscal pathology, additional work is necessary to more fully understand the disease progression that occurs after the meniscus is initially disrupted.

**Figure 2-1: Axial view of medial and lateral meniscus.<sup>1</sup>**

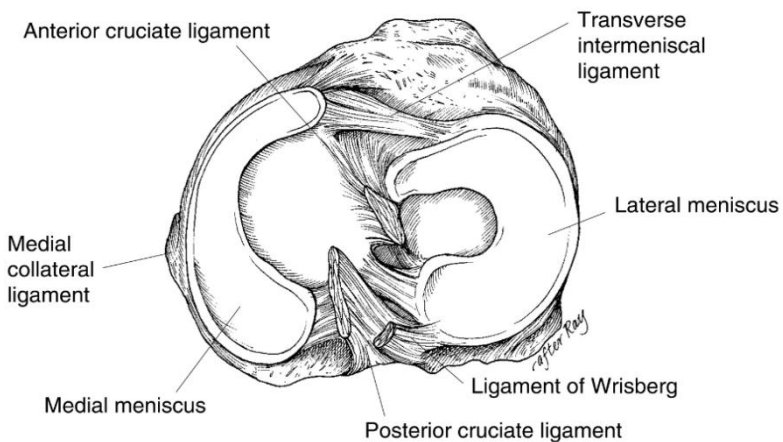


**Figure 2-2: Coronal section of the knee depicting vascular branches into the peripheral border of the medial meniscus.<sup>57</sup>**

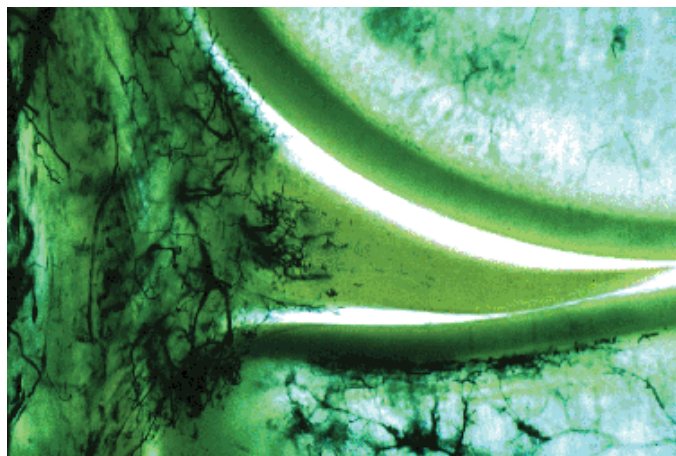
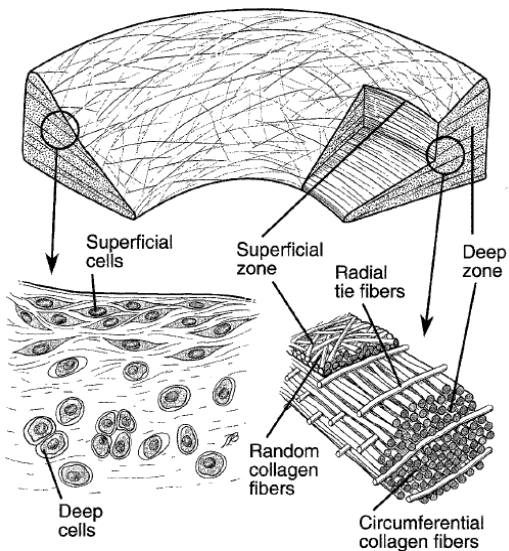


**Figure 2-3: Meniscal collagen ultrastructure.<sup>13</sup>**



## References

1. Renstrom P, Johnson RJ. Anatomy and biochechanics of the menisci. *Clinics in Sports Medicine*. 1990;9(3):523-538.
2. Clark CR, Ogden JA. Development of the menisci of the human knee joint. Morphological changes and their potential role in childhood meniscal injury. *Journal of Bone and Joint Surgery - Series A*. 1983;65(4):538-547.
3. Andersson-Molina H, Karlsson H, Rockborn P. Arthroscopic partial and total meniscectomy: A long-term follow-up study with matched controls. *Arthroscopy*. 2002;18(2):183-189.
4. Chatain F, Robinson AHN, Adeleine P, Chambat P, Neyret P. The natural history of the knee following arthroscopic medial meniscectomy. *Knee Surgery, Sports Traumatology, Arthroscopy*. 2001;9(1):15-18.
5. Bonneux I, Vandekerckhove B. Arthroscopic partial lateral meniscectomy long-term results in athletes. *Acta Orthopaedica Belgica*. 2002;68(4):356-361.
6. Berjon JJ, Munuera L, Calvo M. Degenerative lesions in the articular cartilage after meniscectomy: Preliminary experimental study in dogs. *Journal of Trauma*. 1991;31(3):342-350.
7. Wyland DJ, Guilak F, Elliott DM, Setton LA, Vail TP. Chondropathy after meniscal tear or partial meniscectomy in a canine model. *Journal of Orthopaedic Research*. 2002;20(5):996-1002.
8. Cicuttini FM, Forbes A, Yuanyuan W, Rush G, Stuckey SL. Rate of knee cartilage loss after partial meniscectomy. *Journal of Rheumatology*. 2002;29(9):1954-1956.
9. Mesih M, Zurakowski D, Soriano J, Nielson JH, Zarins B, Murray MM. Pathologic characteristics of the torn human meniscus. *American Journal of Sports Medicine*. 2007;35(1):103-112.
10. Hede A, Svalastoga E, Reimann I. Articular cartilage changes following meniscal lesions. Repair and meniscectomy studied in the rabbit knee. *Acta Orthopaedica Scandinavica*. 1991;62(4):319-322.
11. Cole BJ, Carter TR, Rodeo SA. Allograft meniscal transplantation: Background, techniques and results. *Journal of Bone and Joint Surgery - Series A*. 2002;84(7):1236-1250.

12. Zielinska B, Haut Donahue TL. 3D finite element model of meniscectomy: Changes in joint contact behavior. *Journal of Biomechanical Engineering*. 2006;128(1):115-123.
13. Kawamura S, Lotito K, Rodeo SA. Biomechanics and healing response of the meniscus. *Operative Techniques in Sports Medicine*. 2003;11(2):68-76.
14. Thieman KM, Pozzi A, Ling H, Lewis D. Comparison of contact mechanics of three meniscal repair techniques and partial meniscectomy in cadaveric dog stifles. *Veterinary Surgery*. 2010; 39(3):355-362.
15. Baratz ME, Fu FH, Mengato R. Meniscal tears: the effect of meniscectomy and of repair on intraarticular contact areas and stress in the human knee. A preliminary report. *American Journal of Sports Medicine*. Jul-Aug 1986;14(4):270-275.
16. Vaziri A, Nayeb-Hashemi H, Singh A, Tafti BA. Influence of Meniscectomy and Meniscus Replacement on the Stress Distribution in Human Knee Joint. *Annals of Biomedical Engineering*. 2008;36(8):1335-1344.
17. Arnoczky SP, Warren RF. The microvasculature of the meniscus and its response to injury. An experimental study in the dog. *American Journal of Sports Medicine*. 1983;11(3):131-141.
18. Kobayashi K, Fujimoto E, Deie M, Sumen Y, Ikuta Y, Ochi M. Regional differences in the healing potential of the meniscus - An organ culture model to eliminate the influence of microvasculature and the synovium. *Knee*. 2004;11(4):271-278.
19. Uysal M, Akpinar S, Bolat F, et al. Apoptosis in the traumatic and degenerative tears of human meniscus. *Knee Surgery, Sports Traumatology, Arthroscopy*. Jul 2008;16(7):666-669.
20. Hellio Le Graverand MP, Vignon E, Otterness IG, Hart DA. Early changes in canine menisci during osteoarthritis development: Part I: Cellular and matrix alterations. *Osteoarthritis and Cartilage*. 2001;9(1):56-64.
21. Hashimoto S, Takahashi K, Ochs RL, Coutts RD, Amiel D, Lotz M. Nitric oxide production and apoptosis in cells of the meniscus during experimental osteoarthritis. *Arthritis & Rheumatism*. Oct 1999;42(10):2123-2131.
22. Hellio Le Graverand MP, Vignon E, Otterness IG, Hart DA. Early changes in canine menisci during osteoarthritis development: Part II: molecular alterations. *Osteoarthritis & Cartilage*. Jan 2001;9(1):65-72.

23. Wang P, Zhu F, Lee NH, Konstantopoulos K. Shear-induced interleukin-6 synthesis in chondrocytes: Roles of E prostanoid (EP) 2 and EP3 in cAMP/protein kinase A- and PI3-K/Akt-dependent NF-kappaB activation. *Journal of Biological Chemistry*. 285(32):24793-24804.
24. Zielinska B, Killian M, Kadmiel M, Nelsen M, Haut Donahue TL. Meniscal tissue explants response depends on level of dynamic compressive strain. *Osteoarthritis & Cartilage*. Jun 2009;17(6):754-760.
25. Syal M, Goyal N, Nagi ON, Gupta M. Immunohistochemistry of osteoarthritic meniscus in man. *Bulletin, Postgraduate Institute of Medical Education and Research, Chandigarh*. 2007;41(1):11-16.
26. Melrose J, Smith S, Cake M, et al. Comparative spatial and temporal localisation of perlecan, aggrecan and type I, II and IV collagen in the ovine meniscus: an ageing study. *Histochemistry & Cell Biology*. Sep 2005;124(3-4):225-235.
27. Valiyaveettil M, Mort JS, McDevitt CA, Valiyaveettil M, Mort JS, McDevitt CA. The concentration, gene expression, and spatial distribution of aggrecan in canine articular cartilage, meniscus, and anterior and posterior cruciate ligaments: a new molecular distinction between hyaline cartilage and fibrocartilage in the knee joint. *Connective Tissue Research*. 2005;46(2):83-91.
28. Krenn V, Kurz B, Krukemeyer MG, et al. Histopathological degeneration score of fibrous cartilage: Low- and high-grade meniscal degeneration. *Histopathologischer degenerations-score des faserknorpels: Low-grade- und high-grade-meniskusdegeneration*. 69(7):644-652.
29. Melrose J, Fuller ES, Roughley PJ, et al. Fragmentation of decorin, biglycan, lumican and keratan can is elevated in degenerate human meniscus, knee and hip articular cartilages compared with age-matched macroscopically normal and control tissues. *Arthritis Research & Therapy*. 2008;10(4):R79.
30. Roughley PJ, White RJ. The dermatan sulfate proteoglycans of the adult human meniscus. *Journal of Orthopaedic Research*. Sep 1992;10(5):631-637.
31. Adams ME, Billingham MEJ, Muir H. The glycosaminoglycans in menisci in experimental and natural osteoarthritis. *Arthritis and Rheumatism*. 1983;26(1):69-76.
32. Herwig J, Egner E, Buddecke E. Chemical changes of human knee joint menisci in various stages of degeneration. *Annals of the Rheumatic Diseases*. 1984;43(4):635-640.

33. Nakase T, Takaoka K, Hirakawa K, et al. Alterations in the expression of osteonectin, osteopontin and osteocalcin mRNAs during the development of skeletal tissues in vivo. *Bone & Mineral*. Aug 1994;26(2):109-122.
34. Rees JA, Ali SY. Ultrastructural localisation of alkaline phosphatase activity in osteoarthritic human articular cartilage. *Annals of the Rheumatic Diseases*. Sep 1988;47(9):747-753.
35. Jay GD, Torres JR, Warman ML, Laderer MC, Breuer KS. The role of lubricin in the mechanical behavior of synovial fluid. *Proceedings of the National Academy of Sciences of the United States of America*. 2007;104(15):6194-6199.
36. Schumacher BL, Schmidt TA, Voegtline MS, Chen AC, Sah RL. Proteoglycan 4 (PRG4) synthesis and immunolocalization in bovine meniscus. *Journal of Orthopaedic Research*. 2005;23(3):562-568.
37. Elsaid KA, Fleming BC, Oksendahl HL, et al. Decreased lubricin concentrations and markers of joint inflammation in the synovial fluid of patients with anterior cruciate ligament injury. *Arthritis and Rheumatism*. 2008;58(6):1707-1715.
38. Young AA, McLennan S, Smith MM, et al. Proteoglycan 4 downregulation in a sheep meniscectomy model of early osteoarthritis. *Arthritis Research and Therapy*. 2006;8(2).
39. Fattman CL, Schaefer LM, Oury TD. Extracellular superoxide dismutase in biology and medicine. *Free Radical Biology and Medicine*. 2003;35(3):236-256.
40. Afonso V, Champy R, Mitrovic D, Collin P, Lomri A. Reactive oxygen species and superoxide dismutases: role in joint diseases. *Joint, Bone, Spine: Revue du Rhumatisme*. 2007;74(4):324-329.
41. Marklund SL. Human copper-containing superoxide dismutase of high molecular weight. *Proceedings of the National Academy of Sciences of the United States of America*. 1982;79(24 I):7634-7638.
42. Marklund SL, Bjelle A, Elmquist LG. Superoxide dismutase isoenzymes of the synovial fluid in rheumatoid arthritis and in reactive arthritides. *Annals of the Rheumatic Diseases*. 1986;45(10):847-851.
43. Marklund SL, Holme E, Hellner L. Superoxide dismutase in extracellular fluids. *Clinica Chimica Acta*. 1982;126(1):41-51.
44. Monboisse JC, Borel JP. Oxidative damage to collagen. *EXS*. 1992;62:323-327.

45. Petersen SV, Oury TD, Ostergaard L, et al. Extracellular Superoxide Dismutase (EC-SOD) Binds to Type I Collagen and Protects Against Oxidative Fragmentation. *Journal of Biological Chemistry*. 2004;279(14):13705-13710.
46. Regan E, Flannelly J, Bowler R, et al. Extracellular superoxide dismutase and oxidant damage in osteoarthritis. *Arthritis and Rheumatism*. 2005;52(11):3479-3491.
47. Dankof A, Krenn V, Dankof A, Krenn V. C4d deposits mark sites of meniscal tissue disintegration. *Virchows Archiv*. Aug 2006;449(2):230-233.
48. Papachristou DJ, Papadakou E, Basdra EK, et al. Involvement of the p38 MAPK-NF-kappaB signal transduction pathway and COX-2 in the pathobiology of meniscus degeneration in humans. *Molecular Medicine*. Mar-Apr 2008;14(3-4):160-166.
49. Upton ML, Hennerbichler A, Fermor B, et al. Biaxial strain effects on cells from the inner and outer regions of the meniscus. *Connective Tissue Research*. 2006;47(4):207-214.
50. Upton ML, Chen J, Setton LA, Upton ML, Chen J, Setton LA. Region-specific constitutive gene expression in the adult porcine meniscus. *Journal of Orthopaedic Research*. Jul 2006;24(7):1562-1570.
51. Wildey GM, Billetz AC, Matyas JR, Adams ME, McDevitt CA. Absolute concentrations of mRNA for type I and type VI collagen in the canine meniscus in normal and ACL-deficient knee joints obtained by RNase protection assay. *Journal of Orthopaedic Research*. 2001;19(4):650-658.
52. McHenry JA, Zielinska B, Donahue TL, Zielinska B, Donahue TLH. Proteoglycan breakdown of meniscal explants following dynamic compression using a novel bioreactor. *Annals of Biomedical Engineering*. Nov 2006;34(11):1758-1766.
53. Gupta T, Zielinska B, McHenry J, Kadmiel M, Haut Donahue TL. IL-1 and iNOS gene expression and NO synthesis in the superior region of meniscal explants are dependent on the magnitude of compressive strains. *Osteoarthritis & Cartilage*. Oct 2008;16(10):1213-1219.
54. Voigt H, Lemke AK, Mentlein R, Schunke M, Kurz B. Tumor necrosis factor alpha-dependent aggrecan cleavage and release of glycosaminoglycans in the meniscus is mediated by nitrous oxide-independent aggrecanase activity in vitro. *Arthritis Research & Therapy*. 2009;11(5).

55. Tang Z, Yang L, Zhang J, et al. Coordinated expression of MMPs and TIMPs in rat knee intra-articular tissues after ACL injury. *Connective Tissue Research*. 2009;50(5):315-322.
56. Kobayashi K, Mishima H, Hashimoto S, et al. Chondrocyte apoptosis and regional differential expression of nitric oxide in the medial meniscus following partial meniscectomy. *Journal of Orthopaedic Research*. 2001;19(5):802-808.
57. Arnoczky SP, Warren RF. Microvasculature of the human meniscus. *American Journal of Sports Medicine*. 1982;10(2):90-95.

CHAPTER 3:  
CHARACTERIZATION OF KNEE MENISCAL PATHOLOGY:  
CORRELATION OF GROSS, HISTOLOGIC, BIOCHEMICAL, MOLECULAR,  
AND RADIOGRAPHIC MEASURES OF DISEASE

**Experimental purpose and hypothesis**

Knee menisci are exposed to multiple stresses during daily activities of living. When its fibrocartilaginous structure is altered or damaged, an impediment of its necessary functions will ultimately lead to joint disability caused by osteoarthritis.<sup>1-9</sup> Multiple studies have been conducted analyzing the pathological events that take place within a meniscus after it has been injured; however, there is still much to learn about this complex tissue. The initial step is working to gather critical data that identifies key differences between normal menisci and menisci associated with osteoarthritis.

The overall goal of this study was to comprehensively characterize multiple aspects of meniscal pathology in the presence of OA and correlate clinical and basic science data in pursuit of finding clinically relevant answers for this common problem in people. Toward this goal, the specific aims for this project were: Specific Aim 1: Characterize and correlate the biochemical and molecular markers of OA meniscal disease to gross, histologic, and potential radiographic indicators of meniscal pathology in the human knee, and Specific Aim 2: Delineate which indicators of meniscal pathology are most useful for optimizing diagnostic, therapeutic, and prognostic strategies. Our hypothesis was that patients with OA meniscal disease will have significant differences in protein and molecular markers of extracellular matrix synthesis, degradation, and signaling when compared to age-matched controls, and that these markers will correlate

to gross, histologic, and radiographic measures of meniscal pathology, thereby serving as definitive indicators of disease presence and severity.

## **Materials and methods**

### *Tissue collection, gross evaluation, and tissue storage:*

All procedures were approved by the Institutional Review Board (IRB#1042248) and informed patient consent was obtained before tissue collection. For the pathologic study group, tissue that normally would be discarded during a total knee arthroplasty (TKA) was retrieved. A subjective scoring system was employed for assessing gross pathology at the time of collection. One score was given to the entire meniscus based off the following scoring system: 0 – normal; 1 – all 3 zones present, minimal gross pathology, near-normal shape and size; 2 – all 3 zones present, shape and/or size markedly altered; 3 – 1 or more zones missing due to tissue destruction.

For the Control group, meniscal tissue was obtained from age-matched “normal” cadaveric or above-the-knee amputation specimens. Before the Control menisci were recovered, the joint was assessed to ensure there was grade 1 or less articular cartilage pathology and that there were no osteophytes present. The menisci were then recovered and examined to ensure they were grossly normal. Each meniscus was obtained and stored within 24 hours of death or amputation. This time limit was established in order to prevent excessive degradation of RNA; tissue is stable for 48-96 hours postmortem and postoperatively.<sup>10-12</sup>

After retrieval and transport to the laboratory, each meniscus (medial and lateral) was separated into anterior, medial (body), and posterior sections. Each section was then

further divided into 3 portions for assessment. The sections were divided in a vertical plane allowing for inclusion of the red-red, red-white, and white-white zone for each piece of tissue. The first portion was stored in a 10% formalin solution for subsequent histological examination, the second portion was weighed (wet weight) and stored at -80°C for subsequent biochemical analysis, the third portion was placed within 1 mL of RNAlater® and stored at -80°C for subsequent molecular analysis.

*Histologic evaluation:*

The portion of tissue that was identified for histologic analysis was cut into 5-micron sections and processed routinely for histologic staining. One section was stained with hematoxylin and eosin (H&E). A second section was stained with safranin-O fast green (Saf-O). An additional three sections were cut and stored unstained. Each H&E and Saf-O section was subjectively assessed by one investigator blinded to sample group or number using a scoring system developed specifically for meniscal tissue based on three important categories: (1) Tissue architecture – tissue loss; (2) Cell and matrix (proteoglycan and collagen) content and morphology; and (3) Proliferative response (Figure 3-1).

*Biochemical evaluation:*

The portion that was stored for biochemical analysis was lyophilized and then weighed to obtain its dry weight. The water content was then calculated using the following formula:

$$\text{Water content (\%)} = [(\text{Wet weight} - \text{Dry weight}) / \text{Wet weight}] \times 100$$

The dried tissues were then digested overnight at 60°C in 1 ml of papain digestion solution. The papain solution was created by mixing 2 mM Dithiothreitol, 300 µg/ml papain (14 U/mg; Sigma Chemical Co., St. Louis, MO), and papain solution buffer [20 mM Sodium phosphate (pH 6.8) (0.24 g for 100 ml) plus 1 mM EDTA (0.0372 g for 100 ml)]. The solution was incubated for 10 min at 60°C before use. For tissues that did not fully digest with 1 ml of digestion solution, the remaining tissue was put in another 1 ml of digestion solution and allowed to digest further. Once digestion was complete, the tissue samples were stored at -20°C until subsequent biochemical assays were performed. The final digest was used to determine the glycosaminoglycan content (GAG) and hydroxyproline (HP) content of the tissues. The GAG content of the tissues, which indicates the total proteoglycan content of the tissues, was determined using the DMMB assay (as described below) and reported as µg GAG/mg tissue dry weight. The HP content of the tissues, indicative of the total collagen content of the tissues, was determined by the HP assay (as described below) and reported as µg HP/mg tissue dry weight.

Total sulfated glycosaminoglycan (GAG) content was quantified by 1-9-dimethylmethylene blue (DMMB) spectrophotometric analysis.<sup>13</sup> The GAG concentration was able to be calculated via a standard curve created with serial dilutions of a known concentration of bovine tracheal chondroitin sulfate A (Sigma Chemical Co., St. Louis, MO). A 5 µl aliquot of each standard was mixed with 245 µl of DMMB solution and a 5 µl aliquot of each sample digest solution was mixed with 245 µl of DMMB solution. Absorbance at 525 nm was then determined spectrophotometrically (Beckman DU-65 spectrophotometer, Beckman Instruments, Inc., Fullerton, CA).

Total collagen content in meniscal tissue was evaluated by determination of the hydroxyproline (HP) content using a previously described colorimetric procedure.<sup>14</sup> Commercially available HP (Sigma, St. Louis, MO) was used to generate the standard curve from which the tissue sample HP was calculated. A 50 µl aliquot of each standard and each sample media (meniscal papain digest) was gently mixed with 50 µl of 4 N sodium hydroxide in a 1.2 ml deep-well 96-well polypropylene plate. Each plate was then covered with a silicon sealing mat and a polypropylene cover; then the plates were stacked and sealed by compression via a C-Clamp. The samples were then hydrolyzed by autoclaving at 120°C for 20 min. The hydrolyzate was gently mixed with 450 µl of chloramine T reagent and oxidation was allowed to proceed for 25 minutes at room temperature. Next, 450 µl of Ehrlich's aldehyde reagent was added to each sample, mixed gently, and incubated at 65°C for 20 minutes to allow chromophore development. Absorbance of each sample at 550 nm was determined spectrophotometrically and HP content of explants calculated. HP content determined from this method is provided at a 1:10 dilution, so each value obtained was multiplied by a factor of ten to obtain the final value.<sup>15,16</sup>

*Molecular evaluation:*

RNA was extracted from the portion that was stored for molecular analysis utilizing the TriSpin method. Tissue samples were snap frozen utilizing liquid nitrogen, placed into a cyrocrusher (also cooled in liquid nitrogen), then crushed into a fine powder. The tissue powder was then transferred into a 2 ml o-ring screw cap microcentrifuge tube, which contained three 1.0 mm steel beads and 1 ml of Trizol

(Invitrogen, Carlsbad, CA). The microcentrifuge tube was placed within a mini-bead beater (BioSpec Products, Bartlesville, OK) and ran for 2 minutes at 5000 RPM. The Trizol was transferred to an empty 1.5 ml tube, 1 ml of fresh Trizol was added to the o-ring tube and ran through the beater again; this amount of Trizol was then transferred to a second empty 1.5 ml tube. A 200  $\mu$ l aliquot of Chloroform was added to each homogenate, mixed with a vortex, and then allowed to sit at room temperature for 2 minutes. The samples were centrifuged for 15 minutes at 10000 RPM; the upper aqueous phase was transferred to a new empty 1.5 ml tube (two per sample). A 1  $\mu$ l aliquot of Linear Acrylamide and 500  $\mu$ l of 100% Isopropanol was added to each sample, mixed via vortex, and let stand at room temperature for 10 minutes. The samples were centrifuged for 15 minutes at 10000 RPM, the supernatant was poured off, samples were briefly centrifuged again, and then the remaining supernatant was pipetted off. A 50  $\mu$ l aliquot of RNase free water was added to each sample, next the sample pairs were combined into one tube. A 350  $\mu$ l aliquot of RLT buffer (Qiagen, Valencia, CA) and a 250  $\mu$ l aliquot of 100% Ethanol were added to each sample. The solution was mixed by pipetting, then transferred to an RNeasy MinElute extraction column (Qiagen, Valencia, CA), centrifuged for 20 seconds at 12000 RPM, and the flow through was discarded. The column was transferred to a new collection tube, 500  $\mu$ l RPE buffer was added to the column, centrifuged at 12000 RPM for 20 seconds, and the flow through was discarded again. A 500  $\mu$ l aliquot of 80% ethanol was added to the column and centrifuged for 2 minutes at 12000 RPM, the flow through was discarded, the caps were left open, then centrifuged for another 5 minutes at 12000 RPM. The columns were transferred to a new empty 1.5 ml tube, 14  $\mu$ l of RNase free water was added to the column and centrifuged

for 1 minute at 12000 RPM. The column was discarded and the tube with RNA and RNase free water was treated for DNA contamination via a Turbo DNA-free kit (Ambion, Austin, TX) according to the manufacture's recommendations. A 1.4  $\mu$ l (0.1 volume of RNA) amount of 10X Turbo DNase Buffer and 1  $\mu$ l Turbo DNase was added to the RNA, mixed gently, then incubated for 30 minutes at 37°C. A 1.4  $\mu$ l (0.1 volume of RNA) amount of resuspended DNase inactivation reagent was added, mixed, and allowed to incubate at room temperature for 5 minutes. The solution was centrifuged at 10000 RPM for 1.5 minutes and the supernatant containing mRNA was transferred to a new RNase-free tube and stored at -80°C until ready to proceed.

Before the RNA was reverse transcribed to cDNA, 1  $\mu$ l of each sample was added to 99  $\mu$ l of TE buffer (pH 7.8) and utilized for determination of RNA concentration using a RiboGreen® RNA Quantization Kit. Each sample was mixed with 100  $\mu$ l of the ribogreen dye diluted 1:2000 in TE buffer and RNA concentration was determined by UV spectrophotometry utilizing an internal standard. Next, 500 ng of total RNA from each sample was reverse transcribed to cDNA using an oligo d(T) primer and the Stratascript reverse transcriptase (Stratagene, La Jolla, CA). The 500 ng of sample RNA was mixed with DEPC water and 10 pM of random primers (Integrated DNA Technologies, Coralville, CA) to a final volume of 16  $\mu$ l, incubated at 68°C for 5 minutes, then placed on ice for 3 minutes. A reaction mixture consisting of 1  $\mu$ l Stratascript® enzyme, 1  $\mu$ l 10 mM dNTPs (Promega, Madison, WI), and 2  $\mu$ l 10X Stratascript® buffer was added to each sample to bring the total volume to 20  $\mu$ l. The sample reaction was incubated for 90 minutes at 45°C then held at 4°C utilizing a PE GeneAmp 9700 (Applied Biosystems, Foster City, CA). The sample of cDNA was then

diluted to 200 µl using RNase free water and stored at -20°C until utilization for real-time polymerase chain reaction (PCR).

Real-time PCR was performed using the QuantiTect SYBR green PCR kit (Qiagen, Valencia, CA) and a Rotor-Gene RG-3000 (Corbett Research, Sydney, Australia). Each reaction mixture consisted of 4 µl diluted sample cDNA, 4 µl RNase free water, 10 µl 2X QuantiTect SYBR Green master mix, 1 µl forward primer, 1 µl reverse primer and 0.1 µl HK-UNG. The PCR profile for each test went through an initial incubation of 94°C for 15 minutes followed by 55 cycles of melting (5 seconds at 94°C), annealing (10 seconds at 57°C), and extension (15 seconds at 72°C). The crossing point (C<sub>t</sub>), PCR amplification efficiency, and melt curve analysis was performed to validate the PCR data using the Rotor-Gene software. Each sample was analyzed in duplicate and relative levels of gene expression were determined using Q-Gene.<sup>17</sup> Genes reported to be important in health and disease of meniscal tissue were identified for gene expression analysis. Real time PCR analysis was conducted for genes involved in synthesis (collagens (Col) 1, 2, 3, and 6), degradation (matrix metalloproteinases (MMP-1, -2, -3, -13)), and signaling (vascular endothelial growth factor (VEGF)) using a housekeeping gene ( $\beta$ -actin) as a standard.

*Radiographic evaluation:*

Epidemiologic data, clinical examination findings, radiographs, surgery reports and images, and information regarding outcomes were obtained from chart reviews of patients that underwent TKA. Weight-bearing, anterior-posterior radiographic views were used to determine joint space measurements for the lateral and medial

compartments.<sup>18</sup> Subjective scoring for amount and severity of radiographic OA changes were performed by one investigator (board certified musculoskeletal radiologist), in blinded fashion, as a clinical measure of disease severity.<sup>6,19-21</sup> The radiographic scoring system utilized was the Modified Kellgren and Lawrence grading scale and it was applied to the medial and lateral compartments separately.<sup>19</sup> A total medial and lateral radiographic score was obtained by summing the individual scores for each compartment and was utilized for statistical analysis (if the tibial spines had osteophytes this was applied to the medial and lateral total score).

Osteophytes:

- 0 = none
- 1 = small (definite) osteophyte(s)
- 2 = moderate osteophyte(s)
- 3 = large osteophyte(s)

Narrowing:

- 0 = normal (none)
- 1 = minimal but definite narrowing
- 2 = moderate
- 3 = severe, “bone on bone”

Sclerosis:

- 0 = no sclerosis
- 1 = definite subchondral sclerosis

Chondrocalcinosis:

- 0 = absent
- 1 = present

Osteophytes of tibial spines:

- 0 = normal
- 1 = sharpened spines

Radiographs were not accessible for the Controls. Due to gross evaluation of these joints showing no meniscal or articular cartilage pathology or osteophytosis, it was

presumed the radiographic score for each category would be zero. Joint space measurements were not included for Control specimens.

*Statistical evaluation:*

Statistical analyses were performed using a commercially available software package (SigmaPlot 11.0, Systat Software Inc., San Jose, CA USA). Descriptive statistics (e.g., means and standard deviation) were calculated for each quantitative outcome measure. Relative levels of gene expression were determined using Q-Gene with the housekeeping gene  $\beta$ -actin serving as an internal standard.<sup>17</sup> Data were compared for statistically significant differences using ANOVA or t-test (continuous data) or Mann-Whitney rank sum test (categorical data or when not normally distributed). Outcome measures were compared to determine the presence and strength of correlations using a Pearson Product Moment test or Spearman Rank Order test (when not normally distributed). Correlation values were considered strong if the r value was above 0.6, moderately strong if the r value was between 0.4 and 0.6, and relatively weak if the r value was between 0.2 and 0.4. Significance was set at  $p < 0.05$ .

## **Results**

Twenty-three patients undergoing either a single or bilateral TKA were enrolled in the study. The affected TKA patients in this study had a mean age of 60.2 years with a range of 36-81 years. This amounted to twenty-seven knees, 14 right and 13 left. Six age-matched knees were collected and used as Controls. Tissue from five of the knees were obtained from three patients that were deceased, but had been ambulatory before

perishing. For one of these patients only one knee was utilized for tissue collection due to the other knee containing small osteophytes and some articular cartilage degeneration even though the menisci were “normal” in appearance. The sixth knee that was utilized was obtained from a patient that sustained acute limb ischemia requiring an above-the-knee amputation. The mean age for the Controls was 77 years with a range of 64-87 years. Of the six Control knees, 3 were right and 3 were left.

*Gross evaluation (Table 3-1):*

OA menisci had significantly higher gross pathology scores compared to Control menisci (Overall:  $1.88 \pm 0.69$  vs.  $0.08 \pm 0.28$ ,  $p<0.001$ ) (Medial:  $2.21 \pm 0.6$  vs.  $0.17 \pm 0.38$ ,  $p<0.001$ ) (Lateral:  $1.57 \pm 0.64$  vs.  $0.0 \pm 0.0$ ,  $p<0.001$ ). For OA menisci, medial menisci had significantly higher gross pathology scores compared to lateral menisci ( $2.21 \pm 0.6$  vs.  $1.57 \pm 0.64$ ,  $p<0.001$ ).

*Histologic evaluation (Tables 3-2, 3-2a, 3-2b, and 3-2c):*

For the Tissue Architecture-Loss category, OA tissue had significantly more histologic pathology compared to Controls (Overall:  $1.66 \pm 0.98$  vs.  $0.67 \pm 0.76$ ,  $p<0.001$ ) (Medial:  $1.84 \pm 0.94$  vs.  $0.72 \pm 0.89$ ,  $p<0.001$ ) (Lateral:  $1.48 \pm 1.0$  vs.  $0.61 \pm 0.61$ ,  $p<0.001$ ). OA medial menisci had significantly more histologic pathology compared to OA lateral menisci ( $1.84 \pm 0.94$  vs.  $1.48 \pm 1.0$ ,  $p=0.043$ ).

For the Cell-Matrix category, OA tissue had significantly more morphologic disruption compared to Control tissue (Overall:  $1.52 \pm 0.71$  vs.  $0.58 \pm 0.60$ ,  $p<0.001$ ) (Medial:  $1.59 \pm 0.69$  vs.  $0.72 \pm 0.57$ ,  $p<0.001$ ) (Lateral:  $1.45 \pm 0.73$  vs.  $0.44 \pm 0.62$ ,

p<0.001). OA medial menisci were not significantly different from OA lateral menisci for this category.

For the Proliferative Response category, OA tissue showed significantly more proliferation compared to Control tissue (Overall:  $1.30 \pm 0.84$  vs.  $0.33 \pm 0.53$ , p<0.001) (Medial:  $1.52 \pm 0.82$  vs.  $0.39 \pm 0.61$ , p<0.001) (Lateral:  $1.08 \pm 0.8$  vs.  $0.28 \pm 0.46$ , p<0.001). OA medial menisci had significantly higher scores than OA lateral menisci ( $1.52 \pm 0.82$  vs.  $1.08 \pm 0.8$ , p=0.002).

For the Total Histologic Score, OA menisci showed significantly more pathology when compared to Control menisci (Overall:  $4.47 \pm 2.03$  vs.  $1.58 \pm 1.5$ , p<0.001) (Medial:  $4.95 \pm 1.85$  vs.  $1.83 \pm 1.72$ , p<0.001) (Lateral:  $4.0 \pm 2.11$  vs.  $1.33 \pm 1.24$ , p<0.001). OA medial menisci had significantly higher total histologic pathology scores compared to OA lateral menisci ( $4.95 \pm 1.85$  vs.  $4.0 \pm 2.11$ , p=0.009).

#### *Biochemical Evaluation (Tables 3-3, 3-4, and 3-5):*

Tissue biochemical composition was analyzed for three components critical to meniscal tissue composition and function: water, proteoglycan, and collagen content.

OA menisci had significantly higher water content compared to Control menisci (Overall:  $73.23 \pm 7.54$  vs.  $39.04 \pm 4.22$ , p<0.001) (Medial:  $75.30 \pm 5.92$  vs.  $39.37 \pm 4.41$ , p<0.001) (Lateral:  $71.23 \pm 8.41$  vs.  $38.71 \pm 4.13$ , p<0.001). Medial OA menisci had significantly higher water compared to lateral OA menisci ( $75.30 \pm 5.92$  vs.  $71.23 \pm 8.41$ , p<0.001).

OA menisci had significantly higher proteoglycan content compared to Control menisci (Overall:  $37.78 \pm 20.21$  vs.  $19.98 \pm 13.73$ , p<0.001) (Medial:  $43.47 \pm 20.24$  vs.

$17.27 \pm 13.67$ ,  $p<0.001$ ) (Lateral:  $32.27 \pm 18.75$  vs.  $22.69 \pm 13.63$ ,  $p=0.037$ ). Medial OA menisci had significantly higher proteoglycan content compared to OA lateral menisci ( $43.47 \pm 20.24$  vs.  $32.27 \pm 18.75$ ,  $p<0.001$ ).

The collagen content of OA menisci was significantly higher than that of Control menisci (Overall:  $300.0 \pm 87.77$  vs.  $77.52 \pm 22.21$ ,  $p<0.001$ ) (Medial:  $291.09 \pm 91.87$  vs.  $80.78 \pm 19.39$ ,  $p<0.001$ ) (Lateral:  $308.62 \pm 83.4$  vs.  $74.26 \pm 24.83$ ,  $p<0.001$ ). Unlike the other biochemical measures, medial OA menisci were not significantly different than lateral OA menisci with respect to collagen content.

*Molecular evaluation (Tables 3-6 through 3-14):*

The molecular expression levels of menisci were analyzed for nine genes: Col 1, 2, 3, 6; MMP-1, -2, -3, -13; and VEGF. Unlike some of the previous findings, medial OA menisci were not significantly different than lateral OA menisci with respect to gene expression.

The Col 1 gene expression for OA menisci was significantly higher than that of Control tissue (Overall:  $1.1719 \pm 1.8097$  vs.  $0.0866 \pm 0.1029$ ,  $p<0.001$ ) (Medial:  $1.0016 \pm 1.1005$  vs.  $0.0802 \pm 0.0739$ ,  $p<0.001$ ) (Lateral:  $1.3263 \pm 2.2680$  vs.  $0.0927 \pm 0.1263$ ,  $p<0.001$ ). OA menisci had significantly higher overall Col 2 gene expression compared to Control menisci ( $0.1801 \pm 0.6367$  vs.  $0.0301 \pm 0.0903$ ,  $p=0.008$ ). Medial OA menisci had significantly increased Col 2 expression compared to Control ( $0.1888 \pm 0.7695$  vs.  $0.0064 \pm 0.0102$ ,  $p=0.002$ ), but there was no difference between the lateral OA and Control menisci. The Col 3 expression within OA tissue was significantly higher than the Control tissue (Overall:  $1.408 \pm 2.1544$  vs.  $0.0843 \pm 0.1631$ ,  $p<0.001$ )

(Medial:  $1.1833 \pm 1.3159$  vs.  $0.0682 \pm 0.1268$ ,  $p<0.001$ ) (Lateral:  $1.7504 \pm 2.6819$  vs.  $0.0995 \pm 0.1939$ ,  $p<0.001$ ). Col 6 expression within OA tissue was significantly higher than Control tissue (Overall:  $0.1440 \pm 0.1734$  vs.  $0.0310 \pm 0.039$ ,  $p<0.001$ ) (Medial:  $0.1396 \pm 0.1004$  vs.  $0.0298 \pm 0.0288$ ,  $p<0.001$ ) (Lateral:  $0.148 \pm 0.2205$  vs.  $0.0322 \pm 0.0476$ ,  $p<0.001$ ).

MMP-1 expression was not significantly different for any group analyzed. MMP-2 expression was significantly decreased within OA tissue compared to Control tissue (Overall:  $0.1803 \pm 0.301$  vs.  $0.275 \pm 0.137$ ,  $p<0.001$ ) (Medial:  $0.1506 \pm 0.1164$  vs.  $0.3158 \pm 0.1008$ ,  $p<0.001$ ) (Lateral:  $0.2072 \pm 0.4003$  vs.  $0.2365 \pm 0.1573$ ,  $p=0.025$ ). MMP-3 was also expressed at significantly lower levels within the OA menisci compared to Control menisci (Overall:  $0.03 \pm 0.0405$  vs.  $0.6137 \pm 0.6086$ ,  $p<0.001$ ) (Medial:  $0.0208 \pm 0.0198$  vs.  $0.7098 \pm 0.7771$ ,  $p<0.001$ ) (Lateral:  $0.0382 \pm 0.0513$  vs.  $0.5229 \pm 0.3932$ ,  $p<0.001$ ). MMP-13 expression was significantly higher within OA tissue compared to Controls (Overall:  $0.0016 \pm 0.0132$  vs.  $0.00002 \pm 0.00009$ ,  $p<0.001$ ) (Medial:  $0.0005 \pm 0.0014$  vs.  $0.0 \pm 0.0$ ,  $p<0.001$ ) (Lateral:  $0.0026 \pm 0.0182$  vs.  $0.00003 \pm 0.00013$ ,  $p<0.001$ ).

VEGF expression was significantly decreased for lateral OA menisci compared to Control menisci ( $0.3740 \pm 0.4916$  vs.  $0.9521 \pm 1.7166$ ,  $p=0.007$ ), but no other significant differences were noted.

*Radiographic evaluation (Tables 3-15, 3-16, 3-16a, and 3-16b):*

For OA x-rays, the medial compartment joint space was significantly narrower compared to the lateral compartment ( $2.04 \pm 2.22$  vs.  $6.58 \pm 2.84$ ,  $p<0.001$ ). The

radiographic total score was significantly higher for the medial OA compartment compared to the lateral OA compartment ( $4.79 \pm 1.41$  vs.  $3.08 \pm 1.32$ ,  $p<0.001$ ). As expected, when comparing the OA and Control radiographic scores, the OA group was significantly higher.

*Correlations (Table 3-17):*

A number of strong, moderately strong, and relatively weak correlations were present between the numerous categories analyzed.

For the analyses that allowed for a comparative test between the anterior, body, and posterior sections, no statistically significant differences were noted among the sections of each type of meniscus (Control medial, Control lateral, OA medial, OA lateral).

## **Discussion**

*Gross evaluation:*

When establishing pathological trends through histologic, biochemical, molecular, and clinical measures, it is imperative to link these changes to the gross assessment of the meniscus. As expected, the gross scoring system established for this study was able to statistically distinguish Control menisci from OA menisci. When comparing the medial and lateral OA menisci, it was found that medial menisci had significantly more gross pathology according to the scoring system. This finding correlates with other meniscal and OA findings within the literature. Englund et al assessed the integrity of the medial

and lateral menisci with MRI for 991 randomly selected subjects between the ages of 50 and 90. Of these randomly selected subjects, 35% had meniscal damage and the medial meniscus was significantly affected more than the lateral, 66% vs. 24% respectively (10% were bilateral). They also determined that subjects with a Kellgren and Lawrence grade of 2 or higher had an increased prevalence of meniscal pathology when compared to subjects without such radiographic evidence of OA (82% vs. 25%). This increase in prevalence was even more drastic for subjects with a Kellgren and Lawrence grade of 3 or 4, 95%.<sup>22</sup> Baker et al conducted a review of menisectomies performed in Syracuse, New York from 1973 to 1982. Within this study it was found that 81% of the meniscal injuries affected the medial meniscus.<sup>23</sup> Widuchowski et al analyzed 25,124 knee arthroscopies from 1989 to 2004 and found that chondral lesions were found in 60% of the patients. The articular surfaces affected the most were the patella (36%) and medial femoral condyle (34%). The injury that was most commonly associated with an articular lesion was a medial meniscal tear.<sup>24</sup> Swank et al performed 82 unicompartmental arthroplasties from 1983 to 1987, 75 of which were medial unicompartmental knee arthroplasties (UKA), only 7 were lateral UKA.<sup>25</sup> These studies help to show that the presence of OA is commonly associated with meniscal pathology. OA changes will occur after meniscal injuries, especially when there is a loss of meniscal integrity causing a lack of protection of the articular cartilage.<sup>2-9</sup> In addition, these studies also help prove the fact that medial meniscal pathology is more prevalent. This correlates with our work that highlights a greater presence of gross pathological changes within the medial menisci when compared to lateral for OA patients that required a TKA.

*Histologic evaluation:*

Our next step in evaluation of meniscal pathology was to develop a histologic scoring system. This system was based off typical meniscal characteristic traits that can be easily identified in a blinded fashion. It was important to first assess the structure of the meniscus to see if the normal architecture was intact or if pathology had led to tissue loss. Secondly, different histologic stains allowed for the evaluation of tissue composition. The H&E stain was able to identify normal collagen band alignment when present. The Saf-O stain was able to stain proteoglycans with a red pigment and signify their normal distribution within the meniscus, which are typically found within the central regions of the meniscus and are almost devoid along the outer periphery.<sup>26</sup> Pauli et al has observed that aging will lead to some increased Saf-O staining in the central portion of the meniscus.<sup>27</sup> The distribution of proteoglycans within the middle of the meniscus is compatible with its mechanical role of absorbing compressive loads and translating these loads into circumferential tensile stresses, which are handled by the normal distribution of collagen fibers. Third, when evaluating pathology of the meniscus it is imperative to understand the cellular composition of the tissue, looking for an increased proliferative response of cells from the synovial junction along the abnormal meniscal tissue margins and within the tissue itself. These findings have been observed in other studies where OA menisci had an increased amount of cells in both the superficial and deep layers.<sup>28,29</sup> The categories created to allow for grading of meniscal pathology were as follows: (1) Tissue architecture – tissue loss; (2) Cell and matrix (proteoglycan and collagen) content and morphology; and (3) Proliferative response (Figure 3-1). Totaling these three scores then provided a total severity score for the

meniscal tissue under examination. To help ensure the accuracy of the grading system and to show that histologic scoring does correlate with gross measures but helps to provide a more in depth picture of tissue severity, each of the histologic scores and the total score were correlated with the gross tissue score to assist in evaluating possible trends with respect to other outcome measures.

As hypothesized, OA tissue had significantly increased histologic tissue disruption, increased morphologic disruption, increased cellular proliferation, and increased total microscopic severity when compared to Control tissue samples. Interestingly, just as the gross score was able to distinguish that medial menisci are typically affected more so than lateral OA menisci, all of the histologic scores except for the matrix content score showed a significant increase in pathological changes within the medial OA menisci. This finding again helps to show a relationship between OA and the prevalence of this disease affecting the medial compartment to a higher degree than the lateral compartment.

What was probably even more important to show was that the scoring systems used for the three histologic subgroups had a moderately, strong correlation value between all three of them, correlation value ranged from 0.53 to 0.63. In addition, the total severity score had a strong correlation with each of the individual subgroups, correlation values ranged from 0.81 to 0.89. The histologic scoring system was not only able to distinguish Control from pathologic tissues effectively; it was able to assess three separate characteristic features of meniscal tissue individually and exemplify the progression of OA disease within all three categories with high correlation values between them. As an adjunct, it is expected that histologic scoring should provide a more

accurate and in depth assessment of tissue when compared to gross evaluation. But, a good histologic scoring system should still be able to correlate with the gross evaluation of tissue. In this study, a moderately, strong correlation ( $r=0.51$ ) was present when comparing the total histologic severity score with the gross scoring. This helps to establish the groundwork for comparing other pathologic outcome measures within meniscal tissue for this study to not only the gross score, but to the more in depth, and probably more accurate, histologic scoring system.

*Biochemical evaluation:*

The major components of meniscal tissue consist of water, collagen, and proteoglycans. In 1984 Herwig et al. described that the normal human meniscus contains around 70-75% water, 20-22% collagen, and 0.6-0.8% total glycosaminoglycans. In their study they indicated that water content correlates with the grade of degeneration and increased from about 70 to 85%. Herwig et al. also indicated that the collagen and glycosaminoglycan content expressed per mg of wet weight of tissue decreases in relation to the grade of degeneration. However, when they analyzed the collagen and glycosaminoglycan levels to the dry weight, a consistent correlation with pathological grading could not be found for collagen but the GAG content now increased with more severe pathology ( $r=0.93$ ). It was determined that the main type of GAG was chondroitin 6-sulphate and the proportion of this went from 35% for normal menisci to about 55% in degenerative menisci ( $r=0.84$ ). Due to the percent increase in chondroitin 6-sulphate GAG, the other types of glycosaminoglycans (dermatan sulphate, chondroitin 4-sulphate, and keratin sulphate) had a slight decrease in percentage when comparing normal to

degenerative menisci.<sup>30</sup> A similar finding was demonstrated in a separate study by Adams et al. They found that over time glycosaminoglycan levels would increase within a beagle cranial cruciate ligament transection model.<sup>31</sup> A study by Ghosh et al determined that the dry weight percentage of non-collagenous matrix proteins will increase for degenerative areas of human menisci relative to normal controls.<sup>32</sup> Even though the work by Herwig et al was unable to demonstrate that the collagen dry weight content will increase in degenerative meniscal tissue, a study by Hellio Le Graverand was able to show an increase in collagen with a different means of measurement. Their study analyzed lapine menisci post ACL transection and found that the immunohistochemistry staining of type I and III collagens increased significantly in the medial and lateral menisci, type II increased only in the medial. Their conclusion was that extracellular matrix deposition does occur within the meniscus during the progression of OA. In addition to the findings they had for collagen, they were also able to demonstrate a significant increase in water content for the medial meniscus as it became more degenerative similar to the previous studies that were discussed.<sup>33</sup>

For the study being presented here, a few similarities and a few differences were present when comparing the results with previous studies found in literature. For the water content, this study also found that more degenerative tissue had increased water percentage. The OA tissue had a significantly increased amount of water compared to Controls, and the medial OA menisci had a significantly increased amount of water when compared to the lateral OA menisci. This second finding correlates with the gross and histologic changes that were noted helping to show that the medial meniscus is more commonly affected with increased amounts of pathological changes when compared to the lateral meniscus of OA

patients. In addition, the body and posterior zones of the OA medial meniscus were the two zones that had a statistical increase in water percentage over the OA lateral menisci. This finding correlates with the fact that degenerative pathology typically occurs in the posterior horns of the medial meniscus.<sup>27,34</sup> Interestingly, the water content within the Controls for this study was far less than what has been described in literature, 39% vs. 70-75%. The water percentage for the OA menisci was also less than the reported literature, 73% vs. the high end of 85%.<sup>30</sup> These differences may be due to one of the following two factors: aged normal specimens being utilized for the Control Group instead of true normal menisci; methods of measurement are different between studies (lyophilization vs. acetone-dried specimens). Despite these differences, it is essential to point out the strong correlations that existed between water content and the gross score ( $r=0.61$ ), along with the histologic total score ( $r=0.64$ ). This helps to define the point that water content will definitely increase within meniscal tissue that is more severely affected by OA degeneration.

For this study the proteoglycan content was measured as a ratio between GAG and tissue dry weight. It was found that OA tissue had increased amounts of proteoglycan than Control samples, and medial OA menisci had increased values when compared to lateral OA menisci. These findings mimic the findings by Herwig et al, Adams et al, and Ghosh et al. Just as witnessed with the water percentage, the proteoglycan amount will increase as the tissue becomes more degenerative: OA more than Control, medial more than lateral. It can be postulated that during the process of OA induced meniscal degeneration, proteoglycans that bind water will accumulate and become more prevalent within meniscal tissue. This postulation was further supported by the moderately strong correlations that

existed between proteoglycan content and the gross scores ( $r=0.42$ ) and water percentage ( $r=0.46$ ), along with its relatively weak correlation with the total histologic score ( $r=0.25$ ). The interesting finding that was subjectively noticed in this study was that the amount of red staining for Saf-O histologic evaluation did not increase within the OA tissue. It is hypothesized that the proteoglycans building within degenerative tissue are likely more spread out instead of being localized to the central core of the meniscus; also they may be different in structure and type. These two factors might have prevented the increased amount of proteoglycans from staining as intensely as they do in normal tissue within the midportion of the meniscus.<sup>26</sup> What is very clear from this work is that degenerative menisci experience significant changes with respect to proteoglycan content; it will be important to further evaluate the specific changes that are occurring such as distribution, structure, and types.

The collagen content in this study was measured as a ratio between HP and tissue dry weight. The findings from this study did not match what was described by Herwig et al but it did have some similarities to the study conducted by Hellio Le Graverand. This study identified significant increases in collagen content for OA tissue when compared to Control tissue; this held true for each specific zone that was compared. However, a significant difference was not present when comparing the collagen content of medial and lateral OA menisci as shown when measuring the GAG content and water percentage. It is difficult to definitively say that the collagen content of a meniscus will increase proportionally to the amount of degeneration like what happens with proteoglycan content and water content because of the fact that this study did not show a difference between the medial and lateral OA menisci for collagen content. The collagen content did have a

moderately strong correlation with the gross score ( $r=0.48$ ) and water percentage ( $r=0.40$ ), along with a relatively weak correlation with the total histologic score ( $r=0.33$ ). Due to these findings, it is still possible to hypothesize that as a meniscus goes through degenerative changes, it may attempt a regenerative process with increased collagen deposition, but this will occur in a fashion that lacks appropriate collagenous fiber organization and functionality. This type of finding is what was shown through the experimental OA model performed by Hellio Le Graverand et al: as medial meniscal gross pathology increased, the histologic evaluation showed marked degenerative changes and alteration in cell distribution, the water percentage increased, and the immunohistochemistry intensity of collagens I, II, and III all increased.<sup>33</sup> Further delineation of these collagenous changes with respect to biochemical measures becomes important when trying to understand how the meniscus reacts to injury and the resulting eventual OA pathology.

*Molecular evaluation:*

In order to understand how meniscal tissue reacts to degradation on a molecular level, real time PCR was conducted on a number of mRNAs known to be involved in meniscal pathology. Matrix synthesis genes (Col 1, 2, 3, and 6), matrix degradation genes (MMP-1, -2, -3, -13), and a gene that was predicted to be signaling increased vascularity and cellularity (VEGF) were analyzed. Type I collagen is the predominate collagen within meniscal tissue and can be found throughout the meniscus.<sup>35</sup> Smaller amounts of type II collagen can also be found in the meniscus but tend to be restricted to the inner, nonvascularized portion.<sup>35,36</sup> Only trace amounts of type III and VI collagens

can be found within the meniscus; these collagens have been linked with repair and remodeling processes.<sup>35,37-40</sup> MMP-1 and -13 are collagenases and have been associated with degradation of fibrillar collagens.<sup>41,42</sup> These two collagenases are able to hydrolyze multiple types of collagens to include types I, II, and III; however, MMP-1 has been linked with preferentially hydrolyzing type III collagen and MMP-13 appears to have a more potent activity against type II collagen.<sup>43</sup> MMP-2 is another type of collagenase that is well known to be associated with cleavage of the basement membrane type IV collagen, but it will also degrade denatured collagens and has the potential to degrade type I and VI collagen fibrils.<sup>44,45</sup> MMP-3 is a part of the stromelysin group and has been linked to degradation of proteoglycans such as aggrecan.<sup>46</sup> VEGF has a well-established role of inducing vasculogenesis, cell growth, and cell migration.<sup>47-50</sup>

Katsuragawa et al completed a similar study to the work presented here by comparing the anterior horn of aged normal and end-stage OA menisci with respect to histology and gene expression. In their work, they were able to demonstrate an increase of type I, II, and III procollagens with type III collagen having the most enhanced fold change, reaching 400x.<sup>40</sup> Wildey et al evaluated canine meniscal tissue at 3 and 12 weeks post CCL transection with the goal of measuring expression levels of COL1A1 and COL6A3. Within their study there were noteworthy macroscopic changes in the medial meniscus but not within the lateral meniscus. Even with this finding of gross normality in the lateral meniscus, they found an up-regulation of gene expression for type I and type VI collagen in both menisci; however, the gene expression levels were greater in the medial. It was felt that the increased gene expression in the medial experimental group vs. the lateral reflects the different biomechanical forces the medial

meniscus undergoes during joint instability, which correlates with its macroscopic evaluation. Because of the significant increases in gene expression, range of 20-38 fold increases at 3 weeks and 11-19 fold changes at 12 weeks, it was determined that meniscal tissue will mount a dynamic response when joint injury is present. One additional interesting point they noted was that the control menisci had very low levels of gene expression to begin with. It was concluded that this may be due to relatively little turnover for these proteins within healthy menisci.<sup>37</sup> This finding correlates with the fact that type II collagen within normal femoral condylar articular cartilage also has a very slow turnover rate; measured to have a 300 day mean half-life.<sup>51</sup> Hellio Le Graverand et al is another group that evaluated specific meniscal protein changes post ACL transection; they utilized a rabbit model and looked at meniscal differences at 3 and 8 weeks. Immunohistochemistry was able to show a significant increase in type I, II, and III collagens for the medial meniscus post ACL injury, and a significant increase for types I and III within the lateral menisci. When analyzing these collagens with respect to gene expression, it was once again highlighted that type I, II and III collagens were significantly increased when compared to the controls for the medial meniscus at the 3 week time point. At the 8 week time point, type I and II collagens were still significantly increased. For the lateral meniscus, types I and III were significantly increased at both time points. Type II collagen was not increased in the lateral meniscus for gene expression or immunohistochemistry expression. In addition to collagen gene expression, they evaluated total RNA concentration, a few MMPs, and some proteinase inhibitors. Of major interest, the total RNA yield for the medial meniscus was significantly increased at both time points, and this lead to the conclusion that meniscal

tissue is hypermetabolic after joint injury. For the MMPs tested, the collagenase MMP-1 was found to be elevated in the medial meniscus after 8 weeks, which seemed to correlate to more severe morphological alterations. Of the proteinase inhibitors tested, TIMP-1 was elevated in the medial and lateral menisci for both time points.<sup>33,52</sup> Another study worked to measure changes in gene expression of meniscal tissue dependent on the amount of compressive strain induced. When comparing tissue that was not dynamically loaded to tissue under a 20% strain, representative of the strain remaining on meniscal tissue after 30% of the meniscus has been removed; they found a significant upregulation for MMP-1, -3, -13, and aggrecanase-1. This indicated that increased strains that result after meniscal tissue loss can initiate pathways of enzymatic degradation.<sup>53</sup> Ishihara et al worked to study the presence and affect MMP-3 had on meniscectomy tissue. They described that the ratio of chondrocyte-like cells will increase within OA meniscal tissue and that the amount of MMP-3 activation localized to these cell clusters will also increase (elevated MMP-3 IHC staining). It was felt that MMP-3 could play a significant role in meniscal aggrecan degradation especially in areas where chondrocyte-like cells exist.<sup>54</sup> Becker et al was interested in the impact VEGF had on rabbit menisci after a medial longitudinal laceration was induced either in the peripheral vascular portion or the central avascular portion. The highest VEGF expression via ELISA was found to occur within the central meniscal tissue one week post avascular tear. This was significantly increased over the tear in the peripheral margin and both meniscal tissue samples post tear had more VEGF expression than the contralateral medial meniscus. The amount of VEGF expression from the meniscal tissue post peripheral tear and central tear declined after the one week time point out to the ten week time point; however, they both remained

significantly increased over the contralateral menisci. All peripheral lacerations healed by the ten week time point, but no central lacerations healed. In addition, angiogenesis was noted within the peripheral tears, but even with the increased response of VEGF in the central regions, angiogenesis failed to reach the central meniscal tears. The other interesting finding was that ELISA was unable to detect VEGF in the meniscal tissue obtained from rabbits that had not undergone the operation.<sup>55</sup>

Within our study, all four collagens studied were statistically increased within the OA group compared to Controls. Type III and I collagens had the most drastic increases with 18x and 14x fold changes, respectively. Type II and VI collagens still showed moderate increases with 6x and 5x fold changes, respectively. When just analyzing the medial OA menisci to medial Control menisci, all four collagens remained statistically increased within the OA group. However, of interest was how the type II collagen fold change for the medial menisci had a far greater increase (29x) than the other collagens (17x for Col 3, 12x for Col 1, 5x for Col 6). When comparing the lateral OA and Control menisci, type II collagen no longer showed a significant difference between the two groups and only had a 3x increase. The other three collagens were significantly elevated within the lateral OA menisci (18x for Col 3, 14x for Col 1, 5x for Col 6). It was striking how type II collagen appeared to be affected by localized damage, medial greater than lateral. This type of finding is consistent with the findings in the study performed by Hellio Le Graverand et al.<sup>33,52</sup> However, it is important to note that in this particular study, the mean expression levels of type II collagen within the medial Control menisci were much lower than the lateral Control, but they were not significantly different. This

helped to contribute to the drastic difference in fold changes between the medial and lateral when comparing Control to OA menisci.

The other important finding was how well some of the collagen types correlated with other measures of disease. Types I, III, and VI all had strong or moderately strong correlations with the gross score ( $r=0.61$ ,  $r=0.52$ ,  $r=0.43$ , respectively) and had relatively weak correlations with the total histologic score ( $r=0.36$ ,  $r=0.30$ ,  $r=0.32$ , respectively). This helps to show that as meniscal tissue is more pathologically affected, it will increase its expression of the collagen type that is mainly found within the meniscus (type I), but it will also increase its expression of reparative collagens (types III and VI). In addition, strong and moderately strong correlations also existed between these three collagens and the total collagen content ( $r=0.45$ ,  $r=0.47$ ,  $r=0.61$ , respectively); so as the tissue was increasing its gene expression of these collagens, the actual amount of collagen protein produced was also increasing. Col 1, 3, and 6 also somewhat correlated with the water content % ( $r=0.50$ ,  $r=0.45$ ,  $r=0.30$ , respectively), while all four collagens weakly correlated with the proteoglycan content (Col 1,  $r=0.26$ ; Col 2,  $r=0.36$ ; Col 3,  $r=0.37$ ; Col 6,  $r=0.21$ ). These findings become intriguing because the correlations are now indicating that when meniscal tissue becomes degenerative, it will increase its collagen protein content and gene expression along with its proteoglycan content and water percentage. However, type II collagen did not share a lot of the same correlations as the other collagens. The one correlation it did have similar to the other collages was the fact that it correlated with an increase in proteoglycan content. This finding was particularly interesting since type II collagen and proteoglycans are the major components in cartilage and previous research has indicated that OA menisci will contain increased amounts of

cell clusters that have similar morphology to hypertrophic chondrocytes.<sup>28,29,54</sup> So it can be postulated that OA menisci will not only become more cellular with clusters of cells morphologically similar to chondrocytes, but that these cells will also attempt to lay down an extracellular matrix that is more cartilage-like instead of meniscal-like. Overall, all four collagen markers correlated well with each other showing that OA and degeneration causes a global increase in certain types of collagen (Col 1 with Col 2 ( $r=0.35$ ), Col 3 ( $r=0.83$ ), Col 6 ( $r=0.62$ )) (Col 2 with Col 3 ( $r=0.47$ )) (Col 3 with Col 6 ( $r=0.69$ )).

Out of the other genes tested within this study, it appears that MMP-1 and VEGF expression were the least affected by meniscal pathology, as these genes did not have consistent significant differences between the menisci tested. The other three MMPs tested told a different story. It seems that menisci actually attempt to down regulate certain catabolic metalloproteinases such as MMP-2 and MMP-3 during the progression of OA. MMP-2 decreased by 1.5x within the arthritic menisci; however, when analyzing the medial and lateral OA menisci vs. Controls, the main decrease in gene expression was within the medial menisci (2.1x decrease) instead of the lateral (1.1x decrease). When looking at the anterior, body and posterior sections of the lateral menisci, there was not a statistical difference between Control and OA menisci, but there was a statistical decrease for all three sections within the medial menisci. For MMP-3, there was a much more staggering change. Overall gene expression was decreased by 20x within the OA menisci, and even though there was a significant decrease for both medial and lateral arthritic menisci, the fold change by which arthritis caused a decrease was much higher for the medial menisci (34x decrease for medial, 14x decrease for lateral). Even though it

is very clear that meniscal tissue undergoes a significant amount of degeneration during the progression of OA, it seems that meniscal generated MMP-2 and MMP-3 are not the culprit. If MMP-2 and MMP-3 are playing a role within meniscal tissue breakdown, these factors are probably being released into the joint fluid by other tissues such as the synovium. It has been described that synovial tissue does react to mechanical and inflammatory stresses associated with OA to release catabolic enzymes such as MMP-2 and MMP-3.<sup>56,57</sup> When looking at how these two cytokines correlate with other measures of disease, MMP-2 had some weak associations, but MMP-3 appeared to correlate very well with a number of disease markers. MMP-3 had a strong negative correlation with the gross score ( $r=-0.65$ ) and had a moderately, strong negative correlation with the histologic total score ( $r=-0.42$ ); MMP-2 only weakly correlated with the gross score ( $r=-0.22$ ). MMP-2 had mostly weak negative correlations with the water percentage, proteoglycan content, and the collagen content ( $r=-0.27$ ,  $r=-0.35$ ,  $r=-0.40$ , respectively). MMP-3 however had moderately strong negative correlations with these three measures of disease ( $r=-0.57$ ,  $r=-0.42$ ,  $r=-0.41$ , respectively). In addition, MMP-3 also correlated well with Col 1, Col 3, and Col 6 ( $r=-0.60$ ,  $r=-0.54$ ,  $r=-0.37$ , respectively), but not Col 2. MMP-2 weakly correlated with Col 2 ( $r=-0.22$ ), Col 3 ( $r=-0.28$ ), and Col 6 ( $r=-0.31$ ). Interestingly, MMP-2 and MMP-3 did not correlate with each other. Meniscal tissue appears to be very sensitive to the way these two cytokines affect the breakdown of collagen and proteoglycans. This study was able to highlight their down regulation within meniscal tissue while the degree of OA increased. Meniscal tissue also appears to down regulate these two enzymes while increasing the amount of collagen protein, collagen gene expression, and proteoglycan content all as a futile attempt to repair itself.

This finding appears to be a new finding that has not been described in literature. Previous studies like the work by Ishihara et al attempt to make the conclusion that MMP-3 expression is increased within degenerative meniscal tissue due to increased immunostaining of the antibody against MMP-3 within degenerative meniscal tissue. However, due to the results described here, what may be occurring instead is that MMP-3 can be localized within meniscal tissue causing degradation of extracellular matrix such as aggrecan, but the actual MMP-3 enzyme is being produced by the inflamed synovial tissue while the meniscal tissue is trying to produce less of this enzyme.

MMP-13 had the opposite reaction with increased degradation when compared to MMP-2 and MMP-3. MMP-13 was only detected in one of the Control sections and was expressed in small amounts within all OA samples. Because of this, a 100x fold difference was present between the Control and OA tissue. MMP-13 had a relatively weak correlation with the gross score ( $r=0.37$ ) and histologic total ( $r=0.31$ ) helping to link the possibility that MMP-13 will be expressed within meniscal tissue as it undergoes degeneration. MMP-13 positively correlated with some of the collagens (collagen content ( $r=0.41$ ), Col 1 ( $r=0.24$ ), Col 3 ( $r=0.25$ ), Col 6 ( $r=0.35$ )), but it did not correlate with Col 2 even though MMP-13 has been linked to preferentially degrading type II collagen.<sup>43</sup> The other interesting finding was how there was a relatively weak, negative correlation with MMP-3 ( $r=-0.23$ ). As described earlier, the meniscus attempts to repair itself by increasing certain markers that help with laying down additional extracellular matrix and decreasing other markers that would break down the tissue being built. However, the meniscus does appear to increase its expression of MMP-13 which will lead to some extracellular matrix degradation. Since this gene was not found to be

expressed within Control menisci, it becomes an intriguing question on how potent this proteinase is against meniscal tissue.

*Radiographic evaluation:*

Imaging modalities are a very well accepted way of tracking patients and determining the severity of disease with respect to OA. The most common imaging modality that has been used for decades is radiographic imaging. One of the first radiographic scoring assessments that became widely used was created by Kellgren and Lawrence in 1957.<sup>21</sup> This scoring system, along with modified versions that were created to be slightly more detailed, continue to be used today in clinical practice and for the purpose of data collection.<sup>19,58-72</sup> Even though multiple studies have found correlations between radiographs and various measures of disease, it has been described that x-rays should not be used in isolation when assessing individuals with pain due to every person's level of pain being individualized.<sup>73</sup> One patient may have a high x-ray score but a high threshold for pain resulting in a low pain score, but on the contrary another person may have a lower x-ray score but a low threshold for pain resulting in a high pain score. Within this study, the modified Kellgren and Lawrence scale was used to analyze if the scale would correlate with the other measures of OA disease studied. The goal was to link the meniscal changes that occur on a gross, histologic, biochemical, and molecular level with what can be seen visually on the most common imaging modality used for OA patients, the radiograph.

One limitation within this study was that for the Control knees, it was assumed that a normal radiographic score of 0 would be present for each category. Since a

standing radiograph was not available for these patients, it was felt that this was a reasonable assumption since the femoral condyles, the tibial plateau, and bilateral menisci were all obtained for evaluation. No osteophytes, chondral lesions, or meniscal lesions were noted in the Control tissues collected so it was felt that this would translate to a normal radiographic score. With that limitation noted it was not surprising to find that there was a significant increase in the total radiographic score of OA patients when compared to the presumed normal radiographic score that would be associated with the Control specimens. When just analyzing the medial and lateral compartments of the OA patients, a similar finding was noted as what was seen with other measures of disease. The medial compartment was deemed to be more severely affected due to having a more narrow joint space and a more severe total radiographic score.

The more important finding with respect to the radiographic outcome measures was how well it correlated with the other measures of disease. The radiographic measures within this study can be broken down into two categories: 1) Joint space measurements with an objective outcome, and 2) Modified Kellgren and Lawrence grading scale with a subjective outcome. To a certain degree the joint space measurement is included within the Modified Kellgren and Lawrence grading scale because it does evaluate narrowing, it just isn't as specific as when it is measured with a ruler. When determining which of these two outcome measures depict the severity of meniscal disease more consistently, utilization of the total score from the Modified Kellgren and Lawrence grading scale, when applied to each compartment separately, provided more dependable results. Each time it was determined that the correlation value was significant between the joint space measurement and another outcome measure, there

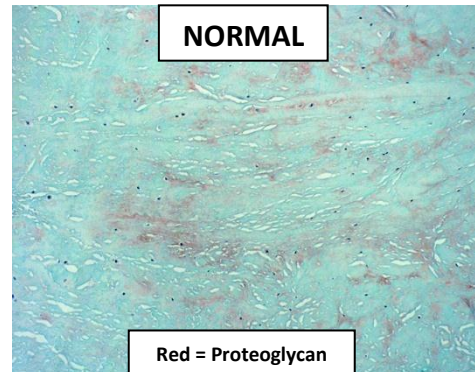
was a higher correlation value between the radiographic total score and that same outcome measure. The limitation of not having joint space measurements for the Control group may have led to these differences. As expected, the highest correlation values for the joint space measurements were with the radiographic narrowing ( $r=-0.90$ ) and radiographic total scores ( $r=-0.87$ ). The radiographic total score helped to provide a clinical correlation to when meniscal pathology is measured grossly ( $r=0.79$ ) and histologically ( $r=0.52$ ). Biochemically, it was clearly shown that meniscal pathology will be associated with increased water, proteoglycan, and collagen content; however, more intriguing was the fact that these measures correlated well with the clinical radiographic score ( $r=0.73$ ,  $r=0.49$ ,  $r=0.44$ , respectively). Lastly, this same principle held true for the molecular measures of disease. Within this study, meniscal pathology was unquestionably associated with increased collagen expression (types I, III, and VI more specifically), decreased MMP-2 and MMP-3 expression, along with increased MMP-13 expression. When analyzing if these markers had the potential to correlate with a clinical assessment, it was clearly demonstrated that the radiographic total score would be able to provide a link between clinical and molecular measures of disease (Col 1,  $r=0.58$ ; Col 3,  $r=0.58$ ; Col 6,  $r=0.51$ ; MMP-2,  $r=-0.30$ ; MMP-3,  $r=-0.61$ ; MMP-13,  $r=0.40$ ). Interestingly, the clinical assessment of a patient with the use of radiographs resulted in some of the highest correlation values with the meniscal indicators of pathology.

## Conclusions

These data have allowed us to draw the following conclusions: (1) Gross, histologic, and radiographic evaluation consistently depict severity of meniscal pathology

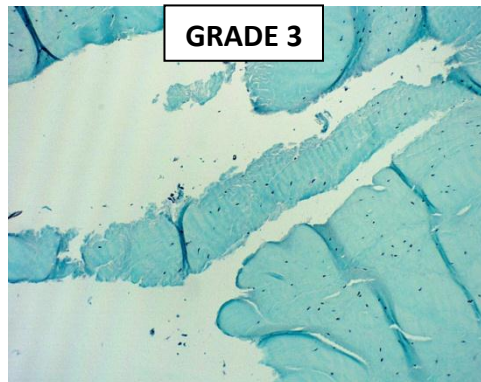
and correlate well with one another; (2) Gross, histologic, and radiographic assessment of menisci and the joint readily distinguishes normal from abnormal; (3) The amount and severity of pathology differs between medial and lateral menisci as determined by clinical (gross and radiographic) and basic science (histologic and biochemical) measures of disease; (4) Strong and significant correlations exist between meniscal basic science markers (histologic, biochemical, and molecular) and clinical indicators of disease (gross and radiographic) for assessment of meniscal pathology; (5) These data suggest that *in vitro* measures of meniscal pathology have potential value for understanding disease mechanisms and predicting clinical disease. Therefore, further investigation is necessary in order to determine which proteoglycans and collagens are being produced at higher levels during pathological events, and to measure gene expression within other genes and assess what other trends exist. An increase in the number of samples for the Control group along with continued effort to obtain true normal meniscal tissue is needed. In addition to normals and OA tissue, meniscectomy tissue from traumatic meniscal tears and degenerative meniscal tears will also need to be obtained for comparison. Additional research is needed to more fully characterize meniscal disorders at both the basic science and clinical level.

**Figure 3-1:**  
**Meniscal tissue**  
**histologic scoring system**



*Tissue Architecture-Tissue Loss*

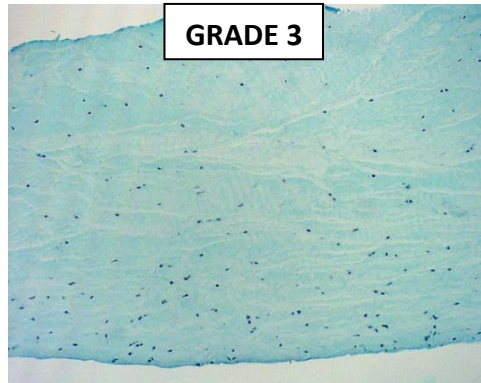
- 0 – normal
- 1 – minimal disruption or loss
- 2 – moderate disruption with loss
- 3 – complete loss of tissue architecture, >50% loss



*Cell and Matrix (PG and Collagen)*

*Content and Morphology*

- 0 – normal
- 1 – minimal alterations of cell and matrix content and morphology
- 2 – moderate alterations of cell and matrix content and morphology
- 3 – severe loss/disruption of cells, PG, and collagen



*Proliferative Response*

- 0 – none
- 1 – minimal proliferation of cells at synovial junction
- 2 – proliferation of cells at synovial junction extending into tissue or surfaces
- 3 – marked proliferation of cells involving majority of remaining tissue

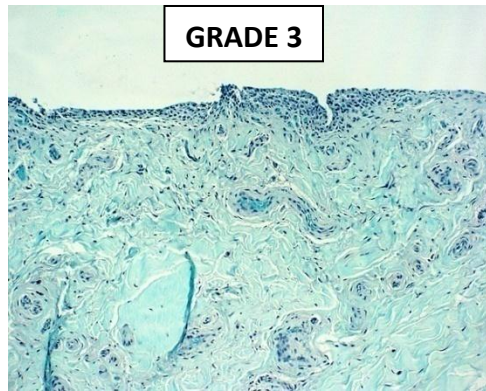


**Table 3-1: Gross score**

	Control	Osteoarthritic	Fold Δ
<b>Overall</b>	<b>0.08 ± 0.28</b>	<b>1.88 ± 0.69 *</b>	<b>22.6x</b>
<b>Medial Meniscus</b>	<b>0.17 ± 0.38</b>	<b>2.21 ± 0.60 *<sup>+</sup></b>	<b>13.2x</b>
<b>Lateral Meniscus</b>	<b>0.00 ± 0.00</b>	<b>1.57 ± 0.64 *</b>	<b>∞</b>

\*p<0.05 when comparing OA to Controls; <sup>+</sup>p<0.05 when comparing Medial to Lateral

**Table 3-2: Histologic total score**

	Control	Osteoarthritic	Fold Δ
<b>Overall</b>	<b>1.58 ± 1.50</b>	<b>4.47 ± 2.03 *</b>	<b>2.8x</b>
<b>Medial Meniscus</b>	<b>1.83 ± 1.72</b>	<b>4.95 ± 1.85 *<sup>+</sup></b>	<b>2.7x</b>
Anterior Horn	1.17 ± 1.47	4.19 ± 1.99 *	3.6x
Body	1.50 ± 1.52	5.36 ± 1.73 *	3.6x
Posterior Horn	2.83 ± 1.94	5.30 ± 1.66 * <sup>+</sup>	1.9x
<b>Lateral Meniscus</b>	<b>1.33 ± 1.24</b>	<b>4.00 ± 2.11 *<sup>+</sup></b>	<b>3x</b>
Anterior Horn	1.67 ± 1.51	4.26 ± 2.53 *	2.6x
Body	1.17 ± 0.75	4.29 ± 1.95 *	3.6x
Posterior Horn	1.17 ± 1.47	3.43 ± 1.69 * <sup>+</sup>	2.9x

\*p<0.05 when comparing OA to Controls; <sup>+</sup>p<0.05 when comparing Medial to Lateral

**Table 3-2a: Histologic architecture score**

	Control	Osteoarthritic	Fold Δ
<b>Overall</b>	<b>0.67 ± 0.76</b>	<b>1.66 ± 0.98 *</b>	<b>2.5x</b>
<b>Medial Meniscus</b>	<b>0.72 ± 0.89</b>	<b>1.84 ± 0.94 *<sup>+</sup></b>	<b>2.5x</b>
Anterior Horn	0.33 ± 0.82	1.48 ± 0.98 *	4.4x
Body	0.50 ± 0.84	2.18 ± 0.85 * <sup>+</sup>	4.4x
Posterior Horn	1.33 ± 0.82	1.85 ± 0.88 <sup>+</sup>	1.4x
<b>Lateral Meniscus</b>	<b>0.61 ± 0.61</b>	<b>1.48 ± 1.00 *<sup>+</sup></b>	<b>2.4x</b>
Anterior Horn	0.50 ± 0.55	1.61 ± 1.23	3.2x
Body	0.83 ± 0.41	1.57 ± 0.87 * <sup>+</sup>	1.9x
Posterior Horn	0.50 ± 0.84	1.24 ± 0.83 <sup>+</sup>	2.5x

\*p<0.05 when comparing OA to Controls; <sup>+</sup>p<0.05 when comparing Medial to Lateral

**Table 3-2b: Histologic matrix score**

	<b>Control</b>	<b>Osteoarthritic</b>	<b>Fold Δ</b>
<b>Overall</b>	<b>0.58 ± 0.60</b>	<b>1.52 ± 0.71 *</b>	<b>2.6x</b>
<b>Medial Meniscus</b>	<b>0.72 ± 0.57</b>	<b>1.59 ± 0.69 *</b>	<b>2.2x</b>
Anterior Horn	0.67 ± 0.52	1.33 ± 0.80	2.0x
Body	0.50 ± 0.55	1.64 ± 0.58 *	3.3x
Posterior Horn	1.00 ± 0.63	1.80 ± 0.62 * <sup>+</sup>	1.8x
<b>Lateral Meniscus</b>	<b>0.44 ± 0.62</b>	<b>1.45 ± 0.73 *</b>	<b>3.3x</b>
Anterior Horn	0.83 ± 0.75	1.48 ± 0.79	1.8x
Body	0.17 ± 0.41	1.57 ± 0.68 *	9.4x
Posterior Horn	0.33 ± 0.52	1.29 ± 0.72 * <sup>+</sup>	3.9x

\*p<0.05 when comparing OA to Controls; <sup>+</sup>p<0.05 when comparing Medial to Lateral**Table 3-2c: Histologic proliferative score**

	<b>Control</b>	<b>Osteoarthritic</b>	<b>Fold Δ</b>
<b>Overall</b>	<b>0.33 ± 0.53</b>	<b>1.30 ± 0.84 *</b>	<b>3.9x</b>
<b>Medial Meniscus</b>	<b>0.39 ± 0.61</b>	<b>1.52 ± 0.82 *<sup>+</sup></b>	<b>3.9x</b>
Anterior Horn	0.17 ± 0.41	1.38 ± 0.86 *	8.3x
Body	0.50 ± 0.55	1.55 ± 0.91 *	3.1x
Posterior Horn	0.50 ± 0.84	1.65 ± 0.67 * <sup>+</sup>	3.3x
<b>Lateral Meniscus</b>	<b>0.28 ± 0.46</b>	<b>1.08 ± 0.80 *<sup>+</sup></b>	<b>3.9x</b>
Anterior Horn	0.33 ± 0.52	1.17 ± 0.94 *	3.5x
Body	0.17 ± 0.41	1.14 ± 0.79 *	6.9x
Posterior Horn	0.33 ± 0.52	0.90 ± 0.62 <sup>+</sup>	2.7x

\*p<0.05 when comparing OA to Controls; <sup>+</sup>p<0.05 when comparing Medial to Lateral**Table 3-3: Water content %**

	<b>Control %</b>	<b>Osteoarthritic %</b>	<b>Fold Δ</b>
<b>Overall</b>	<b>39.04 ± 4.22</b>	<b>73.23 ± 7.54 *</b>	<b>1.9x</b>
<b>Medial Meniscus</b>	<b>39.37 ± 4.41</b>	<b>75.30 ± 5.92 *<sup>+</sup></b>	<b>1.9x</b>
Anterior Horn	38.22 ± 2.79	75.08 ± 6.07 *	2.0x
Body	39.12 ± 4.34	74.66 ± 7.41 * <sup>+</sup>	1.9x
Posterior Horn	40.76 ± 5.94	76.25 ± 3.62 * <sup>+</sup>	1.9x
<b>Lateral Meniscus</b>	<b>38.71 ± 4.13</b>	<b>71.23 ± 8.41 *<sup>+</sup></b>	<b>1.8x</b>
Anterior Horn	39.25 ± 6.00	73.03 ± 8.95 *	1.9x
Body	38.68 ± 4.00	70.02 ± 8.60 * <sup>+</sup>	1.8x
Posterior Horn	38.20 ± 2.34	70.46 ± 7.64 * <sup>+</sup>	1.8x

\*p<0.05 when comparing OA to Controls; <sup>+</sup>p<0.05 when comparing Medial to Lateral

**Table 3-4: Proteoglycan content**

	<b>Control (<math>\mu\text{g}/\text{mg}</math>)</b>	<b>Osteoarthritic (<math>\mu\text{g}/\text{mg}</math>)</b>	<b>Fold <math>\Delta</math></b>
<b>Overall</b>	<b><math>19.98 \pm 13.73</math></b>	<b><math>37.78 \pm 20.21 *</math></b>	<b>1.9x</b>
<b>Medial Meniscus</b>	<b><math>17.27 \pm 13.67</math></b>	<b><math>43.47 \pm 20.24 *^+</math></b>	<b>2.5x</b>
Anterior Horn	$16.08 \pm 13.95$	$44.18 \pm 22.08 *$	2.8x
Body	$21.81 \pm 18.16$	$44.45 \pm 21.92 *^+$	2.0x
Posterior Horn	$13.91 \pm 8.460$	$41.63 \pm 16.94 *$	3.0x
<b>Lateral Meniscus</b>	<b><math>22.69 \pm 13.63</math></b>	<b><math>32.27 \pm 18.75 *^+</math></b>	<b>1.4x</b>
Anterior Horn	$17.41 \pm 7.540$	$36.91 \pm 23.74 *$	2.1x
Body	$25.62 \pm 15.23$	$26.86 \pm 9.850 ^+$	1.1x
Posterior Horn	$25.04 \pm 17.10$	$32.59 \pm 18.76$	1.3x

\*p<0.05 when comparing OA to Controls; <sup>+</sup>p<0.05 when comparing Medial to Lateral

**Table 3-5: Collagen content**

	<b>Control (<math>\mu\text{g}/\text{mg}</math>)</b>	<b>Osteoarthritic (<math>\mu\text{g}/\text{mg}</math>)</b>	<b>Fold <math>\Delta</math></b>
<b>Overall</b>	<b><math>77.52 \pm 22.21</math></b>	<b><math>300.00 \pm 87.77 *</math></b>	<b>3.9x</b>
<b>Medial Meniscus</b>	<b><math>80.78 \pm 19.39</math></b>	<b><math>291.09 \pm 91.87 *</math></b>	<b>3.6x</b>
Anterior Horn	$72.87 \pm 19.12$	$293.99 \pm 97.09 *$	4.0x
Body	$80.35 \pm 21.41$	$293.95 \pm 102.2 *$	3.7x
Posterior Horn	$89.12 \pm 17.22$	$284.91 \pm 77.55 *$	3.2x
<b>Lateral Meniscus</b>	<b><math>74.26 \pm 24.83</math></b>	<b><math>308.62 \pm 83.40 *</math></b>	<b>4.2x</b>
Anterior Horn	$67.70 \pm 14.24$	$316.28 \pm 76.09 *$	4.7x
Body	$70.26 \pm 23.46$	$295.30 \pm 70.76 *$	4.2x
Posterior Horn	$84.81 \pm 33.75$	$313.55 \pm 103.0 *$	3.7x

\*p<0.05 when comparing OA to Controls; <sup>+</sup>p<0.05 when comparing Medial to Lateral

**Table 3-6: Collagen I expression**

	<b>Control</b>	<b>Osteoarthritic</b>	<b>Fold <math>\Delta</math></b>
<b>Overall</b>	<b><math>0.0866 \pm 0.1029</math></b>	<b><math>1.1719 \pm 1.8097 *</math></b>	<b>13.5x</b>
<b>Medial Meniscus</b>	<b><math>0.0802 \pm 0.0739</math></b>	<b><math>1.0016 \pm 1.1005 *</math></b>	<b>12.5x</b>
Anterior Horn	$0.1027 \pm 0.1060$	$1.0881 \pm 1.1097 *$	10.6x
Body	$0.0525 \pm 0.0393$	$0.9676 \pm 1.2862 *$	18.4x
Posterior Horn	$0.0893 \pm 0.0736$	$0.9420 \pm 0.8771 *$	10.6x
<b>Lateral Meniscus</b>	<b><math>0.0927 \pm 0.1263</math></b>	<b><math>1.3263 \pm 2.2680 *</math></b>	<b>14.3x</b>
Anterior Horn	$0.0817 \pm 0.0706$	$1.1116 \pm 1.0079 *$	13.6x
Body	$0.1461 \pm 0.2068$	$2.0679 \pm 3.7650 *$	14.2x
Posterior Horn	$0.0503 \pm 0.0264$	$0.8551 \pm 0.8847 *$	17.0x

\*p<0.05 when comparing OA to Controls; <sup>+</sup>p<0.05 when comparing Medial to Lateral

**Table 3-7: Collagen II expression**

	<b>Control</b>	<b>Osteoarthritic</b>	<b>Fold Δ</b>
<b>Overall</b>	<b>0.0301 ± 0.0903</b>	<b>0.1801 ± 0.6367 *</b>	<b>6.0x</b>
<b>Medial Meniscus</b>	<b>0.0064 ± 0.0102</b>	<b>0.1888 ± 0.7695 *</b>	<b>29.4x</b>
Anterior Horn	0.0013 ± 0.0019	0.3619 ± 1.2898 *	272.9x
Body	0.0053 ± 0.0043	0.1279 ± 0.1950 *	24.2x
Posterior Horn	0.0118 ± 0.0158	0.0604 ± 0.1633	5.1x
<b>Lateral Meniscus</b>	<b>0.0525 ± 0.1229</b>	<b>0.1722 ± 0.4926</b>	<b>3.3x</b>
Anterior Horn	0.0492 ± 0.0735	0.2700 ± 0.7294	5.5x
Body	0.1005 ± 0.2017	0.1090 ± 0.2055	1.1x
Posterior Horn	0.0080 ± 0.0105	0.1252 ± 0.3487	15.6x

\*p<0.05 when comparing OA to Controls; <sup>†</sup>p<0.05 when comparing Medial to Lateral**Table 3-8: Collagen III expression**

	<b>Control</b>	<b>Osteoarthritic</b>	<b>Fold Δ</b>
<b>Overall</b>	<b>0.0843 ± 0.1631</b>	<b>1.4808 ± 2.1544 *</b>	<b>17.6x</b>
<b>Medial Meniscus</b>	<b>0.0682 ± 0.1268</b>	<b>1.1833 ± 1.3159 *</b>	<b>17.4x</b>
Anterior Horn	0.0402 ± 0.0471	1.1567 ± 1.1126 *	28.8x
Body	0.0177 ± 0.0139	1.3805 ± 1.7642 *	78.2x
Posterior Horn	0.1420 ± 0.1977	0.9711 ± 0.8415 *	6.8x
<b>Lateral Meniscus</b>	<b>0.0995 ± 0.1939</b>	<b>1.7504 ± 2.6819 *</b>	<b>17.6x</b>
Anterior Horn	0.0807 ± 0.0989	2.3628 ± 3.1222 *	29.3x
Body	0.1719 ± 0.3246	1.8703 ± 3.1890 *	10.9x
Posterior Horn	0.0459 ± 0.0503	0.9654 ± 1.0868 *	21.0x

\*p<0.05 when comparing OA to Controls; <sup>†</sup>p<0.05 when comparing Medial to Lateral**Table 3-9: Collagen VI expression**

	<b>Control</b>	<b>Osteoarthritic</b>	<b>Fold Δ</b>
<b>Overall</b>	<b>0.0390 ± 0.0310</b>	<b>0.1440 ± 0.1734 *</b>	<b>4.6x</b>
<b>Medial Meniscus</b>	<b>0.0298 ± 0.0288</b>	<b>0.1396 ± 0.1004 *</b>	<b>4.7x</b>
Anterior Horn	0.0357 ± 0.0242	0.1397 ± 0.1157 *	3.9x
Body	0.0253 ± 0.0199	0.1452 ± 0.1080 *	5.7x
Posterior Horn	0.0292 ± 0.0417	0.1327 ± 0.0730 *	4.5x
<b>Lateral Meniscus</b>	<b>0.0322 ± 0.0476</b>	<b>0.1480 ± 0.2205 *</b>	<b>4.6x</b>
Anterior Horn	0.0181 ± 0.0114	0.1373 ± 0.0773 *	7.6x
Body	0.0579 ± 0.0763	0.1978 ± 0.3798 *	3.4x
Posterior Horn	0.0205 ± 0.0232	0.1122 ± 0.0748 *	5.5x

\*p<0.05 when comparing OA to Controls; <sup>†</sup>p<0.05 when comparing Medial to Lateral

**Table 3-10: MMP-1 expression**

	Control	Osteoarthritic	Fold Δ
<b>Overall</b>	<b>0.0007 ± 0.0024</b>	<b>0.0012 ± 0.0044</b>	<b>1.6x</b>
<b>Medial Meniscus</b>	<b>0.0012 ± 0.0033</b>	<b>0.0005 ± 0.0011</b>	<b>0.4x</b>
Anterior Horn	0.0022 ± 0.0048	0.0002 ± 0.0004	0.1x
Body	0.0015 ± 0.0036	0.0006 ± 0.0010	0.4x
Posterior Horn	0.0000 ± 0.0000	0.0008 ± 0.0016	50.3x
<b>Lateral Meniscus</b>	<b>0.0003 ± 0.0009</b>	<b>0.0019 ± 0.0059</b>	<b>5.8x</b>
Anterior Horn	0.0002 ± 0.0004	0.0018 ± 0.0070	7.6x
Body	0.0001 ± 0.0001	0.0021 ± 0.0067	39.2x
Posterior Horn	0.0007 ± 0.0016	0.0017 ± 0.0036	2.5x

\*p<0.05 when comparing OA to Controls; <sup>+</sup>p<0.05 when comparing Medial to Lateral

**Table 3-11: MMP-2 expression**

	Control	Osteoarthritic	Fold Δ
<b>Overall</b>	<b>0.2750 ± 0.1370</b>	<b>0.1803 ± 0.3010 *</b>	<b>0.7x</b>
<b>Medial Meniscus</b>	<b>0.3158 ± 0.1008</b>	<b>0.1506 ± 0.1164 *</b>	<b>0.5x</b>
Anterior Horn	0.3246 ± 0.1262	0.1541 ± 0.1037 *	0.5x
Body	0.3065 ± 0.1136	0.1183 ± 0.1229 *	0.4x
Posterior Horn	0.3178 ± 0.0817 <sup>+</sup>	0.1865 ± 0.1177 *	0.6x
<b>Lateral Meniscus</b>	<b>0.2365 ± 0.1573</b>	<b>0.2072 ± 0.4003 *</b>	<b>0.9x</b>
Anterior Horn	0.1782 ± 0.1025	0.1718 ± 0.2528	1.0x
Body	0.3543 ± 0.1877	0.2982 ± 0.6545	0.8x
Posterior Horn	0.1771 ± 0.1161 <sup>+</sup>	0.1594 ± 0.1241	0.9x

\*p<0.05 when comparing OA to Controls; <sup>+</sup>p<0.05 when comparing Medial to Lateral

**Table 3-12: MMP-3 expression**

	Control	Osteoarthritic	Fold Δ
<b>Overall</b>	<b>0.6137 ± 0.6086</b>	<b>0.0300 ± 0.0405 *</b>	<b>0.05x</b>
<b>Medial Meniscus</b>	<b>0.7098 ± 0.7771</b>	<b>0.0208 ± 0.0198 *</b>	<b>0.03x</b>
Anterior Horn	0.9574 ± 0.9733	0.0237 ± 0.0242 *	0.02x
Body	0.9302 ± 0.8729	0.0230 ± 0.0188 *	0.02x
Posterior Horn	0.2831 ± 0.2726	0.0149 ± 0.0145 *	0.05x
<b>Lateral Meniscus</b>	<b>0.5229 ± 0.3932</b>	<b>0.0382 ± 0.0513 *</b>	<b>0.07x</b>
Anterior Horn	0.3927 ± 0.2485	0.0395 ± 0.0608 *	0.10x
Body	0.6009 ± 0.1673	0.0401 ± 0.0396 *	0.07x
Posterior Horn	0.5751 ± 0.6365	0.0350 ± 0.0520 *	0.06x

\*p<0.05 when comparing OA to Controls; <sup>+</sup>p<0.05 when comparing Medial to Lateral

**Table 3-13: MMP-13 expression**

	<b>Control</b>	<b>Osteoarthritic</b>	<b>Fold Δ</b>
<b>Overall</b>	<b>0.00002 ± 0.00009</b>	<b>0.00158 ± 0.01319 *</b>	<b>100.2x</b>
<b>Medial Meniscus</b>	<b>0.00000 ± 0.00000</b>	<b>0.00052 ± 0.00145 *</b>	<b>∞</b>
Anterior Horn	0.00000 ± 0.00000	0.00030 ± 0.00054 *	∞
Body	0.00000 ± 0.00000	0.00081 ± 0.00228 *	∞
Posterior Horn	0.00000 ± 0.00000	0.00041 ± 0.00064 *	∞
<b>Lateral Meniscus</b>	<b>0.00003 ± 0.00013</b>	<b>0.00256 ± 0.01825 *</b>	<b>83.5x</b>
Anterior Horn	0.00009 ± 0.00023	0.00021 ± 0.00046	2.3x
Body	0.00000 ± 0.00000	0.00015 ± 0.00018 *	∞
Posterior Horn	0.00000 ± 0.00000	0.00734 ± 0.03156 *	∞

\*p&lt;0.05 when comparing OA to Controls; +p&lt;0.05 when comparing Medial to Lateral

**Table 3-14: VEGF expression**

	<b>Control</b>	<b>Osteoarthritic</b>	<b>Fold Δ</b>
<b>Overall</b>	<b>0.6751 ± 1.2867</b>	<b>0.4233 ± 0.6086</b>	<b>0.6x</b>
<b>Medial Meniscus</b>	<b>0.3817 ± 0.4580</b>	<b>0.4777 ± 0.7165</b>	<b>1.3x</b>
Anterior Horn	0.3586 ± 0.4704	0.5184 ± 0.6856	1.5x
Body	0.4065 ± 0.3662	0.6609 ± 0.9389	1.6x
Posterior Horn	0.3763 ± 0.5990	0.2034 ± 0.2070	0.5x
<b>Lateral Meniscus</b>	<b>0.9521 ± 1.7166</b>	<b>0.3740 ± 0.4916 *</b>	<b>0.4x</b>
Anterior Horn	0.4575 ± 0.3031	0.4125 ± 0.4827	0.9x
Body	1.8879 ± 2.8818	0.3555 ± 0.3815	0.2x
Posterior Horn	0.5110 ± 0.2089	0.3494 ± 0.6033 *	0.7x

\*p&lt;0.05 when comparing OA to Controls; +p&lt;0.05 when comparing Medial to Lateral

**Table 3-15: Radiographic measurement**

	Medial (mm)	Lateral (mm)	Fold Δ
<b>OA Joint Space</b>	<b>2.04 ± 2.22 <sup>+</sup></b>	<b>6.58 ± 2.84 <sup>+</sup></b>	<b>3.2x</b>

<sup>+</sup>p<0.05 when comparing Medial to Lateral**Table 3-16: Radiographic total score**

	Control	Osteoarthritic
<b>Overall</b>	<b>0.0 ± 0.0</b>	<b>3.94 ± 1.60 *</b>
<b>Medial Compartment</b>	<b>0.0 ± 0.0</b>	<b>4.79 ± 1.41 **<sup>+</sup></b>
<b>Lateral Compartment</b>	<b>0.0 ± 0.0</b>	<b>3.08 ± 1.32 **<sup>+</sup></b>

\*p<0.05 when comparing OA to Controls; <sup>+</sup>p<0.05 when comparing Medial to Lateral**Table 3-16a: Radiographic osteophyte score**

	Control	Osteoarthritic
<b>Overall</b>	<b>0.0 ± 0.0</b>	<b>1.13 ± 0.61 *</b>
<b>Medial Compartment</b>	<b>0.0 ± 0.0</b>	<b>1.08 ± 0.58 *</b>
<b>Lateral Compartment</b>	<b>0.0 ± 0.0</b>	<b>1.17 ± 0.64 *</b>

\*p<0.05 when comparing OA to Controls; <sup>+</sup>p<0.05 when comparing Medial to Lateral**Table 3-16b: Radiographic narrowing score**

	Control	Osteoarthritic
<b>Overall</b>	<b>0.0 ± 0.0</b>	<b>1.81 ± 0.98 *</b>
<b>Medial Compartment</b>	<b>0.0 ± 0.0</b>	<b>2.42 ± 0.72 **<sup>+</sup></b>
<b>Lateral Compartment</b>	<b>0.0 ± 0.0</b>	<b>1.21 ± 0.83 **<sup>+</sup></b>

\*p<0.05 when comparing OA to Controls; <sup>+</sup>p<0.05 when comparing Medial to Lateral

**Table 3-17: Correlations**

	Gross Score	Histo Arch.	Histo Matrix	Histo Prolif.	Histo Total Score	Water %	GAG Content	Collagen Content	Col 1 Expression	Col 2 Expression
<b>Gross Score</b>		0.37	0.43	0.48	0.51	0.61	0.42	0.48	0.61	X
<b>Histo Architecture</b>	0.37		0.63	0.57	0.89	0.54	0.26	0.23	0.26	X
<b>Histo Matrix</b>	0.43		0.63		0.53	0.83	0.52	X	0.36	0.31
<b>Histo Proliferation</b>	0.48	0.57	0.53		0.81	0.56	0.21	0.26	0.35	X
<b>Histo Total Score</b>	0.51	0.89	0.83	0.81		0.64	0.25	0.33	0.36	X
<b>Water %</b>	0.61	0.54	0.52	0.56	0.64		0.46	0.40	0.50	X
<b>Proteoglycan Content</b>	0.42	0.26	X	0.21	0.25	0.46		X	0.26	0.36
<b>Collagen Content</b>	0.48	0.23	0.36	0.26	0.33	0.40	X		0.45	X
<b>Col 1 Expression</b>	0.61	0.26	0.31	0.35	0.36	0.50	0.26	0.45		0.35
<b>Col 2 Expression</b>	X	X	X	X	X	X	0.36	X	0.35	
<b>Col 3 Expression</b>	0.52	0.22	0.29	0.25	0.30	0.45	0.37	0.47	0.83	0.47
<b>Col 6 Expression</b>	0.43	0.24	0.31	0.26	0.32	0.30	0.21	0.61	0.62	X
<b>MMP-1 Expression</b>	X	X	X	X	X	X	X	X	X	X
<b>MMP-2 Expression</b>	-0.22	X	X	X	X	-0.27	-0.35	-0.40	X	-0.22
<b>MMP-3 Expression</b>	-0.65	-0.31	-0.39	-0.37	-0.42	-0.57	-0.42	-0.41	-0.60	X
<b>MMP-13 Expression</b>	0.37	0.20	0.37	0.23	0.31	0.31	X	0.41	0.24	X
<b>VEGF</b>	X	X	X	X	X	X	X	X	X	0.36
<b>Joint Space</b>	-0.58	-0.20	-0.22	-0.25	-0.29	-0.50	-0.27	X	X	X
<b>XR Osteophyte Score</b>	0.61	0.34	0.43	0.43	0.48	0.56	0.33	0.55	0.62	0.25
<b>XR Narrowing Score</b>	0.79	0.38	0.44	0.43	0.50	0.72	0.50	0.38	0.54	0.28
<b>XR Total Score</b>	0.79	0.39	0.46	0.46	0.52	0.73	0.49	0.44	0.58	0.25

Purple = Strong ( $r \geq 0.6$ )	Green = Moderately Strong ( $0.4 \leq r < 0.6$ )
Red = Relatively Weak ( $0.2 \leq r < 0.4$ )	X = Correlation value less than 0.2 or not significant

**Table 3-17: Correlations (continued)**

	Col 3 Exp.	Col 6 Exp.	MMP-1 Exp.	MMP-2 Exp.	MMP-3 Exp.	MMP-13 Exp.	VEGF Exp.	Joint Space	XR Osteo. Score	XR Nar. Score	XR Total Score
<b>Gross Score</b>	0.52	0.43	X	-0.22	-0.65	0.37	X	-0.58	0.61	0.79	0.79
<b>Histo Architecture</b>	0.22	0.24	X	X	-0.31	0.20	X	-0.20	0.34	0.38	0.39
<b>Histo Matrix</b>	0.29	0.31	X	X	-0.39	0.37	X	-0.22	0.43	0.44	0.46
<b>Histo Proliferation</b>	0.25	0.26	X	X	-0.37	0.23	X	-0.25	0.43	0.43	0.46
<b>Histo Total Score</b>	0.30	0.32	X	X	-0.42	0.31	X	-0.29	0.48	0.50	0.52
<b>Water %</b>	0.45	0.30	X	-0.27	-0.57	0.31	X	-0.50	0.56	0.72	0.73
<b>Proteoglycan Content</b>	0.37	0.21	X	-0.35	-0.42	X	X	-0.27	0.33	0.50	0.49
<b>Collagen Content</b>	0.47	0.61	X	-0.40	-0.41	0.41	X	X	0.55	0.38	0.44
<b>Col 1 Expression</b>	0.83	0.62	X	X	-0.60	0.24	X	X	0.62	0.57	0.58
<b>Col 2 Expression</b>	0.47	X	X	-0.22	X	X	0.36	X	0.25	0.28	0.25
<b>Col 3 Expression</b>		0.69	X	-0.28	-0.54	0.25	0.22	X	0.66	0.53	0.58
<b>Col 6 Expression</b>	0.69		X	-0.31	-0.37	0.35	X	X	0.53	0.45	0.51
<b>MMP-1 Expression</b>	X	X		0.23	X	X	X	X	X	X	X
<b>MMP-2 Expression</b>	-0.28	-0.31	0.23		X	X	-0.24	X	-0.30	-0.23	-0.30
<b>MMP-3 Expression</b>	-0.54	-0.37	X	X		-0.23	X	X	-0.58	-0.59	-0.61
<b>MMP-13 Expression</b>	0.25	0.35	X	X	-0.23		X	X	0.36	0.40	0.40
<b>VEGF</b>	0.22	X	X	-0.24	X	X		X	X	X	X
<b>Joint Space</b>	X	X	X	X	X	X	X		X	-0.90	-0.87
<b>XR Osteophyte Score</b>	0.66	0.53	X	-0.30	-0.58	0.36	X	X		0.59	0.73
<b>XR Narrowing Score</b>	0.53	0.45	X	-0.23	-0.59	0.40	X	-0.90	0.59		0.95
<b>XR Total Score</b>	0.58	0.51	X	-0.30	-0.61	0.40	X	-0.87	0.73	0.95	

Purple = Strong ( $r \geq 0.6$ )	Green = Moderately Strong ( $0.4 \leq r < 0.6$ )
Red = Relatively Weak ( $0.2 \leq r < 0.4$ )	X = Correlation value less than 0.2 or not significant

## References

1. Fithian DC, Kelly MA, Mow VC. Material properties and structure-function relationships in the menisci. *Clinical Orthopaedics and Related Research*. 1990(252):19-31.
2. Andersson-Molina H, Karlsson H, Rockborn P. Arthroscopic partial and total meniscectomy: A long-term follow-up study with matched controls. *Arthroscopy*. 2002;18(2):183-189.
3. Bonneux I, Vandekerckhove B. Arthroscopic partial lateral meniscectomy long-term results in athletes. *Acta Orthopaedica Belgica*. 2002;68(4):356-361.
4. Chatain F, Robinson AHN, Adeleine P, Chambat P, Neyret P. The natural history of the knee following arthroscopic medial meniscectomy. *Knee Surgery, Sports Traumatology, Arthroscopy*. 2001;9(1):15-18.
5. Cicuttini FM, Forbes A, Yuanyuan W, Rush G, Stuckey SL. Rate of knee cartilage loss after partial meniscectomy. *Journal of Rheumatology*. 2002;29(9):1954-1956.
6. Duryea J, Zaim S, Genant HK. New radiographic-based surrogate outcome measures for osteoarthritis of the knee. *Osteoarthritis and Cartilage*. 2003;11(2):102-110.
7. McKinley TO, English DK, Bay BK. Trabecular bone strain changes resulting from partial and complete meniscectomy. *Clinical Orthopaedics and Related Research*. 2003(407):259-267.
8. Wyland DJ, Guilak F, Elliott DM, Setton LA, Vail TP. Chondropathy after meniscal tear or partial meniscectomy in a canine model. *Journal of Orthopaedic Research*. 2002;20(5):996-1002.
9. van Tienen TG, Heijkants RG, de Groot JH, et al. Presence and mechanism of knee articular cartilage degeneration after meniscal reconstruction in dogs. *Osteoarthritis and Cartilage*. 2003;11(1):78-84.
10. Schramm M, Falkai P, Tepest R, et al. Stability of RNA transcripts in post-mortem psychiatric brains. *Journal of Neural Transmission*. 1999;106(3-4):329-335.
11. Yasojima K, McGeer EG, McGeer PL. High stability of mRNAs postmortem and protocols for their assessment by RT-PCR. *Brain Research Protocols*. 2001;8(3):212-218.

12. Kuliwaba JS, Fazzalari NL, Findlay DM. Stability of RNA isolated from human trabecular bone at post-mortem and surgery. *Biochimica et Biophysica Acta - Molecular Basis of Disease*. 2005;1740(1):1-11.
13. Farndale RW, Buttle DJ, Barrett AJ. Improved quantitation and discrimination of sulphate glycosaminoglycans by use of dimethylmethylen blue. *Biochimica et Biophysica Acta - General Subjects*. 1986;883(2):173-177.
14. Reddy GK, Enwemeka CS. A simplified method for the analysis of hydroxyproline in biological tissues. *Clinical Biochemistry*. 1996;29(3):225-229.
15. Freed LE, Hollander AP, Martin I, Barry JR, Langer R, Vunjak-Novakovic G. Chondrogenesis in a cell-polymer-bioreactor system. *Experimental Cell Research*. 1998;240(1):58-65.
16. Tognana E, Chen F, Padera RF, et al. Adjacent tissues (cartilage, bone) affect the functional integration of engineered calf cartilage in vitro. *Osteoarthritis and Cartilage*. 2005;13(2):129-138.
17. Muller PY, Janovjak H, Miserez AR, Dobbie Z. Processing of gene expression data generated by quantitative real-time RT-PCR. *BioTechniques*. 2002;32(6):1372-1379.
18. Vignon E, Piperno M, Le Graverand MPH, et al. Measurement of radiographic joint space width in the tibiofemoral compartment of the osteoarthritic knee: Comparison of standing anteroposterior and Lyon schuss views. *Arthritis and Rheumatism*. 2003;48(2):378-384.
19. Scott Jr WW, Lethbridge-Cejku M, Reichle R, Wigley FM, Tobin JD, Hochberg MC. Reliability of grading scales for individual radiographic features of osteoarthritis of the knee: The Baltimore longitudinal study of aging atlas of knee osteoarthritis. *Investigative Radiology*. 1993;28(6):497-501.
20. Vignon E, Conrozier T, Piperno M, Richard S, Carrillon Y, Fantino O. Radiographic assessment of hip and knee osteoarthritis. Recommendations: Recommended guidelines. *Osteoarthritis and Cartilage*. 1999;7(4):434-436.
21. Kellgren JH LJ. Radiologic assessment of osteoarthritis. *Annals of the Rheumatic Diseases*. 1957;16:494-501.
22. Englund M, Guermazi A, Gale D, et al. Incidental meniscal findings on knee MRI in middle-aged and elderly persons. *New England Journal of Medicine*. 2008;359(11):1108-1115.
23. Baker BE, Peckham AC, Puparo F, Sanborn JC. Review of meniscal injury and associated sports. *American Journal of Sports Medicine*. Jan-Feb 1985;13(1):1-4.

24. Widuchowski W, Widuchowski J, Trzaska T. Articular cartilage defects: Study of 25,124 knee arthroscopies. *Knee*. 2007;14(3):177-182.
25. Swank M, Stulberg SD, Jiganti J, Machairas S. The natural history of unicompartmental arthroplasty: An eight-year follow-up study with survivorship analysis. *Clinical Orthopaedics and Related Research*. 1993(286):130-142.
26. Ghosh P, Taylor TKF. The knee joint meniscus. A fibrocartilage of some distinction. *Clinical Orthopaedics and Related Research*. 1987(224):52-63.
27. Pauli C, Grogan SP, Patil S, et al. Macroscopic And Histopathologic Analysis Of Human Knee Menisci In Aging And Osteoarthritis. *Osteoarthritis and Cartilage*. 19(9):1132-1141.
28. Syal M, Goyal N, Nagi ON, Gupta M. Immunohistochemistry of osteoarthritic meniscus in man. *Bulletin, Postgraduate Institute of Medical Education and Research, Chandigarh*. 2007;41(1):11-16.
29. Le Graverand MPH, Sciore P, Eggerer J, et al. Formation and phenotype of cell clusters in osteoarthritic meniscus. *Arthritis and Rheumatism*. 2001;44(8):1808-1818.
30. Herwig J, Egner E, Buddecke E. Chemical changes of human knee joint menisci in various stages of degeneration. *Annals of the Rheumatic Diseases*. 1984;43(4):635-640.
31. Adams ME, Billingham MEJ, Muir H. The glycosaminoglycans in menisci in experimental and natural osteoarthritis. *Arthritis and Rheumatism*. 1983;26(1):69-76.
32. Ghosh P, Ingman AM, Taylor TK. Variations in collagen, non-collagenous proteins, and hexosamine in menisci derived from osteoarthritic and rheumatoid arthritic knee joints. *Journal of Rheumatology*. 1975;2(1):100-107.
33. Hellio Le Graverand MP, Vignon E, Otterness IG, Hart DA. Early changes in lapine menisci during osteoarthritis development: Part I: Cellular and matrix alterations. *Osteoarthritis and Cartilage*. 2001;9(1):56-64.
34. Greis PE, Bardana DD, Holmstrom MC, Burks RT. Meniscal injury: I. Basic science and evaluation. *The Journal of the American Academy of Orthopaedic Surgeons*. 2002;10(3):168-176.
35. McDevitt CA, Webber RJ. The ultrastructure and biochemistry of meniscal cartilage. *Clinical Orthopaedics and Related Research*. 1990(252):8-18.

36. Upton ML, Chen J, Setton LA. Region-specific constitutive gene expression in the adult porcine meniscus. *Journal of Orthopaedic Research*. 2006;24(7):1562-1570.
37. Wildey GM, Billetz AC, Matyas JR, Adams ME, McDevitt CA. Absolute concentrations of mRNA for type I and type VI collagen in the canine meniscus in normal and ACL-deficient knee joints obtained by RNase protection assay. *Journal of Orthopaedic Research*. 2001;19(4):650-658.
38. Robins SP, Milne G, Duncan A, et al. Increased skin collagen extractability and proportions of collagen type III are not normalized after 6 months healing of human excisional wounds. *Journal of Investigative Dermatology*. 2003;121(2):267-272.
39. Liu SH, Panossian V, Al-Shaikh R, et al. Morphology and matrix composition during early tendon to bone healing. *Clinical Orthopaedics and Related Research*. 1997;(339):253-260.
40. Katsuragawa Y, Saitoh K, Tanaka N, et al. Changes of human menisci in osteoarthritic knee joints. *Osteoarthritis and Cartilage*. 18(9):1133-1143.
41. Shingleton WD, Ellis AJ, Rowan AD, Cawston TE. Retinoic acid combines with interleukin-1 to promote the degradation of collagen from bovine nasal cartilage: Matrix metalloproteinases-1 and -13 are involved in cartilage collagen breakdown. *Journal of Cellular Biochemistry*. 2000;79(4):519-531.
42. Goupille P, Jayson MIV, Valat JP, Freemont AJ. Matrix metalloproteinases: The clue to intervertebral disc degeneration? *Spine*. 1998;23(14):1612-1626.
43. Leeman MF, Curran S, Murray GI. The structure, regulation, and function of human matrix metalloproteinase-13. *Critical Reviews in Biochemistry and Molecular Biology*. 2002;37(3):149-166.
44. Aimes RT, Quigley JP. Matrix metalloproteinase-2 is an interstitial collagenase. Inhibitor-free enzyme catalyzes the cleavage of collagen fibrils and soluble native type I collagen generating the specific 3/4 - and 1/4 -length fragments. *Journal of Biological Chemistry*. 1995;270(11):5872-5876.
45. Veidal SS, Karsdal MA, Vassiliadis E, et al. MMP mediated degradation of type VI collagen is highly associated with liver Fibrosis - Identification and validation of a novel biochemical marker assay. *PLoS ONE*. 2011;6(9).
46. Dodge GR, Jimenez SA. Glucosamine sulfate modulates the levels of aggrecan and matrix metalloproteinase-3 synthesized by cultured human osteoarthritis articular chondrocytes. *Osteoarthritis and Cartilage*. 2003;11(6):424-432.

47. Kowanetz M, Ferrara N. Vascular endothelial growth factor signaling pathways: Therapeutic perspective. *Clinical Cancer Research*. 2006;12(17):5018-5022.
48. Maruotti N, Ribatti D. The role of vascular endothelial growth factor in angiogenesis. *Importancia del factor de crecimiento del endotelio vascular en la angiogenesis*. 2008;16(4):383-386.
49. Patan S. Vasculogenesis and angiogenesis. *Cancer treatment and research*. 2004;117:3-32.
50. Shibuya M, Claesson-Welsh L. Signal transduction by VEGF receptors in regulation of angiogenesis and lymphangiogenesis. *Experimental Cell Research*. 2006;312(5):549-560.
51. Maroudas A. Glycosaminoglycan turn-over in articular cartilage. *Philosophical transactions of the Royal Society of London. Series B: Biological sciences*. 1975;271(912):293-313.
52. Hellio Le Graverand MP, Vignon E, Otterness IG, Hart DA. Early changes in lapine menisci during osteoarthritis development part II: Molecular alterations. *Osteoarthritis and Cartilage*. 2001;9(1):65-72.
53. Zielinska B, Killian M, Kadmiel M, Nelsen M, Haut Donahue TL. Meniscal tissue explants response depends on level of dynamic compressive strain. *Osteoarthritis and Cartilage*. 2009;17(6):754-760.
54. Ishihara G KT, Saito Y, Ishiguro N. Roles of metalloproteinase-3 and aggrecanase 1 and 2 in aggrecan cleavage during human meniscus degeneration. *Orthop Rev (Pavia)*. Oct 10 2009;1(2):10-16.
55. Becker R, Pufe T, Kulow S, et al. Expression of vascular endothelial growth factor during healing of the meniscus in a rabbit model. *Journal of Bone and Joint Surgery - Series B*. 2004;86(7):1082-1087.
56. Wang Y, Yang L, Zhang J, et al. Differential MMP-2 activity induced by mechanical compression and inflammatory factors in human synoviocytes. *MCB Molecular and Cellular Biomechanics*. 2010;7(2):105-114.
57. Tsushima H, Okazaki K, Hayashida M, Ushijima T, Iwamoto Y. CCAAT/enhancer binding protein  $\beta$  regulates expression of matrix metalloproteinase-3 in arthritis. *Annals of the Rheumatic Diseases*. 2012;71(1):99-107.
58. De Klerk BM, Willemsen S, Schiphof D, et al. Development of radiological knee osteoarthritis in patients with knee complaints. *Annals of the Rheumatic Diseases*. 2011.

59. De Seny D, Sharif M, Fillet M, et al. Discovery and biochemical characterisation of four novel biomarkers for osteoarthritis. *Annals of the Rheumatic Diseases*. 2011;70(6):1144-1152.
60. Felson DT, Niu J, Guermazi A, Sack B, Aliabadi P. Defining radiographic incidence and progression of knee osteoarthritis: Suggested modifications of the Kellgren and Lawrence scale. *Annals of the Rheumatic Diseases*. 2011;70(11):1884-1886.
61. Henriksen M, Aaboe J, Bliddal H. The relationship between pain and dynamic knee joint loading in knee osteoarthritis varies with radiographic disease severity. A cross sectional study. *Knee*. 2011.
62. Hoch JM, Mattacola CG, Medina McKeon JM, Howard JS, Lattermann C. Serum cartilage oligomeric matrix protein (sCOMP) is elevated in patients with knee osteoarthritis: A systematic review and meta-analysis. *Osteoarthritis and Cartilage*. 2011;19(12):1396-1404.
63. Honsawek S, Yuktanandana P, Tanavalee A, Saetan N, Anomasiri W, Parkpian V. Correlation between plasma and synovial fluid basic fibroblast growth factor with radiographic severity in primary knee osteoarthritis. *International Orthopaedics*. 2011;1-5.
64. Kawaguchi K, Enokida M, Otsuki R, Teshima R. Ultrasonographic evaluation of medial radial displacement of the medial meniscus in knee osteoarthritis. *Arthritis and Rheumatism*. 2012;64(1):173-180.
65. Murphy SL, Lyden AK, Phillips K, Clauw DJ, Williams DA. Association between pain, radiographic severity, and centrally-mediated symptoms in women with knee osteoarthritis. *Arthritis Care and Research*. 2011;63(11):1543-1549.
66. Ozcakir S, Raif SL, Sivrioglu K, Kucukcakir N. Relationship between radiological severity and clinical and psychological factors in knee osteoarthritis. *Clinical Rheumatology*. 2011;30(12):1521-1526.
67. Saetan N, Honsawek S, Tanavalee A, Tantavisut S, Yuktanandana P, Parkpian V. Association of plasma and synovial fluid interferon- $\gamma$  inducible protein-10 with radiographic severity in knee osteoarthritis. *Clinical Biochemistry*. 2011;44(14-15):1218-1222.
68. Sanghi D, Avasthi S, Mishra A, Singh A, Agarwal S, Srivastava RN. Is radiology a determinant of pain, stiffness, and functional disability in knee osteoarthritis? A cross-sectional study. *Journal of Orthopaedic Science*. 2011;16(6):719-725.

69. Shakoor N, Lee KJ, Fogg LF, et al. The relationship of vibratory perception to dynamic joint loading, radiographic severity, and pain in knee osteoarthritis. *Arthritis and Rheumatism*. 2012;64(1):181-186.
70. Struewer J, Frangen TM, Ishaque B, et al. Knee function and prevalence of osteoarthritis after isolated anterior cruciate ligament reconstruction using bone-patellar tendon-bone graft: long-term follow-up. *International Orthopaedics*. 2011;1-7.
71. Thomas Vangsness C, Burke WS, Narvy SJ, MacPhee RD, Fedenko AN. Human knee synovial fluid cytokines correlated with grade of knee osteoarthritis: A pilot study. *Bulletin of the NYU Hospital for Joint Diseases*. 2011;69(2):122-127.
72. Yusuf E, Bijsterbosch J, Slagboom PE, Rosendaal FR, Huizinga TWJ, Kloppenburg M. Body mass index and alignment and their interaction as risk factors for progression of knees with radiographic signs of osteoarthritis. *Osteoarthritis and Cartilage*. 2011;19(9):1117-1122.
73. Bedson J, Croft PR. The discordance between clinical and radiographic knee osteoarthritis: A systematic search and summary of the literature. *BMC Musculoskeletal Disorders*. 2008;9.

CHAPTER 4:  
CHARACTERIZATION OF MENISCAL PATHOLOGY WITH  
MOLECULAR AND PROTEOMIC ANALYSES

**Experimental purpose and hypothesis**

The meniscus is a complex tissue with key components consisting of water, collagen, proteoglycans, and glycoproteins.<sup>1-3</sup> When the meniscus is damaged, it is inevitable that characteristic alterations of the tissue will occur depending on the type of meniscal insult. Recent technologies have allowed researchers to more broadly analyze tissue alterations on a molecular and proteomic level. The cDNA microarray was developed to evaluate gene expression and detect RNA within tissue after the process of reverse transcription. This allows for a global molecular analysis of the tissue instead of only being able to study isolated genes that were identified by the investigator as relevant. Proteomic analyses have also improved with the addition of mass spectrometry analysis. With a similar principle as microarray technology, mass spectrometry allows for a global proteomic analysis of the tissue. Thus far, these two technologies have been utilized on a limited basis for assessment of menisci. Normal menisci have been compared to hyaline cartilage by means of a cDNA microarray.<sup>4</sup> Microarray analysis was also utilized in a study examining calcium deposition within osteoarthritic menisci.<sup>5</sup> A few recent studies have utilized microarray technology to evaluate the meniscus as it relates to osteoarthritis in murine models.<sup>6,7</sup> Mass spectrometry has been utilized to a lesser degree to evaluate meniscal tissue. One study used mass spectrometry to identify proteins within normal meniscal tissue relative to other tissue types within the body.<sup>8</sup> To our knowledge, no study has been performed utilizing both of these technologies in

conjunction to evaluate normal human meniscal tissue and pathologic human meniscal tissue.

The overall goal of this study was to comprehensively identify molecular and proteomic markers of disease within different cohorts. Toward this goal, the specific aims for this project were: Specific Aim 1: Identify potential molecular trends that exist among aged-normal, meniscectomy, and osteoarthritic meniscal groups via microarray analysis; and Specific Aim 2: Identify potential proteomic trends that exist among aged-normal, meniscectomy, and osteoarthritic meniscal groups via mass spectrometry analysis. Our hypothesis was that meniscal pathology, such as meniscal tears and meniscal degeneration due to osteoarthritis, alters the homeostasis of the meniscus such that molecular and proteomic trends can be identified and correlated with each other to more fully characterize the nature of meniscal disease.

## **Materials and methods**

### *Tissue collection and tissue storage:*

Meniscal tissue collected for the control group was obtained from aged “normal” knee specimens. The tissue was evaluated and recovered by the National Disease Research Interchange organization. Recovery instructions were as follows: (1) recovery of tissue must take place within 24 hours post mortem; (2) no history of meniscal, ACL, or PCL injury; (3) no history of any surgical procedures performed on the knee that tissue is being procured from; (4) ensure there are no meniscal lesions, ACL or PCL disruptions, articular cartilage disruptions, or osteophytes present upon initial evaluation; (5) procure both medial and lateral menisci still intact with the tibial articular cartilage; (6) completely

immerse all tissue within RNAlater®; (7) ship the specimen on dry ice overnight to be further processed within the laboratory. As described in Chapter 3, the 24 hour time limit was established in order to help prevent excessive degradation of RNA once tissue is removed from a living being. Studies indicate that obtaining tissues within 24 hours of death will provide valid data for gene expression outcome measures.<sup>9-11</sup> Once the tissue arrived in the laboratory, the tissue was reassessed to ensure there were minimal to no articular cartilage disruptions, no osteophytes, and the menisci had minimal to no disruptions or degeneration present upon gross examination. Each meniscus (medial and lateral) was separated into their corresponding anterior, medial (body), and posterior sections. One slice of the posterior medial meniscal section was used for this study. The portion obtained was sectioned in a way to remove the red-red zone from the red-white/white-white zone. This was performed by sectioning the peripheral 1/3 of the meniscus from the central 2/3, which consisted of a cut roughly 3 mm from the peripheral rim of the meniscus. The red-white/white-white zone was utilized for this study in order to more closely mimic the type of tissue that would be collected for the meniscectomy groups. The tissue was placed within 1 mL of RNAlater® and stored at -80°C for subsequent molecular and proteomic analyses. Three aged “normal” specimens were collected for this study (Table 4-1).

For the other cohorts, meniscal tissue was obtained from patients that were undergoing meniscal debridement procedures or total knee arthroplasty (TKA) procedures. All procedures were approved by the Institutional Review Board (IRB#1042248) and informed patient consent was obtained before tissue collection. For

the patients undergoing arthroscopy, the ICRS classification system was utilized to grade the amount of cartilage damage present:<sup>12,13</sup>

- 0 – normal
- 1a – fibrillation and/or slight softening
- 1b – additional superficial lacerations and fissures
- 2 – defects extending deeper but less than 50%
- 3a – greater than 50% but not to calcified layer
- 3b – to the calcified layer
- 3c – down to but not through subchondral bone plate
- 3d – blisters present and greater than 50%
- 4a – lesions just through subchondral boneplate
- 4b – deeper defects down into trabecular bone

For the patients undergoing arthroplasty, joint space measurements and the Modified Kellgren and Lawrence (K&L) radiographic grading scale were utilized to determine the grade of cartilage damage.<sup>14</sup> All K&L categories were graded for the medial and lateral compartments separately; then a total score was obtained by adding them together (Chapter 3):

Osteophytes:

- |                            |                                    |
|----------------------------|------------------------------------|
| 0 = none                   | 1 = small (definite) osteophyte(s) |
| 2 = moderate osteophyte(s) | 3 = large osteophyte(s)            |

Narrowing:

- |                   |                                    |
|-------------------|------------------------------------|
| 0 = normal (none) | 1 = minimal but definite narrowing |
| 2 = moderate      | 3 = severe, “bone on bone”         |

Sclerosis:

- |                  |                                    |
|------------------|------------------------------------|
| 0 = no sclerosis | 1 = definite subchondral sclerosis |
|------------------|------------------------------------|

Chondrocalcinosis:

- |            |             |
|------------|-------------|
| 0 = absent | 1 = present |
|------------|-------------|

Osteophytes of tibial spines:

- |            |                      |
|------------|----------------------|
| 0 = normal | 1 = sharpened spines |
|------------|----------------------|

Meniscectomy tissue was collected due to a tear that involved the white-white and red-white zone of the posterior horn of the medial meniscus. The tissue samples were grouped into one of two categories: (1) patients under the age of 40 with an ICRS score

indicating minimal to no articular damage; (2) patients over the age of 50 with an ICRS score indicating moderate to severe articular damage. Three tissue specimens were identified within each category to be included for this study (Table 4-1). Tissue obtained from patients that had undergone a TKA was sectioned in a similar fashion as the normal meniscal tissue. A portion of the posterior medial meniscus was sectioned to remove the red-red zone from the remaining meniscal tissue. Since the meniscal tissue was degenerative due to osteoarthritis, the cut was made roughly 3 mm from the peripheral rim of the meniscus instead of relying on visualizing the meniscus as thirds where the peripheral 1/3 could be sectioned away from the central 2/3. Whatever tissue that remained after cutting away the red/red zone at the 3 mm mark is the tissue that was utilized for analysis in this study. The osteoarthritic tissue was grouped into one of two categories: (1) patients with identifiable medial joint space and a Modified Kellgren and Lawrence radiographic score indicating mild to moderate osteoarthritis; (2) patients with very little medial joint space and a Modified Kellgren and Lawrence radiographic score indicating moderate to severe osteoarthritis. Three tissue specimens were identified from each category to be included within this study (Table 4-1). All tissue samples collected were placed within 1 mL of RNAlater® and stored at -80°C for subsequent molecular and proteomic analyses.

*Microarray analysis:*

RNA was extracted from the stored tissue and treated for DNA contamination utilizing the TriSpin method and Turbo DNA-free kit (Ambion, Austin, TX), respectively, as described in Chapter 3. The only difference was that the lower organic

phase, identified during the Chloroform step of RNA extraction, was saved and stored at -80°C until ready to proceed with the protein extraction protocol.

Before the RNA was amplified, 1 µL of each sample was added to 99 µL of TE buffer (pH 7.8) and utilized for determination of RNA concentration using a RiboGreen® RNA Quantization Kit. Each sample was mixed with 100 µL of the ribogreen dye diluted 1:2000 in TE buffer and RNA concentration was determined by UV spectrophotometry utilizing an internal standard. Next, the mRNA samples were amplified using the MessageAmp Premier RNA Amplification Kit (Ambion, Austin, TX). The first step was reverse transcription to synthesize first strand cDNA. A 5 µL aliquot of mRNA containing 100 ng of mRNA was combined with 5 µL of the First Strand Master Mix, mixed by gentle vortexing, and incubated at 42°C for two hours. Synthesis of second strand cDNA occurred by combining a 20 µL aliquot of the Second Strand Master Mix, gently vortexing, and incubating for 1 hour at 16°C then 10 min at 65°C. In vitro transcription to synthesize biotin-modified aRNA was the next step. A 30 µL aliquot of T7 IVT Master Mix was added to each double-stranded cDNA sample, mixed with gentle vortexing, and incubated at 40°C for 8 hours. The aRNA was purified to remove enzymes, salts, and unincorporated nucleotides. This was accomplished by adding a 60 µL aliquot of aRNA Binding Mix and a 120 µL aliquot of 100% ethanol to each sample within a U-bottom plate, shaken gently for 2 min, and placed on a magnetic stand for 5 min, which allowed the aRNA to bind to the RNA binding beads before aspirating off and discarding the supernatant. A 100 µL aliquot of aRNA Wash Solution was added to each sample, shaken for 1 min, placed on a magnetic stand, then aspiration and discarding of the supernatant occurred once again. This wash cycle was carried out

twice. The purified aRNA was eluted away from the RNA Binding Beads by adding 50  $\mu$ l of preheated aRNA Elution Solution, shaking for 3 min, placing on a magnetic stand, and aspirating the supernatant which contains the eluted aRNA. The aRNA was then quantified using the RiboGreen® RNA Quantization Kit. An equal  $\mu$ g amount of aRNA from each tissue sample within each category (normal, young meniscectomy, older meniscectomy, mild osteoarthritis, and severe osteoarthritis) was combined together so that the 15 total aRNA samples were reduced down to 5 aRNA study group samples, one overall sample for each category being studied. A 20  $\mu$ g amount of biotin labeled amplified RNA was then combined with 8  $\mu$ l of 5X Array Fragmentation Buffer and incubated at 94°C for 35 min. The fragmented aRNA was then stored at -20°C.

The 5 fragmented aRNA samples ( $n=1$  per study category) were then transported to the University of Missouri's DNA core facility for hybridization to the GeneChip Human Genome U133 Plus 2.0 Array (Affymetrix, Santa Clara, CA) according to the manufacturer's protocol. Gene expression data was obtained using an Affymetrix GeneChip Scanner 3000, with the upgrade for high density GeneChips, and GeneChip Operating software. The results available from the microarray procedure provided fold increases or decreases for each human gene between the different subgroups. Initial focus was placed on genes with a 1.5X fold change between at least two out of the five groups.

#### *Proteomics analysis:*

Protein was extracted from the same samples that were used to extract RNA using the TriSpin method. After chloroform was added to the sample suspended in Trizol

Reagent and centrifuged, the upper aqueous phase containing RNA was removed and the lower organic phase was saved, which contained DNA and protein. A 300  $\mu$ L aliquot of 100% ethanol was added to each of the organic phase samples, mixed via inversion, and then centrifuged at 2000 RPM for 5 min. The aqueous phase containing DNA was isolated and discarded. A 1.5 mL aliquot of isopropanol was added, gently vortexed, allowed to sit at room temperature for 10 min, and then centrifuged at 12000 RPM for 10 min. The supernatant was removed and the protein pellet that remained was washed 3 times with 2 mL of wash solution (0.3M guanidine hydrochloride in 95% ethanol). For each wash cycle the protein pellet sat in the wash solution for 20 min before being centrifuged at 7500 RPM for 5 min, then the solution was removed and discarded. A 2 mL aliquot of ethanol was then added to the pellet, vortexed, stored at room temperature for 20 min, then centrifuged at 7500 RPM for 5 min. The pellet was vacuum dried for 10 min then dissolved in a 1% SDS by pipetting.

The EZQ® Protein Quantitation Kit (Molecular Probes, Eugene, OR) was used to quantify the amount of protein in each sample. This was completed by spotting 1  $\mu$ L aliquots of the ovalbumin protein standards and samples on an assay paper. The protein samples were dried; the assay paper was placed in 40 mL of methanol, and gently washed for 5 min. The assay paper was dried again then placed in 40 mL of the EZQ® protein quantitation reagent (Component A), and gently agitated for 30 min. Three, 2 min rinse cycles were performed with a 10% methanol, 7% acetic acid rinse buffer. The assay paper was dried and then analyzed with a fluorescence-based microplate reader. After determining the protein concentration of each sample, a total of 50  $\mu$ g of protein from each sample was precipitated with acetone and the pellet was dissolved in SDS-PAGE

sample buffer. The protein content of each concentrated sample was confirmed using the EZQ® assay.

A pooled sample was then created with 8 µg of each sample within its respective clinical group (normal, young meniscectomy, older meniscectomy, mild osteoarthritis, and severe osteoarthritis). A 25 µL aliquot mixture of 9.375 µL LDS, 3.75 µL reducing buffer, water, and protein solution containing 24 µg of each pooled clinical group was loaded into an 8 cm SDS-PAGE gel. The gel was run at 115 V, 48 mA, 12.5 watts for approximately 1.5 hours. The gel was removed from the cassette and washed three times for 5 min with polisher distilled water; then it was stained overnight with 20 mL of SimplyBlue SafeStain. The gel was washed one more time and then prepared for analysis.

Each lane was cut into 8 equal sections. Each section was cut into smaller 1 mm<sup>3</sup> blocks and placed into one of the wells within a 1 mL 96-well plate. A 500 µL aliquot of 100 mM ammonium bicarbonate buffer was added to each well and agitated for 15 min. Three 15 min wash cycles was performed with a 300 µL wash solution (50 mM ammonium bicarbonate/50% acetonitrile) utilizing gentle agitation. After discarding the wash solution, the gel pieces were rinsed briefly with 300 µL 100% acetonitrile. The rinse solution was discarded then the gel pieces were dehydrated with 300 µL 100% acetonitrile for 20 min with gentle agitation. After discarding the acetonitrile and air-drying the pieces, dithiothreitol (300 µL 10 nM DTT in 100 mM ammonium bicarbonate) was added and incubated for 45 min at 37°C. The DTT solution was removed, then iodoacetamide (300 µL 50 mM IAA in 100 mM ammonium bicarbonate) was added and allowed to react for 45 min in the dark. The IAA was discarded; the gel

pieces were washed with 500 µL of the wash solution for 15 min then rinsed with 500 µL 100% acetonitrile, and dehydrated again with 500 µL 100% acetonitrile for 20 min. The pieces were rehydrated for 2 hours on ice in 30 µL of 0.02 µg/µL trypsin in 40 mM ammonium bicarbonate, 10% acetonitrile, in water. The trypsin solution was then replaced with 30 µL of 40 mM ammonium bicarbonate, 10% acetonitrile, in water; wrapped with aluminum foil, and incubated at 37°C for 18 hours. The plate was centrifuged for 15 sec and then the supernatant (digest solution) was transferred into a new plate and stored on ice. An 8 µL aliquot of extraction solution (60% acetonitrile, 1% formic acid) was added to the digest solution and a 100 µL aliquot of extraction solution was added to the gel pieces and agitated. After a 15 sec centrifugation, the extraction solution was collected and combined with the digest solution. The extraction step was performed again with 50 µL of extraction solution. The pooled digest solution was then frozen with liquid nitrogen and stored at -80°C.

At the University of Missouri's Charles W Gehrke Proteomics Center each digest was analyzed twice (technical replicates). The peptides were separated individually by reversed-phase chromatography coupled to high resolution, high mass accuracy tandem mass spectrometry (LC-MS/MS) on a ThermoFisher Scientific LTQ Orbitrap. Simultaneous identification and quantization was achieved by conducting database searches using the Sorcerer2 Integrated Data Appliance, followed by results parsing using the Scaffold program (Proteome Software, Portland, OR) which incorporated a spectral counting algorithm to produce quantitative data for the identified proteins. The protein quantitative values were analyzed for trends between the different clinical groups.

## **Results**

Meniscal tissue was obtained from three subjects within each cohort being analyzed for this study. Table 4-1 separates the patient's according to category and identifies the patient's age, gender, ICRS score, joint space measurement, and Modified Kellgren and Lawrence radiographic score.

### *Microarray analysis:*

The microarray was able to identify 157 genes that had at least a 1.5x fold change between cohorts. Out of the 157, 26 were repeats, so this left 131 unique genes identified. Of the 131 unique genes, 92 of the genes showed a difference between at least one of the pathologic cohorts and the aged-normal control cohort. Table 4-2 provides an alphabetical list of the genes identified, their respective gene expressions within each group, and their fold change between two groups if the fold change was greater than or equal to 1.5x or less than or equal to 0.67x. Upon further evaluation, 39 genes were found to have potential trends of interest between the aged normal group and the pathologic groups. The genes were categorized into the following subgroups: synthesis (Figure 4-1), vascularity (Figure 4-2), anti-degradation and degradation (Figure 4-3), and signaling pathways (Figure 4-4).

### *Proteomics analysis:*

After the proteins were run on the SDS-PAGE gel, general trends among cohorts could be visualized (Figure 4-5). The LC-MS/MS identified 173 proteins and are organized by molecular weight in Table 4-3. The proteins were evaluated for possible

trends between the aged normal group and the pathologic groups. Fifty-five proteins of interest were subdivided into the following categories: extracellular matrix (ECM) proteins (Figure 4-6), proteins associated with vascularity (Figure 4-7), degradative and potentially anti-degradative proteins (Figure 4-8), cytoskeleton proteins and proteins involved in the glycolysis pathway (Figure 4-9), and proteins associated with signaling (Figure 4-10).

## **Discussion**

Over 6,000 genes and close to 200 proteins (>2700 peptides) have been identified in the meniscus via microarray and proteomic evaluation, respectively.<sup>15,16</sup> When the meniscus undergoes pathological changes, a number of complex events will take place that will alter gene expression and protein synthesis within meniscal tissue. This study was conducted to identify genes and proteins that may be of interest when identifying and characterizing changes within injured menisci. After comparative analyses were conducted between 5 meniscal subgroups, 39 genes and 55 proteins were isolated and categorized according to potential roles in disease mechanisms.

### *Genes and proteins associated with ECM production:*

One major change expected in pathologic menisci is disruption of extracellular matrix. The previous study (Chapter 3) determined that osteoarthritic menisci had increased collagen content along with increased Col 1, Col 2, Col 3, and Col 6 gene expression. The microarray analysis used for the present study support those findings in that the expression levels of Col 1 and Col 2 were again noted to be increased within

injured meniscal tissue. All four pathologic groups had increased expression of these two genes when compared to the aged-normal group. Increased expression of these genes was expected since type I collagen is the predominant collagen in meniscal tissue while type II collagen is found in high concentrations in the inner, nonvascularized portion of menisci.<sup>3,17</sup> What was unexpected was how these two collagens were not identified in high quantities via mass spectrometry. The alpha 3 chain of type I collagen was identified in small quantities, none of the chains of type II collagen were identified, and the protein that had the second highest quantitative value (first was serum albumin) within the meniscal samples was the alpha 3 chain of type VI collagen. Since collagens share considerable homology, it is possible that the proteomic analysis is recognizing one or both of these collagens as a different collagen, possibly as collagen alpha 3 (VI) chain precursor. Two proteins that have associations with type I collagen that were identified were type XII collagen and type 1 procollagen C-proteinase enhancer protein (PCOLCE). Type XII collagen is found in tissues containing fibroblasts and has been described to modify the interactions between collagen I fibrils and the ECM.<sup>18-20</sup> This collagen was identified within the aged-normal group, but very little was present within the younger meniscectomy group and it was absent within the other pathologic groups. When the meniscus is injured, this may be one of the collagens that proteinases destroy immediately and then the meniscus is unable to replace it. PCOLCE functions to cleave type I procollagen so that it can form into a mature triple helical fibril.<sup>21</sup> This protein was increased within all four pathologic groups. Even though the type I collagen protein was not specifically identified, it is reasonable to assume the meniscus attempts to increase production of its main collagen type after it is injured, based on previous work and the

increased gene expression and increase in proteins that participate in its assembly noticed within this study. Unlike the previous study, Col 3 and Col 6 were not identified by the microarray as being increased within the pathologic groups. Cartilage intermediate layer protein 2 (CILP2) on the other hand was increased and the protein created by this gene was described by Bernardo et al to help mediate matrix interactions through associations with collagen VI microfibrils. However, in their mouse osteoarthritic model CILP2 mRNA expression was down-regulated.<sup>22</sup> The study presented here somewhat contradicts Bernardo et al's work since it showed an increased expression of CILP2 in the meniscectomy tissue and the osteoarthritic menisci; however, CILP2 was not identified by mass spectrometry. Mass spectrometry did identify increased amounts of the alpha 1 and alpha 2 chains of type VI collagen within the severe osteoarthritic group. Type VI collagen may be one of the main collagens that the meniscus utilizes for reparative mechanisms. Our previous work (Chapter 3) identified an increased Col 6 gene expression level within osteoarthritic menisci and Wildey et al measured increased Col 6 mRNA levels within menisci post ACL transection.<sup>23</sup>

Our previous study identified an increased amount of proteoglycan content within osteoarthritic menisci. Therefore, a goal of the present study was to identify genes and proteins that could be associated with the increased proteoglycan content. One proteoglycan showed increased gene expression and increased protein levels within all four pathologic groups: osteoglycin (also referred to as mimecan and osteoinductive factor). This proteoglycan had the 5<sup>th</sup> highest quantitative value among the different groups, and its protein levels increased with severity of pathology (osteoarthritic > meniscectomy tissue; meniscectomy tissue from older patients with cartilage

degeneration > meniscectomy tissue from younger patients with minimal cartilage degeneration). Osteoglycin is a keratin sulfate, small leucine-rich proteoglycan (SLRP) that was initially isolated within bone but has also been found within other connective tissues as well.<sup>24-26</sup> This protein can induce ectopic bone formation in the presence of transforming growth factor and has been identified within osteoarthritic cartilage via mass spectrometry.<sup>27,28</sup> Recent findings have indicated that the meniscus becomes calcified during degeneration in association with osteoarthritis; what are relatively unknown are the pathways that initiate the calcium deposition that occurs during this process.<sup>5,29,30</sup> An increase in osteoglycin production may play a significant role in this calcification process of menisci during degeneration. Four other genes potentially involved in the process of bone formation were also found to be increased within the pathologic groups: osteomodulin, bone morphogenetic protein 6 (BMP-6), sulfatase 1, and C-type lectin domain family 3 member B (CLEC3B, also referred to as tetranectin). Osteomodulin (osteoadherin) is another type of SLRP that is expressed by osteoblasts and its expression is restricted to mineralized tissue unlike other SLRPs.<sup>31-33</sup> Osteomodulin expression is up regulated by bone morphogenetic proteins such as BMP-2.<sup>33</sup> The effect of BMP-6 on osteomodulin expression has not been studied; however, BMP-6 does induce bone formation in vivo and some authors have indicated that BMP-6 may have a stronger osteogenic activity than BMP-2 and -7.<sup>34</sup> Extracellular endosulfatases such as sulfatase 1 participate in cell signaling pathways with one mechanism being removal of sulfate groups from heparin sulfate proteoglycans. Sulfatase 1 has been reported to have increased expression in human OA cartilage and findings have suggested they function to enhance BMP signaling in chondrocytes.<sup>35,36</sup>

Tetranectin (CLEC3B) is also found in the ECM and potentially functions in the process of mineralization of bone matrix by binding calcium.<sup>37</sup> These proteins were not identified within the proteomics analysis, but it is plausible to hypothesis that they work synergistically with osteoglycin to induce ossification of meniscal tissue during the degeneration process.

A number of additional SLRPs commonly found within fibrocartilage were also identified during the proteomics analysis: asporin, biglycan, decorin, lumican, fibromodulin, and chondroadherin.<sup>38</sup> Fibromodulin and chondroadherin had a pattern somewhat similar to osteoglycin; however, the other SLRPs had an opposite pattern. Fibromodulin and chondroadherin were associated with slightly higher values in the groups that were associated with cartilage degeneration: older meniscectomy tissue, mild osteoarthritic tissue, and severe osteoarthritic tissue. Fibromodulin and chondroadherin were not increased within the younger meniscectomy group, which did not have significant cartilage pathology. It was intriguing to isolate increased amounts of chondroadherin protein within the groups with cartilage degeneration since it normally binds to type II collagen and this study was able to demonstrate increased Col 2 expression levels.<sup>39</sup> The chondroadherin protein has been isolated in cartilage exposed to inflammatory pathways and appears to impact the complement system along with osteoadherin and fibromodulin.<sup>40-42</sup> Asporin, biglycan, decorin, and lumican were all found to have higher quantitative values in the aged-normal group with decreased levels in the pathologic groups. It is possible that meniscal pathology results in a cascade of events that results in fragmentation of these proteoglycans and these smaller fragments are not recognized effectively by mass spectrometry. Melrose et al helped to confirm this

theory by reporting a consistent increase in fragmentation of decorin within menisci associated with osteoarthritis. They were also able to isolate fragments of biglycan and lumican; however, fibromodulin was not fragmented within the meniscal tissue even though it was fragmented within articular cartilage.<sup>43</sup> Le Graverand et al conducted a rabbit ACL transection study and reported decorin expression to be significantly decreased in medial and lateral menisci at 3 and 8 weeks post transection; however, biglycan expression was increased at 3 and 8 weeks within the medial meniscus.<sup>44</sup> Interestingly, asporin has been found to have increased expression within osteoarthritic articular cartilage and promotes osteoblast collagen mineralization, but in this study asporin gene expression was not significantly different among groups and its protein content was decreased within the pathologic groups.<sup>45,46</sup>

Aggrecan and versican are large aggregating proteoglycans found in fibrocartilage, and both of these are cleaved by aggrecanase-1 (ADAMTS-4) as a part of the arthritic pathway.<sup>38,47,48</sup> Even though aggrecan is one of the main proteoglycans found in meniscal tissue, aggrecan gene expression was not identified as having a fold change greater than 1.5x between two cohorts, and the aggrecan core protein precursor was only identified in small quantities within three out of the five cohorts. As mentioned, versican is also known to be degraded during the progression of osteoarthritis, but it was not identified during the proteomics analysis. However, its gene expression was increased within all the pathologic groups when compared to the aged normal group. It is plausible that this is indicative of an attempted reparative response after injury, but its significance is unknown at this point.

Another gene that was expressed at increased levels within the pathologic groups was dermatopontin. However, the quantitative value for this protein was drastically reduced within the pathologic groups compared to the aged-normal group. Dermatopontin is a small protein found within the ECM that appears to interact with decorin. Studies suggest that dermatopontin and decorin are able to form a complex that binds 3-fold more TGF- $\beta$ 1 than each component individually. Both decorin and dermatopontin can bind type I collagen fibrils and it has been postulated that the complex formed by all three will help anchor TGF- $\beta$  more effectively in the matrix.<sup>49</sup> It is possible that when decorin undergoes fragmentation during the process of meniscal injury, dermatopontin will also be fragmented. Even though the meniscus increases the amount of mRNA produced for this protein, it appears it is unable to produce enough protein to counteract its degradation.

*Genes and proteins associated with vascularity:*

Meniscal pathology is associated with changes in vascularity and this was confirmed in the previous study (Chapter 3) with an increased proliferative response (neovascularization) according to histologic evaluation.<sup>50</sup> Ashraf et al also noted that menisci from knees containing a high degree of chondropathy had increased vascular densities and penetration.<sup>51</sup> When analyzing the microarray and proteomics results; a number of genes and proteins were identified that potentially could be associated with increased vascular responses to injury. One interesting group of genes and proteins isolated was hemoglobin. Hemoglobin alpha 1, hemoglobin beta, and hemoglobin gamma G genes tended to be increased within the groups that had cartilage degeneration

with the severe osteoarthritic group showing much higher expression levels for all three genes and the mild osteoarthritic group showing high levels of expression for alpha and beta chain genes. For the proteomics study, the alpha, beta, and delta chains were present, but not the gamma chain. All three proteins were present at very high levels within the severe osteoarthritic group, but the second highest quantitative value came within the young meniscectomy group and the other cartilage degeneration groups did not have increased values when compared to the aged normal group. It is plausible that the hemoglobin proteins were increased due to the presence of more red blood cells (RBCs) within the meniscus, which would be expected for more severe osteoarthritis with more vascularity and for acute tears of the meniscus that potentially affect the red-red or red-white zones. The question then is whether the RNA and protein isolated from the meniscal tissue is the result of increased RBCs found within the tissue or from the meniscal tissue itself. RBCs do not contain a nucleus, but microarray analysis has demonstrated that circulating RBCs do contain RNA, so it is possible that the RNA present could be coming from the increased presence of RBCs.<sup>52</sup> On the other hand, recent work has demonstrated that other cells besides RBCs will also express hemoglobin. It has been discovered that macrophages will express hemoglobin, and hemoglobin can be isolated within granulation tissue as macrophage invasion occurs.<sup>53</sup> Regardless of the source of hemoglobin RNA and protein found in this study, it is clear that hemoglobin expression and the presence of hemoglobin proteins are involved in the pathologic responses associated with meniscal injuries. A protein related to hemoglobin that also contains a heme group and has oxygen carrying functions is myoglobin. This protein was present within the aged normal control group; however, it followed the

opposite pattern as hemoglobin and was absent within all the pathologic groups. The specific action of myoglobin in the meniscus is unknown and why it potentially is broken down after meniscal injury is also unknown.

The fibronectin protein had some of the highest quantitative values within the pathologic groups. The fibronectin precursor protein and the fibronectin protein were both isolated and found to have high values. The fibronectin gene was not identified, but the fibronectin leucine rich transmembrane protein 2 gene was found to have increased expression in the pathologic groups. Fibronectin is a matrix glycoprotein that is normally found within meniscal tissue and within blood plasma and platelets.<sup>3,54</sup> This protein has also been isolated in synovial fluid as a part of a bound complex with aggrecan in patients that had a meniscal abnormality and pain.<sup>55</sup> Fibronectin fragments have been associated with cartilage chondrolysis, as well as wound healing, and blood clotting pathways.<sup>56,57</sup> Fibronectin is able to cross-link with type I collagen, fibrin, along with other clotting cascade proteins; is able to mediate platelet adhesion; and seems to be associated with newly generated fibroblasts during the early stages of wound healing.<sup>54,58,59</sup> For the study being presented here, it is not clear if the fibronectin proteins are increased because of increased production by meniscal tissue or deposition of fibronectin due to increased vascularity and the inherent response of fibronectin involved in clotting and wound maturation.

Another intriguing finding was the group of proteins that had much higher values within the younger meniscectomy group in comparison to the other pathologic groups and the control group. Three fibrinogen proteins (fibrinogen alpha/alpha-E chain precursor, fibrinogen beta chain precursor, and fibrinogen gamma chain precursor) were

identified to have fairly high quantitative values within the younger meniscectomy group. These proteins had very little, if any, presence within the other pathologic groups, and were not present in the control group. In addition, a protein called transforming growth factor-beta induced protein IG-H3 precursor (TGFBI) followed a similar trend, except it was present in small amounts in the aged control group and it was increased within the other pathologic groups but at lower levels than in the young meniscectomy group. The aquaporin-1 protein followed a similar pattern to TGFBI, but to a lesser degree. Fibrinogen is involved in the last step of the clotting cascade when thrombin converts it into fibrin. It seems reasonable that fibrinogen would be found within the young meniscectomy group as these tears were probably more acute and had some involvement of the red-red or red-white zone. When a meniscal tear involves the peripheral vascular zone, the tissue will respond by forming a fibrin clot at the tear site as an attempt to heal the lesion with a fibrovascular scar.<sup>60</sup> TGFBI is a protein that can be found within platelets and is involved with activation of platelets and induction of thrombus formation on type I collagen.<sup>61</sup> The other protein found to be present in increased amounts within the younger meniscectomy group was aquaporin-1. Aquaporin-1 is a water channel protein within RBCs and also has a function of regulating CO<sub>2</sub> permeability.<sup>62</sup> It would make sense to find additional RBCs in this group as a result of increased access to vascular channels as discussed with respect to hemoglobin protein content. When looking through the microarray data, aquaporin-1 was identified to be increased within all the pathologic groups, but its highest expressions were within the two groups expected to have increased RBCs in the tissue: young meniscectomy and severe osteoarthritis.

Another gene associated with RBCs found to be expressed within the pathologic groups was the Xg blood group protein, which is a RBC surface antigen.<sup>63</sup>

Angiopoietin-like 2 RNA was found to be expressed at higher levels within the pathologic groups when compared to the control group. This protein has been identified in association with inflammatory diseases such as rheumatoid arthritis. The protein can be isolated within the macrophage-like synoviocytes and has been shown to increase inflammation via increased vascular permeability.<sup>64</sup> However, this protein was not isolated within the proteomic analysis. One protein that showed increased values within the control group with little to no presence within the pathologic groups was thrombospondin 1 precursor. Thrombospondin is a protein released from platelets during activation and is a potent antiangiogenic glycoprotein that can also reduce proliferation of different cell lines.<sup>65,66</sup> It would make sense that the meniscal tissue would make efforts to reduce the presence of this protein since it is antiangiogenic and antiproliferative; instead the meniscus appears to work at increasing production of other proteins that are involved with angiogenesis and proliferation.

*Genes and proteins associated with anti-degradation and degradation:*

An important finding within this category was that several proteins that participate in prevention of degradation were found to have much lower quantitative values within the pathologic groups than the control group. It appears that these proteins may be destroyed or cannot be replenished in a timely manner to help counter the degradative nature of meniscal pathology after injury. The extracellular superoxide dismutase precursor protein (SOD3) and the mitochondrial superoxide dismutase

precursor protein (SOD2) were both elevated within the control group, but decreased drastically within the pathologic groups. Reactive oxygen species are commonly produced through cellular metabolism and antioxidants such as superoxide dismutases (SOD) counter the oxygen free radicals produced, thereby protecting tissue such as meniscus from oxidative damage.<sup>67</sup> SOD3 is the predominant SOD in a number of extracellular fluids and reversibly binds to cells via heparin sulphate proteoglycan ligands and also binds to and protects type I collagen.<sup>68-73</sup> SOD3 gene therapy has been utilized within a murine collagen-induced arthritis model and resulted in suppression of joint swelling and deformity, histologically less destruction of cartilage and bone, less infiltration of mononuclear cells, and less proliferation of synovial cells.<sup>74</sup> In a separate in vitro study, SOD was able to protect synovial fluid hyaluronic acid from depolymerizing in the presence of superoxide radicals.<sup>75</sup> It has been identified that osteoarthritic patients will exhibit decreased extracellular SOD levels within their articular cartilage.<sup>76</sup> The study presented here supports the premise of targeting SOD as a potential therapeutic strategy since SOD2 and SOD3 were both decreased within the pathologic groups.

Alpha-1-antichymotrypsin (AACT) precursor and alpha-1-antitrypsin (AAT) precursor are proteins that inhibit neutrophil proteinase activity in extravascular tissues.<sup>77</sup> Both of these proteins were found to have a lower quantitative value within the pathologic groups, which are the groups one would expect to have an increased amount of neutrophil presence. It appears damaged meniscal tissue is unable to increase its production of AACT and AAT to a high enough level to maintain their role of inhibiting proteinase activity. The neutrophil defensin 1 precursor protein followed an opposite

trend. The defensin protein only had increased levels within the osteoarthritic meniscal tissue. Neutrophils utilize defensins to exert rapid and potent microbicidal activities.<sup>78</sup> However, defensins have also been shown to stimulate fibroblast proliferation and increased collagen I, III, VI, and VIII expression.<sup>79</sup> It would be expected that the osteoarthritic groups would contain neutrophils since there is an inflammatory process involved with osteoarthritis; what is unknown is if these defensins lead to degenerative or proliferative responses within pathologic meniscal tissue. When looking through the microarray results, two genes associated with neutrophils were identified. Ectonucleoside triphosphate diphosphoydrolase 1 (ENTPD1) was not expressed at higher levels within the meniscectomy groups, but was found to have increased gene expression for the osteoarthritic tissue (SOA > MOA). ENTPD1 initiates hydrolysis of extracellular ATP that has been released by neutrophils and appears to play an important role in facilitating neutrophil chemotaxis.<sup>80</sup> It is plausible that during the osteoarthritic processes, this protein helps drive the influx of neutrophils and the associated inflammatory mechanisms of disease. The other gene of interest was secretory leukocyte peptidase inhibitor (SLP1). This gene showed highest expression levels within the control group, much less within the meniscectomy groups, and slightly less within the osteoarthritic groups. The protein coded for by this gene inhibits leukocyte elastase; elastase is secreted by neutrophils and macrophages during inflammation and will destroy surrounding tissue.<sup>81,82</sup> It appears the pathologic groups down regulate this gene when meniscal tissue is disrupted, which seems counterintuitive.

An unexpected finding was the number of proteins associated with the immune system that seem to play roles in meniscal pathology: clusterin precursor, complement C4

precursor, complement factor B precursor, Ig kappa chain C region, Ig kappa chain V-IV region precursor, Ig kappa chain V-III region, Ig lambda chain C region, and Ig gamma-1 chain C region. Each protein identified appeared to have higher quantitative values within the control group and decreased values within the pathologic groups. Clusterin, also called apolipoprotein J, is able to bind to complement components and immunoglobulins and has a number of functions, one of which is inhibition of complement-mediated cell lysis.<sup>83</sup> Complement C4 is associated with the classical pathway of the complement system and complement factor B is associated with the alternate pathway. Immunoglobulins are antibodies used to recognize foreign objects so that they can be neutralized. We postulate that the decreased immune system protein levels within the pathologic groups may be due to consumption during the disease progression. Another possibility is that the affected cells are attempting a shift toward a state of synthesis instead of degredative breakdown. One piece of data that could support the latter theory was an increased complement factor I gene expression level within all the pathologic groups, especially the severe osteoarthritic group. This protein functions to cleave the C3b and C4b complement components. The injured tissue may be trying to increase its production of complement factor 1 with the goal of slowing down the progression of the complement system.

Galectin-1 protein had increased quantitative values within the pathologic groups. It was not expressed in the control group; however, it was present within each pathologic group and had an increasing trend: YM < OM < MOA < SOA. It has been proposed that galectin-1 may lead to inhibition of chondrocyte proliferation and anabolic gene expression while it stimulates catabolic processes such as cartilage matrix degradation.<sup>84</sup>

Due to the increasing trend of galectin-1 found within the pathologic groups, it is reasonable to presume that galectin-1 may also stimulate meniscal matrix degradation. Unlike galectin-1, ribonuclease 4 precursor was another protein found to have much higher levels within the control group. Ribonucleases catalyze the degradation of RNA; however, it is unclear why this protein was greatly reduced within all the pathologic groups.

Three additional genes identified to be increased within all four pathologic groups when compared to the control group were the following: secreted frizzled-related protein 2; tumor necrosis factor (ligand) superfamily, member 10 (TNFSF10); and inhibin, beta A (activin A). The secreted frizzled-related protein 2 may play a role in cellular resistance to apoptosis.<sup>85</sup> On the other hand, the protein produced by the TNFSF10 gene preferentially induces apoptosis in transformed cells, but does not appear to destroy normal cells.<sup>86</sup> In theory, the first gene could potentially work to protect healthy meniscal cells while the second gene works to induce death of meniscal cells that are damaged. Inhibin, beta A was the third gene of interest. This gene has identical mRNA as erythroid differentiation factor (activin A) and this molecule may help suppress aggrecanase-mediated cleavage of aggrecan.<sup>87</sup>

*Genes and proteins associated with the cytoskeleton:*

A number of cytoskeletal components were identified in this study within the microarray and proteomic analyses. Vimentin, an intermediate filament larger than microfilaments such as actin and smaller than microtubules and myosin, was identified within both analyses. Vimentin's gene expression was elevated within all four pathologic

groups and its quantitative protein value was elevated within all four pathologic groups as well. When comparing the pathologic groups, the meniscectomy groups had slightly higher gene expression values than the osteoarthritic groups; in addition they had much higher protein quantities, especially within the young meniscectomy group. Since vimentin is a cytoskeleton protein, Hellio Le Graverand et al utilized this protein to evaluate what cellular changes occur in a meniscus after ACL transection. Utilizing antibodies that stain for vimentin filaments, they identified increased cellular proliferation within osteoarthritic menisci, the cells migrated into clusters, and their morphology changed from stellate to round.<sup>88</sup> The present study is the first to report increased production of vimentin within torn menisci in addition to osteoarthritic menisci.

The tubulin polymerization-promoting protein family member 3 gene is involved in microtubule formation and was found to be increased within all four pathologic groups, but was not isolated within the proteomics analysis. Actin 1 and actin 2 were two cytoskeleton proteins that were found to have increased protein values within the pathologic groups. Unlike vimentin, the two actin proteins were only slightly increased within the older meniscectomy and osteoarthritic groups when compared to the aged normal group. However, these two proteins were quite elevated in the younger meniscectomy group. The myosin light chain alkali protein and the transgelin 2 protein, an actin cross-linking protein, were not identified in the aged normal group and had little to no presence within the older meniscectomy and osteoarthritic groups; but, these two cytoskeleton proteins were also elevated in the younger meniscectomy group just like actin. These findings showed some consistency with the work by Mesih et al where they found that patients with meniscal tears who were older than 40 had lower meniscal

cellularity than in patients younger than 40.<sup>89</sup> The younger meniscectomy group for this study contained patients younger than 40 years and this group had increased cytoskeleton proteins relative to the older meniscectomy group, the osteoarthritic groups, and the aged normal group. Increased cytoskeleton proteins as represented by this study may act as a marker of increased cellular density for meniscal pathology; this would need to be further studied for confirmation.

*Genes and proteins associated with signaling and energy pathways:*

In this study, the following genes associated with energy pathways were upregulated within all four pathologic groups: (1) adenylate cyclase 7 (catalyzes formation of cyclic AMP from ATP, cAMP activates protein kinase A which activates phosphorylase kinase, then glycogen phosphorylase is activated causing glycogen degradation); (2) calmodulin 1 also named phosphorylase kinase, delta (stimulates glycogen breakdown into glucose); (3) and phosphoglucomutase 2-like 1 (involved in starch and sucrose metabolism). When looking at the proteomics analysis, the following four proteins were found to be increased within the pathologic groups and all play a role within the glycolysis pathway: (1) enolase 1; (2) glyceraldehyde 3-phosphate dehydrogenase; (3) L-lactate dehydrogenase A chain; (4) and phosphoglycerate mutase 1. When the meniscus is injured, free forms of energy are needed in order to help drive other pathways such as tissue remodeling. Not only are free energy molecules needed, additional hormones also play a role when working to increase metabolic activity. The deiodinase, iodothyronine, type II gene functions to form a protein that activates thyroid hormones and was increased within all pathologic groups. The transthyretin precursor

protein transports thyroid hormones and was found to be increased within the older meniscectomy group and osteoarthritic groups. Thyroid hormones are responsible for the regulation of metabolism within tissues and it appears these hormones may be playing a role in meniscal pathology especially when cartilage degradation is present. A study on end stage osteoarthritic fat pads also demonstrated a significant upregulation of genes involved in metabolism including the thyroid hormone responsive spot gene.<sup>90</sup>

Carbonic anhydrase proteins function in a reversible reaction involving carbon dioxide and water. Three of these carbonic anhydrases were identified in the proteomics analysis. Carbonic anhydrase I and II were both found to be increased within the osteoarthritic groups, especially the severe osteoarthritic group, and were found in either low quantities or not at all within the other groups. Carbonic anhydrase III was only identified within the aged normal group and was not present within the pathologic groups. Two other proteins isolated within the meniscus that appear to be associated with cartilage degeneration were the serine protease HTRA1 precursor protein (regulates insulin growth factor availability) and the fatty acid-binding protein (involved in fatty acid metabolism). One additional protein that appeared to be increased within the meniscal pathologic groups when compared to the aged normal group was annexin A2, which plays a role in signal transduction pathways. For the microarray analysis, ten additional genes potentially involved in important meniscal signaling pathways were increased within all four pathologic groups in comparison to the aged normal group: (1) sphingomyelin synthase 2; (2) tetraspanin 2; (3) adenylosuccinate synthase; (4) Kallmann syndrome 1 sequence; (5) FBJ murine osteosarcoma viral oncogene homolog B; (6) v-fos FBJ murine osteosarcoma viral oncogene homolog; (7) four and a

half LIM domains 1; (8) cell cycle progression 1; (9) UDP-N-acetyl-alpha-D-galactosamine:polypeptide N-acetylgalactosaminyltransferase 7; (10) and UDP-N-acetyl-alpha-D-galactosamine:polypeptide N-acetylgalactosaminyltransferase-like 1.

*Limitations:*

The main limitation of this study was the one value obtained for each cohort. Each group consisted of three samples that were combined together to form one pooled sample per group. The goal of this study was to isolate trends between different pathologic groups and the aged normal group; however, the trends isolated in this study would be more impactful if the three samples per group were kept isolated so that rigorous comparison statistical analyses could have been conducted among cohorts. In addition, it was noted that gene expression values did not always correlate with protein production. There are a number of plausible reasons why a disconnect may exist between mRNA and protein levels. When a gene produces mRNA, the mRNA may be unstable immediately after a ribosome translates the mRNA into a protein. The unstable nature of the mRNA may be intrinsic to that particular mRNA, or pathologic events may increase specific exosome activities of the cell resulting in mRNA degradation. Both pathways may allow for adequate measurement of protein levels if the protein is fairly stable, but the mRNA levels may not correlate. On the other hand, after mRNA transcription, the mRNA may be very stable; however, the protein that is translated from the mRNA may be unstable. The protein may naturally have a short half-life resulting in lower measurable levels, or pathologic events may lead to enzymatic breakdown of the protein soon after it has been translated. Because of the potential disconnects that may occur, it

is important to refrain from assuming high mRNA levels automatically correlates with increased protein content and vice versa. Additional studies analyzing the genes and proteins identified here will need to be performed in order to determine the validity and clinical applicability of these initial results.

## Conclusions

The meniscus undergoes a number of unique changes when subject to pathologic events. As expected, the pathologic tissue showed signs of a haphazard attempt to increase production of extracellular matrix components. The work from this study correlated with our previous study with respect to identifying an increase for certain collagens. One of the novel findings from this study was how osteoglycin may be one of the main proteoglycans accounting for the increased total proteoglycan content that was identified within the pathologic tissue in our previous study. We postulate that this protein likely plays a significant role in ossification of meniscal tissue during the degeneration process. A number of other proteoglycans were also identified, but unlike osteoglycin, both gene and protein levels were not consistently elevated. Osteoglycin has the potential of being a biomarker for meniscal pathology. When analyzing markers for vascularity, hemoglobin and fibronectin were also identified as potential biomarkers. Hemoglobin gene expression and protein levels were increased within the meniscal pathology groups. Fibronectin was elevated and identified as one of the more prevalent proteins within pathologic menisci. Cytoskeleton proteins such as vimentin also have potential of being valuable biomarkers; vimentin was found to have increased gene expression and protein levels within all pathologic groups. In addition, this study was

able to identify a protein of potential therapeutic value. Superoxide dismutases have been described as being depleted during pathologic events that result in reactive oxygen species; this study confirmed that pathologic meniscal tissue will also have minimal levels of SOD. Treatment strategies should be built around increasing the presence of SOD or other free radical scavengers within the joint after an intra-articular injury occurs.

These data provide novel molecular and biochemical information for the investigation of meniscal pathology. To our knowledge, these types of meniscal pathological events have not been characterized with the use of microarray and proteomic mass spectrometry analyses. This study has provided an abundant amount of data, which help to provide a critical understanding of the natural alterations that occur when this fibrocartilage is insulted. Determining and characterizing pathways that are involved in the disruptive nature of meniscal pathology is extremely important. By comparing and correlating the various measures of pathology, definitive indicators of disease presence and severity can be determined. Defining these indicators will allow us to begin to develop algorithms for comprehensive and accurate diagnostic, therapeutic, and prognostic strategies for meniscal disorders in clinical patients.

**Table 4-1: Patient information**

Group	Age (years)	Gender	ICRS Score	Joint Space (mm)	X-Ray Score
AN	64				
AN	70				
AN	78				
YM	28	Male	1a		
YM	33	Male	0		
YM	36	Female	1a		
OM	53	Female	4a		
OM	53	Male	3c		
OM	57	Male	3a		
MOA	44	Male		4	2/18
MOA	59	Male		6.2	2/18
MOA	61	Female		2	4/18
SOA	50	Female		0.6	7/18
SOA	68	Female		0.5	6/18
SOA	69	Male		0.6	12/18

**AN** = Aged normal

**YM** = Posterior medial meniscectomy, younger patients, minimal articular damage

**OM** = Posterior medial meniscectomy, older patients, moderate to severe articular damage

**MOA** = Posterior medial OA meniscus, joint space > 1 mm, mild to moderate radiographic score

**SOA** = Posterior medial OA meniscus, joint space < 1 mm, moderate to severe radiographic score

**Table 4-2: Microarray analysis**

Gene Description														
AN (1)	YM (2)	OM (3)	MOA (4)	SOA (5)	1/2	1/3	1/4	1/5	2/3	2/4	2/5	3/4	3/5	4/5
				actin, alpha, cardiac muscle 1					0.64					
8.95	6.42	8.64	10.02	8.55										
				ADAM metallopeptidase domain 12										
6.67	10.34	7.84	6.28	8.18	0.65					1.64				
				ADAM metallopeptidase domain 12										
6.99	10.66	8.19	6.49	8.29	0.66					1.64				
				adenylate cyclase 7										
5.82	9.69	7.61	7.68	9.09	0.6			0.64						
				adenylosuccinate synthase										
6.41	9.76	9.35	8.95	9.5	0.66									
				ADP-ribosylation factor-like 4C										
10.54	10.29	5.85	6.08	9.2		1.8	1.73		1.76	1.69		0.64	0.66	
				AF4/FMR2 family, member 3										
6.38	8.83	9.86	10.04	8.93		0.65	0.64							
				aldehyde dehydrogenase 1 family, member A2										
8.28	6.5	9.85	10.35	8.49					0.66	0.63				
				angiopoietin-like 2										
6.51	9.86	9.96	10.38	9.89	0.66	0.65	0.63	0.66						
				ankylosis, progressive homolog (mouse)										
6.81	10.24	10.05	9.85	9.5	0.66									
				aquaporin 1 (Colton blood group)										
7.43	10.78	9.6	10.08	11.45				0.65						
				B-cell CLL/lymphoma 2										
5.86	8.64	9.43	9.39	7.58		0.62	0.62							
				beta-1,3-N-acetylgalactosaminyltransferase 2										
5.78	8.27	7.62	7.87	8.68				0.67						
				bone morphogenetic protein 6										
6.17	9.67	8.83	7.86	8.7	0.64									
				brain abundant, membrane attached signal protein 1										
10.43	10.09	6.11	7.24	10.48		1.71			1.65			0.58		
				C1q and tumor necrosis factor related protein 7										
6.01	7.51	8.1	9.48	8.24			0.63							
				calmodulin 1 (phosphorylase kinase, delta)										
7.17	10.26	9.7	9.87	10.92				0.66						
				carbonic anhydrase XII										
9.55	10.16	6.73	6.62	8.85					1.51	1.53				
				carbonic anhydrase XII										
9.57	9.86	6.23	6.31	8.64		1.54	1.52		1.58	1.56				
				carbonic anhydrase XII										
9.61	9.55	5.91	6.33	8.21		1.63	1.52		1.62	1.51				
				cartilage intermediate layer protein 2										
7.44	10.08	11.74	11.84	10.69		0.63	0.63							
				cathepsin D										
7.61	6.81	10.01	10.22	8.7					0.67					
				CD163 molecule										
8.02	9.38	6.41	7.01	10.13								0.63		
				CD163 molecule										
8.83	9.25	6.48	7.08	9.94								0.65		
				CD58 molecule										
5.97	8.28	7.84	7.64	9.02				0.66						
				CDC28 protein kinase regulatory subunit 2										
7.13	8.96	7.13	5.67	7.54						1.58				
				cell cycle progression 1										
6.12	9.45	9.72	9.61	9.09	0.65	0.63	0.64							

**Table 4-2: Microarray analysis (continued)**

Gene Description														
AN (1)	YM (2)	OM (3)	MOA (4)	SOA (5)	1/2	1/3	1/4	1/5	2/3	2/4	2/5	3/4	3/5	4/5
chemokine (C-X-C motif) ligand 14														
6.02	8.97	10.91	7.44	10.27		0.55		0.59						
chromosome 14 open reading frame 147														
5.85	8.83	8.41	8.38	9.06	0.66			0.65						
chromosome 18 open reading frame 1														
6.84	10.51	9.71	10.02	9.96	0.65									
coiled-coil domain containing 80														
5.89	9.43	9.21	8.08	8.79	0.62	0.64								
collagen triple helix repeat containing 1														
10.77	12.46	9.44	7.86	10.36							1.59			
collagen, type I, alpha 1														
6.99	11.66	9.64	8.57	10.99	0.6			0.64						
collagen, type II, alpha 1														
8.04	11.77	13.49	12.44	12.31		0.6	0.65	0.65						
collagen, type IV, alpha 1														
6.39	7.13	6.66	6.92	9.65				0.66						
collagen, type XIV, alpha 1														
7.72	9.1	6	8.72	11.05					1.52				0.54	
complement component 1, q subcomponent, C chain														
7.19	8.64	6.52	6.97	10.37									0.63	
complement component 3														
7.77	7.17	9.75	6.1	7.17								1.6		
complement factor I														
5.97	8.1	8.55	8.15	9.84				0.61						
C-type lectin domain family 2, member B														
9.25	8.72	6.31	6.49	9.69									0.65	
C-type lectin domain family 3, member B														
8.15	12.18	11.68	11.37	12.8				0.64						
cyclin-dependent kinase 6														
5.83	9.23	8.36	6.65	8.32	0.63									
cystin 1														
5.81	8.07	7.53	8.72	7.82			0.67							
cytochrome b-245, beta polypeptide														
5.81	8.35	6.43	6.28	10.01				0.58					0.64	0.63
deiodinase, iodothyronine, type II														
5.7	10.29	9.91	9.76	9.49	0.55	0.58	0.58	0.6						
delta/notch-like EGF repeat containing														
9.98	8.25	10.18	6.3	7.95			1.59					1.62		
dermatopontin														
7.29	10.88	10.8	10.3	11.47				0.64						
dickkopf homolog 3 ( <i>Xenopus laevis</i> )														
6.86	10.78	8.28	9.42	11	0.64			0.62						
Duffy blood group, chemokine receptor														
7.2	5.88	8.22	7.23	9.1							0.65			
ectonucleoside triphosphate diphosphohydrolase 1														
6.77	6.3	6.35	7.78	9.53							0.66		0.67	
ependymin related protein 1 (zebrafish)														
5.84	8.12	8.03	7.54	9.72				0.6						
family with sequence similarity 102, member B														
6.05	9.31	7.87	8.34	9.19	0.65			0.66						
FBJ murine osteosarcoma viral oncogene homolog B														
7.47	9.29	11.86	11.8	12.29		0.63	0.63	0.61						
Fc fragment of IgE, high affinity I, receptor for: gamma polypeptide														
7.23	9.08	6.71	6.96	10.08									0.67	

**Table 4-2: Microarray analysis (continued)**

Gene Description														
AN (1)	YM (2)	OM (3)	MOA (4)	SOA (5)	1/2	1/3	1/4	1/5	2/3	2/4	2/5	3/4	3/5	4/5
fibrillin 1														
5.9	8.82	7.49	7.7	8.93				0.66						
fibronectin leucine rich transmembrane protein 2														
6.08	8.25	7.14	6.86	9.99				0.61						
four and a half LIM domains 1														
6.94	9.65	10.78	10.45	10.85		0.64	0.66	0.64						
G0/G1switch 2														
7.75	7.49	10.17	7.24	6.67										1.52
glutamate-ammonia ligase (glutamine synthetase)														
10.39	7.88	6.67	7	8.62		1.56								
gremlin 1, cysteine knot superfamily, homolog (Xenopus laevis)														
9.74	5.68	10.18	10.45	7.21	1.71				0.56	0.54				
hemicentin 1														
6.12	10.34	7.68	8.06	10.3	0.59			0.59						
hemoglobin, alpha 1														
7.87	6.8	8.37	11.96	12.76			0.66	0.62		0.57	0.53			0.66
hemoglobin, alpha 1														
8.29	7.32	8.6	12.48	13.7			0.66	0.61		0.59	0.53			0.63
hemoglobin, alpha 1														
8.34	6.96	8.52	12.49	13.45				0.62		0.56	0.52			0.63
hemoglobin, alpha 1														
8.42	7.09	8.89	12.85	13.76			0.65	0.61		0.55	0.51			0.65
hemoglobin, alpha 1														
8.45	7.39	8.72	12.53	13.82			0.61		0.59	0.53				0.63
hemoglobin, alpha 1														
10.11	7.95	9.5	13.85	14.37					0.57	0.55				0.66
hemoglobin, beta														
7.61	7.13	8.91	11.72	13.7			0.65	0.56		0.61	0.52			0.65
hemoglobin, beta														
8.2	7.69	9.46	12.05	13.64			0.6		0.64	0.56				
hemoglobin, beta														
8.43	7.74	9.49	12.01	14			0.6		0.64	0.55				
hemoglobin, gamma A														
6.59	6.05	6.88	6.95	9.19										0.66
hemoglobin, gamma G														
6.56	6.31	6.89	7.71	10.45			0.63			0.6				0.66
hemoglobin, gamma G														
6.91	6.13	6.97	7.99	9.88										0.62
hepatic leukemia factor														
5.88	7.75	9.38	8.94	8.41		0.63	0.66							
inhibin, beta A														
7.34	11.6	10.97	10.22	10.49	0.63									
insulin-like growth factor 1 (somatomedin C)														
6.2	8.82	6.75	7.2	10.15			0.61							0.67
insulin-like growth factor 1 (somatomedin C)														
6.99	8.32	5.92	6.75	9.13										0.65
insulin-like growth factor binding protein 3														
7.41	8.38	9.49	5.74	8.23										1.65
insulin-like growth factor binding protein 3														
10.26	10.8	11.82	7.76	10.26										1.52
integral membrane protein 2A														
6.55	5.88	8.01	8.59	9.02										0.65
integrin, alpha 9														
6.65	7.74	6.08	7.98	9.38										0.65

**Table 4-2: Microarray analysis (continued)**

Gene Description														
AN (1)	YM (2)	OM (3)	MOA (4)	SOA (5)	1/2	1/3	1/4	1/5	2/3	2/4	2/5	3/4	3/5	4/5
integrin, alpha M (complement component 3 receptor 3 subunit)														
6.08	7.58	6.07	5.85	8.88										0.66
Kallmann syndrome 1 sequence														
5.91	9.49	9.98	9.79	8.69	0.62	0.59	0.6							
KIAA1881														
6.43	5.78	8.69	6.27	5.95					0.67					
kinesin family member 5C														
6.01	9.62	7.96	7.17	7.85	0.62									
laminin, beta 1														
9.92	8.73	5.75	6.9	9.41		1.72			1.52					0.61
leucine rich repeat containing 17														
7.05	10.23	6.3	6.24	8.04					1.62	1.64				
leucine rich repeat containing 8 family, member C														
6.63	10.09	8.42	8.52	9.32	0.66									
lipoprotein lipase														
6.91	6.6	9.98	7.34	8.64					0.66					
lysozyme (renal amyloidosis)														
7.14	11.33	6.86	6.54	10.6	0.63				1.65	1.73				0.65
major histocompatibility complex, class II, DQ beta 1														
6.1	8.07	5.89	6.15	8.93										0.66
major histocompatibility complex, class II, DR alpha														
6.16	10.53	6.85	7.6	11.47	0.58			0.54	1.54					0.6
major histocompatibility complex, class II, DR alpha														
6.92	10.71	7.06	7.77	11.24	0.65			0.62	1.52					0.63
mannose receptor, C type 1														
6.32	8.06	6.5	6.87	9.6				0.66						
matrix metallopeptidase 2 (gelatinase A, 72kDa gelatinase, 72kDa type IV collagenase)														
13.15	11.66	8.69	9.86	12.17		1.51								
matrix metallopeptidase 9 (gelatinase B, 92kDa gelatinase, 92kDa type IV collagenase)														
7.31	6.04	6.59	6.48	9.29						0.65				
melanoma cell adhesion molecule														
8.22	6.57	8.72	8.72	9.87						0.67				
melanoma cell adhesion molecule														
8.36	5.75	8.46	8.46	9.72						0.59				
membrane-spanning 4-domains, subfamily A, member 6A														
6.01	8.33	6.03	5.89	9.38			0.64							0.64
membrane-spanning 4-domains, subfamily A, member 6A														
6.66	8.69	6.47	6.28	9.49										0.66
membrane-spanning 4-domains, subfamily A, member 6A														
6.71	9.02	6.18	6.59	9.56										0.65
microfibrillar associated protein 5														
5.73	7.39	7.94	6.33	10.96			0.52							0.58
microsomal glutathione S-transferase 1														
7.97	6.15	9.45	8.19	8.98				0.65						
multiple inositol polyphosphate histidine phosphatase, 1														
5.76	9.05	8.45	7.67	7.79	0.64									
myosin, heavy chain 11, smooth muscle														
8.23	6.94	8.23	8.23	10.42						0.67				
nuclear receptor subfamily 2, group F, member 2														
7.75	6.46	8.29	8.22	10.02						0.64				
olfactomedin-like 2A														
7.67	6.53	7.51	9.3	10.05						0.65				
osteoglycin														
8.28	12.6	13.4	12.63	11.92	0.66	0.62	0.66							

**Table 4-2: Microarray analysis (continued)**

Gene Description														
AN (1)	YM (2)	OM (3)	MOA (4)	SOA (5)	1/2	1/3	1/4	1/5	2/3	2/4	2/5	3/4	3/5	4/5
osteomodulin														
6.2	9.26	11.62	10.71	9.8		0.53	0.58	0.63						
osteomodulin														
6.62	8.91	11.25	10.35	9.26		0.59	0.64							
overexpressed in colon carcinoma-1														
5.89	8.92	8.53	7.2	8.38	0.66									
paraneoplastic antigen MA2														
5.68	7.17	8.14	7.32	8.54				0.66						
periostin, osteoblast specific factor														
10.53	11.96	8.1	6.28	10.8		1.68			1.9					0.58
periostin, osteoblast specific factor														
12.68	13.93	10.64	8.64	12.86						1.61				
phosphoglucomutase 2-like 1														
6.36	9.54	8.59	9.07	9.21	0.67									
plasmalemma vesicle associated protein														
7.22	5.81	7.1	7.31	9.02							0.64			
platelet/endothelial cell adhesion molecule														
7.98	6.64	7.94	8.41	10.34							0.64			
pleckstrin homology-like domain, family A, member 1														
5.89	8.59	7.75	8.04	9.12				0.65						
plexin domain containing 1														
6.85	7.41	5.81	6.85	9.25										0.63
plexin domain containing 1														
7.45	8.41	5.7	7.61	9.15										0.62
potassium voltage-gated channel, KQT-like subfamily, member 5														
6.35	8.7	9.76	9.2	8.12		0.65								
prostate androgen-regulated transcript 1														
7.04	9.33	10.72	9.1	8.82	0.66									
RAS, dexamethasone-induced 1														
9.54	6.65	9.77	9.99	9.21						0.67				
RAS-like, estrogen-regulated, growth inhibitor														
5.7	8.38	9.29	9.51	9.1	0.61	0.6	0.63							
sarcolipin														
5.95	8.86	7.69	6.35	9.23				0.64						
scavenger receptor class A, member 5 (putative)														
6.59	6.37	7.91	7.06	10.05				0.66			0.63			
secreted frizzled-related protein 2														
6.05	5.82	6.78	7.75	10.3				0.59		0.57	0.66			
secreted frizzled-related protein 4														
6.3	8.71	5.96	6.27	11.11				0.57				0.54	0.56	
secretory leukocyte peptidase inhibitor														
10.75	6.19	6.65	8.44	8.33	1.74	1.62								
sema domain, immunoglobulin domain, transmembrane domain and short cytoplasmic domain, (semaphorin) 4A														
6.47	5.73	6.48	6.92	9.29							0.62			
serpin peptidase inhibitor, clade E (nexin, plasminogen activator inhibitor type 1), member 1														
6.32	6.14	9.88	8.25	8.15	0.64			0.62						
solute carrier family 16, member 10 (aromatic amino acid transporter)														
5.96	8.12	9.24	7.64	7.75	0.65									
solute carrier family 16, member 10 (aromatic amino acid transporter)														
6.11	8.4	9.41	8.04	7.64	0.65									
solute carrier family 30 (zinc transporter), member 5														
5.8	8.94	8.43	7.99	8.72	0.65			0.67						
solute carrier family 38, member 6														
5.66	8.65	8.35	7.71	8.33	0.65									
solute carrier organic anion transporter family, member 2A1														
7.24	5.8	5.68	7.94	9.1							0.64	0.62		

**Table 4-2: Microarray analysis (continued)**

Gene Description														
AN (1)	YM (2)	OM (3)	MOA (4)	SOA (5)	1/2	1/3	1/4	1/5	2/3	2/4	2/5	3/4	3/5	4/5
sphingomyelin synthase 2														
5.95	9.45	8.8	8.56	9.03	0.63			0.66						
SRY (sex determining region Y)-box 11														
5.68	8.9	8.86	6.17	6.43	0.64	0.64								
sulfatase 1														
7.1	11.43	10.25	9.75	10.98	0.62			0.65						
sulfatase 1														
7.45	11.49	10.22	9.79	11.14	0.65									
tetraspanin 2														
6.16	10.38	10.12	9.78	9.44	0.59	0.61	0.63	0.65						
tetraspanin 2														
6.67	11.32	11.06	10.49	10.31	0.59	0.6	0.64	0.65						
transmembrane protein 176B														
6.05	6.05	6.05	5.71	8.85										0.64
transmembrane protein 200A														
7.72	8.94	8.06	5.8	8.14					1.54					
tubulin polymerization-promoting protein family member 3														
6.77	10.5	8.6	8.89	10.86	0.64			0.62						
tumor necrosis factor (ligand) superfamily, member 10														
5.85	9.03	8.56	8.56	9.09	0.65			0.64						
twist homolog 1 (Drosophila)														
10.04	8.99	6.48	7.58	9.12	1.55									
TYRO protein tyrosine kinase binding protein														
7.4	9.86	6.46	6.94	9.95				1.53						0.65
UDP-N-acetyl-alpha-D-galactosamine:polypeptide N-acetylgalactosaminyltransferase 7 (GalNAc-T7)														
6.13	10.15	9.12	7.75	8.99	0.6									
UDP-N-acetyl-alpha-D-galactosamine:polypeptide N-acetylgalactosaminyltransferase-like 1														
6.53	9.85	9.58	8.83	8.98	0.66									
versican														
5.69	10.4	9.28	9.61	11.07	0.55	0.61	0.59	0.51						
versican														
6.26	9.67	8.56	8.8	10.46	0.65			0.6						
v-fos FBJ murine osteosarcoma viral oncogene homolog														
7.82	10.89	12.99	12.11	12.61		0.6	0.65	0.62						
vimentin														
5.89	9.68	9.93	9.13	9.36	0.61	0.59	0.65	0.63						
von Willebrand factor														
8.71	6.55	9.13	8.15	10.16										0.64
V-set and immunoglobulin domain containing 4														
7.27	8.47	6.26	6.97	9.65										0.65
Xg blood group														
6.38	8.99	8.57	8.95	9.77				0.65						

AN = Aged normal

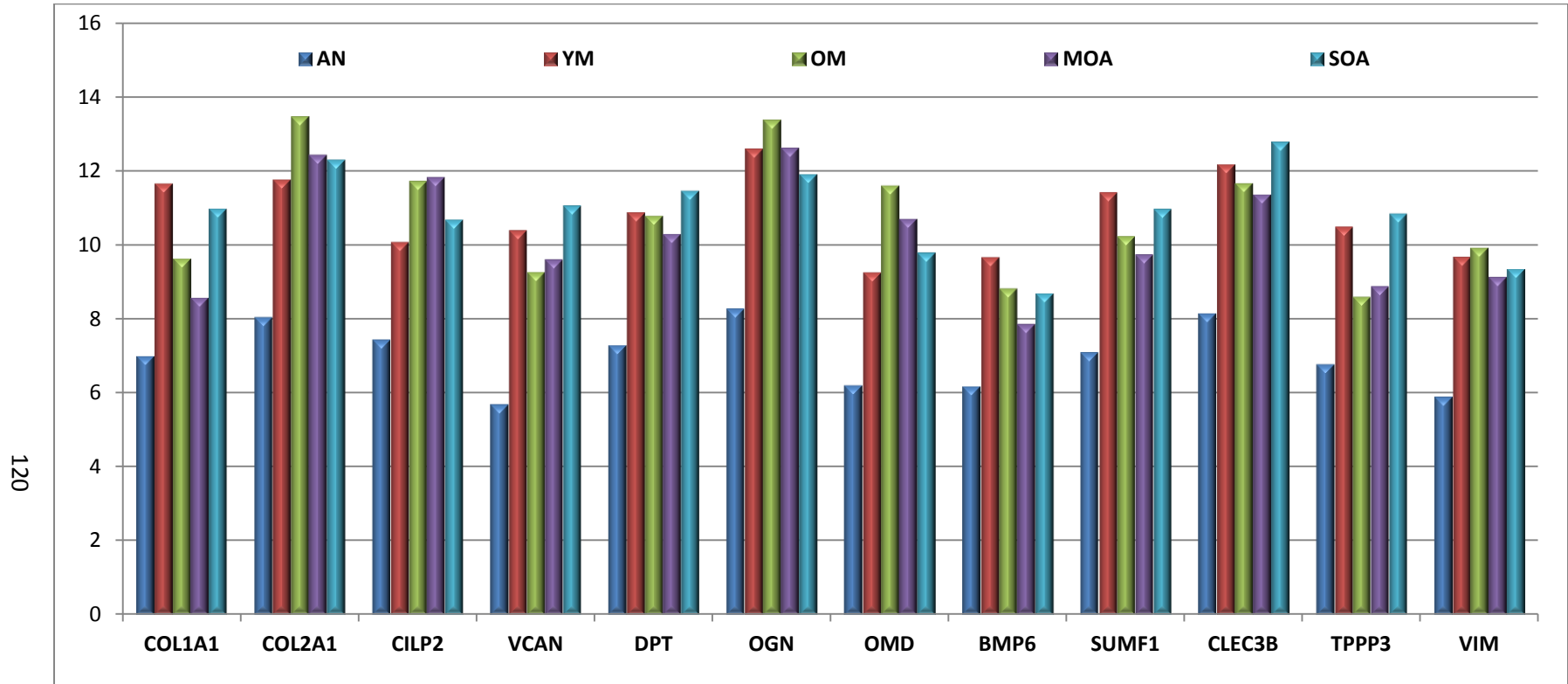
YM = Posterior medial meniscectomy, younger patients, minimal articular damage

OM = Posterior medial meniscectomy, older patients, moderate to severe articular damage

MOA = Posterior medial OA meniscus, joint space &gt; 1 mm, mild to moderate radiographic score

SOA = Posterior medial OA meniscus, joint space &lt; 1 mm, moderate to severe radiographic score

**Figure 4-1: Expression levels of genes associated with synthesis**



AN = Aged-normal

YM = Meniscectomy, younger patients, minimal articular damage

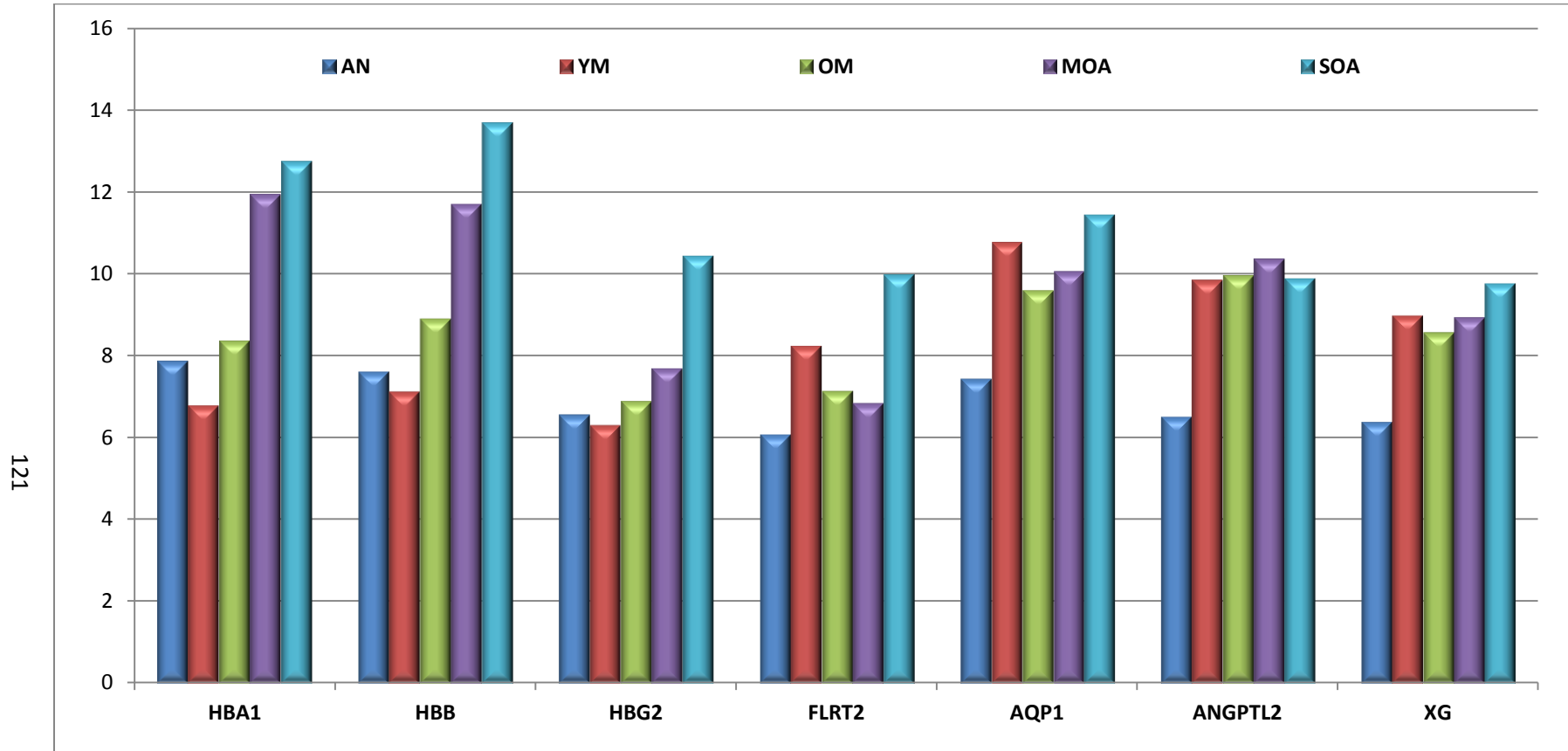
OM = Meniscectomy, older patients, severe articular damage

MOA = Osteoarthritic, identifiable joint space, mild to moderate radiographic score

SOA = Osteoarthritic, minimal joint space, moderate to severe radiographic score

HBA1 = Hemoglobin, alpha 1	COL1A1 = Collagen, type I, alpha 1	COL2A1 = Collagen, type II, alpha 1
CILP2 = Cartilage intermediate layer protein 2	VCAN = Versican	DPT = Dermatopontin
OGN = Osteoglycin (Mimecan)	OMD = Osteomodulin	BMP6 = Bone morphogenetic protein 6
SUMF1 = Sulfatase 1	CLEC3B = C-type lectin domain family 3, member B	TPPP3 = Tubulin polymerization-promoting protein family member 3
VIM = Vimentin		

**Figure 4-2: Expression levels of genes associated with vascularity**



AN = Aged-normal

YM = Meniscectomy, younger patients, minimal articular damage

OM = Meniscectomy, older patients, severe articular damage

MOA = Osteoarthritic, identifiable joint space, mild to moderate radiographic score

SOA = Osteoarthritic, minimal joint space, moderate to severe radiographic score

**HBA1** = Hemoglobin, alpha 1

**HBB** = Hemoglobin, beta

**HBG2** = Hemoglobin, gamma G

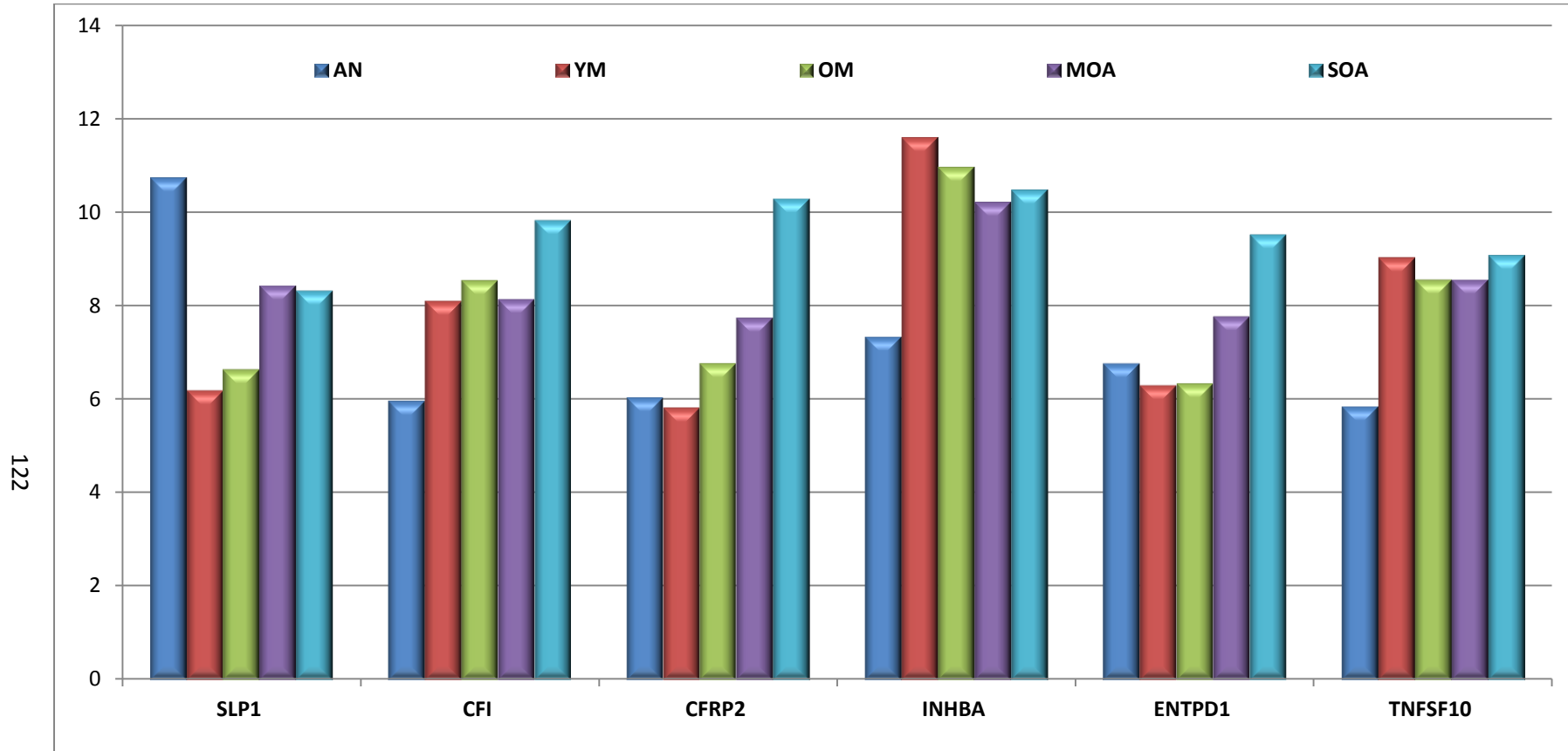
**FLRT2** = Fibronectin leucine rich transmembrane protein 2

**AQP1** = Aquaporin 1 (Colton blood group)

**ANGPTL2** = Angiopoietin-like 2

**XG** = Xg blood group

**Figure 4-3: Expression levels of genes associated with anti-degradation and degradation**



AN = Aged-normal

YM = Meniscectomy, younger patients, minimal articular damage

OM = Meniscectomy, older patients, severe articular damage

MOA = Osteoarthritic, identifiable joint space, mild to moderate radiographic score

SOA = Osteoarthritic, minimal joint space, moderate to severe radiographic score

SLP1 = secretory leukocyte peptidase inhibitor

CFI = Complement factor I

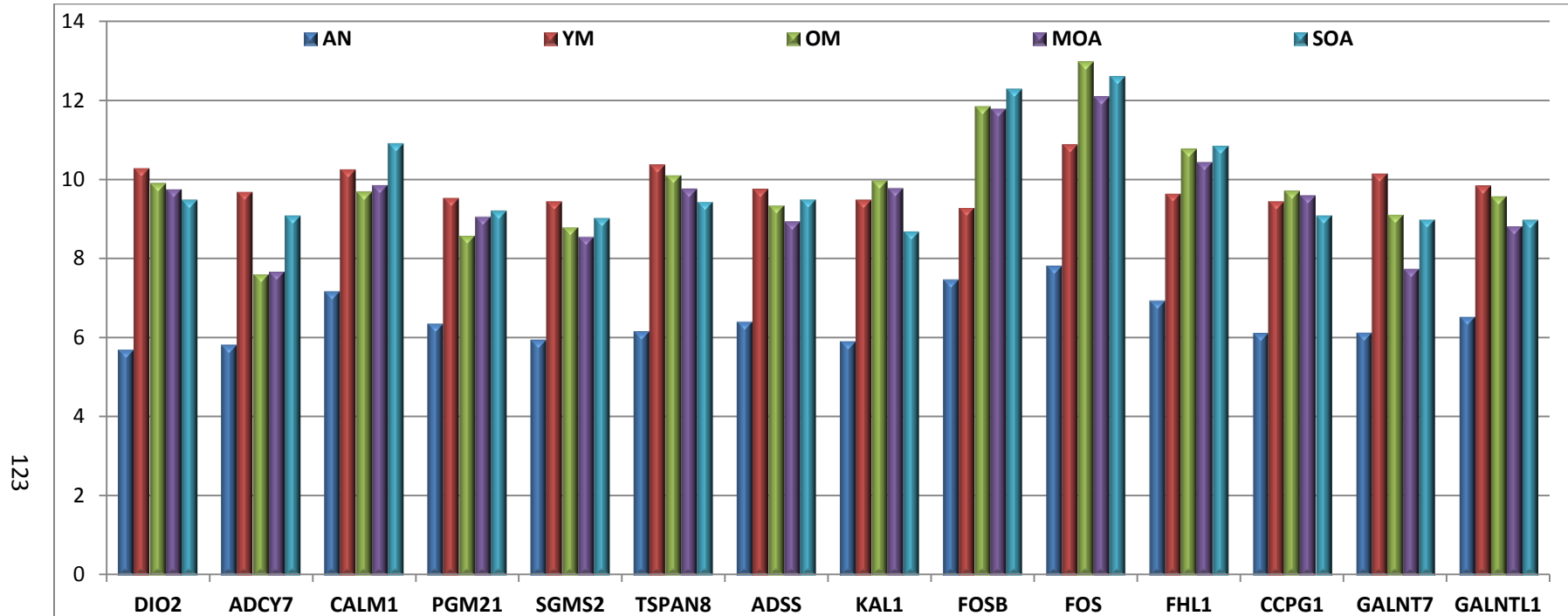
CFRP2 = Secreted frizzled-related protein 2

INHBA = Inhibin, beta A

ENTPD1 = Ectonucleoside triphosphate diphosphohydrolase 1

TNFSF10 = tumor necrosis factor (ligand) superfamily, member 10

**Figure 4-4: Expression levels of genes associated with signaling pathways**



AN = Aged-normal

YM = Meniscectomy, younger patients, minimal articular damage

OM = Meniscectomy, older patients, severe articular damage

MOA = Osteoarthritic, identifiable joint space, mild to moderate radiographic score

SOA = Osteoarthritic, minimal joint space, moderate to severe radiographic score

DIO2 = Deiodinase, iodothyronine, type II

ADCY7 = Adenylate cyclase 7

CALM1 = Calmodulin 1 (phosphorylase kinase, delta)

PGM21 = Phosphoglucomutase 2-like 1

SGMS2 = Sphingomyelin synthase 2

TSPAN8 = Tetraspanin 2

ADSS = Adenylosuccinate synthase

KAL1 = Kallmann syndrome 1 sequence

FOSB = FBXJ murine osteosarcoma viral oncogene homolog B

FOS = v-fos FBX murine osteosarcoma viral oncogene homolog

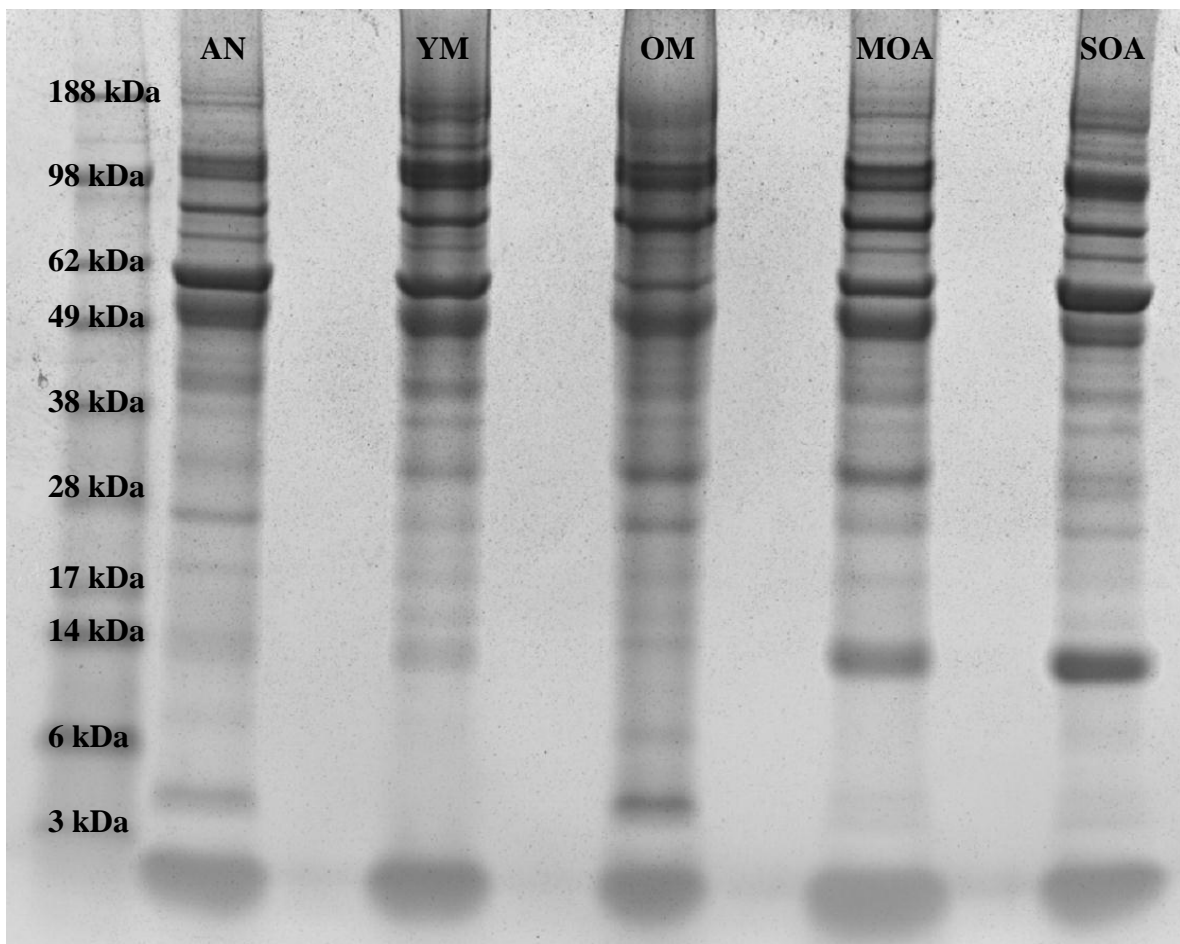
FHL1 = Four and a half LIM domains 1

CCPG1 = Cell cycle progression 1

GALNT7 = UDP-N-acetyl-alpha-D-galactosamine:polypeptide N-acetylgalactosaminyltransferase 7

GALNTL1 = UDP-N-acetyl-alpha-D-galactosamine:polypeptide N-acetylgalactosaminyltransferase-like 1

**Figure 4-5: Proteomics gel**



**AN** = Aged normal

**YM** = Posterior medial meniscectomy, younger patients, minimal articular damage

**OM** = Posterior medial meniscectomy, older patients, moderate to severe articular damage

**MOA** = Posterior medial OA meniscus, joint space > 1 mm, mild to moderate radiographic score

**SOA** = Posterior medial OA meniscus, joint space < 1 mm, moderate to severe radiographic score

**Table 4-3: Proteomics analysis**

Identified Protein	GI #	MW	AN	YM	OM	MOA	SOA
Apolipoprotein B-100 precursor (Apo B-100)	114014	516	0	0.74	0	0	3.71
Tenascin X precursor (TN-X)	9087217	464	4.48	24.46	3.8	43.55	27.49
Collagen alpha 3(VI) chain precursor	5921193	344	1328.19	1192.34	1115.45	1207.48	1201.11
Collagen alpha 1(XII) chain precursor	3182940	333	37.67	1.48	0	0	0
Desmoplakin (DP)	12644130	332	0	6.53	0	0	0
Fibronectin precursor (FN)	2506872	263	420.39	1339.86	1809.43	712.3	1136.21
Aggrecan core protein precursor	129886	250	13.66	0	3.04	6.62	0
Fibronectin (FN)	462100	250	225.72	652.38	1010.58	366.84	587.37
Tenascin precursor (TN)	3915888	241	21.72	106.72	14.6	23.44	108.27
Complement C4 precursor	20141171	193	35.83	3.49	4.71	3.58	19.93
Ras GTPase-activating-like protein	1170586	189	0	0	0	5.25	1.48
Complement C3 precursor	116594	187	25.48	7.51	8.42	29.75	45.11
Alpha-2-macroglobulin precursor (Alpha-2-M)	112911	163	5.5	4.11	0	0	21.45
Collagen alpha 2(I) chain precursor	19855162	129	78.49	47.54	37.94	70.66	35.82
Thrombospondin 1 precursor	135717	129	102.3	4.24	9.49	21.32	11.71
Ceruloplasmin precursor (Ferroxidase)	116117	122	8.25	1.35	0	4.86	15.53
Collagen alpha 1(VI) chain precursor	13878903	109	242.96	252.09	231.94	290.51	417.11
Collagen alpha 2(VI) chain precursor	27808647	109	122.06	128.39	133.16	138.19	217.48
Thrombospondin 4 precursor	549139	106	16.43	13.12	28.33	7.28	16.59
Alpha-actinin 1	112959 (+2)	103	0	7.3	2.41	9.71	3.7
Inter-alpha-trypsin inhibitor heavy chain H1 precursor (Serum-derived hyaluronan-associated protein) (SHAP)	2851501	101	0	0	1.27	6.66	0
Fibrinogen alpha/alpha-E chain precursor	1706799	95	0	215.46	50.71	8.88	4.57
Complement factor B precursor	584908	86	11	3.41	1.81	4.05	4.38
Gelsolin precursor, plasma	121116	86	30.66	24.19	42.2	40.52	34.77
Membrane copper amine oxidase	2501336	85	0	0	15.96	0	0
Cartilage oligomeric matrix protein precursor (COMP)	1705995	83	736.27	315.61	872.16	730.18	476.12
Cartilage oligomeric matrix protein precursor (COMP)	544073	83	259.77	111.54	334.48	209.09	209.98
Fibulin-1 precursor	30581038	77	0	4.55	15.87	0.81	0
Serotransferrin precursor (Transferrin)	136191	77	50.17	43.76	10.84	52.63	72.29
Transforming growth factor-beta induced protein IG-H3 precursor (Beta IG-H3)	2498193	75	12.37	210.2	104.1	31.18	72.67
Lamin A/C (70 kDa lamin)	125962 (+2)	74	0	6.25	4.22	0	3.29
Serum albumin precursor	113576	69	1716.89	1534.92	638.89	1040.49	1770.96
Serum albumin precursor	1351907	69	172.98	939.11	194.13	113.62	240.31

**Table 4-3: Proteomics analysis (continued)**

Identified Protein	GI #	MW	AN	YM	OM	MOA	SOA
Keratin, type II cytoskeletal 1 (Hair alpha protein)	1346343	66	202.2	488.18	205.04	355.06	544.82
Keratin, type II cytoskeletal 2 epidermal	547754	66	100.28	223.72	82.63	231.82	356.12
Keratin, type I cytoskeletal 9	547748	62	148.65	13.84	13.36	41.72	102.28
EH-domain containing protein 2	18203333	61	0	0.57	3.01	0	0
Keratin, type I cytoskeletal 10	547749	60	155.83	640.11	124.89	404.29	524.48
Pyruvate kinase, M2 isozyme	125604 (+1)	58	0	4.55	3.69	4.39	4.03
Fibrinogen beta chain precursor	399492	56	0	68.73	8.79	0	3.85
EGF-containing fibulin-like extracellular matrix protein 1 precursor (Fibulin-3)	9973182	55	0	0	52.15	6.66	15.76
Stromelysin-1 precursor (Matrix metalloproteinase-3) (MMP-3)	116857	54	4.79	1.7	5.69	4.85	0
Vimentin	418249	54	37.42	372.93	297.16	128.16	127.65
Vitronectin precursor	139653	54	49.81	9.55	60.42	17.78	13.97
Antithrombin-III precursor (ATIII)	113936	53	2.05	0	0	0	3.61
Vitamin D-binding protein precursor (DBP)	139641	53	8.89	9.26	3.16	7.62	1.64
Clusterin precursor (Complement cytolytic inhibitor) (Apolipoprotein J)	116533	52	135.37	2.64	53.88	16.11	39.4
Fibrinogen gamma chain precursor	20178280	52	0	55.99	5.05	0	0
Hemopexin precursor (Beta-1B-glycoprotein)	1708182	52	4.1	1.7	0	0.69	2.74
Vimentin	1353212	52	34.97	334.15	259.43	96.17	112.24
Serine protease HTRA1 precursor (L56)	18202620	51	33.85	42.76	222.39	66.87	122.42
ELONGATION FACTOR 1-ALPHA, SOMATIC FORM	119132 (+1)	50	4.83	8.13	3.16	3.7	12.33
Tubulin alpha-1 chain (Alpha-tubulin 1)	135395 (+2)	50	0	7.65	0.63	0	1.48
TUBULIN BETA CHAIN (T BETA-15)	135451 (+5)	50	0	1.74	0	0	0
Keratin, type I cytoskeletal 15	3183049	49	0	80.2	1.26	0	18.04
Alpha-1-antichymotrypsin precursor (ACT)	112874	48	7.07	0.57	0	0	0.55
Procollagen C-proteinase enhancer protein precursor (PCPE) (Type I procollagen COOH-terminal proteinase enhancer)	6919941	48	7.72	16.27	10.74	18.52	18.75
Protein disulfide isomerase A6 precursor	2501205	48	0	4.65	2.53	1.48	0
Alpha enolase (2-phospho-D-glycerate hydro-lyase) (Phosphopyruvate hydratase)	119339	47	22.2	29.63	32.78	49.76	61.16
Alpha-1-antitrypsin precursor (Alpha-1 protease inhibitor) (Alpha-1-antiproteinase)	1703025	47	58.07	14.92	1.87	8.31	12.05
Protein-lysine 6-oxidase precursor (Lysyl oxidase)	417269	47	3.69	9.81	16.45	5.87	0
47 kDa heat shock protein precursor (Collagen-binding protein 1)	123576 (+1)	46	0	4.65	0	0	0
Pigment epithelium-derived factor precursor	20178323	46	22.2	17.43	39	34.07	33.39
Apolipoprotein A-IV precursor (Apo-AIV)	114006	45	78.82	0.58	183.62	44.42	22.13
Phosphoglycerate kinase 1	129902	45	11.48	8.81	10.5	15.69	8.99
Prolargin precursor	1709586	44	523.67	375.71	555.01	517.66	214.74
Asporin precursor (Periodontal ligament associated protein-1)	21541978	43	258.79	129.56	101.66	163.7	65.49
Fibromodulin precursor (Keratan sulfate proteoglycan fibromodulin)	1706876 (+1)	43	31.36	31.64	92.43	51.04	40.53

**Table 4-3: Proteomics analysis (continued)**

Identified Protein	GI #	MW	AN	YM	OM	MOA	SOA
Fibromodulin precursor (Keratan sulfate proteoglycan fibromodulin)	544335	43	23.81	24.03	69.63	45.25	25.98
Lactadherin precursor (Breast epithelial antigen)	2506380	43	91.83	38.34	53.9	115.88	99.4
ACTIN 2, MUSCLE-SPECIFIC	1168320	42	39.47	180.76	63.29	63.74	49.92
ACTIN, MUSCLE	113284	42	34.65	137.77	40.54	43.74	58.91
Biglycan precursor (Bone/cartilage proteoglycan I)	266762	42	292.53	98.72	129.85	218.26	158.83
Chondroadherin precursor	21541994	40	21.23	5.62	44.62	73.99	76.35
Decorin precursor (Bone proteoglycan II)	129951	40	313.19	109.55	177.3	211.26	115.77
Proteoglycan link protein precursor	130310	40	56.16	8.13	39.18	76.49	80.9
Annexin A1 (Phospholipase A2 inhibitory protein)	113944	39	46.13	46.88	86.33	53.36	58.11
Annexin A2 (Placental anticoagulant protein IV)	113950	39	53.57	90.62	126.1	62.63	86.5
Beta-2-glycoprotein I precursor (Apolipoprotein H) (Activated protein C-binding protein)	543826	38	0	3.49	0	0	0
Ig alpha-1 chain C region	113584	38	11.17	1.14	3.01	2.08	6.02
Lumican precursor	20141464	38	257.38	139.02	158.5	202.29	142.84
L-lactate dehydrogenase A chain	126047	37	25.37	70.35	64.15	68.35	69.74
Annexin A4 (Placental anticoagulant protein II) (Carbohydrate-binding protein P33/P41)	1703319 (+1)	36	2.9	6.25	7.4	4.44	10.57
Annexin A5 (Placental anticoagulant protein I) (Thromboplastin inhibitor)	113960	36	94.82	81.2	125.39	60.53	61.94
Apolipoprotein E precursor (Apo-E)	114039	36	423.26	28.59	654.17	120.54	195.82
Glyceraldehyde 3-phosphate dehydrogenase, liver (GAPDH)	120649	36	33.78	73.38	72.06	87.41	49.94
Glyceraldehyde 3-phosphate dehydrogenase, muscle	120643	36	9.65	47.06	43.73	62.22	10.27
Ig gamma-1 chain C region	121039	36	115.32	65.4	49.69	79.83	53.3
Ig gamma-2 chain C region	121043	36	20.54	24.26	14.5	17.05	23.11
L-lactate dehydrogenase A chain (LDH-A) (LDH muscle subunit) (LDH-M)	126048	36	20.28	37.41	26.32	47.09	56.74
Mimecan precursor (Osteoglycin) (Osteoinductive factor) (OIF)	129078	34	506.49	578.8	665.35	921.52	844.3
NADH-cytochrome b5 reductase (B5R)	127846	34	0	2.68	0.82	0	6.86
Erythrocyte band 7 integral membrane protein	114823	32	0	0	0	0	3.43
Apolipoprotein A-I precursor (Apo-AI)	113992	31	79.86	111.9	94.02	30	71.12
Carbonic anhydrase III (Carbonate dehydratase III)	115462	30	18.44	0	0	0	0
14-3-3 protein epsilon (Mitochondrial import stimulation factor L subunit) (Protein kinase C inhibitor protein-1) (KCIP-1) (14-3-3E)	1168198	29	1.23	4.46	1.64	1.17	3.43
Aquaporin-CHIP (Water channel protein for red blood cells and kidney proximal tubule) (Aquaporin 1) (AQP-1) (Urine water channel)	267412	29	2.46	62.35	6.13	3.39	18.25
Carbonic anhydrase I (Carbonate dehydratase I) (CA-I) (Carbonic anhydrase B)	115449	29	0	0	0	30.51	76.62
Carbonic anhydrase II (Carbonate dehydratase II) (CA-II) (Carbonic anhydrase C)	115456	29	1.23	0	0	5.87	11.44
Phosphoglycerate mutase 1 (Phosphoglycerate mutase isozyme B) (BPG-dependent PGAM 1)	20178035	29	6.15	40.15	24.67	16	16.01
Tropomyosin alpha 4 chain (Tropomyosin 4)	136095 (+1)	29	0	14.28	0	0	0
14-3-3 protein zeta/delta (Protein kinase C inhibitor protein-1) (KCIP-1)	112696	28	2.46	10.71	2.47	2.35	3.43

**Table 4-3: Proteomics analysis (continued)**

Identified Protein	GI #	MW	AN	YM	OM	MOA	SOA
Thioredoxin-dependent peroxide reductase, mitochondrial precursor (Peroxiredoxin 3) (Antioxidant protein 1) (AOP-1)	2507171	28	0	2.33	4.25	0	0
Complement factor D precursor (C3 convertase activator) (Properdin factor D) (Adipsin)	3915626	27	30.74	23.2	31.08	30.51	14.87
Triosephosphate isomerase	39932641	27	49.18	52.64	50.17	63.37	59.46
Complement C1q subcomponent, A chain precursor	399138	26	0	3.57	3.29	0	0
Complement C1q subcomponent, B chain precursor	399140	26	0	3.57	2.47	0	0
Complement C1q subcomponent, C chain precursor	20178281	26	0	15.17	9.05	0	10.29
Extracellular superoxide dismutase precursor (EC-SOD)	134635	26	92.22	19.63	19.74	48.11	1.14
Plasma glutathione peroxidase precursor (GSHPx-P) (Extracellular glutathione peroxidase) (GPx-P)	121672	26	0	0	14.87	0	0
C-reactive protein precursor	117486	25	13.53	0	0	0	0
Serum amyloid P-component precursor (SAP)	730704	25	125.98	49.89	112.2	73.3	74.3
Superoxide dismutase, mitochondrial precursor	134665 (+4)	25	11.07	1.16	3.19	0	0
Transmembrane protein	3915893	25	0	8.15	0	0	0
Dermatopontin precursor (Tyrosine-rich acidic matrix protein)	27151769	24	396.78	127.58	150.46	30.79	139.1
Metalloproteinase inhibitor 2 precursor (TIMP-2) (Tissue inhibitor of metalloproteinases-2)	13124588 (+4)	24	2.46	4.66	4.25	0	0
Ras-related protein ARA-3	114088 (+10)	24	0	9.32	16.99	0	0
Ras-related protein Rab-7	131797 (+4)	24	0	0	3.19	0	0
Glutathione S-transferase P	121746	23	4.92	6.99	12.75	5.87	0
Heat shock 27 kDa protein (Stress-responsive protein 27) (Estrogen-regulated 24 kDa protein)	19855073	23	3.69	8.03	8.22	5.87	11.44
Peptidyl-prolyl cis-trans isomerase B precursor (PPIase) (Rotamase) (Cyclophilin B) (S-cyclophilin)	118090	23	0	20.97	4.25	0	0
Ras-related protein Rab-1A (YPT1-related protein)	131786	23	0	6.99	4.25	0	0
Tetranectin precursor (TN) (Plasminogen-kringle 4 binding protein)	267108	23	52.87	90.91	99.54	103.27	38.88
40S ribosomal protein S7 (S8)	134000	22	0	17.47	13.81	0	0
Adenylate kinase isoenzyme 1 (ATP-AMP transphosphorylase) (Myokinase)	20178288	22	0	3.49	2.12	0	0
Complement component C8 gamma chain precursor	116613	22	14.62	20.97	14.87	0	8.23
C-type lectin superfamily member 1 precursor (Cartilage-derived C-type lectin)	20137707	22	0	0	116.84	0	34.97
Peroxiredoxin 1 (Thioredoxin-dependent peroxide reductase 2) (Proliferation-associated protein PAG) (Natural killer cell enhancing factor A)	548453	22	2.46	14.6	6.37	1.17	0
Peroxiredoxin 2 (Thioredoxin-dependent peroxide reductase 1) (Thiol-specific antioxidant protein) (Natural killer cell enhancing factor B)	2507169	22	4.18	17.47	11.68	2.35	16.46
Transgelin 2 (SM22-alpha homolog)	586000	22	0	32.61	1.06	0	0
ADP-ribosylation factor 3	114125	21	0	2.33	4.25	0	16.46
Ras-related protein O-Krev	131854 (+2)	21	0	8.15	7.44	0	0
Alpha crystallin B chain (Alpha(B)-crystallin) (Rosenthal fiber component)	117385	20	7.38	19.8	27.62	3.52	8.23
ARP2/3 complex 20 kDa subunit (p20-ARC) (Actin-related protein 2/3 complex subunit 4)	38372625	20	0	5.82	3.19	0	0
Caveolin-1	13637934	20	0	0	12.75	0	12.34

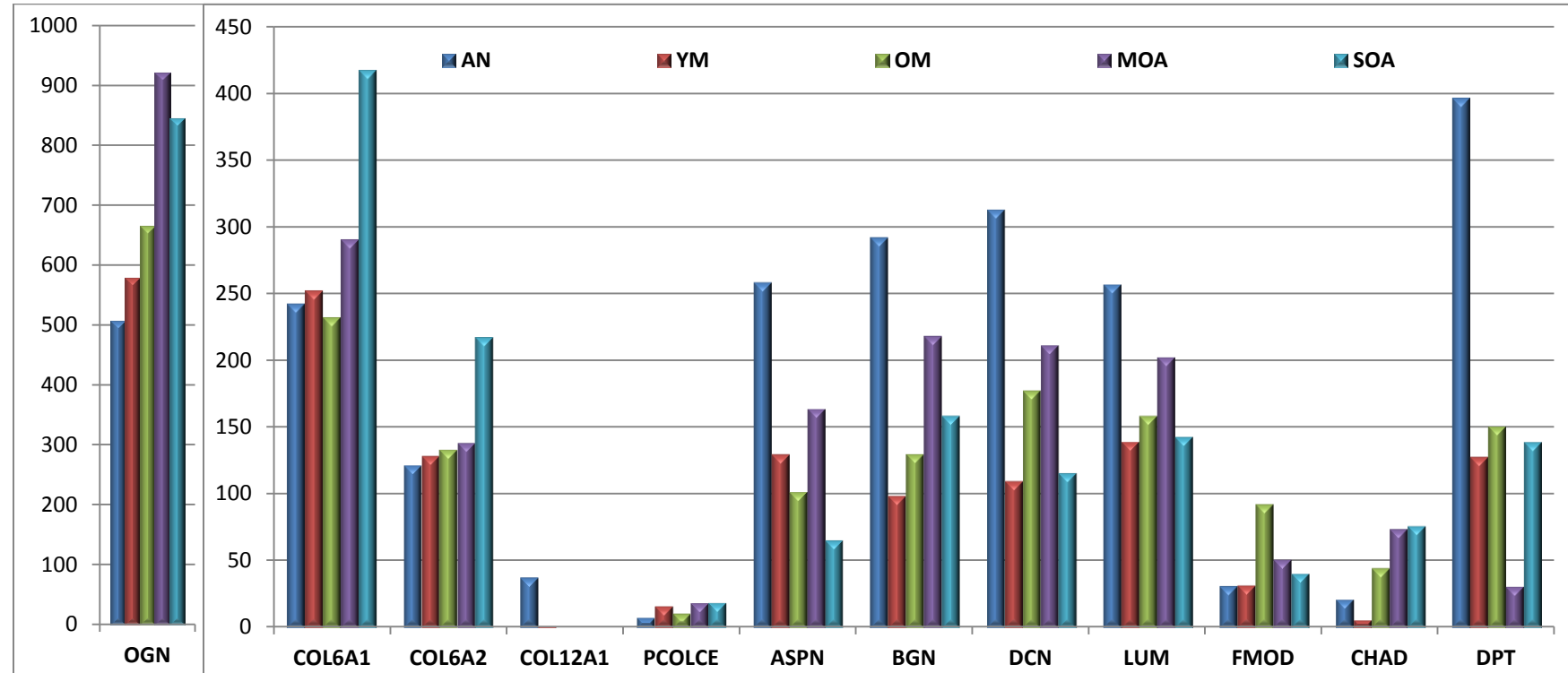
**Table 4-3: Proteomics analysis (continued)**

Identified Protein	GI #	MW	AN	YM	OM	MOA	SOA
Ferritin light chain (Ferritin L subunit)	120523	20	22.98	9.32	13.81	0	0
Cofilin, non-muscle isoform (phosphoprotein)	116848	19	8.36	16.31	11.68	0	14.4
Protein CGI-38	28380040	19	0	2.33	0	0	0
Retinoic acid receptor responder protein 2 precursor (Tazarotene-induced gene 2 protein)	6226227	19	8.36	0	16.99	0	0
Peptidyl-prolyl cis-trans isomerase A (Rotamase) (Cyclophilin A) (Cyclosporin A-binding protein)	118102	18	14.62	24.46	15.93	0	0
Angiogenin precursor (Ribonuclease 5) (RNase 5)	113873 (+1)	17	2.09	1.87	30.51	0	2.06
Lysozyme C precursor (1,4-beta-N-acetylmuramidase C)	126615 (+1)	17	45.96	6.53	22.67	31.07	17.74
Myoglobin	127689	17	45.96	0	0	0	0
Myosin light chain alkali, non-muscle isoform (Smooth muscle myosin alkali light chain) (Nonmuscle myosin light chain 3)	127144 (+3)	17	0	11.65	0	0	0
Nucleoside diphosphate kinase A (NDK A) (NDP kinase A) (Tumor metastatic process-associated protein) (Metastasis inhibition factor nm23)	127981 (+10)	17	0	9.32	4.25	0	0
Ribonuclease 4 precursor (RNase 4)	1710614 (+1)	17	79.38	0	7.63	4.44	14.4
Hemoglobin beta chain	122615	16	105.44	218.55	67.24	139.64	491.31
Hemoglobin delta chain	122713	16	30.21	132.26	30.43	52.71	192.69
Phospholipase A2, membrane associated precursor (Phosphatidylcholine 2-acylhydrolase)	129483	16	31.7	22.13	42.24	18.01	47.31
Superoxide dismutase [Cu-Zn]	134611	16	10.44	8.15	10.62	0	8.23
Transthyretin precursor (Prealbumin)	136464	16	33.42	27.96	266.51	261.91	188.08
Fatty acid-binding protein, adipocyte (Adipocyte lipid-binding protein)	119781	15	15.64	0	33.05	97.66	86.98
Galectin-1 (Beta-galactoside-binding lectin L-14-I) (Lactose-binding lectin 1) (Galaptin)	126155	15	0	7.46	17.8	28.85	40.14
Hemoglobin alpha chain	122366	15	58.49	96.53	23.96	30	217.01
Histone H2A.291.A	121983	15	134.16	128.52	134.37	52.07	74.7
Profilin I	130979	15	0	1.87	3.81	0	0
Histone H2A	121999 (+3)	14	147.55	137.84	139.89	52.07	89.1
Histone H2A.z (H2A/z)	121994	14	62.04	46.17	38.37	16.05	33.27
Histone H2B.I (H2B/I)	7387740 (+2)	14	63.19	93.82	76.78	23.5	34.41
Serum amyloid A protein precursor	134167	14	15.64	0	0	0	0
IG KAPPA CHAIN V-II REGION GM607 PRECURSOR	125790	13	9.84	8.03	0	0	4.57
Ig kappa chain V-IV region precursor	125830 (+1)	13	15.98	6.25	0	3.52	5.72
Late histone H2A.3, gonadal	121979	13	70.89	89.34	103.86	36.02	65.87
Calgizzarin (S100C protein) (MLN 70)	1710818	12	18.77	12.36	22.88	26.64	16.73
Ig kappa chain C region	125145	12	379.27	174.06	92.57	175.78	233.28
IG KAPPA CHAIN V-III REGION WOL	125803 (+2)	12	15.98	8.03	1.64	7.04	5.72
Placental calcium-binding protein (Calvasculin) (S100 calcium-binding protein A4) (MTS1 protein)	115601 (+1)	12	3.13	16.79	11.44	0	0
Calpactin I light chain (P10 protein) (P11) (Cellular ligand of annexin II)	116486 (+1)	11	0	29.84	33.05	0	0
Histone H4	462242	11	287.81	177.28	339.57	144.27	54.54

**Table 4-3: Proteomics analysis (continued)**

Identified Protein	GI #	MW	AN	YM	OM	MOA	SOA
Ig lambda chain C regions	125946	11	213.27	145.12	68.04	118.05	134.66
Neutrophil defensin 1 precursor	30316322 (+1)	10	3.13	0	0	80.47	90.21
Apolipoprotein C-I precursor (Apo-CI)	114016	9	33.81	0	0	40.23	46.91
Ubiquitin	1174860 (+6)	9	0	83.87	65.85	0	0

GI # = GenInfo identifier number, accession number (gi xxxxxx)	MW = Molecular weight (kDa)
AN = Aged-normal	YM = Meniscectomy, younger patients, minimal articular damage
MOA = Osteoarthritic, identifiable joint space, mild to moderate radiographic score	OM = Meniscectomy, older patients, severe articular damage
SOA = Osteoarthritic, minimal joint space, moderate to severe radiographic score	

**Figure 4-6: ECM proteins**

AN = Aged-normal

YM = Meniscectomy, younger patients, minimal articular damage

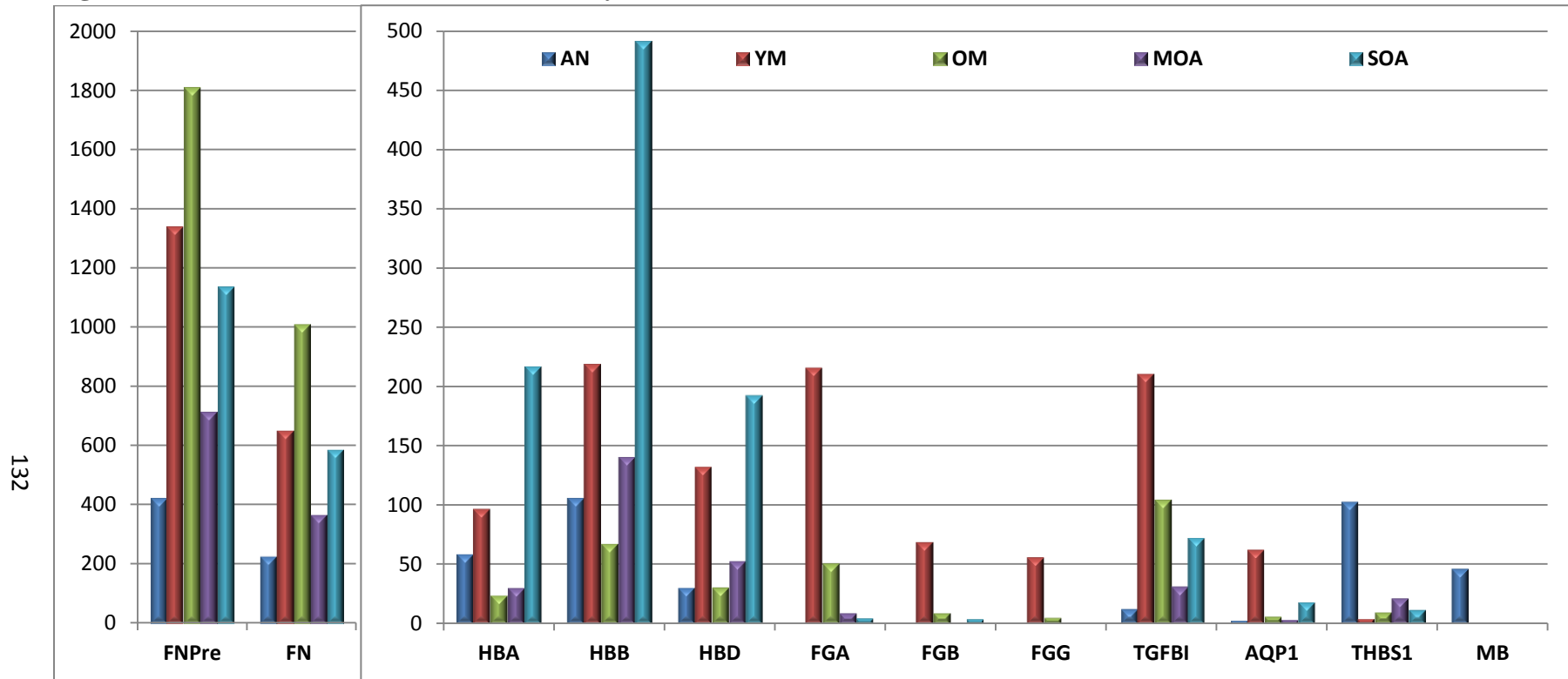
OM = Meniscectomy, older patients, severe articular damage

MOA = Osteoarthritic, identifiable joint space, mild to moderate radiographic score

SOA = Osteoarthritic, minimal joint space, moderate to severe radiographic score

OGN = Mimecan precursor (Osteoglycin)	COL6A1 = Collagen alpha 1 (VI) chain precursor	COL6A2 = Collagen alpha 2 (VI) chain precursor
COL12A1 = Collagen alpha 1 (XII) chain precursor	PCOLCE = Type 1 procollagen C-proteinase enhancer protein	ASPN = Asporin precursor
BGN = Biglycan precursor	DCN = Decorin precursor	LUM = Lumican precursor
FMOD = Fibromodulin precursor	CHAD = Chondroadherin precursor	DPT = Dermatopontin precursor

**Figure 4-7: Proteins associated with vascularity**



AN = Aged-normal

YM = Meniscectomy, younger patients, minimal articular damage

OM = Meniscectomy, older patients, severe articular damage

MOA = Osteoarthritic, identifiable joint space, mild to moderate radiographic score

SOA = Osteoarthritic, minimal joint space, moderate to severe radiographic score

**FNPre** = Fibronectin precursor

**FN** = Fibronectin

**HBA** = Hemoglobin alpha chain

**HBB** = Hemoglobin beta chain

**HBD** = Hemoglobin delta chain

**FGA** = Fibrinogen alpha/alpha-E chain precursor

**FGB** = Fibrinogen beta chain precursor

**FGG** = Fibrinogen gamma chain precursor

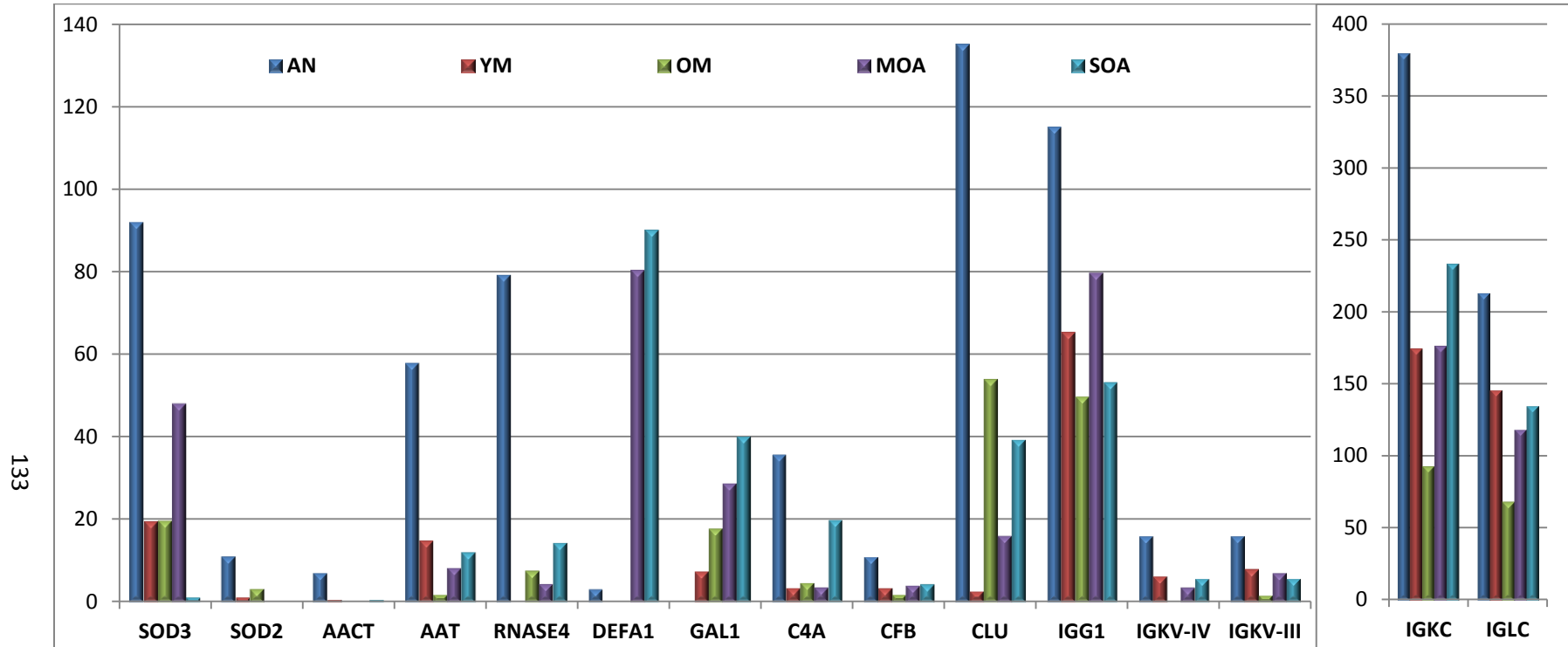
**TGFBI** = Transforming growth factor-beta induced protein IG-H3 precursor

**AQP1** = Aquaporin-1

**THBS1** = Thrombospondin 1 precursor

**MB** = Myoglobin

**Figure 4-8: Degredative and potentially anti-degradative proteins**



AN = Aged-normal

YM = Meniscectomy, younger patients, minimal articular damage

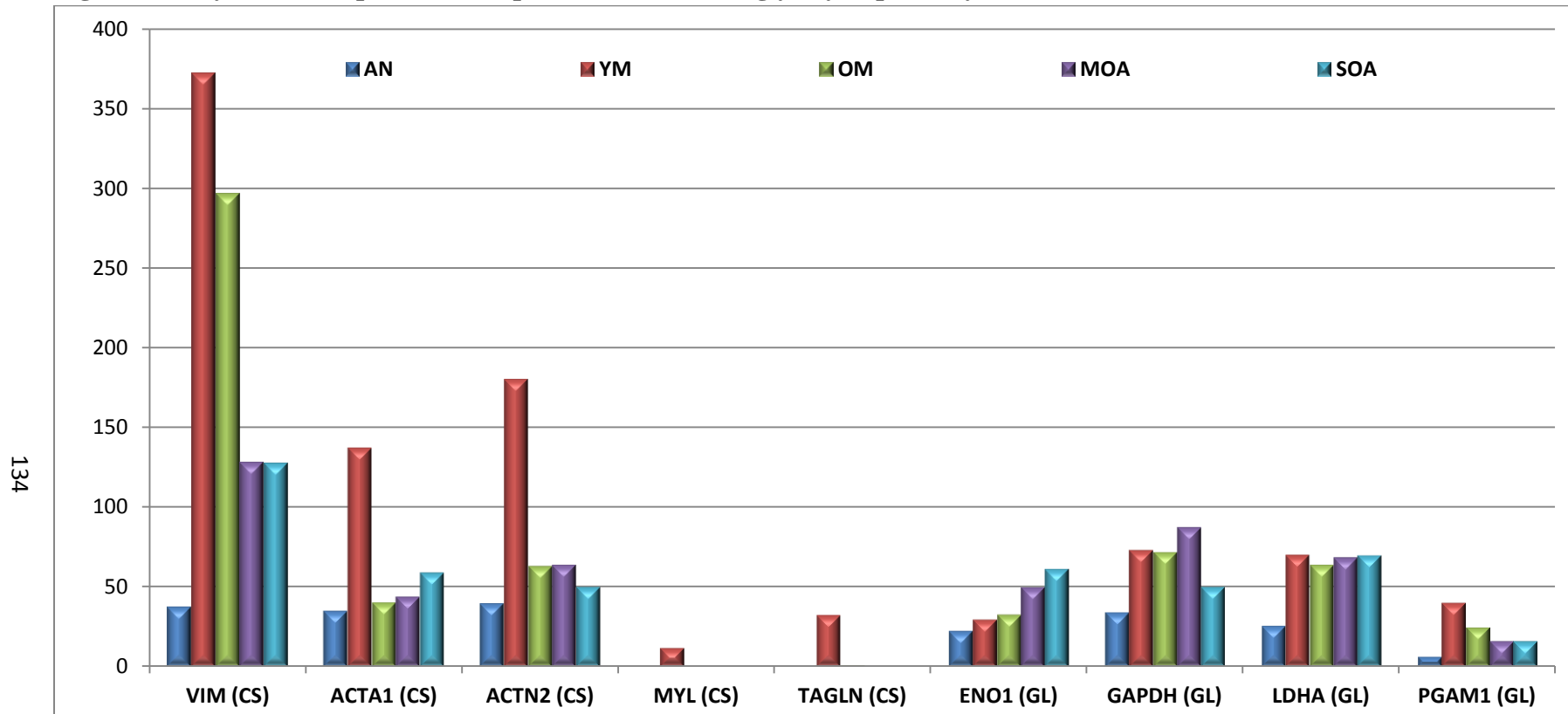
OM = Meniscectomy, older patients, severe articular damage

MOA = Osteoarthritic, identifiable joint space, mild to moderate radiographic score

SOA = Osteoarthritic, minimal joint space, moderate to severe radiographic score

SOD3 = Extracellular superoxide dismutase [Cu-Zn] precursor	SOD2 = Superoxide dismutase [Mn], mitochondrial precursor	AACT = Alpha-1-antichymotrypsin precursor
AAT = Alpha-1-antitrypsin precursor	RNASE4 = Ribonuclease 4 precursor	DEFA1 = Neutrophil defensin 1 precursor
GAL1 = Galectin-1	C4A = Complement C4 precursor	CFB = Complement factor B precursor (C3/C5 convertase)
CLU = Clusterin precursor (Complement cytolysis inhibitor)	IGG1 = Ig gamma-1 chain C region	IGKV-IV = Ig kappa chain V-IV region precursor
IGKV-III = Ig kappa chain V-III region	IGKC = Ig kappa chain C region	IGLC = Ig lambda chain C regions

**Figure 4-9: Cytoskeleton proteins and proteins involved in glycolysis pathway**



AN = Aged-normal

YM = Meniscectomy, younger patients, minimal articular damage

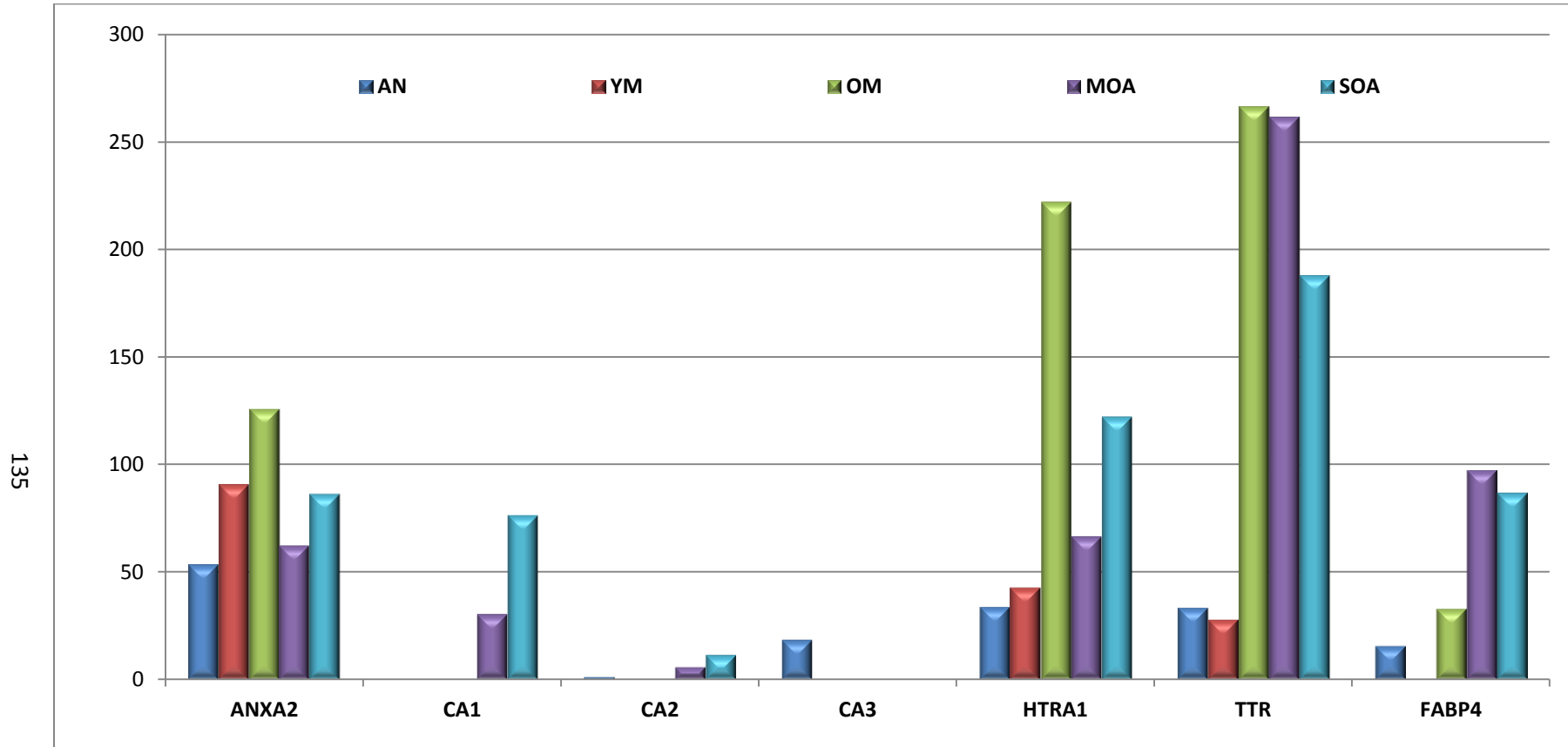
OM = Meniscectomy, older patients, severe articular damage

MOA = Osteoarthritic, identifiable joint space, mild to moderate radiographic score

SOA = Osteoarthritic, minimal joint space, moderate to severe radiographic score

CS = Cytoskeleton	GL = Glycolysis	VIM = Vimentin
ACTA1 = Actin 1	ACTA2 = Actin 2	MYL = Myosin light chain alkali
TAGLN = Transgelin 2	ENO1 = Enolase 1	GAPDH = Glyceraldehyde 3-phosphate dehydrogenase
LDHA = L-lactate dehydrogenase A chain	PGAM1 = Phosphoglycerate mutase 1	

**Figure 4-10: Proteins associated with signaling**



AN = Aged-normal

YM = Meniscectomy, younger patients, minimal articular damage

OM = Meniscectomy, older patients, severe articular damage

MOA = Osteoarthritic, identifiable joint space, mild to moderate radiographic score

SOA = Osteoarthritic, minimal joint space, moderate to severe radiographic score

ANXA2 = Annexin A2

CA1 = Carbonic anhydrase I

CA2 = Carbonic anhydrase II

CA3 = Carbonic anhydrase III

HTRA1 = Serine protease HTRA1 precursor

TTR = Transthyretin precursor

FABP4 = Fatty acid-binding protein, adipocyte

## References

1. Herwig J, Egner E, Buddecke E. Chemical changes of human knee joint menisci in various stages of degeneration. *Annals of the Rheumatic Diseases*. 1984;43(4):635-640.
2. Eyre DR, Muir H. The distribution of different molecular species of collagen in fibrous, elastic and hyaline cartilages of the pig. *Biochemical Journal*. 1975;151(3):595-602.
3. McDevitt CA, Webber RJ. The ultrastructure and biochemistry of meniscal cartilage. *Clinical Orthopaedics and Related Research*. 1990(252):8-18.
4. Ochi K, Daigo Y, Katagiri T, et al. Expression profiles of two types of human knee-joint cartilage. *Journal of Human Genetics*. 2003;48(4):177-182.
5. Sun Y, Mauerhan DR, Honeycutt PR, et al. Calcium deposition in osteoarthritic meniscus and meniscal cell culture. *Arthritis Research & Therapy*. 2010;12(2):R56.
6. Loeser RF, Olex AL, McNulty MA, et al. Microarray analysis reveals age-related differences in gene expression during the development of osteoarthritis in mice. *Arthritis & Rheumatism*. 2012;64(3):705-717.
7. Burleigh A, Chanalaris A, Gardiner MD, et al. Joint immobilization prevents murine osteoarthritis and reveals the highly mechanosensitive nature of protease expression in vivo. *Arthritis & Rheumatism*. 2012;64(7):2278-2288.
8. Onnerfjord P, Khabut A, Reinholt FP, Svensson O, Heinegard D. Quantitative proteomic analysis of eight cartilaginous tissues reveals characteristic differences as well as similarities between subgroups. *Journal of Biological Chemistry*. 2012;287(23):18913-18924.
9. Kuliwaba JS, Fazzalari NL, Findlay DM. Stability of RNA isolated from human trabecular bone at post-mortem and surgery. *Biochimica et Biophysica Acta - Molecular Basis of Disease*. 2005;1740(1):1-11.
10. Schramm M, Falkai P, Tepest R, et al. Stability of RNA transcripts in post-mortem psychiatric brains. *Journal of Neural Transmission*. 1999;106(3-4):329-335.
11. Yasojima K, McGeer EG, McGeer PL. High stability of mRNAs postmortem and protocols for their assessment by RT-PCR. *Brain Research Protocols*. 2001;8(3):212-218.

12. Brittberg M, Peterson L. Introduction of an articular cartilage classification. *ICRS Newsletter*. 1998;1:4.
13. Brittberg M, Winalski CS. Evaluation of cartilage injuries and repair. *Journal of Bone and Joint Surgery - Series A*. 2003;85(SUPPL. 1):58-69.
14. Scott Jr WW, Lethbridge-Cejku M, Reichle R, Wigley FM, Tobin JD, Hochberg MC. Reliability of grading scales for individual radiographic features of osteoarthritis of the knee: The Baltimore longitudinal study of aging atlas of knee osteoarthritis. *Investigative Radiology*. 1993;28(6):497-501.
15. Ochi K, Daigo Y, Katagiri T, et al. Expression profiles of two types of human knee-joint cartilage. *Journal of Human Genetics*. 2003;48(4):177-182.
16. Onnerfjord P, Khabut A, Reinholt FP, Svensson O, Heinegard D. Quantitative proteomic analysis of eight cartilaginous tissues reveals characteristic differences as well as similarities between subgroups. *Journal of Biological Chemistry*. 2012;287(23):18913-18924.
17. Upton ML, Chen J, Setton LA. Region-specific constitutive gene expression in the adult porcine meniscus. *Journal of Orthopaedic Research*. 2006;24(7):1562-1570.
18. Font B, Eichenberger D, Rosenberg LM, Van Der Rest M. Characterization of the interactions of type XII collagen with two small proteoglycans from fetal bovine tendon, decorin and fibromodulin. *Matrix Biology*. 1996;15(5):341-348.
19. Marchant JK, Zhang G, Birk DE. Association of type XII collagen with regions of increased stability and keratocyte density in the cornea. *Experimental Eye Research*. 2002;75(6):683-694.
20. Walchli C, Koch M, Chiquet M, Odermatt BF, Trueb B. Tissue-specific expression of the fibril-associated collagens XII and XIV. *Journal of Cell Science*. 1994;107(2):669-681.
21. Steiglitz BM, Kreider JM, Frankenburg EP, et al. Procollagen C proteinase enhancer 1 genes are important determinants of the mechanical properties and geometry of bone and the ultrastructure of connective tissues. *Molecular and Cellular Biology*. 2006;26(1):238-249.
22. Bernardo BC, Belluoccio D, Rowley L, Little CB, Hansen U, Bateman JF. Cartilage intermediate layer protein 2 (CILP-2) is expressed in articular and meniscal cartilage and down-regulated in experimental osteoarthritis. *Journal of Biological Chemistry*. 2011;286(43):37758-37767.

23. Wildey GM, Billetz AC, Matyas JR, Adams ME, McDevitt CA. Absolute concentrations of mRNA for type I and type VI collagen in the canine meniscus in normal and ACL-deficient knee joints obtained by RNase protection assay. *Journal of Orthopaedic Research*. 2001;19(4):650-658.
24. Funderburgh JL, Corpuz LM, Roth MR, Conrad GW. Identification of the 25 kilodalton corneal keratan sulfate proteoglycan core protein. *Investigative Ophthalmology and Visual Science*. 1996;37(3).
25. Tasheva ES, Koester A, Paulsen AQ, et al. Mimecan/osteoglycin-deficient mice have collagen fibril abnormalities. *Molecular Vision*. 2002;8:407-415.
26. Ujita M, Shinomura T, Kimata K. Molecular cloning of the mouse osteoglycin-encoding gene. *Gene*. 1995;158(2):237-240.
27. De Ceuninck F, Marcheteau E, Berger S, et al. Assessment of some tools for the characterization of the human osteoarthritic cartilage proteome. *Journal of biomolecular techniques: JBT*. 2005;16(3):256-265.
28. Kukita A, Bonewald L, Rosen D, Seyedin S, Mundy GR, Roodman GD. Osteoinductive factor inhibits formation of human osteoclast-like cells. *Proceedings of the National Academy of Sciences of the United States of America*. 1990;87(8):3023-3026.
29. Sun Y, Mauerhan DR. Meniscal calcification, pathogenesis and implications. *Current Opinion in Rheumatology*. 2012;24(2):152-157.
30. Pauli C, Grogan SP, Patil S, et al. Macroscopic and histopathologic analysis of human knee menisci in aging and osteoarthritis. *Osteoarthritis & Cartilage*. 2011;19(9):1132-1141.
31. Nikdin H, Olsson M-L, Hultenby K, Sugars RV. Osteoadherin accumulates in the predentin towards the mineralization front in the developing tooth. *PLoS ONE [Electronic Resource]*. 2012;7(2):e31525.
32. Rehn AP, Cerny R, Sugars RV, Kaukua N, Wendel M. Osteoadherin is upregulated by mature osteoblasts and enhances their in vitro differentiation and mineralization. *Calcified Tissue International*. 2008;82(6):454-464.
33. Rehn AP, Chalk AM, Wendel M. Differential regulation of osteoadherin (OSAD) by TGF-beta1 and BMP-2. *Biochemical & Biophysical Research Communications*. 2006;349(3):1057-1064.
34. Visser R, Arrabal PM, Santos-Ruiz L, Becerra J, Cifuentes M. Basic fibroblast growth factor enhances the osteogenic differentiation induced by bone morphogenetic protein-6 in vitro and in vivo. *Cytokine*. 2012;58(1):27-33.

35. Otsuki S, Hanson SR, Miyaki S, et al. Extracellular sulfatases support cartilage homeostasis by regulating BMP and FGF signaling pathways. *Proceedings of the National Academy of Sciences of the United States of America*. 2010;107(22):10202-10207.
36. Otsuki S, Taniguchi N, Grogan SP, D'Lima D, Kinoshita M, Lotz M. Expression of novel extracellular sulfatases Sulf-1 and Sulf-2 in normal and osteoarthritic articular cartilage. *Arthritis Research and Therapy*. 2008;10(3).
37. Wewer UM, Ibaraki K, Schjorring P, Durkin ME, Young MF, Albrechtsen R. A potential role for tetranectin in mineralization during osteogenesis. *Journal of Cell Biology*. 1994;127(6 I):1767-1775.
38. Benjamin M, Ralphs JR. Biology of Fibrocartilage Cells. Vol 2332004:1-45.
39. Mansson B, Wenglen C, Morgelin M, Saxne T, Heinegard D. Association of chondroadherin with collagen type II. *Journal of Biological Chemistry*. 2001;276(35):32883-32888.
40. Clutterbuck AL, Smith JR, Allaway D, Harris P, Liddell S, Mobasher A. High throughput proteomic analysis of the secretome in an explant model of articular cartilage inflammation. *Journal of Proteomics*. 2011;74(5):704-715.
41. Happonen KE, Sjoberg AP, Morgelin M, Heinegard D, Blom AM. Complement inhibitor C4b-binding protein interacts directly with small glycoproteins of the extracellular matrix. *Journal of Immunology*. 2009;182(3):1518-1525.
42. Sjoberg AP, Manderson GA, Morgelin M, Day AJ, Heinegard D, Blom AM. Short leucine-rich glycoproteins of the extracellular matrix display diverse patterns of complement interaction and activation. *Molecular Immunology*. 2009;46(5):830-839.
43. Melrose J, Fuller ES, Roughley PJ, et al. Fragmentation of decorin, biglycan, lumican and keratocan is elevated in degenerate human meniscus, knee and hip articular cartilages compared with age-matched macroscopically normal and control tissues. *Arthritis Research & Therapy*. 2008;10(4):R79.
44. Hellio Le Graverand MP, Vignon E, Otterness IG, Hart DA. Early changes in lapine menisci during osteoarthritis development part II: Molecular alterations. *Osteoarthritis and Cartilage*. 2001;9(1):65-72.
45. Lorenzo P, Aspberg A, Onnerfjord P, Bayliss MT, Neame PJ, Heinegard D. Identification and characterization of asporin, a novel member of the leucine-rich repeat protein family closely related to decorin and biglycan. *Journal of Biological Chemistry*. 2001;276(15):12201-12211.

46. Kalamajski S, Aspberg A, Lindblom K, Heinegard D, Oldberg A. Asporin competes with decorin for collagen binding, binds calcium and promotes osteoblast collagen mineralization. *Biochemical Journal*. 2009;423(1):53-59.
47. Arner EC. Aggrecanase-mediated cartilage degradation. *Current Opinion in Pharmacology*. 2002;2(3):322-329.
48. Lin EA, Liu CJ. The role of ADAMTSs in arthritis. *Protein and Cell*. 2010;1(1):33-47.
49. Okamoto O, Fujiwara S, Abe M, Sato Y. Dermatopontin interacts with transforming growth factor  $\beta$  and enhances its biological activity. *Biochemical Journal*. 1999;337(3):537-541.
50. Bray RC, Smith JA, Eng MK, Leonard CA, Sutherland CA, Salo PT. Vascular response of the meniscus to injury: effects of immobilization. *Journal of Orthopaedic Research*. 2001;19(3):384-390.
51. Ashraf S, Wibberley H, Mapp PI, Hill R, Wilson D, Walsh DA. Increased vascular penetration and nerve growth in the meniscus: a potential source of pain in osteoarthritis. *Annals of the Rheumatic Diseases*. 2011;70(3):523-529.
52. Kabanova S, Kleinbongard P, Volkmer J, Andree B, Kelm M, Jax TW. Gene expression analysis of human red blood cells. *International Journal of Medical Sciences*. 2009;6(4):156-159.
53. Tommila M, Stark C, Jokilammi A, Peltonen V, Penttinen R, Ekholm E. Hemoglobin expression in rat experimental granulation tissue. *Journal Of Molecular Cell Biology*. 2011;3(3):190-196.
54. Maurer LM, Tomasini-Johansson BR, Mosher DF. Emerging roles of fibronectin in thrombosis. *Thrombosis Research*. 2010;125(4):287-291.
55. Scuderi GJ, Golish SR, Cook FF, Cuellar JM, Bowser RP, Hanna LS. Identification of a novel fibronectin-aggrecan complex in the synovial fluid of knees with painful meniscal injury. *Journal of Bone & Joint Surgery - American Volume*. 2011;93(4):336-340.
56. Johnson A, Smith R, Saxne T, Hickery M, Heinegard D. Fibronectin fragments cause release and degradation of collagen-binding molecules from equine explant cultures. *Osteoarthritis & Cartilage*. 2004;12(2):149-159.
57. Schwarzbauer JE. Alternative splicing of fibronectin: three variants, three functions. *Bioessays*. 1991;13(10):527-533.

58. Matsuda M. [Fibronectin--its functions and roles in tissue repair]. *Nippon Geka Gakkai Zasshi. Journal of Japan Surgical Society*. 1984;85(9):882-886.
59. Mosher DF, Schad PE. Cross-linking of fibronectin to collagen by blood coagulation Factor XIIIa. *Journal of Clinical Investigation*. 1979;64(3):781-787.
60. Arnoczky SP, Warren RF. The microvasculature of the meniscus and its response to injury. An experimental study in the dog. *American Journal of Sports Medicine*. 1983;11(3):131-141.
61. Kim H-J, Kim P-K, Bae SM, et al. Transforming growth factor-beta-induced protein (TGFB $\beta$ /beta ig-h3) activates platelets and promotes thrombogenesis. *Blood*. 2009;114(25):5206-5215.
62. Endeward V, Musa-Aziz R, Cooper GJ, et al. Evidence that aquaporin 1 is a major pathway for CO<sub>2</sub> transport across the human erythrocyte membrane. *FASEB Journal*. 2006;20(12):1974-1981.
63. Fouchet C, Gane P, Cartron JP, Lopez C. Quantitative analysis of XG blood group and CD99 antigens on human red cells. *Immunogenetics*. 2000;51(8-9):688-694.
64. Okada T, Tsukano H, Endo M, et al. Synoviocyte-derived angiopoietin-like protein 2 contributes to synovial chronic inflammation in rheumatoid arthritis. *American Journal of Pathology*. 2010;176(5):2309-2319.
65. Zaslavsky A, Baek K-H, Lynch RC, et al. Platelet-derived thrombospondin-1 is a critical negative regulator and potential biomarker of angiogenesis. *Blood*. 2010;115(22):4605-4613.
66. Hsu C-W, Yuan K, Tseng C-C. The negative effect of platelet-rich plasma on the growth of human cells is associated with secreted thrombospondin-1. *Oral Surgery Oral Medicine Oral Pathology Oral Radiology & Endodontics*. 2009;107(2):185-192.
67. Monboisse JC, Borel JP. Oxidative damage to collagen. *EXS*. 1992;62:323-327.
68. Marklund SL. Human copper-containing superoxide dismutase of high molecular weight. *Proceedings of the National Academy of Sciences of the United States of America*. 1982;79(24 I):7634-7638.
69. Marklund SL, Bjelle A, Elmquist LG. Superoxide dismutase isoenzymes of the synovial fluid in rheumatoid arthritis and in reactive arthritides. *Annals of the Rheumatic Diseases*. 1986;45(10):847-851.

70. Marklund SL, Holme E, Hellner L. Superoxide dismutase in extracellular fluids. *Clinica Chimica Acta*. 1982;126(1):41-51.
71. Marklund SL. Expression of extracellular superoxide dismutase by human cell lines. *Biochemical Journal*. 1990;266(1):213-219.
72. Sandstrom J, Karlsson K, Edlund T, Marklund SL. Heparin-affinity patterns and composition of extracellular superoxide dismutase in human plasma and tissues. *Biochemical Journal*. 1993;294(3):853-857.
73. Petersen SV, Oury TD, Ostergaard L, et al. Extracellular Superoxide Dismutase (EC-SOD) Binds to Type I Collagen and Protects Against Oxidative Fragmentation. *Journal of Biological Chemistry*. 2004;279(14):13705-13710.
74. Iyama S, Okamoto T, Sato T, et al. Treatment of Murine Collagen-Induced Arthritis by Ex Vivo Extracellular Superoxide Dismutase Gene Transfer. *Arthritis and Rheumatism*. 2001;44(9):2160-2167.
75. McCord JM. Free radicals and inflammation: protection of synovial fluid by superoxide dismutase. *Science*. 1974;185(4150):529-531.
76. Regan E, Flannelly J, Bowler R, et al. Extracellular superoxide dismutase and oxidant damage in osteoarthritis. *Arthritis and Rheumatism*. 2005;52(11):3479-3491.
77. Stefansson S, Yepes M, Gorlatova N, et al. Mutants of plasminogen activator inhibitor-1 designed to inhibit neutrophil elastase and cathepsin G are more effective in vivo than their endogenous inhibitors. *Journal of Biological Chemistry*. 2004;279(29):29981-29987.
78. Xiong YQ, Yeaman MR, Bayer AS. In vitro antibacterial activities of platelet microbicidal protein and neutrophil defensin against *Staphylococcus aureus* are influenced by antibiotics differing in mechanism of action. *Antimicrobial Agents & Chemotherapy*. 1999;43(5):1111-1117.
79. Li J, Raghunath M, Tan D, Lareu RR, Chen Z, Beuerman RW. Defensins HNP1 and HBD2 stimulation of wound-associated responses in human conjunctival fibroblasts. *Investigative Ophthalmology & Visual Science*. 2006;47(9):3811-3819.
80. Corriden R, Chen Y, Inoue Y, et al. Ecto-nucleoside triphosphate diphosphohydrolase 1 (E-NTPDase1/CD39) regulates neutrophil chemotaxis by hydrolyzing released ATP to adenosine. *Journal of Biological Chemistry*. 2008;283(42):28480-28486.

81. Vogelmeier C, Biedermann T, Maier K, et al. Comparative loss of activity of recombinant secretory leukoprotease inhibitor and alpha 1-protease inhibitor caused by different forms of oxidative stress. *European Respiratory Journal*. 1997;10(9):2114-2119.
82. Belaaouaj A, Kim KS, Shapiro SD. Degradation of outer membrane protein A in Escherichia coli killing by neutrophil elastase. *Science*. 2000;289(5482):1185-1188.
83. Koch-Brandt C, Morgans C. Clusterin: a role in cell survival in the face of apoptosis? *Progress in Molecular & Subcellular Biology*. 1996;16:130-149.
84. Marsich E, Mozetic P, Ortolani F, et al. Galectin-1 in cartilage: expression, influence on chondrocyte growth and interaction with ECM components. *Matrix Biology*. 2008;27(6):513-525.
85. Lee J-L, Lin C-T, Chueh L-L, Chang C-J. Autocrine/paracrine secreted Frizzled-related protein 2 induces cellular resistance to apoptosis: a possible mechanism of mammary tumorigenesis. *Journal of Biological Chemistry*. 2004;279(15):14602-14609.
86. Wu GS. TRAIL as a target in anti-cancer therapy. *Cancer Letters*. 2009;285(1):1-5.
87. Alexander S, Watt F, Sawaji Y, Hermansson M, Saklatvala J. Activin A is an anticatabolic autocrine cytokine in articular cartilage whose production is controlled by fibroblast growth factor 2 and NF-kappaB. *Arthritis & Rheumatism*. 2007;56(11):3715-3725.
88. Hellio Le Graverand MP, Sciore P, Eggerer J, et al. Formation and phenotype of cell clusters in osteoarthritic meniscus. *Arthritis & Rheumatism*. 2001;44(8):1808-1818.
89. Mesih M, Zurakowski D, Soriano J, Nielson JH, Zarins B, Murray MM. Pathologic characteristics of the torn human meniscus. *American Journal of Sports Medicine*. 2007;35(1):103-112.
90. Gandhi R, Takahashi M, Virtanen C, Syed K, Davey JR, Mahomed NN. Microarray analysis of the infrapatellar fat pad in knee osteoarthritis: relationship with joint inflammation. *Journal of Rheumatology*. 2011;38(9):1966-1972.

CHAPTER 5:  
IDENTIFICATION OF NOVEL SYNOVIAL FLUID BIOMARKERS  
THAT CORRELATE WITH MENISCAL PATHOLOGY

**Experimental purpose and hypothesis**

It is suspected that markers of meniscal disease exist within the synovial fluid. These markers of disease may be released directly by the meniscus or the meniscus may signal the release of these proteins from other tissues into the synovial fluid, which in turn impact the joint as a whole. It is also suspected that some of these proteins may be markers of disease because of their absence from the synovial fluid when a pathologic event occurs. Not only is it imperative to identify meniscal biomarkers that correlate with the degree of pathology progression, it is vital to determine if and how these markers affect the joint in order to establish what therapeutic options can be developed based off these data. As previously described, mass spectrometry has been utilized on a limited basis for assessment of meniscal disease. There are a number of recent articles that have utilized this technology to evaluate human synovial fluid for arthritic conditions.<sup>1-6</sup> Only one known article has used this technology to evaluate meniscal pathology, but this study was evaluating a specific complex of proteins.<sup>7</sup> To our knowledge, mass spectrometry has not been utilized to globally study the synovial fluid associated with different types of meniscal pathology.

The overall goal of this study was to comprehensively identify synovial fluid proteomic markers of disease within different cohorts. Toward this goal, the specific aims for this project were: Specific Aim 1: Develop a synovial fluid processing protocol that allows for adequate protein separation via gel electrophoresis; Specific Aim 2:

Identify potential synovial fluid proteomic trends that exist among the aspirates collected from normal knees, meniscal repairs, meniscectomies, ACL reconstructions with and without meniscal pathology, and total knee arthroplasties via mass spectrometry analysis; and Specific Aim 3: Determine which proteins isolated have diagnostic, prognostic, and therapeutic potential. Our hypothesis was that protein biomarkers can be isolated from synovial fluid aspirates and will correlate with meniscal pathology, such as meniscal tears and meniscal degeneration.

## **Materials and methods**

### *Synovial fluid collection and storage:*

All procedures had been approved by the Institutional Review Board (IRB#1042248) and informed patient consent was obtained before synovial fluid collection. The aspirate samples were divided into one normal group and seven pathologic groups. The pathologic aspirates were collected prior to the patient undergoing an arthroscopic knee procedure or a total knee arthroplasty (TKA) and then stored at -80°C for further evaluation. The groups analyzed were as follows:

- 1) Normal Control (NC)
  - a. Patients under 30 years of age
  - b. Negative history for meniscal, ACL, or PCL injury
  - c. Negative surgical history for either knee
- 2) Meniscal Repair (MR)
  - a. Medial meniscal tear involving the vascular red-red zone
  - b. No presence of ACL, PCL, or lateral meniscal pathology
- 3) Young Meniscal Debridement (YMD)
  - a. Patients under 35 years of age
  - b. Medial meniscal tear involving avascular region
  - c. No presence of ACL, PCL, or lateral meniscal pathology

- 4) Older Meniscal Debridement (OMD)
  - a. Patients older than 50 years of age
  - b. Medial meniscal tear involving avascular region
  - c. No presence of ACL, PCL, or lateral meniscal pathology
- 5) Meniscal Debridement – Total Knee Arthroplasty (MD-TKA)
  - a. Patients have history of arthroscopic meniscal debridement
  - b. Presence of bilateral meniscal degeneration upon gross analysis
- 6) ACL Tear (ACL)
  - a. Patients undergoing ACL reconstruction and have no presence of meniscal lesions
- 7) ACL Tear with Bilateral Meniscal Tears (ACL-BMT)
  - a. Patients undergoing ACL reconstruction and have tears involving bilateral menisci
- 8) ACL Tear – Total Knee Arthroplasty (ACL-TKA)
  - a. Patients have surgical history of ACL reconstruction
  - b. Presence of bilateral meniscal degeneration upon gross analysis

*Proteomics analysis:*

Preparation of each synovial fluid sample involved first being treated with a hyaluronidase solution. The hyaluronidase powder (MP Biomedicals, Solon, OH) was reconstituted with a 0.4 mol/L sodium acetate solution to create a 0.1 TRU/ $\mu$ L concentration of hyaluronidase solution. 18  $\mu$ L of the hyaluronidase solution was added to 90  $\mu$ L of synovial fluid (1:5 ratio of hyaluronidase to synovial fluid) and then allowed to incubate for 90 minutes at 37°C. The samples were then depleted of albumin and IgG using the Sigma Proteoprep Immunoaffinity Kit (Sigma, St. Louis, MO) according to the manufacturer's instructions. A 50  $\mu$ L aliquot of each synovial fluid sample was combined with 50  $\mu$ L of equilibration buffer and then ran through the depletion column. Two columns were utilized for each sample for a total of 100  $\mu$ L of hyaluronidase treated, albumin/IgG depleted synovial fluid. The 100  $\mu$ L was concentrated by

transferring into a 3 kDa filter and centrifuging for 45 minutes at 14,000 RPM and 25°C. The column was then turned over in a new blank tube and centrifuged for 3 minutes at 3,000 RPM in order to remove the concentrated synovial fluid sample from the filter.

The EZQ® Protein Quantitation Kit (Molecular Probes, Eugene, OR) was then used to quantify the amount of protein in each sample as described in Chapter 4. A 50 µg amount of protein was loaded onto an 8 cm SDS-PAGE gel with a 1.5X concentration of LDS and reduction buffer (total amount of 25 µL = 9.375 µL LDS + 3.75 µL reducing buffer + synovial fluid solution + water). The gel was run at 115 V, 48 mA, 12.5 watts for approximately 2 hours. The gel was removed from the cassette and washed three times for 5 min with polisher distilled water; then it was stained overnight with 20 mL of SimplyBlue SafeStain. The gel was washed one more time and then prepared for analysis. Each lane was cut into 12 equal sections of 0.5 cm and then each section was cut into smaller 1 mm<sup>3</sup> blocks and placed into one of the wells within a 1 mL 96-well plate. The samples within the plate were washed, trypsin digested, frozen and analyzed as technical replicates via LC-MS/MS according to the protocol listed in Chapter 4. Simultaneous identification and quantization was achieved by conducting database searches using the Sorcerer2 Integrated Data Appliance, followed by results parsing using the Scaffold program (Proteome Software, Portland, OR) which incorporated a spectral counting algorithm to produce quantitative data for the identified proteins. Each protein was analyzed for trends between the eight clinical groups. In addition, the Scaffold program was utilized to conduct a one-way ANOVA (analysis of variance) statistical analysis without normalization in order to help identify proteins with potential differences between the clinical groups (significance set at p < 0.05).

Proteins of interest were identified and further statistical analyses were then performed using a commercially available software package (SigmaPlot 11.0, Systat Software Inc., San Jose, CA USA). Appropriate descriptive statistics (e.g., means and standard error of the mean (SEM)) were calculated for each clinical group. The data for each protein were compared for statistically significant differences using a one-way ANOVA. If a statistically significant difference was present, the Holm-Sidak method was utilized to perform pairwise comparisons. Significance was set at  $p < 0.05$ .

## Results

A total of twenty-one joint fluid aspirates were analyzed. Table 5-1 lists the patient demographics and meniscal pathology notes that are associated with each synovial fluid sample used for this proteomics study. Table 5-2 alphabetically lists the 296 proteins that were identified via LC-MS/MS along with the average quantitative value for each group studied. The 50 proteins designated with an asterisk had at least one group that was statistically different according to the one-way ANOVA conducted by the Scaffold program. All 296 proteins including the 50 proteins that had a one-way ANOVA p-value less than 0.05 were evaluated for potential trends between the normal and pathologic groups. After evaluating trends for each protein identified by LC-MS/MS, nineteen proteins were identified as proteins of interest and were further analyzed utilizing SigmaPlot in order to determine each protein's ANOVA p-value (Table 5-3). Five of these proteins had lower quantitative values within the normal group when compared to the pathologic groups; the other 14 had a higher quantitative value in the

normal group with decreased values in the pathologic groups. The nineteen proteins were graphed including the mean  $\pm$  SEM for each clinical group (Figures 5-1 through 5-19).

## Discussion

It is crucial to understand the mechanistic actions of the proteins identified. Many of these proteins have been analyzed for other traumatic or inflammatory conditions, but the role they play within intra-articular pathology, specifically meniscal pathology, is not well understood. The following provides a detailed look at each protein of interest and works to describe the potential pathophysiologic role each protein has as it relates to articular pathology. Comprehending these pathways will help us to determine if each protein has the potential of being a biomarker for diagnosis or should be targeted for its potential therapeutic effect.

### *Extracellular Superoxide Dismutase [Cu-Zn] (SOD3):*

Cellular metabolism naturally results in the production and release of reactive oxygen species (ROS) into the joint space. Endogenous antioxidants are created and released in order to counter these species and protect intra-articular tissues from oxidative damage. When an imbalance occurs with either an excess production of ROS and/or a decreased presence of antioxidants, oxidative stress occurs resulting in damage to the surrounding tissues.

One group of antioxidants named superoxide dismutases are able to neutralize two superoxide radicals into oxygen and hydrogen peroxide.<sup>8</sup> Three SOD isozymes have been described; the third was discovered by Marklund et al. in 1982 and was termed

extracellular superoxide dismutase (SOD3). They described this SOD as being the predominant SOD in plasma, synovial fluid, and other extracellular fluids.<sup>9-11</sup> The primary location of SOD3 (99%) is in the extravascular space of tissues reversibly bound to heparin sulphate proteoglycan ligands on the surface of cells and within the interstitial matrix.<sup>12,13</sup> Expression of SOD3 has been shown to be increased by interferon- $\gamma$  and IL-4, but its expression is decreased by TNF- $\alpha$ .<sup>14</sup>

As previously described, superoxide radicals are capable of degrading hyaluronic acid within synovial fluid, but superoxide dismutases have been shown to protect its degradation.<sup>15,16</sup> Collagens are known targets for oxygen free radicals and will be cleaved into small peptides, but SOD3 has the ability to bind to the heparin-binding region of collagen and protect it from oxidative fragmentation.<sup>17,18</sup> When studying oxygen-derived free radical degradation of nasal cartilage, it has been identified that the presence of superoxide dismutase will lead to inhibition of the degradation process.<sup>19</sup> Regan et al. identified how osteoarthritic human cartilage has increased levels of SOD3 mRNA but will have significantly decreased SOD3 protein levels when compared to controls. The osteoarthritic cartilage had decreased levels of immunolocalized SOD3 within the matrix, but increased intracellular staining. The extracellular matrix for the controls had a smooth distribution of SOD3. It was postulated that oxidative stress elicits an initial period of compensation, but an inadequate production of SOD3 and loss of tissue binding sites eventually prevent the ability of SOD3 to adequately counteract the increased amount of ROS that is involved in the pathophysiology of osteoarthritis.<sup>20</sup> In order to study the potential therapeutic effect of SOD3, gene therapy has been used to treat collagen-induced arthritis in a murine model. The mice treated with the SOD3

transgene had suppression of joint swelling and deformity. Histologically, the mice had less destruction of cartilage and bone, less infiltration of mononuclear cells, and less proliferation of synovial cells.<sup>21</sup> A recombinant human superoxide dismutase used within a rodent inflammation model was able to inhibit nitric oxide synthase activity and decrease IL-1 $\beta$  and TNF- $\alpha$  production. Within the study, the inhibitory effect on IL-1 $\beta$  was more pronounced for the superoxide dismutase treatment than for dexamethasone.<sup>22</sup> Superoxide dismutase isolated from bovine erythrocytes has shown some promise as an intra-articular therapy. In multiple clinical trials, one being a double blinded study, it showed superior results in comparison to placebo.<sup>23,24</sup>

This study was able to demonstrate how there is an inadequate amount of SOD3 to account for the oxidative stresses that occur during meniscal injury. As can be seen through the data presented, when meniscal pathology, ACL pathology, or degenerative joint disease occurs, the concentration of SOD3 is reduced when compared to normal patients. SOD3 has the potential of being a biomarker for synovial fluid aspirations. There may be a physiologic normal level of SOD3, but when an injury occurs, the amount of SOD3 will likely fall below this level. This marker does not appear to be specific to meniscal injury as it was low for all pathologies studied. In addition, this is certainly a protein that needs to be studied further as a potential treatment modality for intra-articular injuries. Currently, hyaluronic acid injections are commonly used for osteoarthritis. One research group has looked into binding superoxide dismutase to hyaluronic acid. The conjugate between these two molecules had a higher anti-inflammatory activity than hyaluronic acid or superoxide dismutase on their own.<sup>25</sup> The study presented here was able to demonstrate the reduction of SOD3 within the synovial

fluid and our previous study (Chapter 4) was able to demonstrate the reduction of SOD3 within meniscal tissue. Some initial research evaluating the therapeutic potential of SOD3 has begun, but this needs to be explored in more detail as a treatment option on its own or in combination with other treatment modalities.

*Isoform A and C of Proteoglycan 4 (PRG4):*

Proteoglycan 4 (lubricin) is found along the surfaces of cartilage and menisci and can be isolated within synovial fluid. This molecule is produced by chondrocytes, synovial cells, and meniscal cells and is associated with the normal lubrication of the joint, along with regulating synovial cell adhesion and proliferation.<sup>26,27</sup> This lubricating glycoprotein has been shown to be reduced by the progression of osteoarthritis. Within an ovine model, three months after performing a meniscectomy, a loss of lubricin immunostaining within the articular cartilage was observed, and the mRNA levels were significantly decreased.<sup>28</sup> Intra-articular lubricin levels have been shown to be statistically reduced following an ACL injury when compared to the contralateral uninjured knee, and is deficient within arthritic joints.<sup>27,29</sup> In order to study the therapeutic value of lubricin, a separate study evaluated intra-articular lubricin treatments within an ACL transection rat model. It was noted that the lubricin treatment group reduced the amount of type II collagen degradation.<sup>30</sup> It has been described that lubricin is chondroprotective due to the fact that it can dissipate strain energy.<sup>31</sup> When comparing lubricin to hyaluronic acid within a rat ACL transection model it was noted that lubricin was more effective at reducing cartilage damage.<sup>32</sup>

The results from this study correlate with the early findings that other groups have found with respect to lubricin function and concentration levels within synovial fluid. When meniscal pathology, ACL injury, cartilage degradation, or any combination of the three occurred, there was a reduced amount of lubricin present within the synovial fluid. When constructing a biomarker panel, this protein probably follows a similar pathway to SOD3. There is probably a normal range of lubricin within the joint and when the concentration falls below a certain level, the ability to detect pathology becomes more sensitive. Of additional interest is the therapeutic value that lubricin could provide to intra-articular pathology. A combination product of lubricin and SOD3 would be able to help establish normal joint homeostasis by providing additional lubrication and compensate for the imbalance of ROS. These are two separate mechanisms of action that should be considered when working on treatment methods for joint pathology.

*Apolipoprotein B-100 (APOB):*

APOB was not determined to be significant according to the one-way ANOVA but it did have a trending difference with elevated pathologic levels except for the ACL group when compared to normal. Out of the 18 pathologic synovial fluid samples tested, only 2 had a lower quantitative value than the highest normal value. One sample was in the MR group and was only 50 points lower than the normal mean; the other sample was in the ACL group and had an abnormally low value (quantitative value of 3 vs. normal average of 501), which leads us to believe this is not a standard value and may be an outlier.

APOB is the primary apolipoprotein within very-low-density lipoprotein (VLDL), intermediate-density lipoprotein (IDL), and low-density lipoprotein (LDL). APOB helps with the secretion of cholesterol out of the blood system into the tissues by binding to cell surface receptors and initiating endocytosis. Within the diseased state of atherosclerosis there is more LDL than there are APOB receptors, so the excess LDL has a greater risk of being oxidized by reactive species and picked up by scavenger macrophages known as “foam cells”, which in turn create atherosclerotic lesions.<sup>33</sup> One receptor that has been found to interact with oxidized LDL molecules is the lectin-like oxidized LDL receptor (LOX-1). This receptor has been shown to be induced by the presence of TNF- $\alpha$  or shear stresses within vascular endothelial cells.<sup>34-36</sup> When oxidized LDL interacts with the LOX-1 receptor, an upregulation of monocyte chemotactic protein 1 (MCP-1) occurs, which leads to the influx of monocytes.<sup>37,38</sup> In addition to attracting extra monocytes to the site of the oxidized LDL/LOX-1 receptor interaction, oxidized LDL will act as a potent inhibitor of macrophage motility, so this promotes macrophage retention at this tissue site.<sup>39</sup> The oxidized LDL will also cause apoptosis of the endothelial cells, which might be due to the oxidation products it forms.<sup>40</sup> Not only does oxidized LDL cause apoptosis, it will slow the progression and effectiveness of macrophages clearing apoptotic cells, such as apoptotic fibroblasts. This leads to an increase in MCP-1 along with other potent inflammatory cytokines such as IL-6.<sup>41</sup>

Oxidized LDL is not solely found within atherosclerotic lesions; they are present within other chronic inflammatory environments as well. Foam cells that contain oxidized LDL have been isolated in the synovial membrane from patients with rheumatoid arthritis.<sup>42</sup> In addition, oxidized LDL has been found within synovial fluid of

osteoarthritic patients. These osteoarthritic patients also had increased mRNA and protein expression of the LOX-1 receptor; LOX-1 expression was not found in normal cartilage. The presence of oxidized LDL in culture with these LOX-1 expressing chondrocytes led to decreased viability.<sup>43</sup> In a separate study, oxidized LDL was able to enhance matrix metalloproteinase 3 after interacting with LOX-1.<sup>44</sup> This relationship between oxidized LDL and LOX-1 has also been shown to induce increased leukocyte infiltration, joint swelling, and cartilage destruction in a rat model.<sup>45</sup> Just like what was described for atherosclerosis, oxidized-LDL/LOX-1 binding increases the MCP-1 concentration within cultured articular chondrocytes.<sup>46</sup> The binding of oxidized-LDL/LOX-1 will also cause an increase in VEGF expression levels within chondrocytes, which can enhance the production of MMP-1 and MMP-3.<sup>47-49</sup> Oxidative stress is present within osteoarthritic joints along with joints that sustain a meniscal injury. This is due to a number of mechanisms to include shear stress, compressive forces, and release of cytokines like IL-1 $\beta$  and TNF- $\alpha$ .<sup>50,51</sup> As described, these reactive species will cause LDL oxidation, leading to retention within the joint and interaction with the overexpressed LOX-1 receptor. A number of inflammatory cascades will then result. The study being presented is able to show that the APOB protein found within LDL might be a worthwhile biomarker for meniscal pathology. It was not statistically significant for this study but with an increased study population, a statistical difference may be present.

*C4b Binding Protein Alpha Chain (C4BPA):*

C4b-binding protein has an alpha chain and a beta chain. The beta chain functions to inactivate protein S, which in turn helps with hemostasis. However, the alpha chain seems to participate in the regulation of the complement cascade.<sup>52,53</sup> C4BPA is considered an inhibitor of the classical and lectin pathway, and plays a role in protecting apoptotic cells from the complement pathway. C4BPA will bind the DNA in an apoptotic cell, which helps limit additional complement activation and prevents the release of additional DNA from the cell. The importance of these actions is to limit complement activation toward the dying cell and in turn this will limit the amount of inflammation that is initiated by the cell. The cell is then removed by phagocytosis instead of complement mediated lysis. This protein appears to help regulate the type and amount of inflammation that occurs after cell death while guiding the process of removing these necrotic cells from the tissue.<sup>54,55</sup>

C4BPA is found circulating through plasma and one mechanism of transmigrating from the circulation into tissue is its ability to bind peripheral blood B cells.<sup>56</sup> When an injury occurs within the joint, there is an influx of circulating cells to include lymphocytes. This may be part of the reason why C4BPA is elevated within the pathological groups when compared to the normal group. The other reason for its increase may be due to the joint attempting to bring this protein in to help regulate the complement system. For example, when the meniscus is injured, some meniscal cells will undergo apoptosis. There may be a signaling mechanism that initiates the influx of C4BPA in order to interact with these apoptotic cells and guide them toward a pathway of removal by phagocytosis. This protein appears to be absent or found in very small

amounts within a normal joint. When meniscal injury occurs, it appears that the concentration of this protein in the joint will increase. What was intriguing was how the ACL group without meniscal pathology had a very low value. This could be solely attributed to the small sample size, or this protein may have an increased specificity toward meniscal damage over ACL damage. This theory would need to be evaluated further to determine if the influx of this protein is impacted by the type of joint pathology that occurs.

*Low-density Lipoprotein Receptor Related Protein 1 (LRP1):*

LRP1 is an endocytic receptor that interacts with a number of extracellular components. One of its functions is to facilitate the cellular internalization of aggregated LDL, which contains APOB as described above.<sup>57</sup> As described, oxidized LDL will be found within arthritic joints.<sup>42,43</sup> Oxidized LDL leads to aggregation of the LDL and LRP1 will function to remove it from the extracellular space and internalize it.<sup>58</sup> LRP-1 also has a function of clearing ADAMTS-5, which is an enzyme with potent aggrecan-degrading capabilities. Osteoarthritic chondrocytes appear to have impaired LRP1 mediated endocytosis of ADAMTS-5; with 90% reduction of LRP1 protein levels in the OA cartilage.<sup>59</sup> These factors help to describe why there is a drastic decrease in LRP1 within pathological joints when compared to control synovial fluid.

LRP1 can also be found on cells binding and degrading C4BPA.<sup>56</sup> As described, intra-articular pathology leads to a decrease in LRP1. This could be an extra factor that leads to the increased levels of C4BPA in the pathologic synovial fluid. With more C4BPA present, this protein can interact with the apoptotic cells present helping to

promote removal by phagocytosis. If there was a high amount of LRP1, these receptor proteins would lead to degradation of C4BPA. Without C4BPA, complement mediated lysis would occur, which could initiate additional inflammatory pathways. Another theory that may contribute to the low concentration of LRP1 within pathologic joints is that this receptor could be functioning to degrade the increased amount of C4BPA and this process leads to less available LRP1 to be read by mass spectrometry. The combination of these three proteins could function as potential biomarkers: joint pathology leads to an increase in APOB and C4BPA, along with a decrease in LRP1. It will be imperative to further understand the mechanism of action that initiates these findings.

*Aggrecan (ACAN):*

Aggrecan is a large proteoglycan that can be isolated as one of the main proteoglycans within articular cartilage and can be found at much lower concentration levels within the ACL and PCL. This large proteoglycan has also been isolated within meniscal tissue. When analyzing ovine menisci, aggrecan concentration was highest in the central portion at birth and then increased throughout the rest of the meniscus as they grew older.<sup>60</sup> For canine meniscal tissue, medial menisci were shown to have increased concentrations compared to lateral, and the inner portions had increased concentrations relative to the peripheral.<sup>61</sup> Degradation of aggrecan by aggrecanases has been described as part of the progression of arthritis. Aggrecanases cleave aggrecan and one cleavage site is the interglobular domain, which releases ARGS fragments. One study analyzed the ARGS fragment concentration levels between 26 healthy knees to 269 patients with

one of the following conditions: acute inflammatory arthritis, acute knee injury, chronic knee injury, and knee osteoarthritis. They found a statistically significant increase within all the pathologic groups. The acute inflammatory arthritis group had the highest level of fragments, with the acute injury having the second highest level (ACL and/or meniscal injury).<sup>62</sup> Another group also looked at aggrecan fragments as potential biomarkers. They focused on aggrecanase activity at the interglobular domain and the GAG-bearing region, which produce ARGs and AGEs fragments respectively. They developed mass spectrometry assays that measure ARGs and AGEs aggrecan fragment peptides in biological fluids such as urine and synovial fluid. Using this assay, they were able to show increased levels of these fragments within OA patients when compared to healthy controls within synovial fluid and urine.<sup>2</sup> A separate group created an ELISA assay specific to ARGs and was also able to detect ARGs aggrecan fragments within synovial fluid, serum, and urine.<sup>63</sup> Scuderi et al were able to isolate a protein complex that consisted of fibronectin and the aggrecan G3 domain within patients that had sustained a painful meniscal tear. They then created an ELISA that would identify this specific complex as a biomarker for meniscal injuries.<sup>7</sup> When culturing meniscal tissue with IL-1 $\beta$  or TNF- $\alpha$ , this leads to aggrecan fragmentation with release of GAG into the medium.<sup>64,65</sup>

This study was able to isolate the intact aggrecan protein using mass spectrometry analysis, but it did not recognize the aggrecan fragments as described above. Interestingly, this study showed a decrease in aggrecan concentration for the pathologic groups when compared to the normal group. It is presumed that there is a certain amount of intact aggrecan that can be found in the synovial fluid due to normal homeostasis and

extracellular matrix turnover. When an injury occurs, the aggrecan protein within the matrix and synovial fluid is fragmented causing the synovial fluid concentration of the intact protein to drop and the fragmented protein concentration to increase. Even though the mass spectrometry technology utilized for this study was unable to detect the ARGs and AGEG cleavage fragments; one can hypothesize that these fragments could be isolated within these patients utilizing one of the special assays that were described earlier. In order to more fully characterize the potential of aggrecan as a biomarker for meniscal injury, it will be important to study the concentration of intact aggrecan as well as the aggrecan fragments within synovial fluid. It will be interesting to determine if there is a standard amount of intact aggrecan that is present within synovial fluid and to also determine how much of the fragmented aggrecan results from cleavage of the synovial fluid protein and how much results from the cleavage of tissue proteins. Since articular cartilage and meniscal tissue have a higher concentration of aggrecan than the ACL and PCL, a higher concentration of fragments may result from injuries to these tissues.

*Isoform V0 of Versican Core Protein (VCAN):*

Versican is a proteoglycan that is found in various tissues such as skin, blood vessels, and the nervous system, but it is also normally found within the meniscus.<sup>61</sup> It has been shown that versican plays a role within extracellular connective tissue networks through the binding of fibrillin microfibrils.<sup>66</sup> Versican also binds to hyaluronan and link protein in a similar fashion as aggrecan.<sup>67</sup> Versican is in the same family as aggrecan and it can be catalyzed by one or more members of the ADAMTs family of

metalloproteinases just like aggrecan, such as aggrecanase-1 (ADAMTS-4).<sup>68,69</sup> However, it does not appear to be well understood which versican fragments may possibly be present within intra-articular joint fluid due to meniscal pathology and articular cartilage degradation. This particular mass spectrometry study was able to demonstrate a very similar pattern for versican when compared to aggrecan. There appears to be a normal amount of versican present within the joint that is associated with continual homeostasis of the joint. However, when meniscal pathology occurs, it is possible that versican is fragmented in a similar fashion as aggrecan causing the intra-articular concentration of versican to decrease. The mass spectrometry technology may be able to recognize the versican core protein but the particular search used to analyze the data may not have the fragmented proteins registered. It would be of interest to use an ELISA assay that is specific to versican fragments to see if these fragments are increased for patients with meniscal pathology. Just as aggrecan fragments have been found within the synovial fluid, serum, and urine due to intra-articular pathology; it is possible that the same may hold true for versican fragments.

*Hyaluronan and Proteoglycan Link Protein 1 (HAPLN1):*

Link protein is found within a number of tissues. It is probably most well known as the protein that is abundantly present within cartilage stabilizing the interaction between aggrecan and hyaluronic acid, and has been shown to stabilize the interaction between versican and hyaluronic acid.<sup>67,70</sup> Link proteins are also found within the meniscus.<sup>71</sup> When looking at the concentration of link protein within this study, it coincides with the pattern of aggrecan and versican. The three intact proteins are all

isolated within the synovial fluid of a normal joint, but they appear in lower concentration when intra-articular pathology exists. This helps to indicate that the individual components within the aggrecan/link protein/hyaluronan complex and versican/link protein/hyaluronan complex may undergo degradation simultaneously. It is plausible that a biomarker panel consisting of aggrecan fragments, versican fragments, and link protein fragments may be highly sensitive and specific to intra-articular injuries such as meniscal pathology and articular cartilage degradation. Before creating a biomarker panel, the fragments that result from degradation of the hyaluronan and proteoglycan link protein need to be determined.

*Lymphatic Vessel Endothelial Hyaluronic Acid Receptor 1 (LYVE1):*

LYVE1 is a membrane glycoprotein that binds to hyaluronic acid molecules and initiates its mobilization through lymphatic vessels.<sup>72</sup> Expression of this protein is inhibited by TNF- $\alpha$ . It is also decreased within muscles that undergo degeneration while in the presence of acute inflammation.<sup>73</sup> Acute inflammation is present when the meniscus and ACL are injured and chronic inflammation is present within the osteoarthritic joint. The progression of OA, which involves TNF- $\alpha$ , may be the cause of LYVE1 being found in very low amounts within the pathologic groups when compared to normal synovial fluid samples. It is unknown how inflammatory cytokines such as TNF- $\alpha$  may potentially cause the destruction of this glycoprotein receptor or at the very least reduce the expression of the protein. The question becomes, does this glycoprotein receptor undergo complete degradation and removal into the cell; or will the receptor fragment upon degradation to where a peptide of the degraded protein could indicate the

presence of pathology within the joint. The role of this protein along with the breakdown of this protein relative to articular pathology such as meniscal disease needs to be studied further.

*Cartilage Intermediate Layer Protein 1 (CILP):*

CILP is abundantly found within the extracellular matrix of articular tissues. This glycoprotein is within articular cartilage, meniscus, tendon, ligament, and synovial membranes. The increased expression of this protein has been associated with aging along with early and late stages of osteoarthritis.<sup>74</sup> It has been proposed that there exists an immune response against CILP, which may contribute toward the progression of joint destruction.<sup>75</sup> However, this protein did not have increased concentrations within this particular study. Instead CILP had decreased levels associated with intra-articular pathology when compared to normal. Just like what was observed with aggrecan, versican, and link protein, this protein may undergo fragmentation during the progression of osteoarthritis. An increased concentration of CILP fragments may be present within pathologic joints, which would correlate with the research findings described in the literature. In addition, when analyzing the meniscal tissue via microarray and mass spectrometry, it was observed that CILP2 had increased gene expression levels within the pathologic groups but the CILP proteins were not isolated (Chapter 4). This helps to confirm the theory that CILP may be fragmented when intra-articular pathology exists. It would be interesting to follow the progression of CILP as it is produced and released into the synovial fluid and then possibly broken down during the progression of joint injuries.

If the theory of fragmentation held true, these fragments could also be included within a biomarker panel as described for aggrecan, versican, and link protein.

*Isoform 1 of Collagen Alpha-3 (VI) Chain (COL6A3):*

When analyzing the meniscal tissue via mass spectrometry, the collagen alpha 3 (VI) chain precursor protein had the second highest quantitative value within the aged-normal group and was identified in high quantities for the pathologic meniscal groups studied (Chapter 4). Since type 1 collagen is the predominant collagen in meniscal tissue, it was hypothesized that the proteomic analysis might be identifying multiple collagens (type I, II, and VI) as the collagen alpha 3 (VI) chain precursor protein due to the fact that collagens share considerable homology. The proteomic analysis of the meniscal tissue was able to demonstrate an increased amount of the alpha 1 and alpha 2 chains of type VI collagen within the severe osteoarthritic group (Chapter 4). When we previously looked at Col 6 gene expression, we were able to demonstrate an up regulation within the osteoarthritic meniscal tissue compared to Controls (Chapter 3). When performing mass spectrometry on synovial fluid, it was intriguing to see an increased concentration of COL6A3 within the pathologic groups. This protein did not have a very high quantitative value, but its value was extremely low within the normal group and was identified in higher concentrations for the pathologic groups. As described in Chapters 3 and 4, type VI collagen may be one of the main collagens that the meniscus utilizes for reparative mechanisms. As the meniscus is trying to increase the expression and production of this protein, it may be released into the synovial fluid as well. The COL6A3 protein identified by mass spectrometry may be a fragment of a collagen fibril, and the collagen

being identified could be type I collagen due to the homology of collagen proteins. This protein certainly has the potential of being a potential biomarker for intra-articular pathology. It appears to be increased within synovial fluid after injury and it will be interesting to study if an increased amount of this protein can also be found within serum.

*Haptoglobin (HP) and Isoform 1 of Haptoglobin Related Protein (HRP):*

HP and HRP are proteins that function in binding free hemoglobin released from erythrocytes. When HP binds hemoglobin it helps to reduce the oxidative potential that can be caused by unbound hemoglobin. When increased hemolysis is present, HP is released into the circulatory system. HP is associated with the presence of inflammation, infection, and trauma.<sup>76</sup> HP has been isolated in the knee joint of patients with osteoarthritis and rheumatoid arthritis.<sup>77,78</sup> One study identified HP mRNA within patients with juvenile idiopathic arthritis (JIA) and demonstrated this was statistically significant when compared to non-inflammatory control samples. They concluded that HP is locally produced within the inflamed joints of patients with JIA.<sup>6</sup> HP and HRP may have additional roles within the synovial fluid besides just binding free hemoglobin. Hutadilok et al studied proteins bound to hyaluronic acid within normal and rheumatoid knees and found considerably more HP bound to hyaluronic acid within the pathologic knees. They also demonstrated that hyaluronic acid was more resistant to degradation by oxygen free radicals when it was bound to HP. It was concluded that acute phase proteins such as HP may have a functional role to help protect hyaluronic acid from degradation within an inflammatory environment.<sup>79</sup>

HP and HRP were found in abundance for the pathologic patients when compared to the normal patients for this study. Interestingly, it was noted that within the patients with an isolated ACL tear, the quantitative values were not as high as the groups that contained meniscal pathology. It is possible that HP and HRP not only could be markers for inflammatory diseases, they could also be a marker for meniscal pathology to include acute meniscal tears and degenerative tears. HP and HRP may be produced by the joint or released into the joint attempting to protect the joint against oxidative destruction by binding hemoglobin and protecting hyaluronic acid from degradation. When a meniscal tear occurs, there may be a signal that causes the increased production and influx of HP and HRP. Since these proteins were not isolated within the meniscal tissue (Chapter 4), the question becomes do they come from the circulatory system or does another joint tissue such as the synovial membrane produce it when an injury occurs. Other studies demonstrate that HP is increased in the serum following traumatic events and inflammatory processes.<sup>80,81</sup> So it is possible that an increased amount of these proteins within synovial fluid could be sensitive proteins to help identify meniscal pathology, but they would likely not be specific biomarkers for meniscal pathology.

*Ceruloplasmin (CP):*

Ceruloplasmin mainly functions to carry copper within the body. It also has a function with oxidation of  $\text{Fe}^{2+}$  (ferrous iron) into  $\text{Fe}^{3+}$  (ferric iron), which is required before transferrin can transport the iron molecule within the plasma. Metal binding proteins such as ceruloplasmin are increased within the serum of rheumatoid patients.<sup>81</sup> Rheumatoid patients also appear to have increased serum and synovial fluid

concentrations of ceruloplasmin when compared to osteoarthritic patients. It has been proposed that raised levels of metal-binding proteins may reflect inflammatory activity. Unbound iron is involved in the process of creating hydroxyl radicals; ceruloplasmin may function to bind iron in an attempt to decrease oxygen radical-mediated degradation of hyaluronic acid and normal joint tissue.<sup>82,83</sup>

However, when looking at the data for this study, there was a decrease in the level of ceruloplasmin isolated within the synovial fluid of the pathologic groups when compared to normal. Also of interest was the fact that ceruloplasmin had its lowest values within the acute ACL tear groups where one would expect an increased level of hemolysis due to the initial hemarthrosis that occurs with an ACL tear. Increased hemolysis results in an increased amount of free iron. Even though the mass spectrometry results in this study indicate that the pathologic groups have a lower concentration of ceruloplasmin; this may just mean there is an increased concentration of iron in the pathologic synovial fluid. There may actually be an increased amount of ceruloplasmin overall, but a high amount of ceruloplasmin could be bound to iron preventing it from being recognized by mass spectrometry. When looking at the mass spectrometry results for another iron binding protein, serotransferrin, the normal group also had a slightly higher level than the pathologic groups but this finding was not statistically significant. Iron is not identified during mass spectrometry and if the ceruloplasmin or serotransferrin proteins remain bound to iron during the gel and digest part of the processing protocol, the peptides of these proteins will not be measured by mass spectrometry. This would lead to an inaccurately low synovial fluid concentration when measured by mass spectrometry. However, if this phenomenon of bound vs. free

ceruloplasmin is true, then measurement of free ceruloplasmin may be a potential biomarker. Low levels of free ceruloplasmin within synovial fluid may be representative of joint pathology. This principle needs to be further studied before labeling it as a true biomarker by determining if it is feasible to measure bound vs. unbound ceruloplasmin protein levels within synovial fluid. Other analysis tools should be utilized to help identify and measure the amount of ceruloplasmin within synovial fluid obtained from normal patients and patients with meniscal pathology.

*Beta-2-Microglobulin (B2M):*

B2M is a protein that can be synthesized by all nucleated cells.<sup>84</sup> B2M amyloid deposits will participate in the pathogenesis of osteoarticular pathology by initiating the recruitment and activation of macrophages.<sup>85</sup> B2M has a binding affinity for the synovial membrane and cartilage surfaces. In addition to attracting macrophages, this protein plays a role in presenting peptides to cytotoxic CD8+ T-lymphocytes, presenting lipids to natural killer T-cells, activating the complement system through the classical pathway, and activating synovial fibroblasts to produce MMP-3.<sup>84</sup> Not only does it play a role within inflammation; it also appears to play a significant role with iron metabolism. When B2M is not present, the transfer of iron into the plasma is limited leading to iron overload in tissues.<sup>86,87</sup>

Within this study, the amount of B2M within the synovial fluid appeared to decrease for the pathologic events studied relative to the normal concentration. One proposed theory is that the decrease occurs because B2M is bound to tissue and is influencing the inflammatory cascade that occurs during injury, which leaves less

unbound B2M in the synovial fluid. B2M was not identified within meniscal tissue via mass spectrometry (Chapter 4), so if this theory were true the protein would need to be bound to other articular tissues. A second theory is that the B2M is reduced within pathologic joints because it is interacting with and helping to transfer the excess iron due to hemolysis out of the joint into the plasma. This would leave less free B2M present within the synovial fluid to be read by mass spectrometry. It is also possible that both of these pathways are occurring simultaneously leading to the decreased concentration of B2M within synovial fluid collected from joints that are undergoing pathological changes. Understanding the role of B2M within the joint and further evaluating the concentration levels of B2M within a normal joint vs. a joint where damage has occurred will determine if this protein can serve as a biomarker.

*Fibroblast Growth Factor Binding Protein 2 (FGFBP2):*

Fibroblast growth factor 2 (FGF-2) has been shown to contain chondroprotective properties. One study was able to show that FGF-2 suppresses ADAMTS-5 and delays cartilage degradation.<sup>88</sup> Another study highlighted the fact that FGF-2 suppresses the degradation of aggrecan into ARGs and AGEs neoepitopes in culture.<sup>89</sup> Administration of FGF promotes healing of chondral lesions by stimulating the formation of the extracellular matrix while also inducing chondrocyte proliferation.<sup>90</sup> FGF-2 release from the ECM is dependent on the presence of FGF-BPs, helping to show that FGFBPs play a pivotal role in FGF bioactivation.<sup>91</sup>

This study found the presence of FGFBP2 within joint synovial fluid to be reduced when joint pathology is present. It appears that when meniscal, ACL, or

cartilage pathology is present, FGFBP2 will be less prevalent than within the normal joint. It is unclear on the cause of this reduction within synovial fluid. Potentially, FGFBP2 along with FGF-2 are being utilized in the joint in an attempt to stimulate chondroprotective properties as previously described, and by doing so this leads to a decreased concentration within the joint fluid as the joint is unable to maintain the balance of producing enough FGFBP2 and FGF-2. It is also possible that FGFBP2 is decreased due to cytokine destruction, complement destruction, fragmentation via a protease, or another mechanism. Determining the cause of FGFBP2 reduction will possibly reveal another potential biomarker for meniscal pathology, but will also help define the physiologic imbalance that is occurring.

*Insulin Like Growth Factor Binding Protein 6 (IGFBP6):*

IGF-1 and -2 have been shown to have actions on metabolism such as promoting growth, differentiation, and cell proliferation within tissues.<sup>92</sup> The majority of IGF is bound to one of 6 binding proteins; IGFBP6 has marked preferential affinity for IGF-2 instead of IGF-1. Its main function appears to be regulation and inhibition of IGF-2 actions. IGFBP6 has been shown to promote apoptosis and inhibit the antiapoptotic effect of IGF-2.<sup>93</sup> With respect to osteoarthritis, IGF-2 has been found to be significantly depressed within an ACL transected rabbit model.<sup>94</sup> Since IGF-2 appears to be decreased within the joint after injury, this may explain why IGFBP6 also appeared in lower concentrations within the synovial fluid for the pathologic groups. It is unclear on the impact IGF-2 has on the joint during injury and why it is potentially decreased in the joint after injury. In addition, it becomes unclear on if IGFBP6 is decreased because it

potentially correlates with a low amount of IGF-2, or if it is low because the joint is working to prevent IGFBP6's ability to promote apoptosis and inhibit the antiapoptotic effect of IGF-2. The role of IGF-2 and IFGBP6 with articular injuries such as a meniscal tear will need to be studied further.

*Isoform 1 of Target of Nesh-SH3 Binding Protein (ABI3BP):*

ABI3BP is consistently down regulated in all follicular thyroid carcinomas. It was described that ABI3 are cytoplasmic molecules that interact with tyrosine kinases. One hypothesis is that this protein may negatively regulate cell growth by suppressing tyrosine kinase signaling. So overexpression of these proteins would lead to inhibited cell proliferation, but loss of expression of these proteins lead to thyroid tumorigenesis. In turn this may suggest that ABI3 protein acts as a tumor suppressor molecule.<sup>95</sup>

For this study, ABI3BP was found to have decreased levels within the pathologic study groups. It is plausible that this binding protein is selectively reduced during pathologic events such as meniscal degradation; this reduction may prevent it from stunting cell growth after injury. This pathway is not well described within meniscal and cartilage homeostasis, but it could be a protein of interest to further understand the cellular interactions that occur after injury.

## **Conclusions**

When analyzing intra-articular pathologic events such as meniscal injury and degeneration, it is important to understand the pathophysiological interactions that occur within the meniscal tissue, and also within the synovial fluid. This study worked to

capture a broad spectrum analysis of synovial fluid proteins as it relates to isolated meniscal pathological events and meniscal disease when combined with other pathologic events such as ACL and cartilaginous injuries. In order to study the synovial fluid effectively, we created and optimized a protocol that removed hyaluronic acid, albumin, and immunoglobulin in order to isolate and study the remaining synovial fluid proteins with LC-MS/MS. To our knowledge, proteomics analysis of human synovial fluid from patients with meniscal pathology has not been performed using the protocol we developed for this study. This procedure allowed for improved detection and analysis of the synovial fluid proteome, and identified numerous differences between the normal and pathologic groups.

After analyzing the proteins of interest and better understanding their role as it relates to pathological events, it became evident which ones should be studied further for inclusion within biomarker panels, and which ones should be targeted because of their conceivable therapeutic value. Four proteins (APOB, HP, HRP, and C4BPA) were found to be increased within the pathologic groups and were described as taking part within inflammatory and oxidative stress pathways that affect the meniscus. A biomarker panel highlighting the increased concentration of these proteins may help to diagnose meniscal injuries. In addition, it was determined that further analysis of metal binding proteins such as CP and B2M need to occur. These proteins were decreased within the pathologic groups but it was described that this might be occurring because the majority of these proteins may be bound to iron preventing its ability to be read by mass spectrometry. Further evaluation of bound vs. unbound protein levels will determine the ability of these two proteins to function as biomarkers. The following extracellular matrix proteins were

decreased within the pathologic groups: aggrecan, versican, HAPLN1, and CILP. Supplementary analysis should be performed to determine what fragments are created by known proteinases involved with meniscal pathology when interacting with these proteins. It is presumed that the reason why these proteins are isolated in lower concentration for the pathologic groups is because they are being cleaved by synovial fluid proteinases. If this finding is correct, their intra-articular fragment concentration will be elevated for pathological events such as a meniscal tear. One extracellular matrix protein that was elevated within the synovial fluid for the pathologic groups was COL6A3. Additional studies need to be performed to confirm that type VI collagen is truly elevated in synovial fluid after a meniscal injury especially since mRNA for this protein in addition to the actual protein have both been shown to be elevated within pathologic meniscal tissue (Chapters 3 and 4, respectively). This protein certainly has promise of serving as a meniscal biomarker. A receptor, a receptor related protein, and several binding proteins were also found to be decreased within the pathologic groups and could possibly serve as meniscal biomarkers: LYVE1, LRP1, FGFBP2, IGFBP6, and ABI3BP. These proteins may be decreased for a number of reasons: (1) they may be degraded during the inflammatory process involved with intra-articular injury, (2) the use of these proteins within certain pathways may outbalance the joints ability to produce additional proteins leading to decreased concentrations, or (3) the intra-articular tissues may be down regulating the production of these proteins when an injury occurs. In order to utilize these proteins as biomarkers it will be essential to determine what the normal synovial fluid concentration is and how much each level needs to decrease in order to indicate a pathological event has occurred. In addition to isolating and understanding

which proteins could function as biomarkers, two proteins were identified that need to be evaluated in more depth for their therapeutic potential. Intra-articular pathologic events cause the concentration levels of SOD3 and PRG4 to decrease. In addition, pathologic meniscal tissue has decreased SOD3 concentrations according to mass spectrometry analysis (Chapter 4). These two proteins play a significant role within joint homeostasis by counteracting oxidative stresses and providing lubrication. Developing an intra-articular treatment that consists of these two proteins may help to establish normal joint balance after an injury occurs.

These data provide novel information for the investigation of synovial fluid biomarkers and treatment strategies for meniscal pathology. Importantly, we were able to obtain true normal controls for comparison within this study which is often a major limiting factor in human clinical studies. Additional work is needed in order to increase the sample size of the normal and pathologic synovial fluid samples analyzed, and correlate these values with protein levels found within the serum and urine. Targeted analysis of the identified proteins will further define their diagnostic, prognostic, treatment monitoring, and therapeutic potential.

**Table 5-1: Patient demographics**

<b>Group</b>	<b>Meniscal pathology Notes</b>	<b>Age (yrs)</b>	<b>Gender</b>	<b>ICRS Score</b>
NC	N/A	23	Female	ND
NC	N/A	27	Male	ND
NC	N/A	28	Male	ND
MR	Medial posterior tear	30	Male	1a (LFC)
MR	Medial body tear	36	Female	1a (MFC)
MR	Medial body and posterior tear	37	Male	3a (Patella)
YMD	Medial body tear	25	Female	1a (MFC)
YMD	Medial posterior tear	30	Female	1b (MFC)
YMD	Medial posterior tear	33	Male	0
OMD	Medial posterior tear	53	Male	3c (MTP)
OMD	Medial posterior tear	56	Female	2 (MFC + Patella), 3a (Trochlea)
OMD	Medial posterior tear	56	Male	2 (MFC), 3a (LFC)
MD-TKA	Severe disruption of medial; Moderate disruption of lateral	57	Female	ND
MD-TKA	Mild disruption of medial; Moderate disruption of lateral	66	Female	ND
MD-TKA	Severe disruption of medial; Severe disruption of lateral	67	Male	ND
ACL	Menisci normal in appearance	18	Male	0
ACL	Menisci normal in appearance	23	Male	0
ACL-BMT	Medial body tear repair; Lateral posterior tear debridement	30	Male	2 (MFC)
ACL-BMT	Medial posterior tear repair; Lateral posterior tear repair	36	Male	0
ACL-TKA	Severe disruption of medial; Moderate disruption of lateral	50	Female	ND
ACL-TKA	Moderate disruption of medial; Severe disruption of lateral	57	Male	ND

MFC = Medial femoral condyle

LFC = Lateral femoral condyle

ND = Not determined

**Table 5-2: Proteomics analysis**

IDENTIFIED PROTEINS	MW (kDa)	NC	MR	YMD	OMD	MD-TKA	ACL	ACL-BMT	ACL-TKA
104 kDa protein	104	2.7	0.8	0.0	0.0	0.0	0.0	0.0	0.0
13 kDa protein	13	1.6	1.7	4.8	1.3	3.5	3.5	1.5	1.8
22 kDa protein	22	0.0	0.7	0.0	0.0	0.0	0.0	0.0	0.0
55 kDa protein	55	31.3	28.1	34.2	27.4	31.5	53.9	54.5	63.7
* <i>AIBG Alpha-1B-glycoprotein</i>	54	106.4	95.6	94.4	92.8	73.9	84.2	152.8	120.6
A2M Alpha-2-macroglobulin	163	760.2	1469.4	1789.2	1645.9	1102.9	1446.9	1693.1	829.6
* <i>ABI3BP Isoform 1 of Target of Nesh-SH3</i>	119	19.4	4.7	1.9	3.7	0.6	3.4	3.3	5.8
* <i>ACAN 246 kDa protein</i>	246	314.6	107.8	56.1	71.1	15.0	172.1	32.2	29.3
ACTB Actin, cytoplasmic 1	42	31.2	18.1	17.6	25.5	34.6	26.5	14.0	22.0
ADIPOQ Adiponectin	26	3.2	1.4	0.9	0.3	1.0	3.7	1.4	0.0
AFM Afamin	69	61.9	52.3	63.3	53.1	56.7	28.9	52.3	42.5
AGT Angiotensinogen	53	111.4	40.6	54.6	39.2	86.5	146.7	94.0	63.8
AHSG cDNA FLJ55606, highly similar to Alpha-2-HS-glycoprotein	47	231.8	129.9	259.8	207.7	92.6	190.8	121.5	207.4
ALAD Delta-aminolevulinic acid dehydratase	39	0.0	1.1	0.0	0.0	0.0	0.0	0.0	0.0
ALB Isoform 1 of Serum albumin	69	125.6	146.7	143.2	96.1	103.7	302.5	243.9	220.3
ALB Putative uncharacterized protein ALB	72	39.5	68.3	60.3	31.0	36.5	6.2	8.2	81.7
ALDOA Fructose-bisphosphate aldolase A	39	1.8	0.6	0.0	0.0	1.8	1.1	0.0	0.0
ALS2 Isoform 1 of Alsin	184	0.0	0.0	0.0	3.2	0.4	0.0	0.6	0.7
AMBP Protein AMBP	39	77.8	65.6	75.1	64.4	35.5	57.1	89.7	70.8
* <i>ANXA5 Annexin A5</i>	36	4.5	0.4	0.0	0.0	0.3	1.6	0.0	0.0
APCS Serum amyloid P-component	25	8.8	14.0	13.6	17.1	13.0	13.3	13.7	13.5

**Table 5-2: Proteomics analysis (continued)**

IDENTIFIED PROTEINS	MW (kDa)	NC	MR	YMD	OMD	MD-TKA	ACL	ACL-BMT	ACL-TKA
APOA1 Apolipoprotein A-I	31	2016.5	1260.1	1175.9	1221.5	1457.7	1117.0	569.2	1670.2
APOA2 Apolipoprotein A-II	11	976.5	1113.2	972.5	1297.7	893.5	771.7	525.2	842.6
APOA4 Apolipoprotein A-IV	45	165.0	102.4	102.0	162.3	129.4	123.1	113.0	157.2
APOA4 apolipoprotein A-IV precursor	45	40.0	53.6	0.0	27.6	41.7	0.0	0.0	0.0
APOB Apolipoprotein B-100	516	501.1	940.8	1089.0	868.1	889.0	365.8	879.1	805.2
APOB Putative uncharacterized protein APOB	93	140.5	233.6	281.5	188.7	281.9	44.0	237.2	233.3
APOC1 Apolipoprotein C-I	9	38.6	114.9	88.0	78.2	38.5	17.0	38.2	30.8
APOC2 Apolipoprotein C-II	11	21.9	46.7	47.9	54.0	41.4	30.5	31.0	23.8
APOC3 Apolipoprotein C-III	11	129.8	117.7	132.4	135.2	114.8	74.7	59.8	139.7
APOC4 Apolipoprotein C-IV	15	0.0	6.3	1.1	0.7	0.0	0.0	0.6	0.0
APOD Apolipoprotein D	21	88.4	42.0	27.0	37.4	23.2	41.1	54.8	42.9
APOE Apolipoprotein E	36	111.6	192.6	114.0	175.4	79.8	77.1	152.9	80.3
APOH Beta-2-glycoprotein 1	38	95.1	65.3	80.4	114.1	121.3	129.4	70.0	108.1
APOL1 Isoform 2 of Apolipoprotein L1	46	6.2	22.0	32.3	24.4	13.7	5.4	20.7	15.7
APOM Apolipoprotein M	21	11.4	17.0	11.4	10.5	5.2	3.4	2.8	8.4
ARHGDI B rho GDP-dissociation inhibitor 2	23	0.0	0.0	0.0	0.0	0.3	0.0	0.0	0.0
ARPC4 Actin-related protein 2/3 complex subunit 4	20	2.3	0.0	0.0	0.0	0.7	0.0	0.0	0.0
ATRN Isoform 1 of Attractin	159	7.4	9.6	8.7	9.6	4.2	13.4	5.4	5.5
AZGP1 alpha-2-glycoprotein 1, zinc	34	135.4	97.2	74.9	83.7	69.0	82.3	75.0	81.9
<b>*B2M Beta-2-microglobulin</b>	14	62.7	25.4	30.8	39.9	28.1	27.7	13.4	31.9
BCHE Cholinesterase precursor	73	0.0	0.0	1.2	0.2	1.3	0.0	0.0	0.0
BPGM Bisphosphoglycerate mutase	30	0.0	0.9	0.0	0.0	0.0	0.0	0.0	0.0
BTD Biotinidase	61	1.7	2.0	1.3	0.8	0.4	1.8	0.8	1.1
C1QB complement component 1, q subcomponent, B chain precursor	27	4.7	10.5	1.1	2.5	3.0	2.0	8.1	12.2

**Table 5-2: Proteomics analysis (continued)**

IDENTIFIED PROTEINS	MW (kDa)	NC	MR	YMD	OMD	MD-TKA	ACL	ACL-BMT	ACL-TKA
C1QC Complement C1q subcomponent subunit C	26	2.3	4.5	1.9	1.7	4.6	1.9	1.3	4.8
C1R cDNA FLJ54471, highly similar to Complement C1r subcomponent	82	1.4	4.7	9.3	7.6	12.4	0.4	6.5	9.5
C1S Complement C1s subcomponent	77	0.2	3.6	4.9	2.9	6.9	0.0	2.5	3.3
C2 Complement C2 (Fragment)	83	18.4	9.3	8.9	7.4	8.4	6.0	3.6	10.7
C3 Complement C3 (Fragment)	187	1256.7	1250.2	1396.7	1277.0	1371.4	1251.9	1491.6	1463.0
* <b>C4A Putative uncharacterized protein C4A</b>	193	147.2	182.1	113.5	249.9	135.7	73.8	372.0	275.9
C4B Complement component 4B	193	48.0	0.0	0.0	43.9	3.9	0.0	0.0	0.0
C4B complement component 4B preproprotein	193	470.6	404.5	357.8	497.9	361.2	270.4	632.7	444.2
* <b>C4BPA C4b-binding protein alpha chain</b>	67	0.3	13.5	15.2	16.9	13.8	1.5	41.5	10.5
C4BPB Isoform 1 of C4b-binding protein beta chain	28	0.0	0.6	0.7	1.1	0.3	0.0	0.7	0.0
* <b>C5 Complement C5</b>	188	79.4	87.3	93.6	77.7	85.9	36.4	71.3	79.9
* <b>C6 Complement component 6 precursor</b>	106	28.5	19.3	25.8	19.7	21.9	7.6	13.5	28.5
C7 Complement component C7	94	29.9	14.3	13.6	21.8	25.2	9.2	2.6	6.9
* <b>C8A Complement component C8 alpha chain</b>	65	0.3	4.1	2.6	1.5	5.4	0.0	4.2	2.7
C8B Complement component C8 beta chain	67	0.0	2.9	2.4	1.7	3.4	8.0	9.4	5.7
C8G Complement component C8 gamma chain	22	29.3	38.1	29.2	47.4	33.2	38.4	25.7	62.9
* <b>C9 Complement component C9</b>	63	16.7	24.9	28.2	18.5	27.0	4.0	41.5	32.3
CA1 Carbonic anhydrase 1	29	4.1	31.1	0.6	0.2	6.0	109.7	66.1	5.1
CA2 Carbonic anhydrase 2	29	0.9	8.4	0.0	0.9	1.7	52.9	65.6	10.3
CABIN1 Similar to calcineurin binding protein 1	238	0.0	0.0	0.0	0.0	0.0	1.6	0.0	0.5
CAT Catalase	60	0.0	2.4	0.0	0.0	0.0	0.0	0.0	0.0
CD14 Monocyte differentiation antigen CD14	40	1.5	3.4	4.9	7.6	6.2	1.9	3.6	5.7
CD163 Isoform 1 of Scavenger receptor cysteine-rich type 1 protein M130	125	1.2	0.2	0.2	2.3	2.2	13.0	0.4	0.4
CD248 Isoform 1 of Endosialin	81	0.6	0.0	0.0	0.0	0.0	0.0	0.0	0.0

**Table 5-2: Proteomics analysis (continued)**

IDENTIFIED PROTEINS	MW (kDa)	NC	MR	YMD	OMD	MD-TKA	ACL	ACL-BMT	ACL-TKA
CD5L CD5 antigen-like	38	6.3	14.6	26.7	16.4	17.4	16.0	22.3	30.5
cDNA FLJ55673, highly similar to Complement factor B	141	235.3	181.7	206.2	163.4	177.0	80.0	161.6	206.2
CFD Complement factor D preproprotein	28	25.3	8.3	13.5	18.0	10.3	30.4	3.4	21.5
CFH Isoform 1 of Complement factor H	139	129.2	111.3	177.5	177.3	159.1	334.9	114.0	190.4
CFH Putative uncharacterized protein CFH	44	0.0	5.6	21.8	0.0	9.2	32.5	0.0	24.9
CFHR1;LOC100293069 Complement factor H-related protein 1	38	4.4	3.5	1.8	7.3	5.3	6.3	5.1	6.1
CFHR2;CFHR1 Isoform Long of Complement factor H-related protein 2	31	9.3	6.2	4.7	2.9	3.4	4.7	5.1	6.4
CFI Complement factor I	66	30.7	16.4	25.5	32.6	24.2	17.2	20.0	43.9
CFL1 Cofilin-1	19	2.3	0.0	0.0	0.5	0.0	0.0	0.0	0.0
CHAD Chondroadherin	40	3.7	0.0	0.0	0.0	0.0	0.0	0.0	0.0
CHD5 Chromodomain-helicase-DNA-binding protein 5	223	2.8	1.7	2.5	3.1	1.3	0.4	0.5	1.8
CHI3L1 Chitinase-3-like protein 1	43	0.4	3.3	4.0	2.2	3.0	0.4	3.1	1.8
* <i>CILP Cartilage intermediate layer protein 1</i>	133	22.7	8.2	2.0	4.5	0.0	12.6	3.2	2.6
CLEC3B Tetranectin	23	31.3	15.0	16.5	22.1	13.8	25.4	6.0	34.5
CLU Isoform 1 of Clusterin	58	104.7	86.8	84.4	92.9	52.2	42.9	78.3	98.1
CNDP1 Beta-Ala-His dipeptidase	57	0.0	0.4	0.0	0.0	0.0	0.0	0.0	0.0
COL1A1 Collagen alpha-1(I) chain	139	6.9	4.7	0.1	2.7	4.3	0.0	1.1	0.5
COL1A2 Collagen alpha-2(I) chain	129	1.5	2.2	0.0	0.0	0.0	0.0	0.0	0.0
COL3A1 Isoform 1 of Collagen alpha-1(III) chain	139	0.0	0.0	0.2	1.8	0.5	0.0	2.3	0.5
COL4A2 167 kDa protein	167	0.5	0.0	0.9	0.5	0.0	1.2	0.9	0.0
COL5A1 Collagen type V alpha 1	184	0.2	2.7	1.9	0.4	2.0	3.0	8.2	3.7
* <i>COL6A3 Isoform 1 of Collagen alpha-3(VI) chain</i>	344	0.7	3.2	3.9	3.8	3.9	1.7	12.9	3.9
COMP Cartilage oligomeric matrix protein	83	54.8	23.0	30.2	34.9	40.2	31.3	22.2	34.1
* <i>CP Ceruloplasmin</i>	122	482.5	296.6	362.1	318.8	376.7	219.1	200.9	408.9

**Table 5-2: Proteomics analysis (continued)**

IDENTIFIED PROTEINS	MW (kDa)	NC	MR	YMD	OMD	MD-TKA	ACL	ACL-BMT	ACL-TKA
CPB2 Isoform 1 of Carboxypeptidase B2	48	4.0	1.6	3.0	2.3	2.7	5.4	1.2	4.7
CPN1 Carboxypeptidase N catalytic chain	52	0.0	0.3	0.4	2.2	0.6	0.0	0.8	1.8
* <i>CPN2 Carboxypeptidase N subunit 2</i>	61	4.1	4.2	9.8	8.3	8.5	0.4	11.4	4.1
CRISP3 cDNA FLJ75207	29	0.7	0.5	0.9	0.5	0.4	1.0	0.6	0.2
CRP Isoform 1 of C-reactive protein	25	0.0	0.0	2.1	6.4	0.8	0.0	0.4	1.2
* <i>CRTAC1 Isoform 1 of Cartilage acidic protein 1</i>	71	16.5	9.7	11.3	20.7	22.8	13.4	14.7	23.3
* <i>CST3 Cystatin-C</i>	16	30.2	6.0	10.6	11.5	9.1	20.7	7.9	36.9
DAG1 Dystroglycan	97	0.7	0.0	0.0	0.0	0.0	0.0	0.0	0.0
DCD Dermcidin	11	3.2	0.0	0.0	0.0	2.2	14.6	1.2	1.2
DEFA1;LOCT28358 Neutrophil defensin 1	10	15.0	9.3	7.5	0.0	15.1	0.0	2.4	8.0
DOCK9 Isoform 1 of Dedicator of cytokinesis protein 9	240	0.0	0.0	0.5	0.0	0.4	0.0	0.0	0.0
DSP Isoform DPI of Desmoplakin	332	0.0	0.2	0.0	0.0	0.6	0.0	0.0	0.0
ECM1 Isoform 1 of Extracellular matrix protein 1	61	2.8	4.0	3.1	3.1	3.1	1.1	3.9	3.8
EFEMP1 Isoform 1 of EGF-containing fibulin-like ECM protein 1	55	2.2	6.5	6.6	9.2	6.9	4.9	13.0	9.8
ENO1 Isoform alpha-enolase of Alpha-enolase	47	0.0	0.0	0.0	0.0	0.6	0.0	0.0	0.8
F10 Coagulation factor X	55	3.1	0.8	0.2	2.3	2.2	0.0	0.5	2.9
* <i>F12 Coagulation factor XII</i>	68	15.6	25.9	29.2	22.5	15.8	4.1	21.0	12.6
F13B Coagulation factor XIII B chain	76	0.5	0.7	1.5	0.8	0.3	0.0	1.2	0.0
F2 Prothrombin (Fragment)	70	44.9	50.8	51.0	43.8	45.7	37.7	74.3	50.8
F8 Coagulation factor VIII	267	5.6	6.1	4.2	3.8	0.0	0.0	0.0	0.0
FCN2 Isoform 1 of Ficolin-2	34	0.0	0.0	1.2	0.0	0.0	0.0	0.4	0.0
FCN3 Isoform 1 of Ficolin-3	33	4.0	10.5	13.8	20.5	4.9	2.8	29.5	10.0
FETUB Fetuin-B	42	2.4	1.1	3.6	2.9	3.1	5.7	1.5	1.9
FGA Isoform 2 of Fibrinogen alpha chain	70	90.1	242.0	182.5	269.2	182.7	90.2	284.7	267.9

**Table 5-2: Proteomics analysis (continued)**

IDENTIFIED PROTEINS	MW (kDa)	NC	MR	YMD	OMD	MD-TKA	ACL	ACL-BMT	ACL-TKA
FGB Fibrinogen beta chain	56	43.6	108.9	75.1	120.4	107.2	60.4	157.8	108.9
<b>*FGFBP2 Fibroblast growth factor-binding protein 2</b>	25	10.7	3.9	6.0	5.0	2.4	2.4	3.5	6.4
FGG Isoform Gamma-B of Fibrinogen gamma chain	52	25.9	50.5	48.8	89.5	86.0	47.1	157.1	86.6
FN1 fibronectin 1 isoform 4 preproprotein	256	480.2	563.0	272.7	598.5	428.5	477.3	741.1	855.7
FN1 Isoform 3 of Fibronectin	259	646.5	698.6	351.0	781.1	605.0	685.1	886.3	1132.0
GAPDH Glyceraldehyde-3-phosphate dehydrogenase	36	0.0	0.0	0.0	0.4	0.8	0.0	0.0	1.2
GC Vitamin D-binding protein	53	430.0	242.0	275.7	285.7	245.9	569.5	274.4	240.4
GC vitamin D-binding protein precursor	53	153.6	0.0	82.3	0.0	0.0	0.0	104.7	0.0
GDF5OS Protein GDF5OS, mitochondrial	28	0.6	0.2	0.6	0.3	0.4	3.1	0.0	0.0
GP1BA platelet glycoprotein Ib alpha polypeptide precursor	70	0.0	0.5	0.9	0.4	0.0	0.0	0.3	0.0
GPLD1 Isoform 1 of Phosphatidylinositol-glycan-specific phospholipase D	92	1.8	3.9	5.1	5.5	6.7	0.8	2.3	2.8
GPX3 Glutathione peroxidase 3	26	4.6	1.0	2.5	3.4	0.9	1.2	0.5	4.4
GSN Isoform 1 of Gelsolin	86	75.0	41.4	75.6	76.4	71.9	41.4	54.3	36.2
GSTP1 Glutathione S-transferase P	23	1.3	0.2	0.0	1.1	0.2	0.0	0.0	1.2
HABP2 Hyaluronan-binding protein 2	63	3.7	1.9	3.0	1.9	1.4	1.1	2.2	3.8
<b>*HAPLN1 Hyaluronan and proteoglycan link protein 1</b>	40	19.5	6.5	1.9	2.6	0.0	13.9	2.1	2.0
HBA2;HBA1 Hemoglobin subunit alpha	15	391.6	583.3	135.0	89.3	350.2	104.5	50.6	167.8
HBB Hemoglobin subunit beta	16	671.1	1157.3	223.2	167.8	587.1	167.4	73.1	342.5
HBD;HBB Hemoglobin subunit delta	16	280.5	435.1	79.6	31.4	169.7	24.8	20.4	161.5
HBG2 Hemoglobin subunit gamma-2	16	32.7	88.4	8.9	0.0	66.7	0.0	0.0	0.0
HCG2010697	11	42.0	41.5	39.6	62.9	85.7	32.4	72.8	74.6
HGFAC Hepatocyte growth factor activator	71	2.1	0.9	0.5	1.6	1.8	0.8	0.4	0.5
<b>*HP Haptoglobin</b>	47	511.4	1956.3	2270.0	1811.1	2003.0	988.3	1162.7	1817.8
HP;HPR Isoform 1 of Haptoglobin-related protein	39	72.1	802.2	747.8	599.2	328.4	113.1	340.1	239.7

**Table 5-2: Proteomics analysis (continued)**

IDENTIFIED PROTEINS	MW (kDa)	NC	MR	YMD	OMD	MD-TKA	ACL	ACL-BMT	ACL-TKA
HPX Hemopexin	52	346.8	263.2	255.3	253.5	221.3	263.4	296.7	302.7
HRG Histidine-rich glycoprotein	60	131.6	121.2	103.6	112.5	109.6	85.1	97.8	210.7
HRV Fab 025-VL	13	1.5	4.1	7.9	5.1	1.9	0.7	1.5	1.0
HSPG2 Basement membrane-specific heparan sulfate PG core protein	469	9.0	1.5	2.0	4.2	0.4	3.6	1.2	4.6
Ig gamma lambda chain V-II region DOT	12	0.0	0.0	0.0	0.0	0.4	0.0	0.0	0.0
Ig kappa chain V-I region Ka	12	0.2	0.0	0.1	0.8	1.8	0.4	0.0	0.5
Ig kappa chain V-I region Ni	12	2.7	2.0	3.6	3.4	3.1	2.2	1.1	1.0
Ig kappa chain V-I region Roy	12	0.0	0.0	0.1	2.3	0.0	0.0	0.0	0.0
Ig kappa chain V-III region CLL	14	4.1	2.0	3.8	5.8	5.5	4.9	1.3	1.9
Ig kappa chain V-III region HIC	14	33.2	29.0	78.2	47.8	57.6	27.6	30.9	29.6
Ig kappa chain V-IV region B17	15	21.2	25.5	31.2	28.4	23.0	18.8	15.6	20.3
Ig kappa chain V-IV region JI	15	0.0	3.3	3.1	2.3	2.4	4.4	3.7	3.6
*IGFALS Insulin-like growth factor-binding protein complex acid labile chain	66	48.5	29.2	49.7	15.1	19.1	15.8	24.3	26.6
*IGFBP4 Insulin-like growth factor-binding protein 4	28	2.6	2.2	3.5	5.2	3.7	1.9	1.0	12.8
*IGFBP6 Insulin-like growth factor-binding protein 6	25	22.8	6.1	3.1	5.6	1.7	8.4	2.7	8.9
IGHA1 cDNA FLJ14473 fis, clone MAMMA1001080, highly similar to Homo sapiens SNC73 protein (SNC73) mRNA	53	284.9	245.8	415.2	586.1	413.1	386.3	715.8	237.1
IGHD Isoform 2 of Ig delta chain C region	47	1.2	1.6	2.1	0.0	1.8	0.7	6.0	2.3
IGHG2 Putative uncharacterized protein DKFZp686C15213	51	1.5	2.6	6.2	5.1	3.8	0.6	4.6	2.7
IGHG3 FLJ00385 protein (Fragment)	56	0.0	0.0	1.7	2.0	1.3	0.0	0.0	0.0
IGHM 52 kDa protein	52	59.5	106.1	194.8	126.8	120.3	105.3	269.0	155.6
IGHM Full-length cDNA clone CS0DD006YL02 of Neuroblastoma of Homo sapiens	41	0.0	9.0	37.5	16.0	16.2	0.0	40.6	0.0
IGHM Isoform 2 of Ig mu chain C region	52	0.0	0.0	0.0	0.0	31.7	0.0	17.7	0.0

**Table 5-2: Proteomics analysis (continued)**

IDENTIFIED PROTEINS	MW (kDa)	NC	MR	YMD	OMD	MD-TKA	ACL	ACL-BMT	ACL-TKA
IGHV4-31;LOC100293211;IGHG1;IGH@ cDNA FLJ78387	52	4.6	2.4	12.2	3.7	4.6	1.3	7.9	2.0
*IGHV4-31;LOC100293211;IGHG1;IGH@ protein	51	2.7	1.4	7.1	18.9	15.8	4.1	17.5	11.3
*IGHV4-31;LOC100293211;IGHG1;IGH@ Putative uncharacterized protein DKFZp686G11190	52	0.8	4.5	10.7	19.5	16.5	4.3	10.2	4.1
IGJ immunoglobulin J chain	18	8.8	18.9	23.8	25.7	18.3	9.1	5.5	25.3
IGK@ IGK@ protein	26	204.9	247.4	477.6	426.4	526.9	225.9	185.0	278.7
IGK@ IGK@ protein	26	227.8	239.8	504.7	385.3	480.2	245.9	237.6	260.8
IGKV1-5 Ig kappa chain V-I region HK102	13	11.4	7.7	15.0	15.5	5.8	8.3	3.6	8.5
IGKV1-5 Ig kappa chain V-II region GM607 (Fragment)	13	17.7	21.0	23.9	18.6	21.0	12.1	10.7	10.3
IGKV3-20 IGK@ protein	26	87.3	116.6	312.7	155.4	183.3	42.6	95.0	166.0
IGLC2;IGLV2-11;IGLV1-40;IGLV2-14;IGLV3-21;LOC100290557;IGLC1;LOC100293277;IGL@;IGLV1-44;IGLC3;LOC100290481;LOC100293440 hypothetical protein XP_002348153	28	78.9	113.8	159.0	133.4	163.5	99.1	99.9	87.2
*IGLC2;IGLV2-11;IGLV1-40;IGLV2-14;IGLV3-21;LOC100290557;IGLC1;LOC100293277;IGL@;IGLV1-44;IGLC3;LOC100290481;LOC100293440 IGL@ protein	25	104.5	116.8	142.7	141.2	56.0	0.0	96.0	70.9
IGLC2;IGLV2-11;IGLV1-40;IGLV2-14;IGLV3-21;LOC100290557;IGLC1;LOC100293277;IGL@;IGLV1-44;IGLC3;LOC100290481;LOC100293440 Putative uncharacterized protein	25	22.0	22.1	30.4	20.2	12.3	8.5	3.3	4.8
IGLC2;IGLV2-11;IGLV1-40;IGLV2-14;IGLV3-21;LOC100290557;IGLC1;LOC100293277;IGL@;IGLV1-44;IGLC3;LOC100290481;LOC100293440 similar to Ig lambda chain	30	0.7	0.0	0.9	0.3	0.2	2.0	0.5	1.7
IGLC2;IGLV2-11;IGLV1-40;IGLV2-14;IGLV3-21;LOC100290557;IGLC1;LOC100293277;IGL@;IGLV1-44;IGLC3;LOC100290481;LOC100293440 V2-7 protein	13	9.3	11.2	8.4	7.5	6.2	6.4	8.8	6.8
IGLV2-18 V1-5 protein	13	1.4	1.4	3.4	2.5	2.0	2.5	3.2	2.2
IGLV4-69 V5-6 protein	13	0.0	0.3	1.1	0.0	0.1	0.6	0.2	0.0

**Table 5-2: Proteomics analysis (continued)**

IDENTIFIED PROTEINS	MW (kDa)	NC	MR	YMD	OMD	MD-TKA	ACL	ACL-BMT	ACL-TKA
IGLV6-57 Amyloid lambda 6 light chain variable region PIP	13	0.4	0.3	1.3	1.0	0.9	0.4	0.0	0.2
IGLV7-43 Ig lambda chain V region 4A	12	1.3	1.8	1.3	0.5	0.7	0.0	0.9	1.4
Immunglobulin light chain variable region (Fragment)	11	1.1	3.0	2.5	0.0	2.8	0.0	0.0	1.1
INS;INS-IGF2;IGF2 Isoform 1 of Insulin-like growth factor II	20	8.9	3.7	6.5	8.4	4.2	7.0	4.8	11.5
ITIH1 Inter-alpha-trypsin inhibitor heavy chain H1	101	95.8	134.5	158.7	107.6	104.3	143.4	222.0	111.4
ITIH2 Inter-alpha-trypsin inhibitor heavy chain H2	106	126.0	163.0	185.5	125.1	131.7	153.4	231.3	152.1
ITIH3 Isoform 1 of Inter-alpha-trypsin inhibitor heavy chain H3	100	9.3	13.2	12.0	9.1	12.8	2.8	6.4	14.2
* <b>ITIH4 ITIH4 protein</b>	104	135.2	124.0	128.1	111.7	123.6	41.8	89.2	168.4
JUP Junction plakoglobin	82	0.0	0.0	0.0	0.0	0.6	0.0	0.0	0.0
KLKB1 Plasma kallikrein	71	3.4	14.3	11.9	9.0	8.3	0.7	9.6	9.1
KNG1 Isoform HMW of Kininogen-1	72	0.0	0.5	1.2	0.2	0.0	0.0	0.0	0.0
KNG1 Isoform LMW of Kininogen-1	48	148.5	124.5	135.1	112.7	93.4	95.1	103.2	117.2
KPRP Keratinocyte proline-rich protein	64	0.0	1.1	0.8	0.9	1.9	2.7	0.8	3.8
KRT1 Keratin, type II cytoskeletal 1	66	634.8	392.5	377.1	458.5	741.1	926.7	588.5	548.3
KRT10 Keratin, type I cytoskeletal 10	59	409.7	188.5	188.1	250.9	445.5	674.8	392.5	377.6
KRT13 Isoform 1 of Keratin, type I cytoskeletal 13	50	0.0	0.0	6.7	0.0	16.8	0.0	0.0	0.0
KRT13 keratin 13 isoform b	46	0.0	0.0	4.5	0.0	13.0	0.0	0.0	0.0
* <b>KRT14 Keratin, type I cytoskeletal 14</b>	52	76.8	29.2	30.3	23.9	73.4	131.3	40.2	61.7
* <b>KRT16 Keratin, type I cytoskeletal 16</b>	51	26.1	16.4	6.9	6.8	32.1	91.5	3.2	8.5
KRT2 Keratin, type II cytoskeletal 2 epidermal	66	343.5	141.3	166.3	148.8	275.4	452.9	221.2	279.2
KRT31 Keratin, type I cuticular Ha1	47	0.8	1.8	0.0	0.0	0.0	0.0	3.2	0.0
KRT5 Keratin, type II cytoskeletal 5	62	70.4	18.5	24.5	27.0	77.6	104.2	37.1	49.9
* <b>KRT6C Keratin, type II cytoskeletal 6C</b>	60	17.0	16.1	31.4	10.0	44.4	103.8	8.7	11.0
KRT82 Keratin, type II cuticular Hb2	57	0.0	1.3	0.0	0.0	0.0	0.0	0.4	0.0

**Table 5-2: Proteomics analysis (continued)**

IDENTIFIED PROTEINS	MW (kDa)	NC	MR	YMD	OMD	MD-TKA	ACL	ACL-BMT	ACL-TKA
KRT83 Keratin, type II cuticular Hb3	54	0.4	4.0	0.0	0.0	0.7	0.0	5.1	0.0
KRT9 Keratin, type I cytoskeletal 9	62	217.4	119.2	100.9	90.1	248.5	270.5	153.0	191.6
Lambda-chain	25	224.0	212.5	228.8	306.1	256.8	154.3	282.1	205.8
LDHA L-lactate dehydrogenase	40	6.8	4.2	1.4	4.6	2.6	3.0	2.5	6.0
LDHB L-lactate dehydrogenase B chain	37	5.5	3.1	0.0	1.3	1.2	1.0	0.0	0.0
LEP Leptin	19	0.0	0.0	0.0	0.0	0.0	68.6	59.7	0.0
LGALS3BP Galectin-3-binding protein	65	1.6	0.0	0.0	0.0	1.3	0.8	0.0	0.0
* <i>LOC100126583;IGHA2 Putative uncharacterized protein DKFZp686C02218 (Fragment)</i>	54	74.8	78.5	147.2	219.6	150.8	12.2	277.2	83.8
LOC100133511 hypothetical protein, partial	145	0.0	139.2	0.0	17.9	0.0	0.0	306.9	0.0
LOC284297 Scavenger receptor cysteine-rich domain-containing protein LOC284297	116	0.0	0.2	0.3	0.4	5.7	0.0	1.2	1.0
LOC650405 similar to hCG2042707	16	1.9	1.5	1.4	1.4	1.7	0.4	0.2	0.4
LPA Apolipoprotein(a)	501	4.6	1.5	13.4	2.8	39.6	1.2	6.2	9.9
LRG1 Leucine-rich alpha-2-glycoprotein	38	29.5	19.6	15.8	29.6	18.9	22.5	21.1	37.3
* <i>LRP1 Prolow-density lipoprotein receptor-related protein 1</i>	505	80.8	12.4	9.5	8.4	3.6	4.1	1.7	7.8
LTF Lactoferrin	78	2.0	2.8	1.7	3.2	0.8	2.2	0.3	2.7
LUM Lumican	38	45.3	31.8	40.9	46.6	48.4	32.6	48.7	55.3
* <i>LYVE1 Lymphatic vessel endothelial hyaluronic acid receptor 1</i>	35	10.1	1.5	1.7	0.5	0.3	1.6	0.0	0.0
LYZ Lysozyme C	17	0.0	0.0	0.0	1.3	5.1	1.6	0.0	2.5
MASP2;WHAMM Isoform 1 of Mannan-binding lectin serine protease 2	76	1.1	1.0	0.9	1.6	0.0	1.0	1.1	1.3
MB Myoglobin	17	0.0	0.0	0.0	1.6	0.0	12.7	0.0	0.0
MDH1 Malate dehydrogenase	39	1.1	1.0	0.0	0.0	0.0	0.0	0.0	0.0
MMP3 Stromelysin-1	54	0.0	0.0	0.8	1.3	9.1	0.0	6.3	0.0
MST1 Hepatocyte growth factor-like protein homolog	79	1.2	1.8	1.3	0.5	0.6	0.0	0.0	1.9

**Table 5-2: Proteomics analysis (continued)**

IDENTIFIED PROTEINS	MW (kDa)	NC	MR	YMD	OMD	MD-TKA	ACL	ACL-BMT	ACL-TKA
* <i>MYOC Myocilin</i>	57	9.7	1.0	0.5	0.0	0.0	3.3	0.0	0.5
Myosin-reactive IG kappa chain variable region (Fragment)	12	0.0	0.6	4.2	0.0	0.6	0.0	0.0	0.5
* <i>Myosin-reactive IG light chain variable region (Fragment)</i>	12	10.8	13.2	23.1	14.6	8.0	9.1	3.2	4.9
OGN cDNA FLJ59205, highly similar to Mimecan	41	2.3	2.2	0.3	1.9	0.5	0.0	0.0	1.2
ORM1 Alpha-1-acid glycoprotein 1	24	149.8	127.6	124.8	150.5	150.0	160.8	144.6	243.9
ORM2 Alpha-1-acid glycoprotein 2	24	48.4	78.5	49.4	65.3	73.3	85.4	49.6	123.9
PCOLCE Procollagen C-endopeptidase enhancer 1	48	0.0	1.0	0.2	2.7	0.7	0.3	2.4	2.3
PEBP4 Phosphatidylethanolamine-binding protein 4	26	1.4	0.2	0.0	0.0	0.0	0.7	0.0	0.0
PFN1 Profilin-1	15	5.0	0.6	0.0	2.5	2.4	0.0	1.0	2.3
PGAM1 Phosphoglycerate mutase 1	29	0.2	0.2	0.0	0.0	0.8	0.3	0.0	0.5
* <i>PGLYRP2 Isoform 1 of N-acetylmuramoyl-L-alanine amidase</i>	62	15.0	20.6	18.0	15.1	13.6	6.5	22.8	22.5
PLG Plasminogen	91	123.5	75.6	78.8	68.5	91.8	32.1	50.6	73.7
PLTP Phospholipid transfer protein, isoform CRA_c	57	0.6	3.9	9.3	5.8	4.9	0.0	18.2	1.8
POLQ DNA polymerase theta	305	0.5	2.4	1.4	5.0	14.6	3.0	3.6	13.8
* <i>PON1 Serum paraoxonase/arylesterase 1</i>	40	30.3	42.4	43.2	51.5	40.2	20.2	44.9	33.4
* <i>POSTN Isoform 1 of Periostin</i>	93	0.0	0.0	0.0	0.0	0.0	0.0	10.0	0.0
PPIA Peptidyl-prolyl cis-trans isomerase A	24	7.3	1.5	1.8	3.5	4.9	8.7	0.0	0.0
PRDX1 Peroxiredoxin-1	22	0.0	0.0	0.0	1.1	0.0	14.4	2.7	0.0
PRDX2 Peroxiredoxin-2	22	4.9	7.0	0.0	0.5	0.3	0.0	0.0	3.7
* <i>PRG4 Isoform A of Proteoglycan 4</i>	151	340.4	141.7	134.2	160.2	160.8	91.1	96.8	177.3
PRG4 Isoform C of Proteoglycan 4	141	194.4	27.8	0.0	8.8	53.0	0.0	0.0	0.0
PROCR Endothelial protein C receptor precursor	31	3.1	1.2	1.4	3.9	1.9	1.1	0.5	1.7
* <i>PROS1 Vitamin K-dependent protein S</i>	75	3.5	8.0	10.9	8.3	7.7	1.1	11.7	5.8
PRSS3 Isoform A of Trypsin-3	33	20.2	17.5	22.0	27.7	31.8	24.3	8.9	26.1

**Table 5-2: Proteomics analysis (continued)**

IDENTIFIED PROTEINS	MW (kDa)	NC	MR	YMD	OMD	MD-TKA	ACL	ACL-BMT	ACL-TKA
PTGDS Prostaglandin D2 synthase 21kDa	23	2.2	2.4	2.0	3.1	1.3	3.7	0.7	2.5
Putative uncharacterized protein	26	279.8	296.3	540.7	498.9	645.8	319.4	314.7	352.8
Putative uncharacterized protein ENSP00000374810	13	0	2	3	2	0	0	1	0
Putative uncharacterized protein ENSP00000374812	13	14.7	11.4	22.5	20.1	18.1	11.8	9.5	12.9
PZP Isoform 1 of Pregnancy zone protein	164	87.9	222.1	229.7	136.9	175.5	0.0	108.0	54.3
RBP4 Retinol-binding protein 4	23	259.7	120.5	169.3	161.8	133.1	123.3	74.6	183.1
RCTPI1;TPI1 triosephosphate isomerase 1 isoform 2	31	0.6	0.2	0.0	0.0	0.5	0.7	0.0	0.0
REV25-2 (Fragment)	15	1.1	1.8	5.7	1.6	2.7	1.8	1.2	1.7
*RNASE1 Ribonuclease pancreatic	18	3.8	0.0	0.3	0.0	0.2	3.1	0.5	1.4
*S100A8 Protein S100-A8	11	0.0	0.7	4.3	4.4	19.9	12.9	2.3	8.4
S100A9 Protein S100-A9	13	0.0	0.7	3.3	0.5	12.9	6.9	1.3	0.0
*SAA2;SAA1 Serum amyloid A protein	14	10.5	1.0	17.9	26.6	2.6	0.0	1.3	23.0
*SAA2;SAA1 serum amyloid A2 isoform a	14	1.4	0.3	10.5	14.5	2.5	0.0	1.3	6.9
SAA4 Serum amyloid A-4 protein	15	124.9	111.2	148.7	131.4	138.6	96.0	79.1	152.8
SEPP1 Selenoprotein P	43	0.2	0.6	0.7	1.4	2.7	1.9	1.7	1.7
SERPINA1 Isoform 1 of Alpha-1-antitrypsin	47	2343.5	1593.5	1826.8	1705.2	2004.6	5023.7	2968.0	1920.5
SERPINA10 Protein Z-dependent protease inhibitor	55	0.0	0.0	0.4	0.2	1.0	0.0	0.0	0.3
SERPINA3 cDNA FLJ35730 fis, clone TESTI2003131, highly similar to ALPHA-1-ANTICHYMOTRYPSIN	51	287.1	193.9	257.5	199.0	211.1	586.3	391.5	259.9
SERPINA4 Kallistatin	49	11.6	8.1	8.9	8.8	12.8	16.5	5.3	9.1
*SERPINA5 Plasma serine protease inhibitor	46	0.7	0.2	1.2	4.2	0.7	0.9	0.0	3.4
SERPINA6 Corticosteroid-binding globulin	45	29.4	14.0	17.1	11.9	10.0	47.2	37.3	18.8
SERPINA7 Thyroxine-binding globulin	46	18.3	8.6	3.9	5.5	11.2	13.6	10.7	10.9
SERPIN C1 Antithrombin-III	53	365.1	278.0	288.1	250.8	248.0	753.6	438.0	289.6

**Table 5-2: Proteomics analysis (continued)**

IDENTIFIED PROTEINS	MW (kDa)	NC	MR	YMD	OMD	MD-TKA	ACL	ACL-BMT	ACL-TKA
SERPIND1 Serpin peptidase inhibitor, clade D (Heparin cofactor), member 1	60	39.7	42.7	47.8	31.1	28.6	24.8	40.4	32.2
SERPINF1 Pigment epithelium-derived factor	46	73.0	45.8	43.5	62.2	28.9	29.7	40.8	73.2
SERPING1 Plasma protease C1 inhibitor	55	109.9	61.4	89.9	61.2	71.6	51.3	71.4	63.6
SHBG Isoform 1 of Sex hormone-binding globulin	44	4.6	5.0	1.4	3.4	1.4	0.0	1.8	1.2
Single-chain Fv (Fragment)	26	0.7	0.4	0.6	1.1	0.7	0.0	0.9	0.3
SOD1 Superoxide dismutase [Cu-Zn]	16	2.6	1.7	0.0	0.5	0.4	0.0	0.0	0.0
*SOD3 Extracellular superoxide dismutase [Cu-Zn]	26	37.2	16.9	3.5	3.0	0.9	9.0	2.3	3.6
*SPARCL1 SPARC-like protein 1	75	7.4	2.2	1.2	1.7	0.5	0.8	0.4	2.5
TF Serotransferrin	77	2263.9	1779.4	1568.5	1816.5	1532.1	1512.7	1836.3	2021.6
TGFB1 Transforming growth factor-beta-induced protein ig-h3	75	0.2	0.0	0.0	0.2	0.6	0.0	0.6	0.0
THBS4 Thrombospondin-4	106	0.0	3.4	1.4	3.6	5.3	0.0	0.0	2.4
TIMP1 Metalloproteinase inhibitor 1	23	0.9	0.8	0.0	0.2	0.6	0.3	0.0	1.2
TIMP2 Metalloproteinase inhibitor 2	24	5.7	2.9	1.7	4.6	1.0	0.8	1.0	4.1
TNC Isoform 1 of Tenascin	241	0.0	0.2	1.0	0.0	0.2	0.0	1.4	0.4
TNXB Isoform XB of Tenascin-X	456	1.6	1.0	2.4	0.7	0.0	0.8	0.0	0.9
TPM3 Isoform 2 of Tropomyosin alpha-3 chain	29	2.4	1.3	0.6	0.5	0.8	0.4	1.6	0.3
TTR Transthyretin	16	533.3	400.2	396.6	448.9	301.5	545.7	400.9	333.1
VASN Vasorin	72	1.4	0.0	2.0	1.0	2.1	0.4	1.3	1.0
*VCAN Isoform V0 of Versican core protein	373	34.4	20.0	15.0	7.0	10.4	20.5	11.6	16.4
*VTN Vitronectin	54	85.5	65.4	98.7	73.7	35.9	42.0	45.4	78.3
YWHAZ 14-3-3 protein zeta/delta	28	0.7	0.6	0.0	0.8	0.7	0.6	0.0	0.0
ZCCHC11 Isoform 1 of Zinc finger CCHC domain-containing protein 11	185	9.2	8.7	8.3	6.0	17.5	7.9	10.7	10.3

\*Proteins have a p<0.05 according to a one-way ANOVA performed by the Scaffold program

**Table 5-3: Proteins of Interest**

PROTEINS OF INTEREST	NC	MR	YMD	OMD	MD-TKA	ACL	ACL-BMT	ACL-TKA	ANOVA p-value
Extracellular Superoxide Dismutase [Cu-Zn] (SOD3)	37.2	16.9	3.5	3.0	0.9	9.0	2.3	3.6	0.004
Isoform A of Proteoglycan 4 (PRG4-A)	340.4	141.7	134.2	160.2	160.8	91.1	96.8	177.3	0.121
Isoform C of Proteoglycan 4 (PRG4-C)	194.4	27.8	0.0	8.8	53.0	0.0	0.0	0.0	0.001
Apolipoprotein B-100 (APOB)	501.1	940.8	1089.0	868.1	889.0	365.8	879.1	805.2	0.243
C4b Binding Protein Alpha Chain (C4BPA)	0.3	13.5	15.2	16.9	13.8	1.5	41.5	10.5	0.059
Low-density Lipoprotein Receptor Related Protein 1 (LRP1)	80.8	12.4	9.5	8.4	3.6	4.1	1.7	7.8	<0.001
Aggrecan (ACAN)	314.6	107.8	56.1	71.1	15.0	172.1	32.2	29.3	0.004
Isoform V0 of Versican Core Protein (VCAN)	34.4	20.0	15.0	7.0	10.4	20.5	11.6	16.4	0.132
Hyaluronan and Proteoglycan Link Protein 1 (HAPLN1)	19.5	6.5	1.9	2.6	0.0	13.9	2.1	2.0	<0.001
Lymphatic Vessel Endothelial Hyaluronic Acid Receptor 1 (LYVE1)	10.1	1.5	1.7	0.5	0.3	1.6	0.0	0.0	<0.001
Cartilage Intermediate Layer Protein 1 (CILP)	22.7	8.2	2.0	4.5	0.0	12.6	3.2	2.6	0.036
Isoform 1 of Collagen Alpha-3(VI) Chain (COL6A3)	0.7	3.2	3.9	3.8	3.9	1.7	12.9	3.9	<0.001
Haptoglobin (HP)	511.4	1956.3	2270.0	1811.1	2003.0	988.3	1162.7	1817.8	0.084
Isoform 1 of Haptoglobin Related Protein (HRP)	72.1	802.2	747.8	599.2	328.4	113.1	340.1	239.7	0.240
Ceruloplasmin (CP)	482.5	296.6	362.1	318.8	376.7	219.1	200.9	408.9	0.011
Beta-2-Microglobulin	62.7	25.4	30.8	39.9	28.1	27.7	13.4	31.9	0.022
Fibroblast Growth Factor Binding Protein 2 (FGFBP2)	10.7	3.9	6.0	5.0	2.4	2.4	3.5	6.4	0.021
Insulin Like Growth Factor Binding Protein 6 (IGFBP6)	22.8	6.1	3.1	5.6	1.7	8.4	2.7	8.9	0.002
Isoform 1 of Target of Nesh-SH3 Binding Protein (ABI3BP)	19.4	4.7	1.9	3.7	0.6	3.4	3.3	5.8	0.003

**Figure 5-1: Extracellular Superoxide Dismutase [Cu-Zn]**

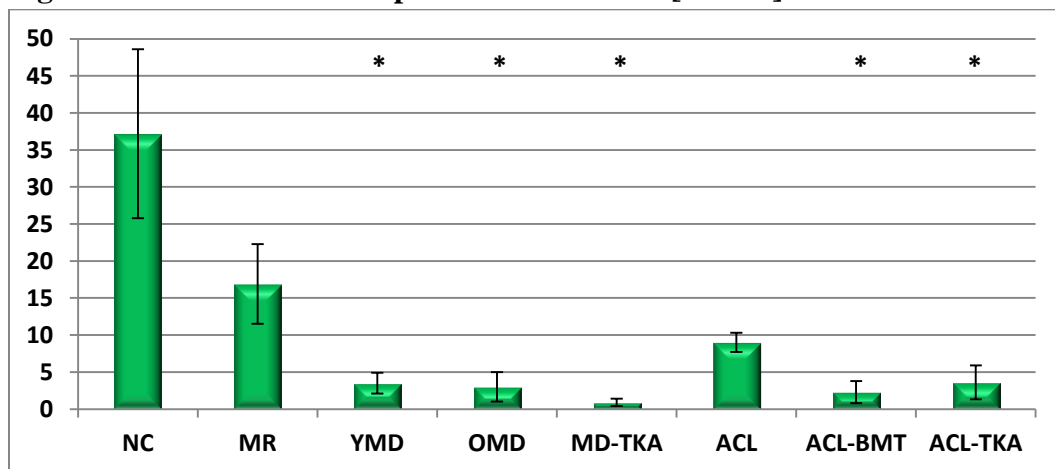


**Figure 5-2: Isoform A of Proteoglycan 4**

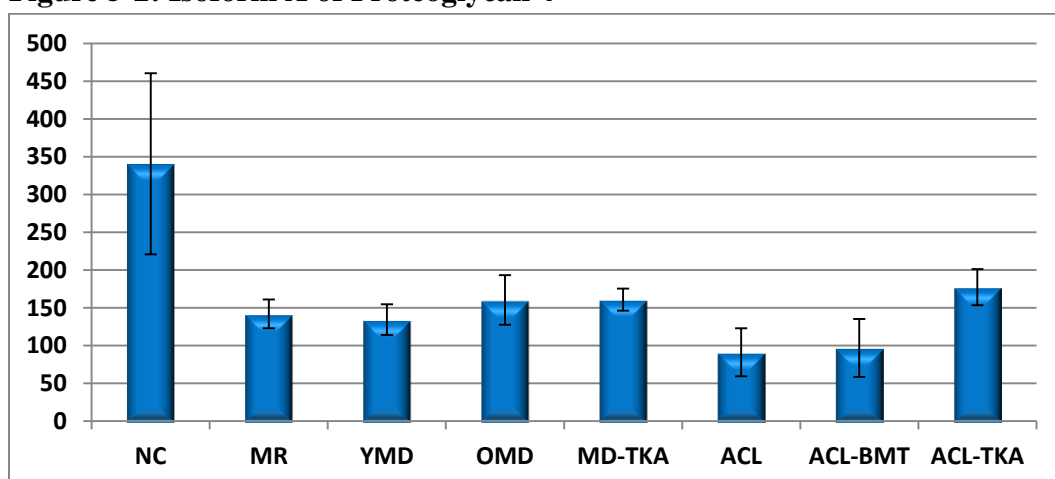
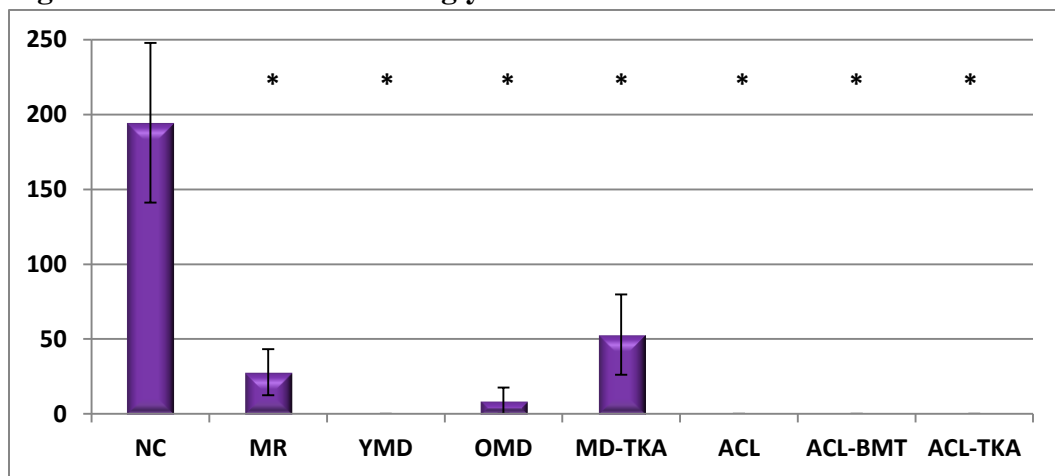


**Figure 5-3: Isoform C of Proteoglycan 4**



\* Significantly different than NC

**Figure 5-4: Apolipoprotein B-100**

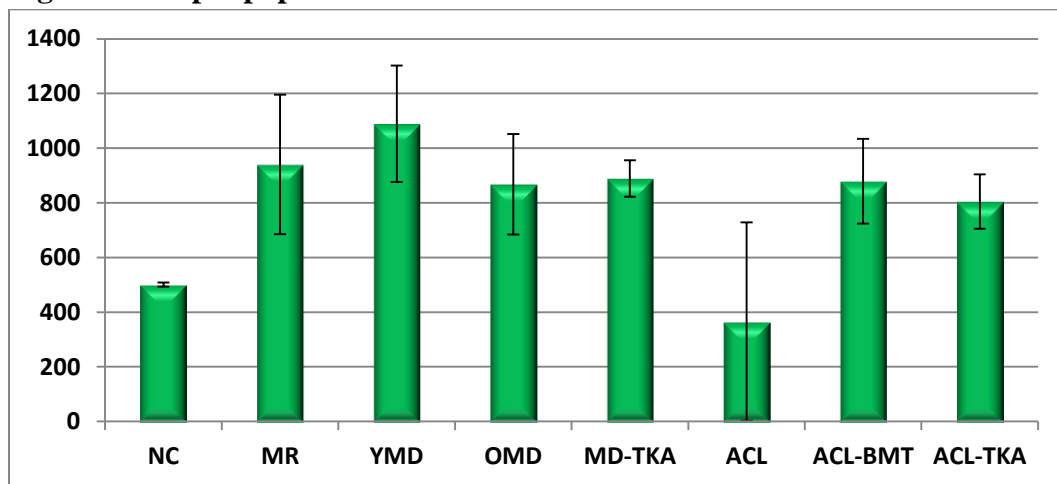


**Figure 5-5: C4b Binding Protein Alpha Chain**

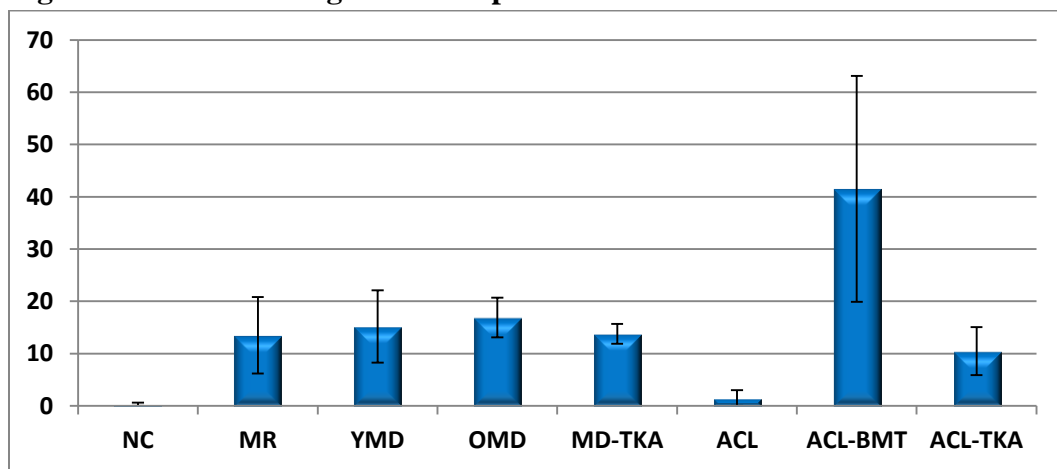
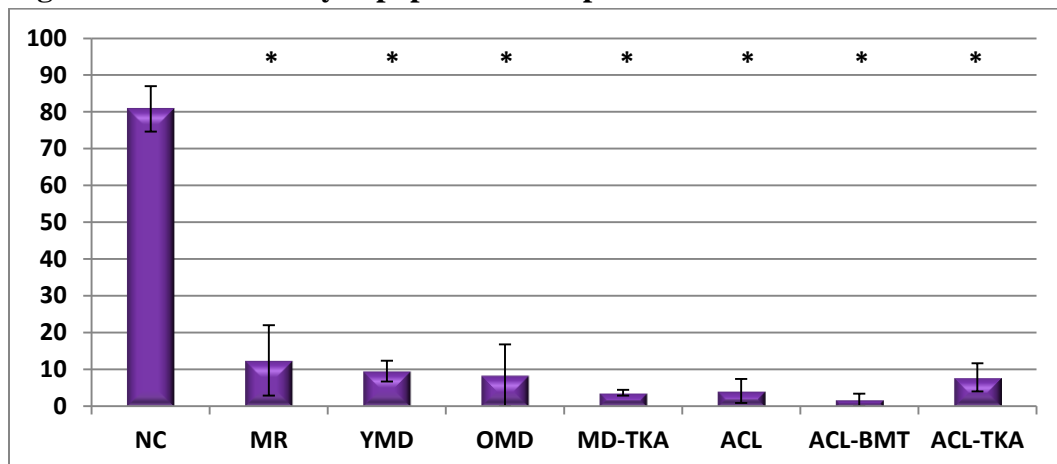
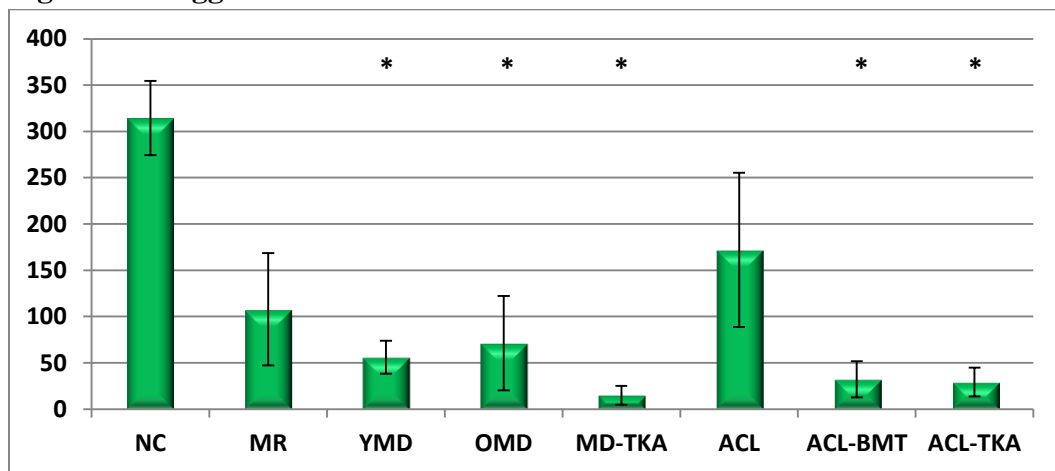


**Figure 5-6: Low-density Lipoprotein Receptor Related Protein 1**



\* Significantly different than NC

**Figure 5-7: Aggrecan**



\* Significantly different than NC

**Figure 5-8: Isoform V0 of Versican Core Protein**

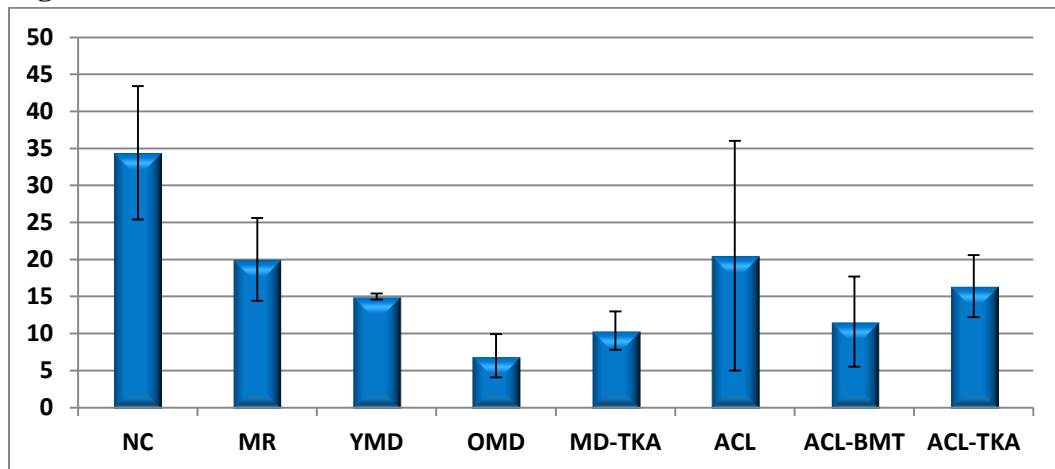
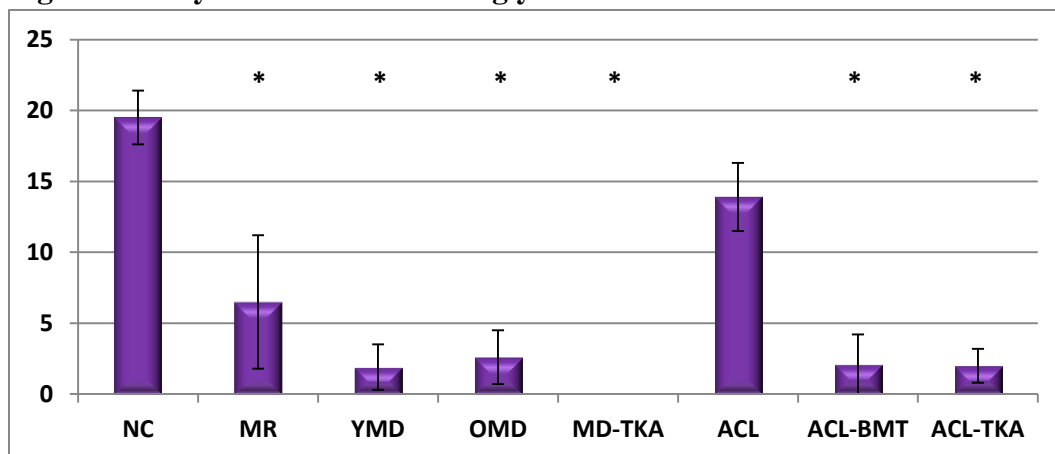
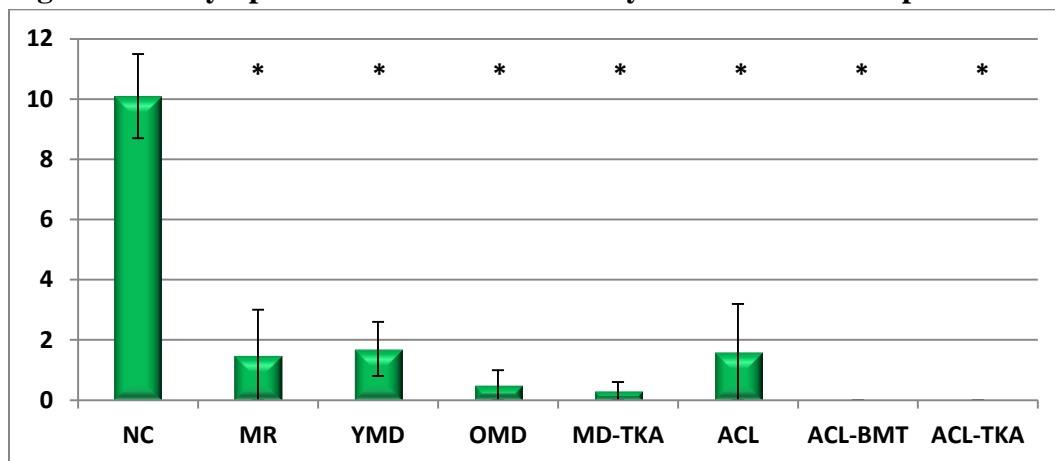


**Figure 5-9: Hyaluronan and Proteoglycan Link Protein 1**



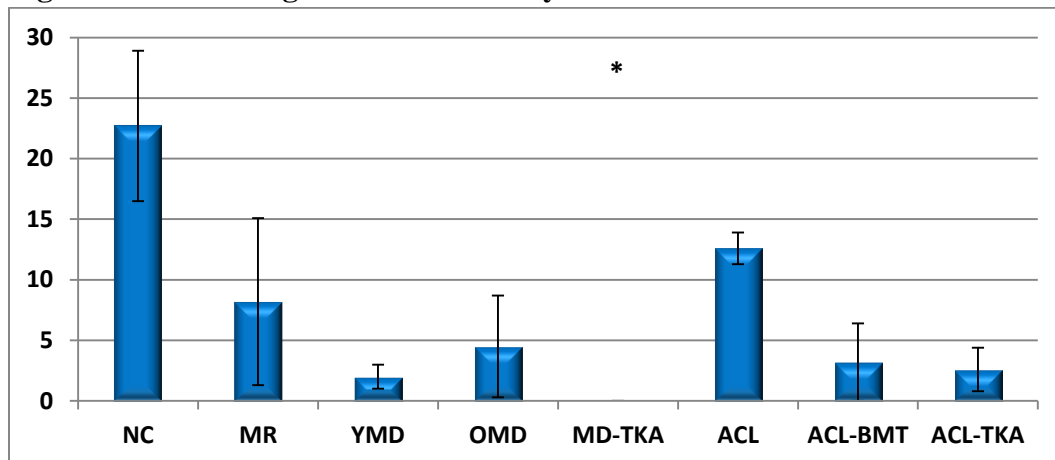
\* Significantly different than NC

**Figure 5-10: Lymphatic Vessel Endothelial Hyaluronic Acid Receptor 1**



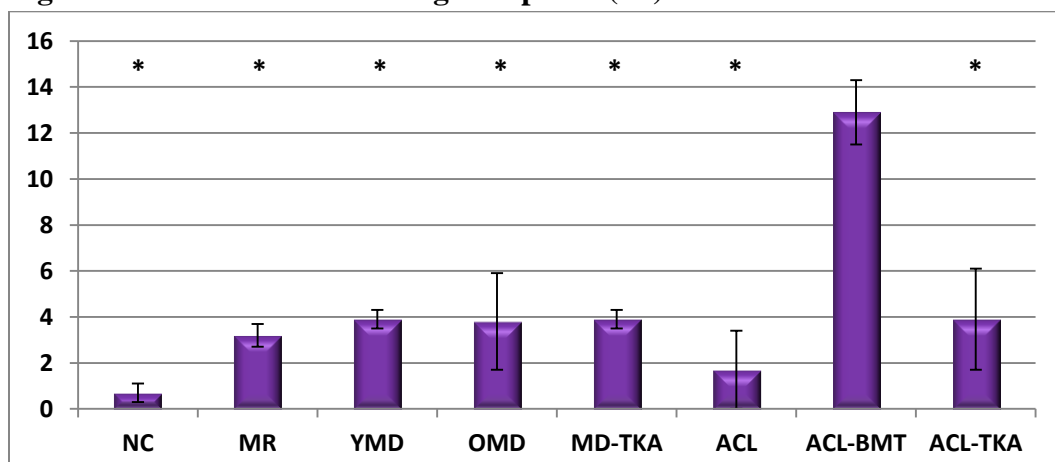
\* Significantly different than NC

**Figure 5-11: Cartilage Intermediate Layer Protein 1**



\* Significantly different than NC

**Figure 5-12: Isoform 1 of Collagen Alpha-3 (VI) Chain**



\* Significantly different than ACL-BMT

**Figure 5-13: Haptoglobin**

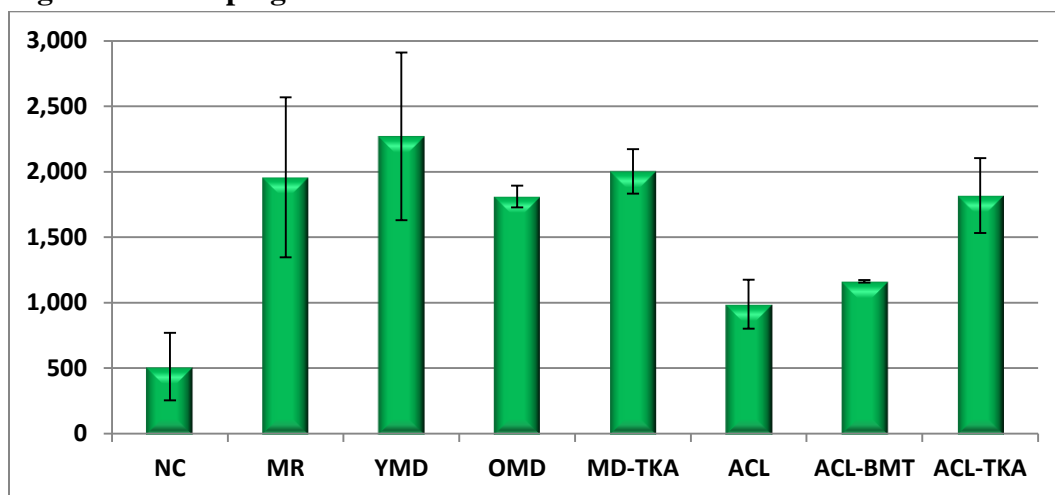


**Figure 5-14: Isoform 1 of Haptoglobin Related Protein**

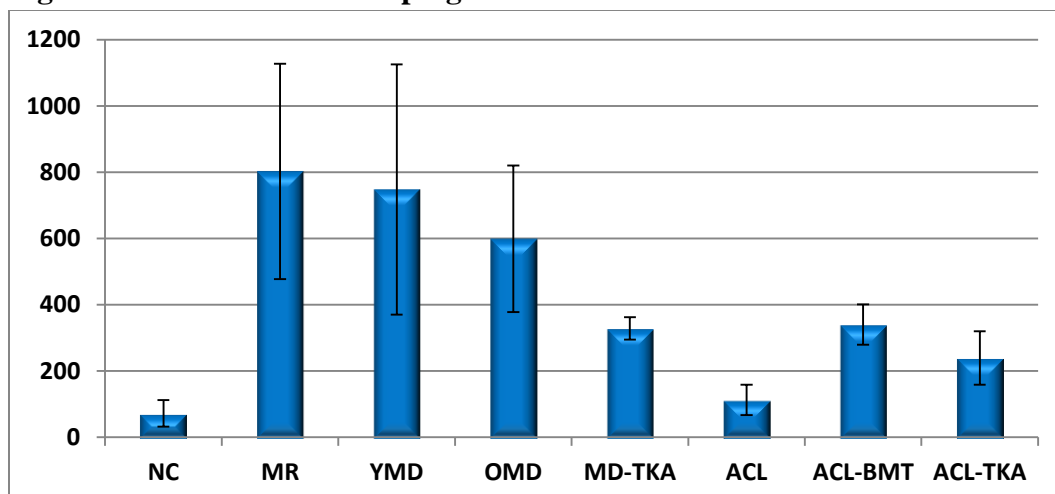
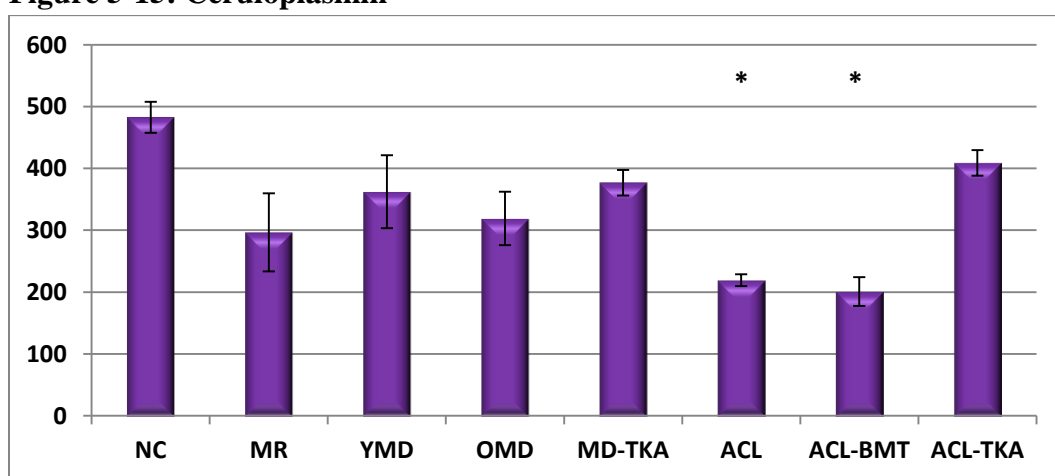
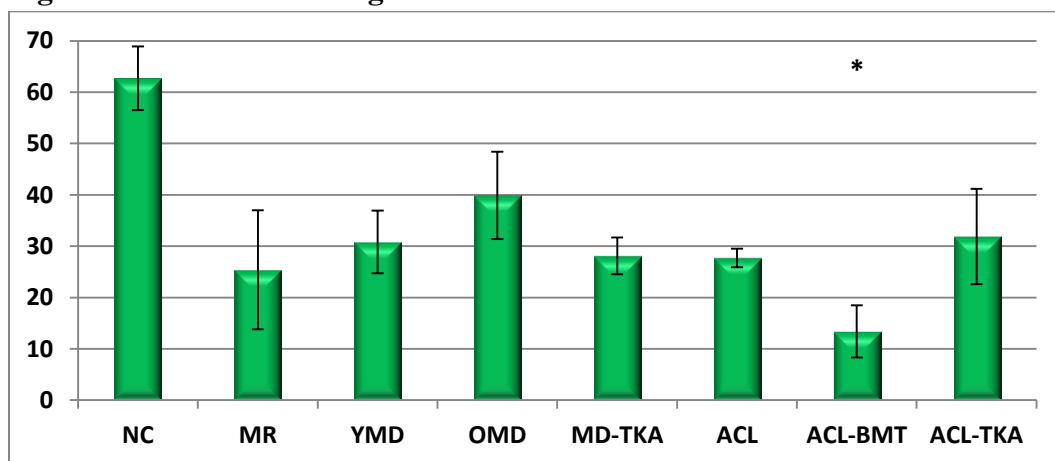


**Figure 5-15: Ceruloplasmin**



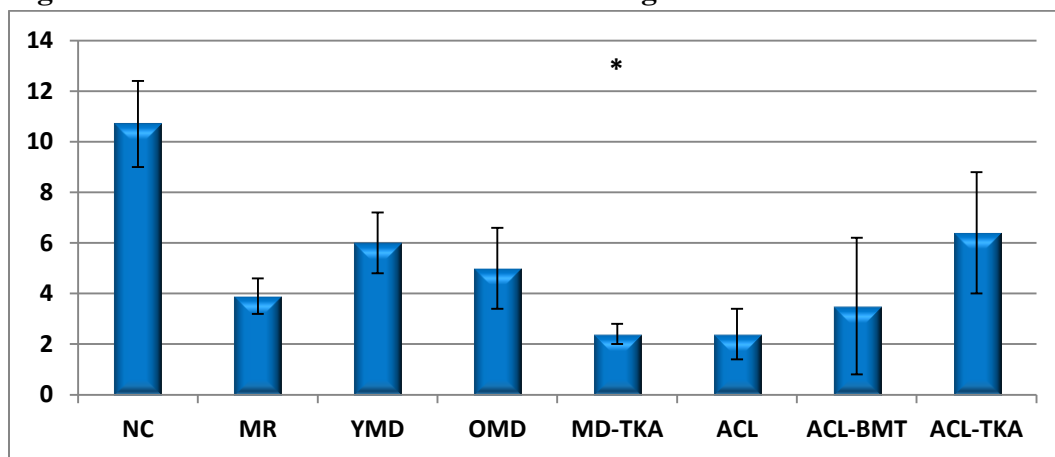
\* Significantly different than NC

**Figure 5-16: Beta-2-Microglobulin**



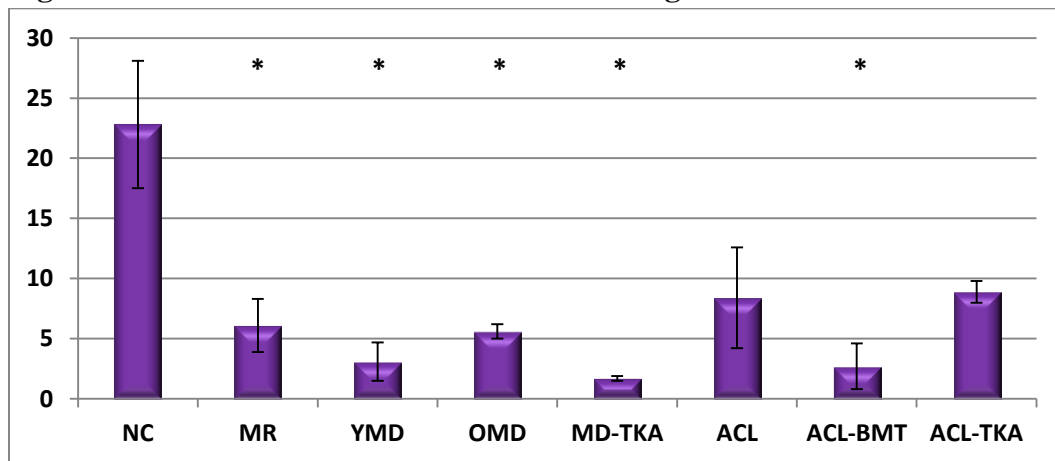
\* Significantly different than NC

**Figure 5-17: Fibroblast Growth Factor Binding Protein 2**



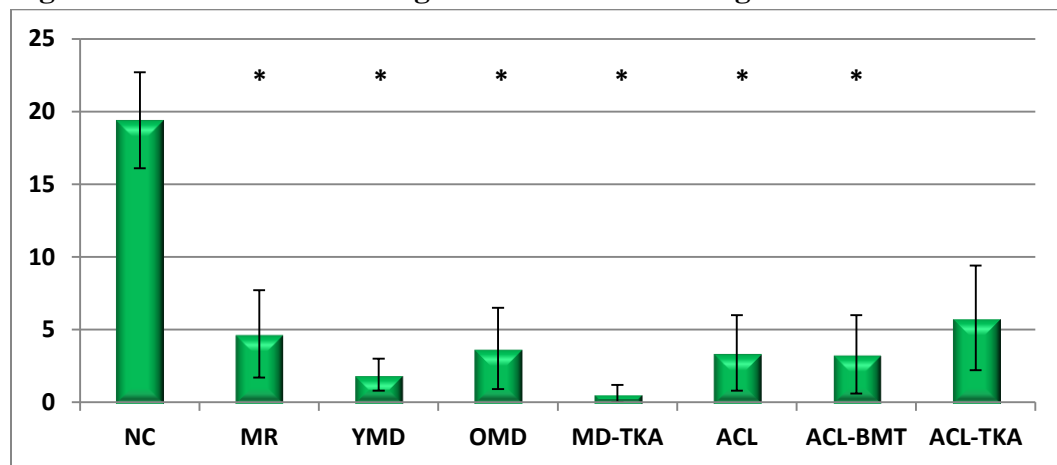
\* Significantly different than NC

**Figure 5-18: Insulin Like Growth Factor Binding Protein 6**



\* Significantly different than NC

**Figure 5-19: Isoform 1 of Target of Nesh-SH3 Binding Protein**



\* Significantly different than NC

## References

1. Baillet A, Trocme C, Berthier S, et al. Synovial fluid proteomic fingerprint: S100A8, S100A9 and S100A12 proteins discriminate rheumatoid arthritis from other inflammatory joint diseases. *Rheumatology*. 2010;49(4):671-682.
2. Dufield DR, Nemirovskiy OV, Jennings MG, Tortorella MD, Malfait AM, Mathews WR. An immunoaffinity liquid chromatography-tandem mass spectrometry assay for detection of endogenous aggrecan fragments in biological fluids: Use as a biomarker for aggrecanase activity and cartilage degradation. *Analytical Biochemistry*. 2010;406(2):113-123.
3. Giera M, Ioan-Facsinay A, Toes R, et al. Lipid and lipid mediator profiling of human synovial fluid in rheumatoid arthritis patients by means of LC-MS/MS. *Biochimica et Biophysica Acta*. 2012;1821(11):1415-1424.
4. Mateos J, Lourido L, Fernandez-Puente P, et al. Differential protein profiling of synovial fluid from rheumatoid arthritis and osteoarthritis patients using LC-MALDI TOF/TOF. *Journal of Proteomics*. 2012;75(10):2869-2878.
5. Pan X, Huang L, Chen J, Dai Y, Chen X. Analysis of synovial fluid in knee joint of osteoarthritis: 5 proteome patterns of joint inflammation based on matrix-assisted laser desorption/ionization time-of-flight mass spectrometry. *International Orthopaedics*. 2012;36(1):57-64.
6. Rosenkranz ME, Wilson DC, Marinov AD, et al. Synovial fluid proteins differentiate between the subtypes of juvenile idiopathic arthritis.[Erratum appears in Arthritis Rheum. 2011 Mar;63(3):669]. *Arthritis & Rheumatism*. 2010;62(6):1813-1823.
7. Scuderi GJ, Woolf N, Dent K, et al. Identification of a complex between fibronectin and aggrecan G3 domain in synovial fluid of patients with painful meniscal pathology. *Clinical Biochemistry*. 2010;43(10-11):808-814.
8. Fattman CL, Schaefer LM, Oury TD. Extracellular superoxide dismutase in biology and medicine. *Free Radical Biology and Medicine*. 2003;35(3):236-256.
9. Marklund SL. Human copper-containing superoxide dismutase of high molecular weight. *Proceedings of the National Academy of Sciences of the United States of America*. 1982;79(24 I):7634-7638.
10. Marklund SL, Bjelle A, Elmquist LG. Superoxide dismutase isoenzymes of the synovial fluid in rheumatoid arthritis and in reactive arthritides. *Annals of the Rheumatic Diseases*. 1986;45(10):847-851.

11. Marklund SL, Holme E, Hellner L. Superoxide dismutase in extracellular fluids. *Clinica Chimica Acta*. 1982;126(1):41-51.
12. Marklund SL. Expression of extracellular superoxide dismutase by human cell lines. *Biochemical Journal*. 1990;266(1):213-219.
13. Sandstrom J, Karlsson K, Edlund T, Marklund SL. Heparin-affinity patterns and composition of extracellular superoxide dismutase in human plasma and tissues. *Biochemical Journal*. 1993;294(3):853-857.
14. Stralin P, Marklund SL. Multiple cytokines regulate the expression of extracellular superoxide dismutase in human vascular smooth muscle cells. *Atherosclerosis*. 2000;151(2):433-441.
15. McCord JM. Free radicals and inflammation: protection of synovial fluid by superoxide dismutase. *Science*. 1974;185(4150):529-531.
16. Gao F, Koenitzer JR, Tobolewski JM, et al. Extracellular superoxide dismutase inhibits inflammation by preventing oxidative fragmentation of hyaluronan. *Journal of Biological Chemistry*. 2008;283(10):6058-6066.
17. Monboisse JC, Borel JP. Oxidative damage to collagen. *EXS*. 1992;62:323-327.
18. Petersen SV, Oury TD, Ostergaard L, et al. Extracellular Superoxide Dismutase (EC-SOD) Binds to Type I Collagen and Protects Against Oxidative Fragmentation. *Journal of Biological Chemistry*. 2004;279(14):13705-13710.
19. Burkhardt H, Schwingel M, Menninger H. Oxygen radicals as effectors of cartilage destruction. Direct degradative effect on matrix components and indirect action via activation of latent collagenase from polymorphonuclear leukocytes. *Arthritis and Rheumatism*. 1986;29(3):379-387.
20. Regan E, Flannelly J, Bowler R, et al. Extracellular superoxide dismutase and oxidant damage in osteoarthritis. *Arthritis and Rheumatism*. 2005;52(11):3479-3491.
21. Iyama S, Okamoto T, Sato T, et al. Treatment of Murine Collagen-Induced Arthritis by Ex Vivo Extracellular Superoxide Dismutase Gene Transfer. *Arthritis and Rheumatism*. 2001;44(9):2160-2167.
22. Zhang Y, Wang J-Z, Wu Y-J, Li W-G. Anti-inflammatory effect of recombinant human superoxide dismutase in rats and mice and its mechanism. *Acta Pharmacologica Sinica*. 2002;23(5):439-444.
23. Huskisson EC, Scott J. Orgotein in osteoarthritis of the knee joint. *European Journal of Rheumatology & Inflammation*. 1981;4(2):212-218.

24. McIlwain H, Silverfield JC, Cheatum DE, et al. Intra-articular orgotein in osteoarthritis of the knee: a placebo-controlled efficacy, safety, and dosage comparison. *American Journal of Medicine*. 1989;87(3):295-300.
25. Sakurai K, Miyazaki K, Kodera Y, Nishimura H, Shingu M, Inada Y. Anti-inflammatory activity of superoxide dismutase conjugated with sodium hyaluronate. *Glycoconjugate Journal*. 1997;14(6):723-728.
26. Schumacher BL, Schmidt TA, Voegtline MS, Chen AC, Sah RL. Proteoglycan 4 (PRG4) synthesis and immunolocalization in bovine meniscus. *Journal of Orthopaedic Research*. 2005;23(3):562-568.
27. Lotz M. Osteoarthritis year 2011 in review: biology. *Osteoarthritis & Cartilage*. 2012;20(3):192-196.
28. Young AA, McLennan S, Smith MM, et al. Proteoglycan 4 downregulation in a sheep meniscectomy model of early osteoarthritis. *Arthritis Research and Therapy*. 2006;8(2).
29. Elsaid KA, Fleming BC, Oksendahl HL, et al. Decreased lubricin concentrations and markers of joint inflammation in the synovial fluid of patients with anterior cruciate ligament injury. *Arthritis and Rheumatism*. 2008;58(6):1707-1715.
30. Jay GD, Fleming BC, Watkins BA, et al. Prevention of cartilage degeneration and restoration of chondroprotection by lubricin tribosupplementation in the rat following anterior cruciate ligament transection. *Arthritis and Rheumatism*. 2006;52(8):2382-2391.
31. Jay GD, Torres JR, Warman ML, Laderer MC, Breuer KS. The role of lubricin in the mechanical behavior of synovial fluid. *Proceedings of the National Academy of Sciences of the United States of America*. 2007;104(15):6194-6199.
32. Teeple E, Elsaid KA, Jay GD, et al. Effects of supplemental intra-articular lubricin and hyaluronic acid on the progression of posttraumatic arthritis in the anterior cruciate ligament-deficient rat knee. *American Journal of Sports Medicine*. 2011;39(1):164-172.
33. Podrez EA, Schmitt D, Hoff HF, Hazen SL. Myeloperoxidase-generated reactive nitrogen species convert LDL into an atherogenic form in vitro. *Journal of Clinical Investigation*. Jun 1999;103(11):1547-1560.
34. Sawamura T, Kume N, Aoyama T, et al. An endothelial receptor for oxidized low-density lipoprotein. *Nature*. Mar 6 1997;386(6620):73-77.

35. Kume N, Murase T, Moriwaki H, et al. Inducible expression of lectin-like oxidized LDL receptor-1 in vascular endothelial cells. *Circulation Research*. Aug 10 1998;83(3):322-327.
36. Murase T, Kume N, Korenaga R, et al. Fluid shear stress transcriptionally induces lectin-like oxidized LDL receptor-1 in vascular endothelial cells. *Circulation Research*. Aug 10 1998;83(3):328-333.
37. Cushing SD, Berliner JA, Valente AJ, et al. Minimally modified low density lipoprotein induces monocyte chemotactic protein 1 in human endothelial cells and smooth muscle cells. *Proceedings of the National Academy of Sciences of the United States of America*. Jul 1990;87(13):5134-5138.
38. Li D, Mehta JL. Upregulation of endothelial receptor for oxidized LDL (LOX-1) by oxidized LDL and implications in apoptosis of human coronary artery endothelial cells: evidence from use of antisense LOX-1 mRNA and chemical inhibitors. *Arteriosclerosis, Thrombosis & Vascular Biology*. Apr 2000;20(4):1116-1122.
39. Mertens A, Holvoet P. Oxidized LDL and HDL: antagonists in atherosclerosis. *FASEB Journal*. Oct 2001;15(12):2073-2084.
40. Heermeier K, Leicht W, Palmethofer A, Ullrich M, Wanner C, Galle J. Oxidized LDL suppresses NF-kappaB and overcomes protection from apoptosis in activated endothelial cells. *Journal of the American Society of Nephrology*. Mar 2001;12(3):456-463.
41. Khan M, Pelengaris S, Cooper M, et al. Oxidised lipoproteins may promote inflammation through the selective delay of engulfment but not binding of apoptotic cells by macrophages. *Atherosclerosis*. Nov 2003;171(1):21-29.
42. Winyard PG, Tatzber F, Esterbauer H, Kus ML, Blake DR, Morris CJ. Presence of foam cells containing oxidised low density lipoprotein in the synovial membrane from patients with rheumatoid arthritis. *Annals of the Rheumatic Diseases*. Sep 1993;52(9):677-680.
43. Simopoulou T, Malizos KN, Tsezou A. Lectin-like oxidized low density lipoprotein receptor 1 (LOX-1) expression in human articular chondrocytes. *Clinical & Experimental Rheumatology*. Jul-Aug 2007;25(4):605-612.
44. Kakinuma T, Yasuda T, Nakagawa T, et al. Lectin-like oxidized low-density lipoprotein receptor 1 mediates matrix metalloproteinase 3 synthesis enhanced by oxidized low-density lipoprotein in rheumatoid arthritis cartilage. *Arthritis & Rheumatism*. Nov 2004;50(11):3495-3503.

45. Nakagawa T, Akagi M, Hoshikawa H, et al. Lectin-like oxidized low-density lipoprotein receptor 1 mediates leukocyte infiltration and articular cartilage destruction in rat zymosan-induced arthritis. *Arthritis & Rheumatism*. Sep 2002;46(9):2486-2494.
46. Akagi M, Ueda A, Teramura T, Kanata S, Sawamura T, Hamanishi C. Oxidized LDL binding to LOX-1 enhances MCP-1 expression in cultured human articular chondrocytes. *Osteoarthritis & Cartilage*. Feb 2009;17(2):271-275.
47. Kanata S, Akagi M, Nishimura S, et al. Oxidized LDL binding to LOX-1 upregulates VEGF expression in cultured bovine chondrocytes through activation of PPAR-gamma. *Biochemical & Biophysical Research Communications*. Sep 29 2006;348(3):1003-1010.
48. Enomoto H, Inoki I, Komiya K, et al. Vascular endothelial growth factor isoforms and their receptors are expressed in human osteoarthritic cartilage. *American Journal of Pathology*. Jan 2003;162(1):171-181.
49. Pufe T, Harde V, Petersen W, et al. Vascular endothelial growth factor (VEGF) induces matrix metalloproteinase expression in immortalized chondrocytes. *Journal of Pathology*. Mar 2004;202(3):367-374.
50. Henrotin Y, Kurz B, Aigner T. Oxygen and reactive oxygen species in cartilage degradation: friends or foes? *Osteoarthritis & Cartilage*. Aug 2005;13(8):643-654.
51. Henrotin YE, Bruckner P, Pujol JP, Pujol JPL. The role of reactive oxygen species in homeostasis and degradation of cartilage. *Osteoarthritis & Cartilage*. Oct 2003;11(10):747-755.
52. Garcia OC, Sanchez-Corral P, Rodriguez de Cordoba S. Isoforms of human C4b-binding protein: II. Differential modulation of the C4BPA and D4BPB genes by acute phase cytokines. *Journal of Immunology*. 1995;155(8):4037-4043.
53. Sanchez-Pernaute O, Esparza-Gordillo J, Largo R, et al. Expression of the peptide C4b-binding protein beta in the arthritic joint. *Annals of the Rheumatic Diseases*. 2006;65(10):1279-1285.
54. Blom AM, Villoutreix BO, Dahlb, et al. Functions of human complement inhibitor C4b-binding protein in relation to its structure. *Archivum Immunologiae et Therapiae Experimentalis*. Mar-Apr 2004;52(2):83-95.
55. Sjoberg AP, Trouw LA, Blom AM. Complement activation and inhibition: a delicate balance. *Trends in Immunology*. Feb 2009;30(2):83-90.

56. Blom AM, Villoutreix BO, Dahlb, et al. Complement inhibitor C4b-binding protein-friend or foe in the innate immune system? *Molecular Immunology*. Apr 2004;40(18):1333-1346.
57. Llorente-Cortes V, Otero-Vinas M, Camino-Lopez S, Costales P, Badimon L. Cholestryl esters of aggregated LDL are internalized by selective uptake in human vascular smooth muscle cells. *Arteriosclerosis, Thrombosis & Vascular Biology*. 2006;26(1):117-123.
58. Satchell L, Leake DS. Oxidation of low-density lipoprotein by iron at lysosomal pH: implications for atherosclerosis. *Biochemistry*. 2012;51(18):3767-3775.
59. Yamamoto K, Troeberg L, Scilabria SD, et al. LRP-1-mediated endocytosis regulates extracellular activity of ADAMTS-5 in articular cartilage. *FASEB Journal*. 2013;27(2):511-521.
60. Melrose J, Smith S, Cake M, et al. Comparative spatial and temporal localisation of perlecan, aggrecan and type I, II and IV collagen in the ovine meniscus: an ageing study. *Histochemistry & Cell Biology*. Sep 2005;124(3-4):225-235.
61. Valiyaveettill M, Mort JS, McDevitt CA, Valiyaveettill M, Mort JS, McDevitt CA. The concentration, gene expression, and spatial distribution of aggrecan in canine articular cartilage, meniscus, and anterior and posterior cruciate ligaments: a new molecular distinction between hyaline cartilage and fibrocartilage in the knee joint. *Connective Tissue Research*. 2005;46(2):83-91.
62. Larsson S, Lohmander LS, Struglics A, et al. Synovial fluid level of aggrecan ARGS fragments is a more sensitive marker of joint disease than glycosaminoglycan or aggrecan levels: a cross-sectional study. *Arthritis Research & Therapy*. 2009;11(3):R92.
63. Swearingen CA, Carpenter JW, Siegel R, et al. Development of a novel clinical biomarker assay to detect and quantify aggrecanase-generated aggrecan fragments in human synovial fluid, serum and urine. *Osteoarthritis and Cartilage*. 18(9):1150-1158.
64. Lemke AK, Sandy JD, Voigt H, et al. Interleukin-1alpha treatment of meniscal explants stimulates the production and release of aggrecanase-generated, GAG-substituted aggrecan products and also the release of pre-formed, aggrecanase-generated G1 and m-calpain-generated G1-G2. *Cell and Tissue Research*. 340(1):179-188.
65. Voigt H, Lemke AK, Mentlein R, Schunke M, Kurz B. Tumor necrosis factor alpha-dependent aggrecan cleavage and release of glycosaminoglycans in the meniscus is mediated by nitrous oxide-independent aggrecanase activity in vitro. *Arthritis Research & Therapy*. 2009;11(5).

66. Isogai Z, Aspberg A, Keene DR, et al. Versican interacts with fibrillin-1 and links extracellular microfibrils to other connective tissue networks. *Journal of Biological Chemistry*. Feb 8 2002;277(6):4565-4572.
67. Matsumoto K, Shionyu M, Go M, et al. Distinct interaction of versican/PG-M with hyaluronan and link protein. *Journal of Biological Chemistry*. Oct 17 2003;278(42):41205-41212.
68. Sandy JD, Westling J, Kenagy RD, et al. Versican V1 proteolysis in human aorta in vivo occurs at the Glu441-Ala442 bond, a site that is cleaved by recombinant ADAMTS-1 and ADAMTS-4. *Journal of Biological Chemistry*. Apr 20 2001;276(16):13372-13378.
69. Arner EC. Aggrecanase-mediated cartilage degradation. *Current Opinion in Pharmacology*. 2002;2(3):322-329.
70. Binette F, Cravens J, Kahoussi B, Haudenschild DR, Goetinck PF. Link protein is ubiquitously expressed in non-cartilaginous tissues where it enhances and stabilizes the interaction of proteoglycans with hyaluronic acid. *Journal of Biological Chemistry*. Jul 22 1994;269(29):19116-19122.
71. McDevitt CA, Webber RJ. The ultrastructure and biochemistry of meniscal cartilage. *Clinical Orthopaedics and Related Research*. 1990(252):8-18.
72. Banerji S, Ni J, Wang S-X, et al. LYVE-1, a New Homologue of the CD44 Glycoprotein, Is a Lymph-specific Receptor for Hyaluronan. *Journal of Cell Biology*. 1999;144(4):789-801.
73. Wardrop KE DJ. Proinflammatory signals and the loss of lymphatic vessel hyaluronan receptor-1 (LYVE-1) in the early pathogenesis of laminin alpha-2 deficient skeletal muscle. *J Histochem Cytochem*. 2010.
74. Mori M, Nakajima M, Mikami Y, et al. Transcriptional regulation of the cartilage intermediate layer protein (CILP) gene. *Biochemical & Biophysical Research Communications*. Mar 3 2006;341(1):121-127.
75. Tsuruha J, Masuko-Hongo K, Kato T, Sakata M, Nakamura H, Nishioka K. Implication of cartilage intermediate layer protein in cartilage destruction in subsets of patients with osteoarthritis and rheumatoid arthritis. *Arthritis & Rheumatism*. Apr 2001;44(4):838-845.
76. Dobryszycka W. Biological functions of haptoglobin--new pieces to an old puzzle. *European Journal of Clinical Chemistry & Clinical Biochemistry*. Sep 1997;35(9):647-654.

77. Yamagiwa H, Sarkar G, Charlesworth MC, et al. Two-dimensional gel electrophoresis of synovial fluid: method for detecting candidate protein markers for osteoarthritis. *Journal of Orthopaedic Science*. 2003;8(4):482-490.
78. Willumsen L, Friis J. A comparative study of the protein pattern in serum and synovial fluid. *Scandinavian Journal of Rheumatology*. 1975;4(4):234-240.
79. Hutadilok N, Ghosh P, Brooks PM. Binding of haptoglobin, inter-alpha-trypsin inhibitor, and alpha 1 proteinase inhibitor to synovial fluid hyaluronate and the influence of these proteins on its degradation by oxygen derived free radicals. *Annals of the Rheumatic Diseases*. May 1988;47(5):377-385.
80. Conner JG, Eckersall PD, Ferguson J, Douglas TA. Acute phase response in the dog following surgical trauma. *Research in Veterinary Science*. Jul 1988;45(1):107-110.
81. Li TW, Zheng BR, Huang ZX, et al. Screening disease-associated proteins from sera of patients with rheumatoid arthritis: a comparative proteomic study. *Chinese Medical Journal*. Mar;123(5):537-543.
82. Ahmadzadeh N. The role of metal binding proteins and proteinase inhibitors in rheumatoid synovial fluids. *Japanese Journal of Rheumatology*. 1990;2(2-3):127-137.
83. Ahmadzadeh N, Shingu M, Nobunaga M, Yasuda M. Correlation of metal-binding proteins and proteinase inhibitors with immunological parameters in rheumatoid synovial fluids. *Clinical and Experimental Rheumatology*. 1990;8(6):547-551.
84. Heegaard NH, Heegaard NHH. beta(2)-microglobulin: from physiology to amyloidosis. *Amyloid*. 2009;16(3):151-173.
85. Hou FF, Owen WF, Jr., Hou FF, Owen WF, Jr. Beta 2-microglobulin amyloidosis: role of monocytes/macrophages. *Current Opinion in Nephrology & Hypertension*. Jul 2002;11(4):417-421.
86. Santos M, Schilham MW, Rademakers LH, Marx JJ, de Sousa M, Clevers H. Defective iron homeostasis in beta 2-microglobulin knockout mice recapitulates hereditary hemochromatosis in man. *Journal of Experimental Medicine*. Nov 1 1996;184(5):1975-1985.
87. de Sousa M, Reim, x00E, et al. Iron overload in beta 2-microglobulin-deficient mice. *Immunology Letters*. Feb 1994;39(2):105-111.

88. Chia SL, Sawaji Y, Burleigh A, et al. Fibroblast growth factor 2 is an intrinsic chondroprotective agent that suppresses ADAMTS-5 and delays cartilage degradation in murine osteoarthritis. *Arthritis & Rheumatism*. Jul 2009;60(7):2019-2027.
89. Sawaji Y, Hynes J, Vincent T, Saklatvala J. Fibroblast growth factor 2 inhibits induction of aggrecanase activity in human articular cartilage. *Arthritis and Rheumatism*. 2008;58(11):3498-3509.
90. Cuevas P, Burgos J, Baird A. Basic fibroblast growth factor (FGF) promotes cartilage repair in vivo. *Biochemical & Biophysical Research Communications*. Oct 31 1988;156(2):611-618.
91. Abuharbeid S, Czubayko F, Aigner A, Abuharbeid S, Czubayko F, Aigner A. The fibroblast growth factor-binding protein FGF-BP. *International Journal of Biochemistry & Cell Biology*. 2006;38(9):1463-1468.
92. Martinelli CE, Jr., Cust, x00F, et al. [Physiology of the GH-IGF axis]. *Arquivos Brasileiros de Endocrinologia e Metabologia*. Jul 2008;52(5):717-725.
93. Bach LA, Bach LA. IGFBP-6 five years on; not so 'forgotten'? *Growth Hormone & Igf Research*. Jun 2005;15(3):185-192.
94. Hellio Le Graverand MP, Vignon E, Otterness IG, Hart DA. Early changes in lapine menisci during osteoarthritis development: Part II: molecular alterations. *Osteoarthritis & Cartilage*. Jan 2001;9(1):65-72.
95. Latini FRM, Hemerly JP, Oler G, Riggins GJ, Cerutti JM. Re-expression of ABI3-binding protein suppresses thyroid tumor growth by promoting senescence and inhibiting invasion. *Endocrine-Related Cancer*. 2008;15(3):787-799.

## VITA

Dr. Brandon L. Roller was born July 16, 1981 in Ozark, Alabama. After several years of travel, his family settled in Jefferson City, Missouri where he graduated from Jefferson City High School and was awarded salutatorian in 1999. He went on to attend the University of Missouri and received a Bachelor of Science in Biochemistry with the honor of summa cum laude in 2003. He continued his studies at the University of Missouri and received his Doctor of Medicine in 2007. He was accepted into the Department of Orthopaedic Surgery residency program at the University of Missouri, completing an internship with the Department of General Surgery in 2008. After serving as the Orthopaedic Research Resident through 2009, he elected to forgo the remainder of his orthopaedic residency training and pursue a career in the orthopaedic device industry. In 2009 he was hired by Arthrex, Inc. as a Product Manager of Orthobiologics. In 2012 he was promoted to Senior Product Manager of Orthobiologics and continues to hold this position.